OFFICE OF CIVILIAN RADIOACTIVE WASTE MANAGEMENT
ANALYSIS/MODEL COVER SHEET

Complete Only Applicable Items

1. QA: QA

2. ☒ Analysis	Check all that apply	3. ☒ Model	Check all that apply
Type of Analysis	☐ Engineering ☐ Performance Assessment ☒ Scientific	Type of Model	☒ Conceptual Model ☐ Abstraction Model ☒ Mathematical Model ☐ System Model ☒ Process Model
Intended Use of Analysis	☐ Input to Calculation ☒ Input to another Analysis or Model ☒ Input to Technical Document ☒ Input to other Technical Products	Intended Use of Model	☐ Input to Calculation ☒ Input to another Model or Analysis ☒ Input to Technical Document ☒ Input to other Technical Products
Describe use:	Primary use of results is to develop upper boundary conditions for the UZ site-scale flow and transport models.	Describe use:	Primary use of results is to develop upper boundary conditions for the UZ site-scale flow and transport models.

4. Title:

Simulation of Net Infiltration for Modern and Potential Future Climates

5. Document Identifier (including Rev. No. and Change No., if applicable):

ANL-NBS-HS-000032 REV 00

6. Total Attachments:	7. Attachment Numbers - No. of Pages in Each:
15	I-26, II-43, III-34, IV-16, V-30, VI-40, VII-28, VIII-20, IX-25, X-19, XI-23, XII-9, XIII-28, XIV-16, XV-14

		Printed Name	Signature	Date
8.	Originator	Joseph A. Hevesi	Joseph A. Hevesi	6/16/00
9.	Checker	Dwight Hoxie	Dwight Hoxie	06/16/00
10.	Lead/Supervisor	Alan Flint	Alan L Flint	6/16/00
11.	Responsible Manager	Robert Craig	Robert Craig	6/16/00

12. Remarks: Approved AMR

DISCLAIMER

This contractor document was prepared for the U.S. Department of Energy (DOE), but has not undergone programmatic, policy, or publication review, and is provided for information only. The document provides preliminary information that may change based on new information to be used specifically for Total System Performance Assessment analyses. The document is a preliminary lower-level contractor document and is not intended for publication or wide distribution.

Although this document has undergone technical reviews at the contractor organization, it has not undergone a DOE policy review. Therefore, the views and options of authors expressed may not state or reflect those of the DOE. However, in the interest of the rapid transfer of information, we are providing this document for your information per your request.

OFFICE OF CIVILIAN RADIOACTIVE WASTE MANAGEMENT
ANALYSIS/MODEL COVER SHEET

Complete Only Applicable Items

1. QA: QA

2. ☒ Analysis — Check all that apply		3. ☒ Model — Check all that apply	
Type of Analysis	☐ Engineering ☐ Performance Assessment ☒ Scientific	Type of Model	☒ Conceptual Model ☐ Abstraction Model ☒ Mathematical Model ☐ System Model ☒ Process Model
Intended Use of Analysis	☐ Input to Calculation ☒ Input to another Analysis or Model ☒ Input to Technical Document ☒ Input to other Technical Products	Intended Use of Model	☐ Input to Calculation ☒ Input to another Model or Analysis ☒ Input to Technical Document ☒ Input to other Technical Products
Describe use: Primary use of results is to develop upper boundary conditions for the UZ site-scale flow and transport models.		Describe use: Primary use of results is to develop upper boundary conditions for the UZ site-scale flow and transport models.	

4. Title:

Simulation of Net Infiltration for Modern and Potential Future Climates

5. Document Identifier (including Rev. No. and Change No., if applicable):

ANL-NBS-HS-000032 REV 00

6. Total Attachments:	7. Attachment Numbers - No. of Pages in Each:
15	I-26, II-43, III-30, IV-16, V-30, VI-40, VII-28, VIII-20, IX-25, X-19, XI-23, XII-9, XIII-28, XIV-16, XV-14

	Printed Name	Signature	Date
8. Originator	Joseph A. Hevesi	Joseph A. Hevesi	6/16/00
9. Checker	Dwight Hoxie	Dwight O Hoxie	06/16/00
10. Lead/Supervisor	Alan Flint	Alan L Flint	6/16/00
11. Responsible Manager	Robert Craig	Robert Craig	6/16/00

12. Remarks: Approved AMR

INFORMATION COPY

LAS VEGAS DOCUMENT CONTROL

OFFICE OF CIVILIAN RADIOACTIVE WASTE MANAGEMENT
ANALYSIS/MODEL REVISION RECORD

Complete Only Applicable Items

2. Analysis or Model Title:

Simulation of Net Infiltration for Modern and Potential Future Climates

3. Document Identifier (including Rev. No. and Change No., if applicable):

ANL-NBS-HS-000032 REV 00

4. Revision/Change No.	5. Description of Revision/Change
Draft 00A	2-28-00 Initial Draft prepared for OQA Audit M&O-ARP-00-04
Draft 00A-1	3-9-00 AP-3.14Q Input request
Draft 00A-2	3-23-00 Initial check draft
REV00B	4-27-00 Initial check copy concurrence draft
REV 00C	5-11-00 Back Check /Review copy
REV 00D	Date 6/05/00 AP-2.14Q Review Concurrence/Final Check Copy
REV 00E	Date 06/15/00 PCG Final Check Copy
REV 00	Date 06/16/00 Approved AMR

CONTENTS

CONTENTS (CONTINUED)

Page

CONTENTS (CONTINUED)

Page

FIGURES

Page

FIGURES (CONTINUED)

Page

FIGURES (CONTINUED)

Page

FIGURES (CONTINUED)

Page

TABLES

Page

TABLES (CONTINUED)

Page

ACRONYMS

AMR	Analysis/Modeling Report
CRWMS M&O	Civilian Radioactive Waste Management System Management & Operating Contractor
DEM	Digital Elevation Model
DIRS	Document Input Reference System
DOE	United States Department of Energy
DTN	Data Tracking Number
ENSO	El Niño Southern Oscillation
GIS	Geographic Information System
ID	Identification
IFR	Instantaneous Flow Routing
MAP	Mean Annual Precipitation
MAT	Mean Annual Temperature
NCDC	National Climatic Data Center
NOAA	National Oceanic and Atmospheric Administration
NTS	Nevada Test Site
NWS	National Weather Service
OCRWM	Office of Civilian Radioactive Waste Management
PTn	Paintbrush nonwelded hydrogeologic unit
QARD	Quality Assurance Requirements and Description
TBV	To Be Verified
TCw	Tiva Canyon welded hydrogeologic unit
TIC	Technical Information Center
USGS	United States Geological Survey
UTM	Universal Transverse Mercator
UZ	Unsaturated Zone
YMP	Yucca Mountain Site Characterization Project

1. PURPOSE

This Analysis/Model Report (AMR) describes enhancements made to the infiltration model documented in Flint et al. (1996) and documents an analysis using the enhanced model to generate spatial and temporal distributions over a model domain encompassing the Yucca Mountain site, Nevada. Net infiltration is the component of infiltrated precipitation, snowmelt, or surface water run-on that has percolated below the zone of evapotranspiration as defined by the depth of the effective root zone, the average depth below the ground surface (at a given location) from which water is removed by evapotranspiration. The estimates of net infiltration are used for defining the upper boundary condition for the site-scale 3-dimensional Unsaturated-Zone Ground Water Flow and Transport (UZ flow and transport) Model (CRWMS M&O 2000a). The UZ flow and transport model is one of several process models abstracted by the Total System Performance Assessment model to evaluate expected performance of the potential repository at Yucca Mountain, Nevada, in terms of radionuclide transport (CRWMS M&O 1998). The net-infiltration model is important for assessing potential repository-system performance because output from this model provides the upper boundary condition for the UZ flow and transport model that is used to generate flow fields for evaluating potential radionuclide transport through the unsaturated zone. Estimates of net infiltration are provided as raster-based, 2-dimensional grids of spatially distributed, time-averaged rates for three different climate stages estimated as likely conditions for the next 10,000 years beyond the present. Each climate stage is represented using a lower bound, a mean, and an upper bound climate and corresponding net-infiltration scenario for representing uncertainty in the characterization of daily climate conditions for each climate stage, as well as potential climate variability within each climate stage. The set of nine raster grid maps provide spatially detailed representations of the magnitude and distribution of net-infiltration rates that are used to define specified flux upper boundary conditions for the UZ flow and transport model.

The model development, calibration, and application conducted in this analysis were performed pursuant to AMR Development Plan TDP-NBS-HS-000016 (USGS 2000a). This analysis consists of (1) modifications to the 1996 model code INFIL V1.0 (Flint et al., 1996, Appendix V), (2) an updating of input parameters defining the new model INFIL V2.0 (STN 10307-2.0-00), (3) calibration of the new model using stream flow records, (4) the development of daily climate input representative of potential future climate stages, and (5) application of the model to provide net-infiltration estimates for a lower, mean, and upper bound climate scenario within each potential future climate stage. Estimation of the timing and duration of the potential future climate stages, which consist of a modern, a monsoon, and a glacial transition climate stage, is documented in "Future Climate Analysis" (USGS 2000b). The characterization of precipitation and air temperature for the upper and lower bound climate scenarios within the monsoon and glacial transition climate stages is also described in USGS (2000b).

This AMR documents the development, calibration, and application of the enhanced model, and also the historical development of the conceptual and numerical models used to provide spatially and temporally distributed estimates of net infiltration over the area of the UZ flow and transport model and the potential repository. The document describes all inputs, procedures, and assumptions used to obtain estimates of net infiltration and provides a descriptive summary of

model results. This AMR provides complete documentation of the net-infiltration model and its application, and Scientific Notebooks were not used to document model development.

2. QUALITY ASSURANCE

The activities documented in this Analysis/Model Report (AMR) were evaluated in accordance with QAP-2-0, *Conduct of Activities,* and were determined to be subject to the requirements of the U.S. DOE Office of Civilian Radioactive Waste Management (OCRWM) *Quality Assurance Requirements and Description* (QARD) (DOE 2000). This evaluation is documented in Wemheuer (1999; activity evaluation for work package WP 8191213UU1, UZ PMR Rev 0 for SRCR Analysis and Writing). This AMR has been prepared in accordance with procedure AP-3.10Q, *Analyses and Models.*

3. COMPUTER SOFTWARE AND MODEL USAGE

The software listed in Table 3-1 was appropriate for the intended application, and was used only within the range of validation in accordance with AP-SI.1Q, *Software Management.* Software, as appropriate, was obtained from Configuration Management and its status may be confirmed by review of the Document Input Reference System database. The main body of computer software used for this analysis consists of developed FORTRAN routines and programs. The primary model program for obtaining estimates of net infiltration is INFIL V2.0 (STN 10307-2.0-00), which is a modified version of INFIL V1.0 (Flint et al., 1996). ARCINFO V6.1.2 (STN: 10252-6.1.2-00),[1] was the only non-exempt software application acquired outside of the Yucca Mountain Site Characterization Project (YMP) that was needed for the AMR. No previous models were used in this analysis.

Table 3-1. Computer software used to develop estimates of net infiltration (Attachment I)

All electronic files consisting of source data, developed model inputs, model outputs, and post-processing results were maintained and processed according to the seven compliance criteria listed in AP-SV.1Q, *Control of Electronic Management of Data,* (Process Control Evaluation for Supplement V). The work activities documented in the AMR were dependent on electronic media to store, maintain, retrieve, modify, update, and transmit quality affecting information. As part of the work process, electronic databases, spreadsheets, and sets of files were required to hold information intended for use to support the licensing position. In addition, the work process required the transfer of data and files electronically from one location to another.

To provide adequate controls for protecting data and electronic files from damage and destruction during their prescribed lifetime, back-up copies of all electronic files were created and are maintained on two different media types: removable magnetic disk drives and optical CD-ROMs. Two sets of back-up files are maintained on each media type, and the complete set of electronic files on the two media types are maintained at two separate locations (Room 5004, Placer Hall, 6000 J Street, Sacramento CA 95819-6129, and 8815 Crusheen Way, Sacramento CA 95828). The location and description of individual files are catalogued and documented at

[1] ARCINFO is a registered trademark of ESRI, 210 Business Center Court, Redlands, CA 92373.

each location. The files on the magnetic media are readily retrieved using any AT-compatible PC equipped with IOMEGA[2] 2GB JAZ drives (files are maintained on both 1 and 2 GB IOMEGA JAZ disks). The files on CD-ROMs are readily retrieved using any AT-compatible PC equipped with a standard CD-ROM drive. Access to both media types at the two locations is controlled and secured. For archived and compressed files, standard "unzipping" utilities are required for accessing files and data. File integrity and accuracy is maintained using standard file checking utilities and also by checking calculated statistics for data files and model input and output files. For example, each simulation performed using the program INFIL V2.0 includes a set of simple output statistics calculated using the input data prior to the actual simulation, and this provides a check to ensure that the input files have not been corrupted. For all electronic file transfers and file archiving, adequate controls are provided using standard operating system utilities and file checking operations to ensure that data transfers and/or file compressions are error free. The use of the input computer files in developing and applying the net infiltration model is summarized in Section 6 and documented more fully in Attachment IV. The model input files are available from the Model Warehouse under the net infiltration model output data DTN: GS000308311221.000.

4. INPUTS

4.1 DATA AND PARAMETERS

All data sets and parameters used in the development, calibration, and application of the net-infiltration model to estimate net infiltration for modern and potential future climates are listed in Table 4-1. These data and parameters consist of the set of digitized topographic, geologic, and soil maps; soil and bedrock hydrologic properties; and modern and projected future climatic data that are appropriate to and required for the development and application of the distributed-parameter, quasi-three-dimensional, water-balance approach to watershed modeling that is the basis for the net infiltration model. Data qualification efforts, as needed, will be documented in accordance with AP-SIII.2Q, *Qualification of Unqualified Data and the Documentation of Rationale for Accepted Data*, and documented separately from this AMR.

Table 4-1. Data sets used for model development, calibration, and application. (Attachment I)

4.2 CRITERIA

This AMR complies with the DOE interim guidance (Dyer, 1999). Subparts of the interim guidance that apply to this analysis/modeling activity are those pertaining to the characterization of the Yucca Mountain site (Subpart B, Section 15), the compilation of information regarding hydrology of the site in support of the License Application (Subpart B, Section 21(c)(1)(ii)), and the definition of hydrologic parameters and conceptual models used in performance assessment (Subpart E, Section 114(a)).

[2] IOMEGA and JAZ are registered trademarks of the Iomega Corp., 1821 West Iomega Way, Roy, Utah 84067.

4.3 CODES AND STANDARDS

No specific formally established codes or standards have been identified as applying to this analysis.

5. ASSUMPTIONS

The assumptions pertaining to this analysis are grouped according to the following types of investigations conducted: (1) development of the conceptual model of net infiltration, (2) development of the numerical model of net infiltration, (3) model calibration and comparison to independent methods, (4) model application and the representation of three climate stages (modern, monsoon, and glacial transition), including the upper bound, mean, and lower bound climate scenarios within each climate stage, and (5) development of estimated input parameter distributions and climate inputs in support of the net infiltration uncertainty analysis documented in CRWMS M&O (2000b). Significant or general assumptions pertaining to this analysis/model are noted below. These assumptions are used throughout this AMR and do not require further confirmation.

The numerical representation of the conceptual model depends on the assumption that simplification of physical processes characterized by the conceptual model can be achieved while maintaining a sufficient level of accuracy in the mathematical approximation of these physical processes. This assumption is supported, in part, by model calibration and model validation.

It is assumed on the basis of numerous YMP peer reviews and several publications (e.g. Hatton, 1998, pp. 5-7, 16), that the use of INFIL V2.0, which uses a distributed parameter, quasi-three-dimensional water-balance approach, and associated assumptions, is appropriate for the complexity of this analysis/model and is relevant in this large-scale application of providing the upper boundary condition to the UZ flow and transport model. It is noted that this approach does not necessarily represent the physics of infiltration in soils, but uses a water volume calculation approach in the mathematical and numerical models. This model has been compared successfully to several independent approaches to estimating net infiltration and recharge, and more rigorous methods based, for example, on detailed numerical solution of the differential equations of ground-water and surface-water flow are not feasible for use in this large-scale application.

The infiltration model and analysis documented in this AMR are based on the assumption that the 1996 infiltration model, which was based on the distributed-parameter, water-balance approach and was calibrated using a variety of field data collected from 1984 through 1995, adequately represents the major features and processes controlling present-day and future infiltration at Yucca Mountain. The principal basis for the assumptions, discussed below, is that the resulting net-infiltration model quantitatively accounts for all major water inflow and outflow processes on a cell-by-cell basis and strictly imposes the conservation of total water mass within each model cell. The calculation results do not account for error propagation from the various components of the mass balance, such as measurement error associated with the various model inputs.

For the purpose of estimating potential surface net-infiltration rates and resulting percolation fluxes at the potential repository horizon, it is assumed that the climate scenarios developed in USGS (2000b) are representative of possible future climate conditions. Assumptions and uncertainties regarding the estimated monsoon and glacial transition potential future climate scenarios, including the timing and duration of each estimated future climate stage, are documented in USGS (2000b).

Within each cell of the model domain, water is assumed to move vertically downward within soil and bedrock, and that on a 30m x 30m grid block basis, there is no lateral diversion within the root zone. This is a viable assumption based on several calculations of specific conditions at the site. Given a land surface slope of approximately 4 to 6 degrees, the sine of the gravity vector is 0.07 to 0.10. The saturated hydraulic conductivity of the alluvium is 5.6E-6 m/s to 6.7E-6 m/s and the porosity is 35 percent (Attachment IV, Table IV-4). Using Darcy's equation and assuming fully saturated flow in a lateral downslope direction, with a perched system at the bedrock/alluvium contact that parallels the soil surface, the distance that lateral flow would travel in 30 days is approximately 3 to 6 m, thereby not moving beyond the 30m x 30m grid block area. If the slope were 45 degrees, the distance would be an order of magnitude greater. According to Hatton (1998), 1-dimensional, distributed-parameter, water-balance models are appropriate for use unless the excess rainfall generates overland flow (which is accommodated by flow routing in INFIL V2.0), or with the development of saturated conditions in soil profiles on slopes. The above calculation, and the fact that slopes have very thin soil cover and the underlying fractured bedrock has a high saturated hydraulic conductivity, negate this as a significant concern. On the other hand, if water were to move from one grid block downslope to the next grid block at the soil/bedrock contact, in a three-dimensional model configuration, this volume would be additive and would continue downslope until the slope was reduced, resulting in a shorter lateral travel distance. The total slope would only be affected in the uppermost and lowermost grid blocks. This component of error is considered to be insignificant relative to the spatial resolution required for the site-scale UZ ground water flow model.

Net infiltration is assumed to occur as fracture flow through the Tiva Canyon welded hydrogeologic unit (TCw) that is considered within the root zone. This assumption is based on relative changes in measured water content profiles that indicates that the penetration rates of the wetting front exceeded that calculated from the saturated hydraulic conductivity of the matrix alone. An assumption is also made that saturated fracture flow is maintained only for the duration that saturated conditions are maintained along the soil-bedrock interface. This assumption is based on interpretations of relative changes in the time series of water content profiles measured in boreholes by neutron logging (Flint and Flint, 1995), and corresponding nearby measurements of water potential at the soil/bedrock contact indicating saturated or near saturated conditions (see Figure 6-6A). The net infiltration rate for the time periods when net infiltration is occurring is assumed to be numerically equivalent to the bulk saturated hydraulic conductivity of the bedrock. This model does not use pressure gradients to induce flow and does not consider positive pressure heads.

The stream-flow routing algorithm is not an approximate solution to the governing partial differential equations of surface water flow (various forms of the St. Venant equations). Kinematic and inertia effects, flood waves and backwater effects are not being modeled. Additional factors not being considered are density changes due to temperature changes

throughout the water profile, gravitational acceleration, resistance terms, viscosity changes due to sediment load, phase changes, changes in fluid hydraulics due to shifts from turbulent to laminar flow, flow dispersion and dynamic shifts in channel geometry due to concurrent stream bed erosion and deposition. The only physical process being represented by this model is the lateral redistribution and subsequent infiltration of the runoff water volume and it is assumed that this can be adequately modeled based on elevation alone. In addition, the details of positive heads in active channels are insignificant relative to the uncertainty of available input parameters required to accurately define stream channel geometry for the entire stream channel network represented by this model.

It is assumed that changes in liquid properties, such as viscosity and density, on the saturated field-scale hydraulic conductivity of soil and bedrock are insignificant. This assumption is justified because temperature variations in the near-surface environment that could affect the viscosity or density of water are expected to be small and because dissolved constituents that could affect the density of water are expected to be present in insignificant concentrations.

While there is evidence that there is negligible downward flow occurring during long time-periods of no precipitation, it is included as an assumption. Very small changes in volumetric water content cannot be measured using neutron logging, which assumes that changes less than 0.006 m^3/m^3 are within the error of the measurement. Drainage under a unit gradient during time periods when soil water content is below field capacity can be calculated and an example is included in Section 6.1.5.

Model uncertainty is being addressed through parameter input distributions that are being developed as a part of the net infiltration model uncertainty analysis (CRWMS M&O 2000b). Input distributions are developed for 12 selected parameters (estimated a-priori as being potentially significant, see Section 6.10.2) from those included in the model control file. The parameters included in the model control file are discussed in Section 6.3.3. The developed distributions are based on assumptions of upper and lower bounds for each of the selected parameters. Additionally, the distribution type for each selected parameter is assumed. CRWMS M&O (2000b) should be consulted for complete documentation of the assumptions and their bases.

6. ANALYSIS/MODEL: CONCEPTUAL MODEL OF INFILTRATION AND MODEL DEVELOPMENT, CALIBRATION, AND APPLICATION

The conceptual and numerical models of net infiltration for Yucca Mountain were developed by Flint et al. (1996) and described and simulated the natural hydrologic system. The models were based on thorough analysis of extensive field data collected during 1984 through 1995. The current (1999) model development does not completely replace the 1996 model, but supplements and enhances the 1996 model, particularly with respect to evapotranspiration from the root zone and the infiltration of surface run-on in the channels of washes. In addition, the current (1999) model uses updated model inputs for bedrock geology and soil depth.

The net-infiltration modeling process requires a combination of applications using Geographic Information System (GIS) applications, field measurements (or acquisition of existing field data), parameter estimation, visualization and analysis, and the application of developed

FORTRAN codes. The FORTRAN codes are used for pre-processing model input, the implementation of process modeling for simulating net infiltration, and for post-processing of model results, which includes the development of net-infiltration estimates for a given climate scenario by averaging separate model simulation results. The process modeling for net infiltration consists primarily of an hourly energy balance and a daily water balance simulation for a continuous multi-year period. The daily net-infiltration rates are averaged over the duration of the simulation for each model node[3] to obtain spatially distributed, time-averaged net-infiltration rates.

The net infiltration model and analysis documented in this AMR are concerned specifically with estimating the spatial distribution of net infiltration in the vicinity of the potential Yucca Mountain repository under present-day and projected future climatic conditions. In accordance with the screening criteria listed in Attachment 6 of AP-3.15Q, *Managing Technical Product Inputs,* the net infiltration model and analysis are of Level 2 importance in addressing the factors of the post-closure safety case for the potential repository in the unsaturated zone at Yucca Mountain. The net infiltration model is founded on the application of standard distributed-parameter water-balance methods to estimate net infiltration as discussed, for example, in Hatton (1998), and yields net infiltration estimates that, as discussed in this section, are within the range of and consistent with the results of other methods that have been used to estimate net infiltration and recharge in the Yucca Mountain region. On this basis, the net infiltration model and analysis documented in this AMR are deemed to be appropriate for providing estimates of net infiltration that serve as input to and the upper boundary condition for the site-scale UZ flow and transport model.

6.1 CONCEPTUAL MODEL OF INFILTRATION

The following sections provide a brief overview of the conceptual model of net infiltration for the purpose of describing the physical processes that are represented by the mostly deterministic, process-based, numerical model of net infiltration. A more thorough description of the conceptual model of net infiltration is provided in Flint et al. (1996, pp. 8-26).

6.1.1 Definition of Net Infiltration

The conceptual model defines net infiltration as water that has percolated from the land surface to below the root zone. The root zone herein is defined as the zone from the ground surface to some variable depth in soil or bedrock from which infiltrated water is readily removed on an annual or seasonal basis by evapotranspiration. The depth of the root zone can be estimated from field studies but cannot be defined precisely. In addition, the depth of the root zone depends on variable climate and surface conditions controlling vegetation and other factors affecting evapotranspiration and is thus transient and spatially variable. Infiltration is the movement of water across the air/soil or air/bedrock interface, and percolation is defined as the downward movement of water within the unsaturated zone.

[3] In this report, model nodes are also referred to as model cells or model grid cells, and represent locations in space for which corresponding model calculations are made. The nodes are points at the centers of horizontally equidimensional, square grid cells that can be used to define representative areas for each node.

6.1.2 Overview of the Conceptual Model of Infiltration

The current conceptual model of infiltration at Yucca Mountain identifies effective precipitation, which is the ratio of precipitation to potential evapotranspiration, as the most significant environmental factor controlling net infiltration at Yucca Mountain. Precipitation averages 170 mm/yr over the study area but is temporally and spatially variable (Hevesi et al., 1992). On an annual basis effective precipitation is low because potential evapotranspiration is much higher than precipitation. However, on a daily basis, effective precipitation can be high, particularly during periods with large and frequent winter storms. For example, the average penetration depth of infiltration[4] into the soil/bedrock profile fluctuates on a seasonal basis for a given location, but tends to be greatest in the winter due to lower evapotranspiration demands, higher amounts of precipitation, and slow snow melt.

The second most significant environmental factor controlling net infiltration is soil depth. When there is sufficient precipitation to produce net infiltration, the spatial distribution is generally defined by the spatial variability of soil depth. Field measurements indicate that when the soil/bedrock contact reaches near-saturated conditions (see Figure 6-6A), fracture flow is initiated in the bedrock (as evidenced by changes in water content profiles), increasing the hydraulic conductivity by several orders of magnitude. Soils exceeding 6 meters in thickness eliminate the infiltration of water to the soil/bedrock contact except in channels (Flint and Flint, 1995). Storage capacity in the soil profile is large enough that most water from precipitation is held in the root zone and removed by evapotranspiration processes. Soils that are less than 6 meters deep do not have enough storage capacity to store the volume of precipitation, and often allow near-ponding conditions to occur at the soil/bedrock contact, particularly when the soil depth is less than 0.5 meters.

The third factor controlling net infiltration is bedrock permeability. At Yucca Mountain welded tuffs of the Tiva Canyon welded (TCw) hydrogeologic unit, and nonfractured, nonwelded tuffs of the Paintbrush nonwelded (PTn) hydrogeologic unit are the principal rock types present in surface exposures or directly under soils. The saturated hydraulic conductivity of the nonwelded PTn matrix is higher than the TCw matrix (Flint, 1998, Table 7). The fractures in the welded tuff increase the saturated hydraulic conductivity of those rocks but due to channeling and the presence of inactive as well as active fractures (Liu et al., 1998), the unsaturated bulk conductivity is generally not more than that of the matrix of the nonwelded tuffs. The lower storage capacity of the fractured, welded tuffs allows moisture that has infiltrated to penetrate more deeply than in the nonwelded tuffs. Hydraulic properties of fractures calculated for this study depend on fracture aperture and whether or not the fractures are open or filled with calcium carbonate or siliceous materials. Based on numerical simulations of water flow through a block of variably saturated fractured tuff, Kwickis et al. (1998, p. 60) suggest that the infiltration of water into a fractured welded tuff, such as the TCw, will be controlled by the water potential at the soil-bedrock interface. Because the apertures and the air-entry water potentials of unfilled fractures (Kwicklis et al., 1998) are larger than the overlying soils (see Attachment IV, Table IV-4), the initiation of fracture flow should occur only under saturated or near-saturated conditions.

[4] The penetration depth of infiltration is identified by the maximum depth at which a wetting front is observed based on geophysical logs.

Fracture densities and matrix permeabilities are variable among the geologic units at Yucca Mountain.

Shallow infiltration processes at Yucca Mountain can be described on the basis of four infiltration zones that can be identified based on the manner in which volumetric water content changes with depth and time (Flint and Flint, 1995). The zones, which correlate with topographic position, are described as follows: (1) Ridgetops are flat to gently sloping, of higher elevation than the other zones, and have thin soils composed of both eolian deposits and soils developed in place from the weathering process. These soils often have higher clay content and higher water-holding capacity compared to soils on sideslopes and alluvial terraces. The ridgetops generally are located where the bedrock is moderately to densely welded and fractured. The presence of thin soil and fractured bedrock results in the deeper penetration of moisture following precipitation compared to other topographic positions. In some locations where runoff is channeled, large volumes of water can infiltrate. For the present-day arid climate, runoff generally is restricted to the upper headwater portions of drainages and to locations downstream of areas that have very thin soils underlain by relatively impermeable bedrock. (2) Sideslopes are steep, commonly have thin to no soil cover, and are usually developed in welded, fractured tuff. The steepness of the slopes creates conditions conducive to rapid runoff. The low storage capacity of the thin soil cover and the exposure of fractures at the surface may enable small volumes of water to infiltrate to greater depths, especially on slopes with north-facing exposures and therefore lower evapotranspiration demands. Shallow alluvium at the bases of the slopes can easily become saturated and initiate flow into the underlying fractures. (3) Alluvial terraces are flat, broad deposits of layered rock fragments and fine soil with a large storage capacity. Little runoff is generated on the terraces and the precipitation that falls there does not move below a depth of one to two meters before it is removed evapotranspiration. Consequently, this zone contributes the least to net infiltration in the drainage basin. (4) Active channels are similar to the terraces but are located in a position to collect and concentrate runoff that, although occurring infrequently, can penetrate deeply. Although local net infiltration can be high for some channel locations, under the current arid climate this mechanism is not considered a major contributor to the total volume of net infiltration at Yucca Mountain, because runoff is infrequent and because the channels areas include only a very small percentage of the total drainage basin area.

6.1.3 The Hydrologic Cycle

In the conceptual model, the hydrologic cycle is used to identify, define, and separate the various field-scale components and processes controlling net infiltration (Figure 6-1; all figures referenced in Section 6 are included in Attachment II, Figures). The hydrologic cycle is a basic conceptual tool used to visualize and define the various components of the field-scale water balance (Maidment, 1993, Figure 1.2.1, p. 1.4; Freeze and Cherry, 1979, Figure 1.1, p. 3). The hypothetical starting point of the hydrologic cycle is precipitation, which for current (modern) climate at Yucca Mountain occurs primarily as rain but can also occur as snow. Precipitation can accumulate on the ground surface,[5] infiltrate the soil or exposed bedrock[6] surfaces, contribute to runoff, or accumulate as snow. The contribution of precipitation to runoff generation depends on

[5]Some precipitation can also be intercepted and temporarily stored by vegetation surfaces, but this component of the hydrologic cycle is negligible at the study site.

[6]In this report, bedrock is used as a general term referring to all consolidated rock material that is either exposed (outcropping) or overlain by unconsolidated soil material.

precipitation intensity relative to soil and exposed bedrock hydraulic conductivity, and also on the available storage capacity of soil and shallow bedrock with thin or no soil cover. Water accumulated in the snow pack can sublimate into the atmosphere or become snowmelt, which can then infiltrate, evaporate, or contribute to runoff. Rain or snowmelt that becomes runoff accumulates in surface depressions and basins or contributes to surface water flow, which is routed to downstream locations as run-on.[7] Run-on contributes to either infiltration or accumulated surface-water run-on at downstream locations. Infiltrated water percolates through the root zone as either saturated or unsaturated ground water and is subject to evapotranspiration. Water percolating through the root zone is available as potential net infiltration, but the actual net-infiltration rate is limited by the bulk (or field-scale) saturated hydraulic conductivity of the bedrock or soil underlying the root zone. In the conceptual model, the bulk saturated hydraulic conductivity represents a weighted averaging of the field-scale matrix and fracture saturated hydraulic conductivity. Estimates of saturated hydraulic conductivity were calculated using these measured values of fracture conductivity for the percentage of area covered by the fracture per square meter of rock, given the fracture density and aperture size available for water to flow through. This was added to the saturated hydraulic conductivity of the rock matrix and weighted averages of bulk saturated hydraulic conductivity of bedrock, on the basis of percentages of matrix and fractures, were calculated by lithostratigraphic unit (see Attachment IV, Part 2). When infiltration from rain, snowmelt, or surface-water run-on occurs at a rate greater than the bulk saturated hydraulic conductivity of a subsurface layer, water will begin to fill the available storage capacity of the overlying soil. When the total storage capacity is exceeded, runoff is generated. While runoff can occur while the subsurface is still unsaturated due to precipitation exceeding the saturated hydraulic conductivity of the soil, this is on a small scale, and irrelevant to modeling of 30m x 30m grid blocks.

Figure 6-1. Field-scale water balance and processes controlling net infiltration. (Attachment II)

In the Yucca Mountain area, the hydrologic cycle can be limited to atmospheric, surface, and shallow sub-surface processes because contributions from ground water discharge and the deep unsaturated zone are insignificant relative to the other components of the cycle[8] (there is no perennial stream flow at the site).

6.1.4 Evapotranspiration

Evapotranspiration is the combined process of bare-soil evaporation and transpiration (excluding evaporation from open water bodies) (Freeze and Cherry, 1979, p. 4). Transpiration is the uptake and transfer of water to the atmosphere by vegetation. Transpiration is much more efficient than bare-soil evaporation in removing water from sub-surface soils and fractured bedrock. Evapotranspiration is a function of the potential evapotranspiration rate, the availability of water at the ground surface and within the root zone, vegetation characteristics such as timing of plant growth and root density, and the chemical and hydrologic properties of the root zone. The

[7] In this report, runoff is specifically defined as the volume or depth of water accumulation on the ground surface prior to being routed as surface-water flow, whereas run-on is defined as the volume or depth of the routed surface-water flow.

[8] Vapor flow enhanced by barometric pumping and temperature gradients also contributes to the water balance at the site but has been shown to be insignificant relative to precipitation, evapotranspiration, runoff, and net infiltration.

processes are not independent, but in general the primary factors controlling evapotranspiration are potential evapotranspiration, water availability, vegetation density, and seasonal vegetation growth. The more saturated the soil (or fractured bedrock) and the denser the vegetation, the closer the transpiration rate is to the potential evapotranspiration rate. If the soil (or fractured bedrock) becomes drier than what is conceptually referred to as the wilting point, transpiration will not occur even though there may be some residual water in the root zone. The redistribution of water within the root zone affects the total evapotranspiration rate because bare-soil evaporation extends approximately depths of only 10 to 30 cm, and the density and growth of roots within the root zone in general is typically observed to decrease with depth. The estimate of the depth of bare-soil evaporation is based on field measurements of water potential with depth, and above about 20-30 cm the water potential values are too dry (see Figure 6-6A) for extraction by plant roots. The more quickly water redistributes to lower depths the greater the potential for net infiltration to occur because the overall susceptibility of water in the root zone to removal by evapotranspiration decreases with depth. At depths greater than the root zone vapor flow and matric suction potentials can result in upward unsaturated flow or exfiltration back into the root zone; but total water losses from these processes are considered negligible relative to evapotranspiration within the relatively thin root zone.

The potential evapotranspiration rate is determined by the energy balance and depends primarily on net radiation, air temperature, ground heat flux, the slope of the saturation-vapor density curve, and advective energy from wind (McNaughton and Spriggs, 1989; Priestley and Taylor, 1972; Flint and Childs, 1991). Net radiation depends primarily on solar radiation and surface characteristics including topography and albedo. For the current climate at Yucca Mountain, the average annual potential evapotranspiration rate is approximately six times greater than the average annual precipitation rate (Hevesi et al., 1994b, p. 2326); thus, on an annual basis, most of the precipitation is removed from the site by evapotranspiration. However, on a daily basis, the precipitation, snowmelt, or surface-water run-on rate, can be much higher than the potential evapotranspiration rate, especially during the winter when the potential evapotranspiration rate is at a minimum.

6.1.5 Net Infiltration

Net infiltration at Yucca Mountain is dominantly an episodic process that tends to occur only under wetter than average conditions or in response to isolated but intense storms (Flint et al., 1996; Flint and Flint, 1995; Hevesi et al., 1994a). For upland areas having thin soils and rooting depths, the occurrence of net infiltration requires saturated or near-saturated conditions at the soil/bedrock interface and within shallow bedrock fractures to initiate flow through open or filled fractures (see Section 6.1.2). Assuming that active roots can extend into bedrock along open or partially filled fractures, a maximum effective rooting depth of approximately two meters is estimated for fractured bedrock, with a much lower root density and water storage capacity relative to soils. For locations with thick soils, the occurrence of net infiltration requires percolation through a deeper average rooting depth that is estimated to be approximately 6 meters (Flint et al., 1996; Flint and Flint, 1995).

For larger storm or snowmelt events, water can accumulate in the root zone more rapidly than it can be removed by evapotranspiration. This is especially true during winter when potential evapotranspiration is at a minimum due to shorter days, lower sun angle, and lower air

temperatures and root activity is either diminished or dormant. The downward percolation rate through the root zone under these conditions depends primarily on the storage capacity of the root zone and the field capacity and hydraulic conductivity of the soil and bedrock. The total storage capacity of the soil is defined as the porosity minus the residual water content multiplied by the soil depth. Field capacity is defined as the water content of the near surface soil profile (i.e., the root zone) at which drainage becomes negligible (several orders of magnitude less than the saturated flux rate) (Jury et al., 1991, p. 150). Field capacity is an old soil physics concept intended to provide a characteristic index of how much water may be retained from a rainfall event after redistribution has ceased. In actual field conditions, water drains continually under gravity. However, in coarse-textured soils such as those found at Yucca Mountain, the drainage rate falls to an insignificant level within a few days, after which the water content is changing at such a slow rate that a field capacity concept has practical value (Jury et al., 1991, p. 150). In skeletal soils found in southwestern Oregon, the water content at a measured mean value of -0.07 bars for field capacity was obtained (Flint and Childs, 1984). Flint and Childs (1984) argued that the water content at close to –0.1 bars was more appropriate for field capacity than the assumption of –0.33 bars that was commonly used, based on soil textures common to agricultural fields. This publication and other large scale studies conducted in major metropolitan water districts in southern California and regional watershed studies in Japan, provide support for the use of the field capacity concept in the gravelly sandy soils located at Yucca Mountain. For thick soils, reaching or exceeding field capacity at a depth of 6 meters tends to occur only for locations subject to concentrated surface-water flow, such as active stream channels and the base of steep sideslopes. For upland areas with thin soils, the percolation rate through the root zone depends on the field-scale storage capacity, and once exceeded, the hydraulic conductivity of bedrock. Thus, the effective field capacity of the root zone in upland areas is determined by bedrock lithology, fracture characteristics (density, aperture, filling), and the characteristics of the soil/bedrock interface, in addition to the characteristics of the overlying soil. The water potential that corresponds to the volumetric water content measured at field capacity is considered to be –0.1 bars and is shown for the soils used for modeling infiltration at Yucca Mountain in Attachment IV, Geospatial Input for INFIL V2.0 FY99.

Two exercises are conducted to illustrate the negligible value of drainage at water contents below the field capacity value of –0.1 bars. Using values of soil properties listed in Attachment IV, Table IV-4, unsaturated hydraulic conductivity was calculated for soils with average water potentials at 0.025 bars, –0.1 bars (field capacity), and -0.5 bars. At 0.025 bars the unsaturated hydraulic conductivity is reduced about 2 orders of magnitude below that of the saturated hydraulic conductivity, with a value of 10.7 mm/day. At field capacity the rate drops to 4 orders of magnitude, with an unsaturated hydraulic conductivity of 0.25 mm/day. Once below field capacity, at 0.5 bars, the rate drops to 6 orders of magnitude, which is 0.003 mm/day. As the evapotranspiration rate at about –0.2 bars is approximately 2-3 mm/day, the soil dries quickly to very low drainage rates.

A calculation of drainage for measured soil water contents was done for a borehole located in an active channel, illustrating relatively wet conditions. For borehole N1, located in Pagany Wash where the channel is about 3 m in cross-section, and the soil is 8.3 m deep, drainage from the soil was calculated as the unsaturated hydraulic conductivity at an average volumetric water content from below an estimated zone of evapotranspiration, 3 m, to the bottom of the alluvium. For monthly measurements made for the period of 1984 through 1995, the drainage was calculated to

be 0.5 mm/yr in this active channel with periodic runoff. Flux was calculated as described in Section 6.3.4 for this borehole, using the average water content for 2 m of soil below 6 m in depth. Increases in average water content between monthly measurements were summed for values that were greater than the measurement error of 0.006 m^3/m^3. The total flux calculated for the 10 year period was 83.5 mm/yr (when distributed over a 30 m grid cell, this equates to about 10 mm/yr.). The drainage due to gravity from the soil for this borehole was 0.6% of the total flux calculated for the borehole. Boreholes located in topographic locations where runoff is unlikely, such as terraces, have soils that are generally much drier, potentially reducing the drainage by several orders of magnitude below that calculated for this borehole. As the net infiltration flux calculated in these locations are also much lower, the contribution of drainage to the total flux in the borehole would be higher, but the drainage, even at somewhat moist ranges of between –1 bar and –5 bars, the drainage ranges from 0.2 mm/yr to 0.001 mm/yr.

In general, the volume of net infiltration occurring at Yucca Mountain under conditions of unsaturated ground-water flow when the root zone is drier than field capacity either in upland areas with thin soils or in locations with thick soils is considered negligible compared to the volume of net infiltration occurring as saturated flow through bedrock fractures or through thick soils that have reached or exceeded field capacity (see Figure 6-5) (Flint et al., 1996; Flint and Flint, 1995; Hevesi et al., 1994b; Nichols, 1987).

6.2 NUMERICAL REPRESENTATION OF THE CONCEPTUAL MODEL

The numerical model is a digital representation of the mathematical concepts that describe the conceptual model of net infiltration described in Section 6.1. In most cases, an exact mathematical formulation of the physical processes being modeled is not required and in many cases is not possible. An application of approximate mathematical formulations is an essential requirement for computational efficiency and practical applicability of the numerical model. The level of accuracy needed for an approximate representation depends on the sensitivity of the UZ flow and transport models to net infiltration, in conjunction with the level of accuracy needed for results obtained with the models to evaluate potential repository performance (CRWMS M&O, 2000a).

6.2.1 Accuracy and Precision of Model Calculations

The simulation of net infiltration primarily involves a water-balance calculation and the application of the conservation of mass principle. All water-balance calculations are performed as water-depth balances (which are easily converted to volume balances[9]), and thus an assumption is made that calculation errors due to temperature effects on water density are negligible relative to the level of precision needed for net-infiltration estimates.

Model calculations are performed using double precision variables and standard FORTRAN77 programming language. The model code performs several internal mass balance checking calculations that are used to test the precision of the overall water-balance simulation (program testing and software validation are described thoroughly in the software qualification documentation). For estimated average annual net-infiltration rates, model results are provided

[9] Model calculations are performed as water-depth balances, and are converted to volume balances based on model grid cell area, which is 900 square meters for all model grid cells.

for each model grid cell to the nearest 0.00001-millimeter (mm) water depth for all components of the water balance to allow for additional mass-balance checking using post-processing procedures. This level of precision does not indicate the level of accuracy in model results. Based on the average number of significant figures in model input, the number of significant figures that can be applied to model results should not exceed two. This level of output accuracy is subjectively based on the average level of precision in model inputs.

6.2.2 Accuracy of Input Parameters

The accuracy of all model inputs could not be fully quantified at the time of this activity. Uncertainty in model inputs was not incorporated into the results developed in this analysis/model report. A preliminary uncertainty analysis is provided by CRWMS M&O (2000b), and will be used in the UZ Flow and Transport Process Model Report (CRWMS M&O 2000a) to provide a limited evaluation of model accuracy and uncertainty based on estimated bounds and distributions for a few selected input parameters. The development of input distributions for the selected parameters is discussed in Section 6.10.2.

6.3 GENERAL DESCRIPTION OF MODELING PROCEDURE

6.3.1 Overview of Distributed-Parameter Water-Balance Model

The distributed-parameter, water-balance model developed as the FORTRAN program INFIL V2.0 follows the conceptual model of infiltration discussed in Section 6.1, and is represented using a storage volume approach for modeling the root-zone. The total root-zone water storage capacity is calculated using the 30m x 30m area of each grid cell multiplied by the depth of the root-zone (including soil and bedrock layers) . The root-zone water balance calculation used to model net infiltration is illustrated by Figure 6-2. Infiltration into the root-zone and net infiltration through the root-zone is calculated independently for all grid cells and corresponding root-zone storage volumes. Because all grid cells have equal areas, the root-zone water storage terms are calculated as 1-dimensional vertical storage depths, which can easily be converted to volumes based on grid cell areas. The components of the root-zone water balance are determined for each layer using the water content of each layer. For water contents less than or equal to the water content at field capacity, infiltration is set to zero and water loss due to evapotranspiration from that layer is modeled as an empirical function of relative saturation (with relative saturation based on porosity and the residual water content) and potential evapotranspiration (Flint and Childs, 1991). For water contents greater than the water content at field capacity, water losses due to both infiltration and evapotranspiration from the layer are calculated. Infiltration into the underlying layer is set equal to the bulk saturated hydraulic conductivity of that layer (in millimeters per day). If the available water for net infiltration (calculated based on the amount of water remaining after evapotranspiration losses have been calculated) is less than the maximum infiltration amount determined using saturated hydraulic conductivity, water loss to infiltration is set equal to the amount of available water in the layer. For the lowermost root-zone layer in thick (6 meters or greater) soils, the daily water loss to infiltration is used to determine net infiltration. For upland areas with shallow soils where the root-zone is modeled as having a lowermost layer in bedrock, the amount of water available to evapotranspiration losses is calculated using the fracture porosity and the thickness of the bedrock layer. Once the water content of the bedrock layer has reached the limit defined by the

fracture porosity, if water continues to infiltrate or percolate into the bedrock layer, net infiltration is calculated based on either the saturated hydraulic conductivity of the bedrock layer or the amount of available water (whichever determines the lower net infiltration amount).

On a daily basis, precipitation, snowmelt, and surface water run-on are added (as water depth) to the top layer of the root-zone profile at each grid cell. The surface water run-on depth is calculated as runoff generated and routed from upstream grid cells. If the amount of precipitation, snowmelt, and run-on added to the top layer exceeds the maximum daily amount calculated using the saturated hydraulic conductivity of the soil, then runoff (set equal to the amount of excess water) occurs at that grid cell location and is routed to the downstream grid cell. Surface-water flow depths are routed as part of an instantaneous flow routing algorithm representing a daily water balance. All overland flow is routed as a time-independent flow depth for each grid cell within a 24-hour time step (the physics of overland flow are not considered in this type of model). Daily surface water flow volumes are calculated using grid cell areas and converted to standard stream discharge units (cubic-feet-per-second) for comparison with measured stream flow records.

For locations where the lowermost root-zone layer is in bedrock, net infiltration is numerically equal to the bulk saturated hydraulic conductivity of the underlying bedrock (in millimeters/day) for the period of time where the water content of the lowermost root-zone layer exceeds the field capacity of that layer. Net infiltration is simulated as the bulk saturated hydraulic conductivity of the underlying bedrock when the water content of the bedrock root-zone layer equals the fracture porosity of that layer. This condition is maintained only as long as the field capacity of the bottom soil layer (the soil layer above the bedrock layer) is exceeded. Thus, for upland areas with shallow soils, net infiltration is simulated as an episodic process requiring saturated conditions at the soil/bedrock interface and throughout the effective flow path of the bedrock layer included in the root-zone.

For locations with thick (greater than 6 meters) soil, net infiltration does not require saturated conditions at the bottom of the root zone, but does require that the water content of the bottom soil layer exceeds the field capacity of the layer. For upland areas, it is assumed that water ponded at the soil/bedrock interface and saturating the effective flow path through the bedrock root-zone layer percolates below the root-zone as net infiltration on a daily basis under a unit gradient. In all cases, water losses due to evapotranspiration are simulated for all root zone layers having a water content greater than residual prior to the calculation of net infiltration. During winter when potential evapotranspiration is at a minimum, ponded or saturated conditions at the soil/bedrock interface and throughout the effective flow path of the bedrock root-zone layer may exist for several days. Thus the total net infiltration is calculated as approximately the saturated hydraulic conductivity multiplied by the number of days net infiltration occurred. For days when the amount of water available for net infiltration is less than the limit set by the saturated hydraulic conductivity of the bedrock (this condition applies only to the last day of an extended net infiltration event), net infiltration equals the amount of water available to net infiltration in the lowermost root-zone layer.

The daily water balance model is applied over a continuous multi-year period and is driven by the continuous daily climate input provided for the total simulation period. The daily net infiltration rates calculated for each grid cell location are used to calculate an average annual net

infiltration rate for each grid cell based on the total simulation period. The average annual net infiltration rate is calculated in units of length per time (millimeters per year), and can be directly applied as a specified flux upper boundary condition for the UZ flow and transport model.

Figure 6-2. The daily root-zone water-balance used to model net infiltration. (Attachment II)

6.3.2 Overview of Modeling Procedure

The net infiltration modeling procedure begins with building a geospatial input parameter base grid using the selected digital elevation model (DEM) to define the base-grid geometry. The development of the geospatial input parameter base grid and the separate watershed modeling domains requires the application of Geographic Information Systems (GIS) to transfer available digitized map data, which is in a vector-based format, onto the grid-cell of the raster-based format of the DEM (a process referred to as rasterization). The vector-based map coverages used as input by the net infiltration model include bedrock geology and soil type maps. In addition to the rasterization procedure, GIS applications are also used for calculating slope and aspect as well as latitude and longitude coordinates for all grid cells. Geospatial parameters that are not available as either raster-based or vector-based map coverages are developed using a series of FORTRAN routines that are applied sequentially. The routines are used to overlay three separate bedrock geology maps (after rasterization), estimate soil thickness, calculate the blocking ridge parameters, calculate surface water flow routing parameters, and extract the watershed model domains.

The DEM (DTN: GS000308311221.006) selected for defining the grid geometry is the composite DEM used for the original net infiltration model (Flint et al., 1996) that was developed from two standard USGS 7.5 minute 30-meter DEMs (Busted Butte and Topopah Spring NW). The two DEMs (DTN:GS000200001221.003) were combined into a composite DEM (DTN: GS000308311221.006) by using the ARCINFO, ARC-EDIT, ARC-PLOT, and ARC-GRID modules, utilizing a series of standard commands within the various modules. The grid geometry of the composite DEM (DTN: GS000308311221.006) is based on the Universal Transverse Mercator (UTM) projection (zone 11, NAD27) and consists of 691 rows in the north-south direction and 367 columns in the east-west direction covering a rectangular area centered over Yucca Mountain and the potential repository site, with the following corner coordinates:

Northwest corner:	544,661 meters easting, 4,087,833 meters northing
Northeast corner:	555,641 meters easting, 4,087,833 meters northing
Southeast corner:	555,641 meters easting, 4,067,133 meters northing
Southwest corner:	544,661 meters easting, 4,067,133 meters northing

The elevation provided by the composite DEM (253,597 values) is the primary geospatial parameter used by the net infiltration model. Elevation is used to define the surface-water flow-routing network, which is in turn used to define watershed-modeling domains which are extracted from the base grid and modeled separately as closed hydrologic systems. Elevation is used to define slope, aspect, and blocking ridge parameters for modeling incoming solar

radiation that is in turn used in an energy balance calculation for modeling potential evapotranspiration. The calculated slope is also used to model soil thickness. Additional uses of elevation values in the net infiltration model include estimation of spatially distributed daily climate input (precipitation and air temperature).

In addition to the geospatial input parameters, the daily climate input and the model parameter inputs are defined prior to application of the net infiltration model. Daily climate input includes precipitation and air temperature. Model parameters include soil properties, bedrock properties, and root-zone parameters. An initial condition consisting of the root-zone water content is also defined prior to model application.

Following the development of the base grid, the following 11 steps summarize the net-infiltration modeling procedure used for this analysis:

1. Acquisition and/or development of GIS map coverages and the application of ARCINFO V6.1.2. for the rasterization of geospatial parameters onto the base grid defined by the digital elevation model (DEM) for Yucca Mountain. Conversion of grid cell coordinates to both UTM zone 11 and geographic (latitude and longitude) using ARCINFO V6.1.2.

2. Calculation of topographic parameters, including grid cell slope and aspect using ARCINFO V6.1.2, and 36 blocking-ridge angles for each grid cell using the routine BLOCKR7 V1.0 (the blocking-ridge angles used in the geospatial-parameter input file for INFIL V2.0 are the same as those used in the input file for the 1996 INFIL V1.0 model).

3. Estimation of soil depth and refinement of bedrock geology (rock-type identification) using the programs GEOMAP7 V1.0, GEOMOD4 V1.0, and SOILMAP6 V1.0.

4. Calculation of surface-water flow routing parameters for each model grid cell using the DEM and the programs SORTGRD1 V1.0 and CHNNET16 V1.0.

5. Identification of watershed outflow locations using TRANSFORM[10] V3.3 for raster data visualization and output from CHNNET16 V1.0. Extraction of watershed modeling domains, including calibration modeling domains, using the DEM, the identified outflow locations, the calculated surface-water flow-routing parameters, and the program WATSHD20 V1.0.

6. Development of a daily climate input file (mod3-ppt.dat) for model calibration and modern climate simulations using available precipitation records from monitoring sites within the study area and in the proximity of Yucca Mountain. Development of mod3-ppt.dat is performed within an EXCEL spreadsheet (mod3-ppt.xls) using a linear interpolation method.

7. Estimation of pre-calibration model coefficients and initial conditions for root-zone water contents.

[10] TRANSFORM is a registered trademark of Fortner Software LLC, 100 Carpenter Dr, Sterling, VA 20164.

8. Calibration of root-zone model coefficients included as input in model control file for modeling program INFIL V2.0 by comparing simulation results for calibration watersheds against streamflow records.

9. Development of 100-year daily climate input files for modern climate scenarios using available precipitation records from the Nevada Test Site stations 4JA and Area 12 Mesa and the programs MARKOV V1.0 (STN 10142-1.0-00) and PPTSIM V1.0. (STN 10143-1.0-00) Development of daily climate input for future climate scenarios using the routine DAILY09 V1.0 and seven selected analog records from the EARTHINFO[11] database.

10. Application of INFIL V2.0 (STN 10307-2.0-00) using developed daily climate input (mod3-ppt.dat, 4ja.s01, area12.s01, nogales.inp, hobbs.inp, rosalia.inp, spokane.inp, stjohn.inp, beowawe.inp, and delta.inp), calibrated or estimated root-zone model coefficients, and watershed modeling domains for net-infiltration simulations.

11. Development of net-infiltration estimates for nine separate climate scenarios by averaging or sampling from individual net-infiltration simulations using the routine MAPADD20 V1.0. Development of descriptive statistics for results over the areas of the potential repository boundary and the UZ flow and transport-modeling domain using SURFER[12] V6.04 and the routine MAPSUM01 V1.0. Development of model results as GIS coverages using ARCVIEW[13] V3.1, TRANSFORM V3.3, and SURFER V6.04

Figure 6-3 provides a generalized illustration of the various model components required for simulating spatially distributed net-infiltration rates.

Figure 6-3. Major components of the net-infiltration modeling process. (Attachment II)

6.3.3 Overview of Model Input

User-defined model inputs for INFIL V2.0 consist of four general groups: (1) geospatial parameters, (2) hydrologic properties, (3) empirical model coefficients, and (4) daily climate input. Additional model coefficients are defined within the model source code. A detailed description of model inputs is provided in Sections 6.2 through 6.7. A detailed description of model input files, including descriptions of file formats, model options, and input and output options, is provided in the users manuals for INFIL V2.0, prepared under the software qualification procedure *AP-SI.1Q, Software Management.*

The data acquired or developed and used as input for modeling net infiltration consist of either ASCII digital data or proprietary formats for acquired software applications (ARCINFO map coverages, EARTHINFO data formats). All model input required directly for simulating net infiltration using the developed model code INFIL V2.0 is provided by three separate ASCII files:

[11] EARTHINFO is a registered trademark of EarthInfo Inc., 5541 Central Avenue, Boulder, CO 80301.
[12] SURFER is a registered trademark of Golden Software, Inc, 809 14th Street, Golden, CO 80401-1866
[13] ARCVIEW is a registered trademark of ESRI, 210 Business Center Court, Redlands, CA 92373

1. **Model control file:** specifies input and output options, input and output file names, modeling options, simulation period, model coefficients, and hydrologic properties.

2. **Daily climate input file:** defines the temporal domain for the model simulation and consists primarily of day number and daily precipitation amount in millimeters. The file can also include daily maximum, minimum, and mean air temperature in degrees Celsius, and snowfall accumulation in water equivalent millimeter data (measured snowfall data are not used by INFIL V2.0, see Section 6.4.3).

3. **Geospatial parameter input file:** consists of location coordinates and spatially variable grid cell parameters for all grid cells defining the model domain. Grid cell variables include elevation, slope, aspect, surface-water flow-routing parameters, soil type, soil depth, bedrock type, and 36 blocking ridge parameters.

As will be documented subsequently in this AMR, the infiltration model will be applied over the domain of the site-scale UZ flow and transport model (CRWMS M&O, 2000a).

6.3.4 Assumptions Concerning Model Calibration

Data used for model calibration are listed in Table 4-1 and in the attachments and are described in detail in Flint et al. (1996) as well as various sections throughout this report. They include soil hydrologic properties, bedrock hydrologic properties, vertical water-content profiles in soils and bedrock, and meteorological data. It is assumed that the 1996 infiltration model that was calibrated using these data is an adequate starting point for the enhancements included in the 1999 model and that the 1999 model calibration may build on the calibration performed in 1996. The calibration of the 1996 model is described in Section 6.8.3. The 1999 model calibration uses stream flow measurements from USGS gaging stations for 1994 and 1995 (DTN: GS941208312121.001, GS960908312121.001).

The 1996 infiltration model was calibrated using water-content profiles at Yucca Mountain obtained by geophysical logging a network of up to 98 boreholes with neutron-moisture probes at monthly or weekly intervals during 1984 through 1995. Analysis of depth versus time water-content changes from this network provided critical information for the development of the conceptual model, particularly with respect to relative magnitudes of net infiltration for different topographic locations (Flint et al., 1996; Flint and Flint, 1995; Hevesi et al., 1994b). Depth versus time water-content profiles indicated the importance of thin soils, saturated fracture flow, periods of heavy precipitation (and/or snowmelt), and surface water run-on; in providing the conditions needed for the occurrence of episodic net-infiltration pulses. For example, the depth versus time water-content profile measured at borehole UZ-N15 (Flint et al., 1996, Figure 32; DTN: GS940708312212.011, GS941208312212.017, GS950808312212.001, GS960108312212.001) indicates the occurrence of three major episodes of net infiltration through bedrock in response to wetter than average conditions during the winters of 1992-93 and 1994-95 (Figure 6-4). The UZ-N15 site is at a ridgetop location in the headwater part of the upper Pagany Wash channel, has relatively thin soils, and based on field observations, received surface-water run-on during the winters of 1992-93 and 1994-95. The net-infiltration pulses indicated in Figure 6-4 cannot be supported by the measured bedrock matrix hydraulic conductivity alone. In order to measure the changes in water content noted in this figure using

neutron moisture meters, it is necessary to have detectable changes in the volumetric water content. The rapid downward advance of the wetting front observed at this site suggests fracture flow is necessary as the matrix permeability is very low, therefore fracture flow through welded tuff is required, which was verified by independent measurements of water potential using heat dissipation probes at the soil-bedrock contact at a nearby site not affected by the existence of a borehole (Flint et al., 1996, Figure 35; DTN: GS960908312211.004). While the fractures may or may not be saturated in all locations during episodic high precipitation events accompanied by surface run-on, in this particular case, field observation at a nearby trench indicated that the fractures were fully saturated. The thin soils, fractured bedrock, and concentrated surface-water flow all contributed to rapid percolation of infiltrated water well below the depth of the effective root zone. In general, the collective time-averaged net-infiltration rates calculated at all borehole sites (DTN: GS960508312212.008) using the measured water-content changes indicate the occurrence of significant net infiltration at Yucca Mountain during 1989–95 (Figure 6-5) and a strong negative correlation between soil depth (DTN: GS960508312212.007) and net-infiltration rates (Flint and Flint, 1995).

Figure 6-4. Measured water-content profiles at borehole UZN-15 for 1993-95. (Attachment II)

Figure 6-5. Estimates of average net-infiltration rates at Yucca Mountain calculated using changes in measured water-content profiles obtained for the period 1989–95 from a network of monitoring boreholes, compared to depth of alluvium at each borehole. (Attachment II)

Drilling neutron-probe boreholes in the fractured tuffs at Yucca Mountain may introduce additional fractures or enhance the flow in the existing network, causing an overestimate of net infiltration. An independent estimate of net infiltration was developed using 1 year of water-potential measurements from heat-dissipation probes near borehole USW UZ-N15 (Figure 6-6A). The probes were installed laterally from a small trench that was backfilled. Measurements were made at four depths: 7.0, 15.0, 36.5, and 73.7 cm (the soil/bedrock interface). By early March, within 2 weeks of installation, winter precipitation saturated the soil from the soil-bedrock interface to within 36 cm of the soil surface, and heat-dissipation probes at both 36.5 cm and 73.7 cm were saturated. The probe at the soil/bedrock interface (73.7 cm) remained saturated until the end of March and then dried out to less than -10 bars by September. The probes closer to the surface dried out faster, and the near-surface probes became wetter periodically due to summer precipitation events.

The moisture-retention curve for this location (Attachment IV, Geospatial Input Data for INFIL V2.0 FY99) was used to convert water potential to water content (Figure 6-6B). The rate of water loss was calculated between selected dates by using the change in water content. In early March the profile changed at a rate of more than 10 mm/day, but dropped to less than two mm/day within 30 days. The evaporation rate was estimated to be no more than two mm/day on the basis of potential evapotranspiration calculations using the Priestley-Taylor equation (Priestley and Taylor, 1972), yielding a maximum flux into the bedrock of eight mm/day. The flux for 30 days averaged five mm/day to yield a total flux into the bedrock of 150 mm. The estimate for the nearby borehole (USW UZ-N17; DTN: GS960508312212.008) was 110 mm for the same time period.

Figure 6-6. Graphs of water-potential measurements near borehole USW UZ-N15 using heat dissipation probes (DTN: GS960908312211.004), (A) measured at four depths for 1995 and (B) used to calculate flux. (Attachment II)

Changes in water-content profiles through time measured in boreholes located in active channels with thick soils were used to develop and calibrate a modified Priestley-Taylor evapotranspiration model (Hevesi et al., 1994b). Initial model calibrations conducted using INFIL V1.0 in 1996 consisted of a generalized (site-wide) calibration of the modified Priestley-Taylor model coefficients (DTN: GS000300001221.009) were based primarily on the calculated changes in the measured profiles (Flint et al., 1996, Figure 41; also discussed in Section 6.8.3). Model calibration using INFIL V2.0 was conducted using stream flow records from five gaging sites on Yucca Mountain that were operational from 1994 through 1995 and included two significant storm events measured during the winter of 1994-95 (DTN: GS941208312121.001, GS960908312121.001). A description of the model calibration procedure and the results of model calibration are provided in Section 6.8. Net infiltration is assumed to occur as saturated, or near-saturated, fracture flow through the TCw. An assumption is made that the fracture flow is maintained only through the thickness of the TCw within the root-zone, which is estimated to be less than 2 meters. Because of expected capillary barrier effects at the soil bedrock interface, it is assumed that fracture flow is maintained only for the duration that saturated conditions are maintained along the soil-bedrock interface. The spatial resolution of this fracture flow is much higher than that of the site-wide model, and therefore may not be well represented by the site-wide model. During infiltration events the contribution of the matrix of the bedrock to net infiltration is extremely small compared to the flow within the fractures. If the matrix is unsaturated it makes even less of a contribution. Therefore the saturation of the rock matrix is not taken into consideration. Rather, once the alluvium at the bedrock contact becomes saturated it is assumed that fracture flow is initiated, piston flow is assumed, and the fracture flow is accompanied by the small proportion of matrix saturated hydraulic conductivity. This also accounts for those few locations when sparsely fractured, nonwelded tuff is underlying alluvium.

Assumptions regarding the appropriateness of various calibration procedures can be supported using comparisons of model results with independent methods to determine if model results vary considerably from other approaches of estimating net infiltration or recharge in the same environment. The spatially averaged net-infiltration rates for the nine climate scenarios were compared against estimates of recharge obtained using independent studies at various locations in the southern Basin and Range Province as a method of model comparison (Maxey and Eakin, 1950; Winograd, 1981; Lichty and McKinley, 1995; Harrill and Prudic, 1998; Dettinger, 1989). Although this method of model comparison is useful as a qualitative assessment of model results, it cannot be used to quantify levels of confidence or model uncertainty (due in part to the unknown accuracy of the independent results). A comparison with independent results does not necessarily validate (or invalidate) the accuracy of the model in representing the physical processes developed in the conceptual model.

6.4 MODEL COMPONENTS AND PROCESSES

The INFIL V2.0 model algorithm consists of three main loops for performing a daily simulation of net infiltration over all model cells comprising a watershed model domain. Figure 6-7 provides a flow chart illustration of the general model algorithm and the primary loop (day-of-

year loop), which is driven by the daily climate input file and carries the simulation through the time domain. Nested within the primary loop is a grid cell loop for performing a daily water balance calculation at each grid cell location and within each layer of the root zone. [The root zone was subdivided into layers based on the estimated maximum depth of bare-soil evaporation and an estimated variation in root density. In general, the layering represents a decrease in root density with increased depth in the root zone, particularly at locations with thick soils (greater than 6 meters).] The daily root-zone water balance consists of simulating precipitation, snowmelt, sublimation, evapotranspiration, changes in water content for each root-zone layer, net infiltration, and runoff generation. Nested within the water-balance loop is an hourly loop for modeling potential evapotranspiration based on the simulation of incoming solar radiation and effects on total solar radiation due to blocking ridges using the SOLRAD sub-model and the routine BLOCKR7 (Flint et al., 1996; Flint and Childs, 1987).

After the completion of the water-balance loop, a surface-water flow-routing subroutine is called if runoff was generated at any grid cell. Surface-water flow is routed at the end of the day as a time-independent (instantaneous) total daily flow depth across each grid cell. The routing algorithm connects all grid cells horizontally using surface-water flow-routing parameters included in the geospatial parameter input file. Surface-water flow is coupled to the water-balance calculation by allowing surface water to infiltrate into downstream grid cells according to the available root-zone storage capacity, soil hydraulic conductivity, and estimates for effective surface-water flow area and stream flow duration. The infiltrated water is added to the grid cell's antecedent root-zone water-content term used in the following day's water-balance calculation. The surface-water flow depth routed across the grid cell defining the outflow location of the watershed is converted to a daily mean discharge flow rate, in cubic feet per second (cfs),[14] which can be compared to measured stream flow for model calibration.

Figure 6-7. Flow chart of the model algorithm used for simulating net infiltration. (Attachment II)

Time-averaged net-infiltration rates are calculated by accumulating the simulated daily net-infiltration amounts obtained at the end of the daily water-balance loop. Time average rates also are calculated for the remaining components of the water balance (precipitation, snowmelt, sublimation, evapotranspiration, infiltrated run-on, root-zone water-content change, and runoff) for all model grid cells and are included in the main output file used for developing the net-infiltration results. The time-averaged rates for all components of the water balance simulated at each grid cell are averaged over the watershed model domain and compared against the time-averaged watershed outflow to check the consistency of the simulated water balance for the entire watershed.

Output from INFIL V2.0 also includes spatially averaged daily water-balance terms for all components of the water balance. The daily output indicates the average inflow, outflow, and change in storage rates over the area of the watershed being simulated. The spatially averaged daily water balance is compared against the simulated daily outflow to provide a water-balance check for each day simulated. The simulated daily water balance rates are averaged over time and compared against the spatially averaged water-balance rates simulated at each grid cell as an

[14] Cubic feet per second is a standard unit used for volume discharge rates in surface water hydrology

additional method of checking the consistency of the simulated water balance for the entire watershed.

6.4.1 Daily Water and Energy Balance

The estimation of spatially distributed net-infiltration rates consists of a daily simulation of net infiltration in response to a daily water- and energy-balance calculation performed separately for all model elements within a watershed bounded by surface-water flow divides. The daily water-balance calculation used in INFIL V2.0 is:

$$R_{off} = P - SF + IR_{on} + SM - SB - S - ET - I \qquad \text{(Eq. 1)}$$

where I = net infiltration, P = precipitation (rain and snow), SF = snowfall, SB = sublimation, SM = snowmelt, S = change in water-content storage within the root zone, ET = evapotranspiration, IR_{on} = infiltrated surface-water run-on, and R_{off} = surface-water runoff generated by excess precipitation, snowmelt, or run-on. It is important to note that runoff, not net infiltration, is calculated as the solution to the water-balance equation. A unit gradient is assumed and net infiltration is incorporated in the water-balance formulation as a temporary potential net-infiltration term and is limited by the field-scale-saturated hydraulic conductivity of the soil or bedrock underlying the root zone. A detailed description of the method used for calculating net infiltration is provided in Sections 6.4.5 and 6.4.6.

The daily water-balance calculation performed for a root zone is illustrated in Figure 6-2, which was discussed in Section 6.3.1. In this figure water balance of the root zone is schematically represented for a single soil layer. In modeling the daily water-balance, parameters affecting the daily water balance, such as soil thickness, soil and bedrock properties, and various surface and vegetation characteristics, are uniquely defined for each grid cell. The difference between field capacity and residual water content is commonly referred to as available water capacity in soil science terms and that is the water available for plants. Therefore this is the zone in which the transpiration part of evapotranspiration processes take place. The infiltration rate of precipitation, snowmelt, or surface-water run-on into the root zone from the land surface is limited by the saturated hydraulic conductivity of the grid cell soil type (or the bulk saturated hydraulic conductivity of the grid cell bedrock type in cases of no soil cover). Precipitation and surface-water flow rates are defined using an estimated 2-hour storm duration for summer storm events and an estimated 12-hour storm duration for winter storm events. If the precipitation or snowmelt rate exceeds the saturated hydraulic conductivity of the top root-zone layer, the excess precipitation or snowmelt is added to the runoff term for that grid cell. During the simulation of surface-water flow, the infiltration of surface-water run-on is also limited by the saturated hydraulic conductivity of the top root-zone layer. Surface-water run-on exceeding the saturated hydraulic conductivity of the top root-zone layer is added to the runoff term routed to the downstream grid cell.

As noted in Figure 6-2, infiltration is represented as equal to recharge. This is not entirely the case because in a deep unsaturated zone there are several mechanisms that may remove a small amount of water and the timing of recharge is not accounted for. At Yucca Mountain there are unsaturated zone groundwater ages of over 7,000 years.

6.4.2 Daily Climate Input

Infiltration occurs in response to daily precipitation that occurs in particular temporal and spatial patterns. Stochastic representations of infiltration would be required to predict infiltration for long time periods without daily input; however, no infiltration data are available for the development of long-term patterns. Therefore, using stochastic representations of precipitation and daily input to simulate infiltration is appropriate.

The daily climate input file is the primary control for the timing and duration of the simulation. The daily climate input file defines the time domain through which the simulation occurs by providing a real-time sequential input of daily climate parameters. The file is ASCII column formatted and at minimum consists of the year number, the day of year number, and the total daily precipitation amount but can also consist of maximum, minimum, and average daily air temperature, along with total daily snowfall accumulation.

The primary input provided by the daily climate-input file is total daily precipitation, in millimeters, and this drives the daily water-balance calculation. Average daily air temperature, in degrees Celsius, is not required as input, but if not provided in the daily climate input file, this parameter is modeled internally by INFIL V2.0 using Equation 20 from Flint et al. (1996):

$$T = T1\text{-}T2\ \{\mathrm{Sin}[(D/366)*2*\pi + 1.3]\} \qquad \text{(Eq. 2)}$$

where T = modeled daily air temperature, D = day of year number, T1 = mean annual air temperature, and T2 = mean seasonal variation of average daily air temperatures above the mean during summer and below the mean during winter (the ½ amplitude of the sine wave). T1 and T2 were calculated as 17.3 and 11.74 degrees Celsius, respectively, using measured air temperature data from Yucca Mountain (DTN: GS000208312111.002).

The daily climate input file provides point values of total daily precipitation and average daily air temperature for a given day of the simulation. These values are representative of the conditions at locations having elevations of approximately 1,400 meters, which represents the approximate average elevation of the land surface above the potential repository. Precipitation and air temperature are distributed spatially across all model grid cells using empirical elevation models. The precipitation/elevation correlation, caused by the adiabatic cooling of air masses interacting with mountainous terrain, has been studied in the southern Nevada region and correlation models between elevation and annual as well as seasonal precipitation amounts have been defined (French, 1983; Hevesi et al., 1992; Hevesi and Flint, 1998). The precipitation/elevation correlation model used in INFIL V2.0 for modern climate was from Hevesi and Flint (1998, Table 4) for the sample of 114 precipitation stations with a minimum of 8 years of record (DTN: GS960108312111.001), where the coefficients in the table are based on mean annual precipitation transformed as ln(MAP) x 1,000. The model estimated mean annual precipitation distributions using the relation:

$$P_d^k = P_d * \exp(0.0006458*E + 4.317)/MAP \qquad \text{(Eq. 3)}$$

where P_d^k = the elevation-corrected daily precipitation estimate (in millimeters) for day d at model element k, P_d = the point precipitation estimated for day d provided by the daily climate

input file, E = elevation (in meters), and MAP = mean annual precipitation (in millimeters). For the monsoon and glacial transition climate scenarios, the slope defined by Equation 3 was adjusted to account for assumed changes in the precipitation/elevation correlation based on estimates of precipitation-elevation correlations presented by Thompson et al. (1999), indicating a reduction in orographic effects on precipitation for wetter paleoclimates.

Atmospheric pressure decreases with increasing altitude. Consequently, stirring of an atmospheric layer causes rising parcels of air to cool by adiabatic expansion, and sinking parcels to correspondingly warm by compression. The net effect of this is a vertical decrease in temperature with increase in elevation called the adiabatic lapse rate. The adiabatic lapse rate, or air temperature/elevation correlation is cited in numerous references as about 9.8 degrees C per kilometer and was cited for this work using Maidment (1993, p. 2.27):

$$T_d^k = 0.0098 * (1400.-E^k) + T_d \qquad \text{(Eq. 4)}$$

where T_d^k is the elevation-adjusted air temperature for grid cell k based on elevation E and daily air temperature T_d (either provided in the daily climate-input file or simulated using Equation 2). The elevation E is subtracted from the estimated mean elevation for the potential repository area that is indicated in the equation as 1,400 m. This is the approximate average ground surface elevation of the potential repository.

Cloud cover is a variable affecting the energy-balance calculation and is indirectly accounted for in the model as an empirical function of daily precipitation magnitude. For days with precipitation, the modeled clear-sky potential evapotranspiration rate is reduced according to:

$$APET_d = PET_d/[(4*P_d/25.4) + 1] \qquad \text{(Eq. 5)}$$

where APET = adjusted potential evapotranspiration for day d (in millimeters), PET_d = the Priestley-Taylor modeled clear-sky potential evapotranspiration for day d (PET is discussed further in Section 6.4.4), and P_d = modeled daily precipitation for day d. The coefficient 25.4 converts inches to millimeters, and the value 4 is an estimate that reduces the PET by approximately 25 percent due to cloud cover that exists whenever it rains. The assumption is that the energy for ET is reduced in the presence of clouds (associated with precipitation) and the more rain there is, the less ET there is. The model is fairly insensitive to this value.

6.4.3 Snow Pack Sub-Model

Precipitation is simulated as snowfall for a grid cell location if the average air temperature is less than or equal to 0 degrees Celsius. When snowfall occurs, all precipitation for that day is assumed to occur as snow at that location. However, because air temperature is distributed spatially using the elevation correlation model, snowfall and snow pack accumulation may occur at higher elevation cells while rain occurs at lower elevations within the same watershed.

Snowfall is accumulated into a snow pack storage term and is removed from the root-zone water balance. If snow pack exists and the air temperature is less than 0 degrees Celsius, water is removed from the snow pack by using an empirical sublimation-saltation-suspension model under the assumption that in upland areas advective wind-transport processes tend to cause snow removal rather than deposition over most areas. The three processes are grouped into a single

empirical "sublimation" model that also includes evaporation of snowmelt and sublimation (but not saltation and suspension) when the air temperature exceeds 0 degrees Celsius:

$$SB^k = A1 * APET^k,\ T^k <= 0 \text{ (sublimation/advective losses)} \quad \text{(Eq. 6)}$$
$$SB^k = A2 * APET^k,\ T^k > 0 \text{ (evaporation of snowmelt and sublimation)}$$

where SB^k = total snow pack losses to the atmosphere (in millimeters), $APET^k$ is the cloud cover adjusted Priestley-Taylor potential evapotranspiration rate[15], (in millimeters/day), and T^k is the average air temperature simulated for grid cell k (in degrees Celsius). The model coefficients were estimated based on limited information indicating the average percentage of snow pack losses due to sublimation and advective energy processes (Maidment, 1993, pp. 7.4-7.10). For all simulations using the snow pack sub-model, A1 was set to 0.1 and A2 was set to 0.3 in the model control file. This is an assumed relation to account for an increase in snow pack losses to the atmosphere when the average daily air temperature is above freezing. If a snow pack exists and air temperature is greater than 0 degrees Celsius, a combined sublimation of snow and evaporation of snowmelt is simulated, and the APET term is reduced by the sublimation/evaporation rate SB to provide a potential transpiration rate for the root zone. Thus, the model allows reduced transpiration to occur when a snow pack exists but only if air temperature is higher than 0 degrees. For all days when air temperature is 0 degrees or less, transpiration is set to zero, and only sublimation can occur, provided a snow pack exists.

If air temperature is greater than 0 degrees Celsius, snowmelt is simulated as an empirical linear function of average daily air temperature (Maidment, 1993, pp. 7.4-7.10) using a standard temperature index modeling approach:

$$SM^k = A * T^k \quad \text{(Eq. 7)}$$

where SM is the modeled snowmelt (in millimeters) for grid cell k; T is the modeled average daily air temperature (degrees Celsius) for grid cell k; and A was set to 1.78, which is the coefficient used for modeling snowmelt in the Sierra Nevada during April (Maidment, 1993, Table 7.3.7, p. 7.24) The simulated snowmelt is carried back into the root-zone water-balance calculation as an influx term.

6.4.4 Potential Evapotranspiration and the Net Radiation Sub-Model

Total daily potential evapotranspiration is modeled for each grid cell using the Priestley-Taylor equation (Priestley and Taylor, 1972):

$$PET_d^k = \alpha * [S/(S + \gamma)_d^k * (RN_d^k - GH_d^k) / 2.45*10^6] \quad \text{(Eq. 8)}$$

where PET_d^k is potential evapotranspiration (in millimeters) on day d for grid cell k; S is the slope of the saturation vapor pressure-temperature curve; γ is the psychometric constant; RN is modeled net radiation; and GH is estimated ground-heat flux, which is modeled using Equation 22 from Flint et al. (1996):

[15] The potential evapotranspiration rate used in the sublimation model uses a Priestley-Taylor α coefficient value of 1.26 to account empirically for the advective component of the total energy balance and is not necessarily equivalent to the values of the coefficient used in the root-zone model.

$$GH = -20 + 0.386(RN) \quad \text{(Eq. 9)}$$

and $2.45*10^6$ converts the energy units to millimeters of water. In Equation 8, α is used as an empirical scaling factor to account for the missing advective energy term in the Priestley-Taylor equation. For wet conditions having freely evaporating surfaces, α is often set to 1.26 (Priestley and Taylor, 1972; Flint and Childs, 1991; DTN: GS000300001221.009). For dry conditions, available moisture becomes the limiting factor controlling actual evapotranspiration, and α can be modeled as an empirical scaling function, α', using a relative saturation term (Flint and Childs, 1991). In the root-zone water-balance sub-model, α' is defined as an empirical function of relative saturation within the root zone by using a method described in Section 6.2.6.

The $S/(S+\gamma)$ term is modeled as a function of average daily air temperature by using Equation 19 from Flint and et al. (1996):

$$S/(S+\gamma)_d^k = -13.281 + 0.083864 * TA_d^k - 0.00012375 * (TA_d^k)^2 \quad \text{(Eq. 10)}$$

where TA^k is the average daily air temperature on day d for grid cell k, in Kelvins. Equation 10 was defined using parameter values obtained from performing a regression on data from Campbell (1977, Table A.3), and provides an indication of the relative effect of air temperature on potential evapotranspiration, which varies for different temperature ranges. In Figure 6-8, Equation 10 is compared with selected values taken from (Campbell, 1977, Table A.3) to illustrate the greater relative change in the $S/(S+\gamma)$ term for the lower air temperatures in the range –5 to 5 degrees Celsius as compared to temperatures in the range of 25 to 35 degrees Celsius. For example, a decrease in air temperature from 5 to 0 degrees Celsius results in a 17 percent reduction in $S/(S+\gamma)$ and thus potential evapotranspiration, while a decrease in air temperature from 35 to 30 degrees Celsius causes only a 5 percent reduction in the $S/(S+\gamma)$ term.

Figure 6-8. Relative effect of air temperature change on the modeled $S/(S+\gamma)$ term of the Priestley-Taylor equation used for estimating potential evapotranspiration. (Attachment II)

Total daily net radiation is the primary component of the energy balance determining potential evapotranspiration and is modeled using Equation 21 from Flint et al. (1996):

$$RN_d^k = -71 + 0.72 * K_d^k\downarrow \quad \text{(Eq. 11)}$$

where RN is total net radiation, in w/m^2, on day d for model element k, and $K\downarrow$ is simulated incoming solar radiation which is modeled using a version of the SOLRAD program developed by Flint and Childs (1987). To account for seasonal changes in the solar trajectory as well as terrain effects across model elements, SOLRAD calculates solar position on an hourly[16] basis from sunrise to sunset as a function of the day of year and geographic position of each grid cell (Flint and Childs, 1987). Terrain effects (blocking ridges) on incoming solar radiation are modeled using topographic parameters calculated from the DEM and included as input in the geospatial parameter file. Topographic parameters include grid cell slope, aspect, and 36

[16] The time step is a user-specified option included in the model control file. Although a 1-hour time step is allowed, a 2-hour time step was used to reduce simulation run time.

blocking ridge angles that define shading effects and reductions in skyview for every 10 degrees in the horizontal plane, starting with the UTM northing axis as the 0-degree azimuth. Shading causes a reduction in direct beam radiation, and diminished skyview decreases diffuse radiation. These effects can become important in rugged mountainous terrain.

6.4.5 Root-Zone Sub-Model: Infiltration, Percolation, and Redistribution

Water infiltrating and percolating (see Section 6.1.1 for definitions) through the multi-layered root-zone system is modeled as a cascading piston-flow process. Downward percolation is modeled as a "forward" cascade initiated by adding the total volume of water infiltrating the top layer of the root zone to the antecedent water content of the layer. The new water content is calculated using the layer thickness and compared against the field capacity defined by the grid cell soil type. The volume of water exceeding the field capacity becomes downward percolation that is added to the antecedent water content of the underlying layer, and the new water content of the underlying layer is compared against the field capacity of that layer. If the potential percolation volume exceeds the saturated soil hydraulic conductivity or the saturated bulk bedrock hydraulic conductivity of the underlying layer, the downward percolation rate is set equal to the saturated hydraulic conductivity of the underlying layer, and the excess water volume is added to a temporary storage term for the overlying layer. The process is repeated for each soil and bedrock layer in the root zone (in the case of the model used in this analysis/modeling activity, a maximum of three soil layers and one bedrock layer were used) until the bottom layer is reached, which completes the forward cascade.

The volume of water that has percolated into the bottom bedrock layer (which may be zero if the field capacity of an overlying layer was not exceeded) is compared against the effective root-zone storage capacity of the bedrock. If a bedrock layer exists in the root zone, the effective root-zone storage capacity of the bedrock layer is calculated based on the estimated root-zone depth, the estimated soil depth, and the estimated effective fracture porosity of the rock type (a more complete description of estimated root-zone depths in bedrock is provided in Section 6.5). The volume of water exceeding the bedrock storage capacity is the potential net-infiltration volume. For thick soils, there is no bedrock layer in the root zone. The thickness of the bedrock root-zone layer is set to zero, the effective fracture porosity for the bottom bedrock layer becomes zero, and all water exceeding the field capacity of the bottom soil layer (the third soil layer) is potential net infiltration unless limited by the saturated bulk hydraulic conductivity of the underlying soil or bedrock. For locations where the soil depth is estimated to be 6 meters or greater, the underlying bedrock properties are defined using alluvium/colluvium properties. Based on analysis of neutron moisture meter data (Flint and Flint, 1995), the maximum depth of infiltration in non-channel alluvial locations is 6 meters, therefore there is no need to provide bedrock properties in these locations. The actual net-infiltration volume is calculated after evapotranspiration is simulated throughout the root zone and is limited by the bulk saturated hydraulic conductivity of the underlying rock type. The potential net-infiltration volume exceeding the bulk saturated hydraulic conductivity is added to the temporary storage term of the bottom root-zone layer.

Starting with the bottom root-zone layer, a reverse cascade is performed to determine if runoff is generated. The volume of water in the temporary storage term is compared against the total storage capacity of each layer defined by the porosity (or effective fracture porosity in the case of bedrock) and layer thickness. If the volume of water in the temporary storage term exceeds the

storage capacity, the excess water is added to the temporary storage term of the overlying layer. The process is repeated until the top layer is reached, completing the reverse cascade. The volume of water in the temporary storage term exceeding the storage capacity of the top layer is added to the potential runoff volume calculated for that grid cell. The final runoff volume is calculated following the simulation of evapotranspiration from the root zone.

6.4.6 Root-Zone Sub-Model: Evapotranspiration, Runoff, and Net Infiltration

After the completion of the reverse cascade and the placement of excess water into temporary storage terms, evapotranspiration is simulated for each root-zone layer using a dynamic root-zone weighting function and the modified Priestley-Taylor equation (discussed in Section 6.4.4). Evapotranspiration is simulated only for days with air temperature greater than 0 degrees Celsius. The dynamic weighting is based on calculated relative saturations for each root-zone layer and the relative distribution of water (based on saturation) throughout all layers. The purpose of the dynamic weighting is to increase root activity for the wettest layer. Static root density weights are also incorporated into the dynamic weighting function, setting an upper limit on root activity within each layer. For the top soil layer, the bare-soil evaporation term is added to the transpiration term. Using the calculated weighting terms, evapotranspiration is simulated by applying a form of the modified Priestley-Taylor equation developed by Flint and Childs (1991, coefficients in DTN: GS000300001221.009) to each layer of the root zone:

$$Et^k = \alpha' * PET^k \qquad \text{(Eq. 12)}$$
$$\alpha' = \sum_i \{wgt_i * [a^k (1-\exp(b^k * relsat_i^k))]\}$$

where Et^k is total root-zone evapotranspiration for grid cell k; PET^k is the adjusted clear-sky simulated equilibrium[17] potential evapotranspiration rate for grid cell k; $relsat_i^k$ is the relative saturation calculated for layer i within grid cell k; a^k and b^k are the Priestley-Taylor model coefficients for grid cell k supplied as soil- and rock-type input parameters in the model control file (in this analysis, the coefficients were identical for all soil and rock types but were varied between different climate scenarios and between soils and rocks). After water contents for each layer are reduced according to the calculated evapotranspiration rates, the final runoff and net-infiltration terms are calculated, and the new water-content terms for each root-zone layer are up-dated for the following day's water-balance calculation.

6.4.7 Surface-Water Flow-Routing Sub-Model

At the completion of the root-zone water balance loop, the surface-water flow sub-model is called if the runoff accumulation term is greater than zero (at least one grid cell has generated runoff). The sub-model uses an instantaneous flow routing (IFR) method to perform an efficient time-independent simulation of surface-water flow. The purpose of the routing algorithm is to calculate the lateral redistribution of water throughout the watershed domain and to allow for the infiltration of surface water as it is routed. The surface water flow routing algorithm is fully coupled with the algorithm used to calculate infiltration into the root zone. There is no need to predict a flood wave, peak flows, or backwater effects, and thus a finite difference approximation

[17] The equilibrium potential evapotranspiration rate is calculated using $\alpha = 1.0$, and is used to represent the non-advective component of the energy balance.

of the St. Venant equations is not required. The IFR method assumes that the duration of surface-water flow at Yucca Mountain is less than 24 hours, which is generally supported by the available stream flow records and field observations (Savard, 1995; Flint et al., 1996, Figure 23; DTN: GS960908312121.001). For the purpose of calculating daily net infiltration, it is not necessary to perform surface water flow routing at time steps less then the daily water balance, especially when stream flow events are known to be episodic and have duration less then 24 hours (at least for current climate conditions).

The routing is performed using parameters calculated by the routine CHNNET16 V1.0 and included in the geospatial parameter input file. The routing parameters identify downstream cell connections for all cells in the model domain. The flow routing routine determines which of eight surrounding grid cells is the lowest in elevation and calculates the flow directions for each grid cell by first sorting the entire base-grid based on elevation, then using a standard D8 convergent flow routing algorithm in the routine. Multiple cells are allowed to route to a single cell, but any given cell can route to only one downstream grid cell (as opposed to two in cases of flow dispersion). In this way, channels are defined for every watershed. In general it is adequate to drive all flow along one connected node pair. The flow routing algorithm models convergent flow only. Inaccuracies resulting from a lack of flow dispersion are not significant within the area of the potential repository, and are not significant within most areas of the UZ flow and transport model. Inaccuracies resulting from a lack of flow dispersion tend to increase as flow is routed across more gently sloping alluvial fans, particularly in cases where the stream channel becomes braided or is not well defined.

The IFR sub-model repeats the infiltration and percolation simulation performed in the water-balance loop, providing a 2-dimensional coupling of surface-water flow and infiltration. As with precipitation and snowmelt, infiltration of run-on is a function of the storage capacity and hydraulic conductivity of the underlying soils and bedrock. The fraction of the total grid cell area affected by surface-water flow is defined in the model control file and is used to scale the bulk hydraulic conductivity of the grid cell as a means of limiting total infiltration volumes along the width of the active channel. The scaling is performed by using an estimate of the average fraction of the total grid cell area wetting by surface water flow. For example, if the scaling factor is 0.1, only 10 percent of the 30m x 30m area of the grid cell is wetted, on average, by surface water. Thus the effective saturated hydraulic conductivity used to limit the volume of water infiltrating into the grid cell is multiplied by 0.1 to account for the reduction in area. Saturated conditions along the active channel are assumed for estimated storm duration of 2 hours for summer storms and 12 hours for winter storms. Positive pressure heads are assumed to be negligible and are not included in the calculation of infiltration volumes. The increase in water content for each layer in the root zone is stored and included in the following day's root-zone water-balance calculation.

Surface water that is routed off the model grid is stored as an outflow term. For watershed model domains, there is only one outflow point and the outflow term represents stream discharge from the watershed. The outflow term is incorporated into a global mass-balance calculation using:

$$D = \sum R_{off}^{k} - \sum IR_{on}^{k} = \sum P^{k} + \sum SM^{k} - \sum SB^{k} - \sum S^{k} - \sum ET^{k} - \sum I^{k} \qquad \text{(Eq. 13)}$$

where D is the watershed outflow, P is defined for this equation as rainfall, and the water balance terms defined in Equation 1 are summed for all grid cells k in the watershed. Equation 13 is calculated for each day of the simulation as means of verifying the mass balance over the modeling domain.

6.5 MODEL GRID GEOMETRY AND WATERSHED MODELING DOMAINS FOR THE YUCCA MOUNTAIN SITE

All acquired and estimated geospatial parameters required as input for INFIL V2.0 are combined into a single ASCII file defining the base-grid for all extracted watershed model grids (DTN: GS000308311221.004). The geospatial parameter input files defining watershed model domains are extracted as separate files from the developed base-grid using the routine WATSHD20 V1.0 (discussed in Section 6.5.3). All FORTRAN routines (GEOMAP7 V1.0, GEOMOD4 V1.0, SOILMAP6 V1.0, and BLOCKR7 V1.0) and acquired software applications (ARCINFO V6.1.2) used in the development of the base-grid geospatial parameter input file are listed in Table 3-1.

6.5.1 Spatial Discretization and the Base-Grid

The net infiltration modeling procedure begins with building a geospatial input parameter base grid using the selected digital elevation model (DEM) to define the base-grid geometry. The DEM (DTN: GS000308311221.006), selected for defining the grid geometry is the composite DEM used for the original net infiltration model (Flint et al., 1996) that was developed from two standard USGS 7.5 minute 30-meter DEMs (Busted Butte and Topopah Spring NW). The two DEM's (DTN: GS000200001221.003) were combined into a composite DEM (DTN: GS000308311221.006) by using the ARCINFO GRID module. Within this module a command MERGE is used to perform the combining process. Once the two DEM's are combined, it was necessary to convert the projection coordinates from decimal-degrees into UTM coordinates. This was done using the standard ARCINFO PROJECT command. The grid geometry of the composite DEM (DTN: GS000308311221.006) is based on the Universal Transverse Mercator projection (zone 11, NAD27, DTN: GS000200001221.003) and consists of 691 rows in the north-south direction and 367 columns in the east-west direction covering a rectangular area centered over Yucca Mountain and the potential repository site, with the following corner coordinates:

Northwest corner:	544,661 meters easting, 4,087,833 meters northing
Northeast corner:	555,641 meters easting, 4,087,833 meters northing
Southeast corner:	555,641 meters easting, 4,067,133 meters northing
Southwest corner:	544,661 meters easting, 4,067,133 meters northing

The 253,597 elevation values provided by the composite DEM is the primary geospatial parameter used by the net infiltration model. The development of the geospatial parameter input grid and the separate watershed modeling domains requires the application of Geographic Information Systems (GIS) to transfer available digitized map data, which is in a vector-based format, onto the grid-cell or raster-based format of the DEM (a process referred to as rasterization).

Figure 6-9 is a shaded relief representation of the Yucca Mountain DEM and includes the location of the 1999 UZ flow model boundary, the 1999 design potential repository boundary, and the trace of the main Exploratory Studies Facility drift. Also shown are the locations of the neutron borehole sites used to calibrate the 1996 model as well as provide core samples for measuring bedrock hydraulic conductivity (see Attachment IV). Figure 6-9 illustrates the level of detail provided by the DEM in terms of representing discrete topographic features by using elevation, which is the primary geospatial-input parameter for the net-infiltration model. The DEM has an average elevation of 1,237 meters, a minimum elevation of 918 meters along the southern perimeter, and a maximum elevation of 1,969 meters along the northern perimeter.

Figure 6-9. Yucca Mountain DEM used to define geospatial-input parameters and watershed modeling domains. (Attachment II)

DEM elevations in the base grid are used for calculating and estimating geospatial-input parameters and are also used directly as an input in the developed geospatial-parameter input file. Section 6.3.2 discusses the application of elevation directly as an input parameter for INFIL V2.0 calculations, which includes estimating the spatial distribution of precipitation and air temperature. Sections 6.5.2 and 6.5.3 discuss the application of DEM elevations for calculating flow-routing parameters and developing watershed model domains using the routines SORTGRD1 V1.0, and CHNNET16 V1.0. Section 6.4.4 describes the application of DEM elevations for calculating topographic parameters, which include slope, aspect, and blocking ridge angles, using ARCINFO V6.1.2 and the routine BLOCKR7 V1.0.

6.5.2 Development of the Surface Drainage Network

To generate watershed-modeling domains, the surface-water drainage network was defined using the base grid supplied as output from SOILMAP6 V1.0 and GEOMOD4 V1.0. Flow directions were calculated for each grid cell using a 2-step process. For the first step, the entire base grid is sorted by elevation using the routine SORTGRD1 V1.0. In the second step, flow-routing directions are calculated based on a standard D8 routing algorithm (flow is routed to one of eight adjacent grid cells having the lowest elevation) using the routine CHNNET16 V1.0.

CHNNET16 V1.0 is a convergent flow routing algorithm; multiple cells are allowed to route to a single cell, but any given cell can route to only one downstream grid cell (as opposed to two in cases of flow dispersion). The CHNNET16 V1.0 algorithm provides a method for routing through surface depressions in the DEM, which were found to be numerous. The surface depressions are in part a characteristic of poorly established drainage networks across alluvial fans and basins in arid and semiarid environments. Surface depressions are also caused by inaccuracy in the DEM in terms of both elevation values and grid resolution. If the DEM grid is too coarse relative to channel dimensions it cannot accurately capture the natural channel, and this problem tends to be most severe on broad alluvial fans and basins as opposed to upland areas where the drainage network is more accurately defined by the rugged terrain. The CHNNET16 V1.0 routing algorithm allows DEM surface depressions of up to 20 layers deep (20 grid cells need to be crossed before surface flow escapes the depression), and this was found to be greater than the largest depression encountered in the Yucca Mountain DEM. In addition to the flow routing parameters, output from CHNNET16 V1.0 includes a flow accumulation term,

which indicates the number of upstream cells for each grid cell in the initial model grid (Figure 6-10).

Figure 6-10. Number of upstream cells indicating the numerical channel network. (Attachment II)

6.5.3 Development of Watershed Model Domains

Division of the net-infiltration model domain into a set of smaller, isolated watershed model domains was needed to decrease simulation run-times for INFIL V2.0 by allowing the simulation to be distributed over multiple computer processors. The isolated watershed domains allow for a more efficient analysis of the impact of watershed characteristics on simulation results. Additionally, the smaller, closed modeling systems enable a more efficient mass balance checking because each model domain is a single watershed with only one outflow location.

To develop a composite watershed-modeling domain consisting of all watersheds either overlying or immediately adjacent to the area of the site-scale UZ flow and transport model, the boundary of the UZ model was overlain on the numerically defined drainage networks obtained from CHNNET16 V1.0. The outflow cell (the discharge point for all upstream grid cells) of each major drainage network affecting the UZ model area was identified using TRANSFORM for a visual analysis of the flow accumulation map (Figure 6-11). A total of 10 separate watershed model grids were extracted using the routine WATSHD20 V1.0, which executes a reverse flow-routing algorithm to identify all model cells upstream from the selected outflow cell. The model grid defining the extracted watershed domain includes the active grid cells upstream from the outflow cell and also an outer perimeter layer of inactive cells that are needed as boundary cells during surface-water flow routing. The perimeter cells are also used in the mass-balance checking calculation performed using Equation 13 to ensure that outflow is consistent with the cumulative mass balance calculated for all grid cells in the watershed model domain.

Whether or not the calculated flow divides accurately represent the natural system depends on the resolution and accuracy of the DEM, and the accuracy of the flow routing algorithm in capturing the true channel network. An assumption was made that the accuracy of the DEM and the accuracy of the D8 flow routing algorithm was adequate for the purpose of this modeling activity. This assumption was based in part on the knowledge that the model results would be interpolated onto the coarser mesh of the UZ flow and transport model. The assumption was also based on the knowledge that a static DEM was being used to represent topography for the next 10,000 years. In other words, an accurate representation of the present-day channel network at Yucca Mountain is considered to be irrelevant given that the active channel network is likely to change significantly over a 10,000-year period, particularly if wetter climates develop.

Figure 6-11. Isolation of the drainage networks overlying the area of the UZ flow and transport model. (Attachment II)

The main watersheds included in the composite watershed model area are Yucca Wash, Drill Hole Wash, Dune Wash, Solitario Canyon #1, and Plug Hill[18] (Figure 6-12). Additional drainages that were included in the composite model to provide a buffer zone along the western edge of the UZ model are Jet Ridge #1, Jet Ridge #2, Jet Ridge #3, Solitario Canyon #2, and Solitario Canyon #4. The watershed model domains were restricted to the western side of the Fortymile Wash channel because the Yucca Mountain DEM captures only a small part of the lower Fortymile Wash drainage, and complete watersheds cannot be defined for most sections of the DEM east of Fortymile Wash. With the exception of Yucca Wash, and Jet Ridge #1, all watersheds are fully defined by the DEM. For Yucca Wash, northern sections of the watershed are missing because the DEM does not extend far enough north (the northern perimeter of the watershed is defined by the DEM boundary). The missing area is small relative to the total watershed area, and the only potential impact occurs in the Yucca Wash channel along the northeastern perimeter of the UZ flow and transport model area. For Jet Ridge #1, the lowermost segment of the eastern perimeter is defined by the DEM boundary. The missing eastern section of Jet Ridge #1 is an insignificant area that does not affect results obtained for the UZ flow and transport model area.

Figure 6-12. Location of 10 watershed model domains included in the composite watershed model area overlying the area of the UZ flow and transport model. (Attachment II)

6.6 GEOSPATIAL INPUT PARAMETERS

The parameters included in the geospatial-parameter input file defining each watershed model domain are: grid cell identifier, UTM easting (meters), UTM northing (meters), latitude (decimal degrees), longitude (decimal degrees), row identifier, column identifier, downstream grid cell identifier, number of upstream cells, elevation (meters), slope (degrees inclination from horizontal), aspect (degrees from north), soil-type identifier, soil depth class identifier, soil depth (meters), rock-type identifier, topographic position identifier, vegetation-type identifier, percent vegetation cover, and 36 blocking-ridge angles.

6.6.1 Topographic Parameters (Slope, Aspect, and Blocking Ridges)

Topographic parameters, such as the flow-routing parameters discussed in Section 6.5.2, are calculated directly from the DEM and included in the geospatial-parameter input file. Additional topographic parameters include slope, aspect, and blocking ridge angles, which are required by the SOLRAD routine in the potential evapotranspiration sub-model. Slope is also a required input parameter for estimating soil depths using the routine SOILMAP6 V1.0. Slope and aspect were calculated for the 1996 version of the net-infiltration model (Flint et al., 1996) using standard GIS applications in ARCINFO V6.1.2.

The 36 blocking ridge angles (degrees of inclination above horizontal) are calculated at each 10-degree horizontal arc (with the azimuth aligned in the UTM northing direction) for each grid cell using the routine BLOCKR7 V1.0. Calculations were performed using the DEM as input and a

[18]The names selected for the extracted watershed modeling domains are not necessarily the established geographic names for these physiographic features. They are used here only as a means of identifying the separate watershed models.

technique for approximating the 10-degree horizontal angles based on northing and easting grid cell distances. The blocking ridge parameters cannot account for topographic influences outside of the DEM, and thus the blocking ridge effect is only partly accounted for along the perimeter of the DEM.

6.6.2 Soil-Depth Classes

A soil-depth-class map consisting of four separate soil-depth classes was developed for the 1996 net-infiltration model (Flint et al., 1996, Figure 13; DTN: GS960508312212.007). The four depth classes represent different ranges in actual soil depths that were estimated using a combination of Quaternary geologic maps, field observations, and soil depth recorded at borehole sites (Flint and Flint, 1995, Table 2). Depth class #1 identifies locations with soil depths ranging from 0 to 0.5 meter and primarily occurs in rugged upland areas. Depth class #2 identifies deeper soils ranging from 0.5 to 3.0 meters occurring at mid to lower side-slope locations in upland areas affected by slumps, slides, and other mass-wasting processes. Depth class #3 identifies locations in the transition zone between upland areas and alluvial fans or basins with intermediate soil depths ranging from 3 to 6 meters. Depth class #4 identifies soils with depths of 6 meters or greater. The soil-depth classes were used to estimate soil depths based on calculated slope and an empirical soil-depth model described in Attachment IV.

6.6.3 Soil Types

A soil-type classification map is defined in Flint et al. (1996; Figure 14, DTN: GS960508312212.007). The soil-type classification is based on a recombination of mapped Quaternary surficial deposits and defines 10 unique soil types based primarily on differences in soil texture (Figure 6-13). Soil texture and porosity data were obtained using field samples and laboratory measurements (DTN: GS950708312211.002) as described in Flint et al. (1996; p. 42). Soil hydrologic properties consisting of hydraulic conductivity, residual water content, and field capacity were both measured and estimated using the soil texture data as described in Flint et al. (1996, p. 41) and Attachment IV. The soil hydrologic properties included directly as model input (using the model control file) for INFIL V2.0 consist of porosity, field capacity, residual water content, and saturated hydraulic conductivity, and are the same as the properties used in the 1996 version of the net-infiltration model (INFIL V1.0) which are listed in Flint et al. (1996, Table 4, p. 42) and Attachment IV.

Figure 6-13. Recombined soil classes used in the 1996 net-infiltration model. (Attachment II)

6.6.4 Bedrock Geology

Bedrock geology was defined for each grid element using three different ARCINFO map coverages and a vector to raster conversion performed by ARCINFO. Figure 6-14 indicates the areal coverage of the three maps: the 1:6,000-scale Bedrock Geologic Map of the central block area by Day et al. (1998, DTN: GS971208314221.003), the Preliminary Geologic Map of Yucca Mountain by Scott and Bonk (1984, DTN: MO0003COV00095.000), and the Geologic Map of the Topopah Spring Northwest Quadrangle by Sawyer et al. (1995, DTN: GS000300001221.010). Within the UZ flow and transport model area, bedrock geology for the

net-infiltration model (which is defined as a unique integer identifier for each rock type in the geospatial-parameter input file) is primarily defined by Day et al. (1998). Bedrock geology for the northern and southern perimeter sections of the UZ flow and transport model area is defined by Scott and Bonk (1984).

Figure 6-14. Overlay of the three geologic maps used to define rock types underlying the root zone and included in the bottom root-zone layer. (Attachment II)

Bedrock geology for the 1996 version of the net-infiltration model was defined by the Scott and Bonk (1984; DTN: MO0003COV00095.000) and the Sawyer et al. (1995, DTN: GS000300001221.010) map coverages (Flint et al., 1996, Figure 10). To incorporate the Day et al. (1998) geology for INFIL V2.0, the rasterized version of the Day et al. (1998) map coverage (DTN: GS971208314221.003) was integrated with the bedrock geology defined by the 1996 version of the geospatial input file (DTN: GS000308311221.004) using the routine GEOMAP7 V1.0. Figure 6-15 indicates that for some locations within the Day et al. (1998) geologic map coverage, bedrock geology for the net-infiltration model is defined by GEOMAP7 V1.0 using the Scott and Bonk (1984) geologic map (DTN: MO0003COV00095.000). The purpose of including the Scott and Bonk (1984) geology (DTN: MO0003COV00095.000) within the Day et al. (1998) map coverage (DTN: GS971208314221.003) is to estimate bedrock geology for some locations mapped by Day et al. (1998) as alluvium or colluvium and having intermediate soil depths less than 6 meters (as defined by the soil depth class map from Flint et al. (1996, Figure 13; DTN: GS960508312212.007). Locations having intermediate soil depths primarily occur in the transition from upland areas to alluvial fans and basins. Assigning a bedrock type of colluvium or alluvium to grid cells having a soil depth less than 6 meters was considered problematic in terms of modeling net infiltration. Conceptually, all grid cells with a soil depth less than 6 meters should be underlain by a consolidated bedrock type to avoid inconsistency in terms of the assigned soil depth and the estimated root-zone depth. The available geologic maps, however, are representations of the surface geology and do not necessarily indicate bedrock geology for locations having one to 6 meters of soil cover. In general, the consolidated bedrock geology defined by Scott and Bonk (1984) extends farther into the intermediate soil-depth areas then the consolidated bedrock geology defined by Day et al. (1998) and thus was substituted by GEOMAP7 V1.0 for the colluvium or alluvium defined by Day et al. (1998) at many locations with intermediate soil depths.

To ensure that a consolidated rock type was defined as the bedrock geology for all grid cells having less than 6 meters of soil, the routine GEOMOD4 V1.0 was applied to the geospatial parameter file created by GEOMAP7 V1.0. GEOMOD4 V1.0 also performs a modification of the depth-class #3 boundary defined in Flint et al. (1996, p. 40) for all cases where the boundary was found to be inconsistent with the updated bedrock geology. The algorithm creates a new buffer zone of intermediate soil depths defined by depth class #3 using the updated alluvium/colluvium – consolidated bedrock boundary. The result is that the modified depth-class parameters defined by GEOMOD4 V1.0 do not allow for grid cells with depth class #4 (thick soils) to be adjacent to grid cells with thin soils (depth classes #1 and #2). All thin soils are separated from the thick soils by at least one grid cell assigned to depth class #3. Once the soil-depth classes are finalized, GEOMOD4 V1.0 identifies all grid cells having less than 6 meters of soil and alluvium or colluvium as bedrock and interpolates the bedrock geology based on the

most prevalent consolidated rock type found within a search neighborhood of one to two grid cell layers.

Bedrock geology is represented in the geospatial-parameter-input file using a unique integer identifier for each rock type (see Attachment IV for details). The identifier is linked to an estimated bulk (field-scale) saturated hydraulic conductivity in the model control file. The bulk saturated hydraulic conductivity represents a combination of the saturated hydraulic conductivity of the matrix (Flint, 1998, DTN: GS000308312231.002) and the saturated hydraulic conductivity of fracture-fill material (DTN: GS950708312211.003) based on the fracture density of the particular rock type. The saturated hydraulic conductivity of the fracture fill material was measured in the laboratory and averaged 43.2 mm/d (DTN: GS950708312211.003) (see Attachment IV). Estimates of saturated hydraulic conductivity were calculated using these values of fracture conductivity for the percentage of area covered by the fracture per square meter of rock, given the fracture density and size of aperture available through which water can flow. This was added to the saturated hydraulic conductivity of the rock matrix and weighted averages of bulk bedrock saturated hydraulic conductivity were calculated on the basis of percentages of matrix and fractures by lithostratigraphic unit. These calculations are also provided in Flint et al. (1996, Table 2), in DTN: GS000308311221.004, and in Attachment IV. Bulk saturated hydraulic conductivity values for the updated Day et al. (1998) geology rock types were defined using lithologic correlations with the Scott and Bonk (1984) geology (DTN: MO0003COV00095.000). In general, the number of unique bedrock units with different bulk hydraulic conductivity values decreased with the incorporation of the Day et al.(1998) geology. Figure 6-15 shows the bulk bedrock hydraulic conductivity for the three combined geologic map coverages. The bulk saturated hydraulic conductivities range from a minimum of less than 10 mm/year for densely welded tuffs with low matrix hydraulic conductivity and relatively small fracture densities to a maximum of more than 100,000 mm/year for alluvium and colluvium.

Figure 6-15. Estimated field-scale saturated hydraulic conductivity of bedrock or soils underlying the root zone. (Attachment II)

6.7 ESTIMATED ROOT-ZONE DEPTH AND VERTICAL LAYERING

6.7.1 Estimated Soil Depth

Soil depth is estimated using a combination of the soil-depth class map and an estimated linear relation between soil depth and slope within each depth class. The empirical soil-depth model is based on an assumed soil depth/slope correlation (DTN: GS000308311221.004), Attachment IV, within the soil depth classes defined for the 1996 version of the net-infiltration model (Flint et al., 1996; DTN: GS960508312212.007). The conceptual soil-depth model for depth class #1 assumes that soils are thinnest at summit and ridge-crest areas as well as steep side slopes. Thicker soils are expected to occur at the relatively gently sloping shoulder areas that define the transition between summit or ridge-crest areas and steep sideslope areas. Thicker soils are also expected to occur for more gently sloping foot-slope locations. The model for soil-depth class 1 is defined by:

$$D = 0.03 * S + 0.1, S \leq 10 \qquad \text{(Eq. 14)}$$
$$D = 0.013 * (10 - S) + 0.4, 10 < S < 40$$

$$D = 0.01, S \geq 40$$

where D = soil depth (in meters), and S = slope (degrees). The model for depth class #2 is defined by:

$$\begin{aligned} D &= 2 - (0.05 * S), \quad S < 32 \\ D &= 0.4, \quad S \geq 32 \end{aligned} \qquad \text{(Eq. 15)}$$

and the model for depth class #3 is defined by:

$$\begin{aligned} D &= 6 - (0.16 * S), \quad S \leq 25 \\ D &= 2.0 \end{aligned} \qquad \text{(Eq. 16)}$$

For depth class #4, soil depth is set to a uniform depth of 6 meters.

Figure 6-16 shows the spatial distribution of estimated soil depth (DTN: GS000308311221.004) with relatively thin soils less than 0.2 meter deep along steep sideslopes, and thicker upland soils 0.3 to 0.4 meter along ridge-top and shoulder areas. All locations having a soil depth of 6 meters (as indicated by the color gray in Figure 6-13) are underlain by alluvium or colluvium rock-types. The six-meter soil depth represents only the depth of the root zone, not the actual soil depth.

Figure 6-16. Estimated soil depth using the 1996 soil-depth class map and calculated land-surface slope. (Attachment II)

6.7.2 Estimated Root-Zone Depth

The estimated soil-depth map is used to estimate the depth of the root zone by using an empirical model based on field observations and neutron moisture meter data analyses:

$$\begin{aligned} RZ^k &= SD^k + [RZc - (SD^k/RZd)], \quad [RZc - (SD^k/RZd)] \geq 0 \\ RZ^k &= SD^k, \quad [RZc - (SD^k/RZd)] \leq 0 \end{aligned} \qquad \text{(Eq. 17)}$$

where RZ is the estimated root-zone depth (in meters) at grid location k; SD is the estimated soil depth at grid location k; and RZc and RZd are coefficients supplied as input in the model control file. The coefficients are used to adjust the depth of the root zone extending into bedrock for locations with thin soils. For example, for the modern climate simulations, RZc and RZd were both set to 2, and thus the extension of the root zone into bedrock was limited to locations with soil depth less than four meters. Using Equation 17, the root zone extends two meters into bedrock for locations having no soil, one meter into bedrock for locations having two meters soil depth, and 1.5 meters into bedrock for locations having one meter soil depth. The empirical model defined by Equation 17 is consistent with the estimated root-zone depth defined in Flint et al. (1996, Table 5) and is derived on the basis of field observations of rooting depth into bedrock, and evaluation of measurements of extraction of water within the estimated root zone in bedrock, using neutron moisture meters.

6.7.3 Estimated Root-Zone Layering and Root-Zone Density

Root-zone layers are defined to represent differences in root-zone density, storage capacity, and hydrologic properties affecting evapotranspiration and percolation within the root zone. The layers are used to model vertical percolation and redistribution of water in the root zone, as described in Sections 6.4.5 and 6.4.6. The top layer is used to model both bare-soil evaporation and shallow transpiration. Three lower root-zone layers, which include two soil layers and the bottom bedrock layer, are used for modeling transpiration only. The thickness of each of the four root-zone layers is variable and is defined by the soil-depth map. The thickness of the bottom bedrock layer, $RZ4^k$, is the extension of the root zone into bedrock, as defined using Equation 17 above. The thickness of each of the three soil root-zone layers is defined using:

$$\begin{aligned} RZ1^k &= SD^k \qquad SD^k \le RZa \\ RZ2^k &= 0 \\ RZ3^k &= 0 \end{aligned} \qquad \text{(Eq. 18)}$$

$$\begin{aligned} RZ1k &= Rza \qquad RZa \le SDk \le RZb \\ RZ2^k &= SD^k - RZa \\ RZ3^k &= 0 \end{aligned}$$

$$\begin{aligned} RZ1^k &= RZa \qquad RZb \ge SD^k \\ RZ2^k &= RZb - RZa \\ RZ3^k &= SD^k - RZb \end{aligned}$$

where RZ1 is the top root-zone layer thickness (in meters) for grid cell k; RZ2 is the second soil layer thickness; and RZ3 is the third soil layer thickness. Model coefficients RZa and RZb define the maximum thickness of the soil layers. For example, for the modern climate scenarios, RZa = 0.3 and RZb = 1.5, and thus the maximum thickness of the top layer is 0.3 meter, the maximum thickness of the second layer is 1.2 meters, and the maximum thickness of the third layer is 4.5 meters. According to this model, root zones in upland locations with thin soils less than 1.5 meters deep consist of one or two soil layers and one bedrock layer, while alluvial fan terraces having 6 meters or greater soil thickness have three soil layers and no bedrock layer.

The multi-layered root-zone model represents variable root-zone properties between layers by using a set of model coefficients specific to each layer. The model coefficients consist of two root-density-weighting factors for each layer (including the bedrock layer) and are defined in the model control file. These root-density-weighting factors were assumed, but are partially based on field observations of root distributions of various plant types at Yucca Mountain. Soil storage capacities are defined for the three soil layers using the soil-type ID assigned to each grid cell in the geospatial-parameter input file, soil porosity, and soil thickness. The bedrock fracture porosity (a coefficient included in the model control file) and the thickness of the bedrock layer define the storage capacity of the bedrock layer. For all simulations performed in this analysis/model activity, a fracture porosity of 0.02 was determined for the modern climate during model calibration based on comparisons of simulated versus measured stream flow. This value is consistent with model results from CRWMS M&O (2000a, Section 2.5.2.3). The total water-storage capacity of the root zone is a function of the estimated root-zone depth, soil depth, soil porosity, and the bedrock fracture porosity. Figure 6-17 illustrates the calculated total water-

storage capacity of the root zone. Minimum storage capacities of approximately 40 mm occur in upland areas with very thin soils and indicate the root-zone water storage capacity of fractured bedrock. Maximum storage capacities of more than 1,000 mm occur at locations with thick alluvium and no bedrock layer included in the root zone.

Figure 6-17. Total water-storage capacity of the modeled root zone, including bedrock and soil layers. (Attachment II)

6.8 MODEL CALIBRATION

The 1996 model was initially calibrated by comparing model-calculated volumetric water contents and infiltration rates with those obtained through analysis of time-series water-content profiles from the network of boreholes described in Section 6.3.4 and in Flint et al. (1996). Evapotranspiration parameters were adjusted during these calibrations which are presented in detail in Section 6.8.3. Because the 1996 model did not account for infiltration from surface-water runoff in channels, it was necessary to increase precipitation input to the model to obtain a good match with the borehole water-content profiles, particularly during wet years.

Because the 1999 infiltration model has the capability to route surface runoff and calculate the resulting infiltration in channels, the calibration approach for the 1999 model differed from that for the 1996 model. Accordingly, the 1999 infiltration model was calibrated through comparison of simulated and measured daily mean discharge at five stream gages in operation at Yucca Mountain during 1994–95 (DTN: GS941208312121.001, GS960908312121.001). To facilitate the trial-and-error calibration process using smaller watershed domains with reduced simulation run-times, calibration watershed models were extracted using the routine WATSHD20 V1.0 (as described in Section 6.5.3) and the locations of the stream-gaging sites. The simulated run-on depth for the grid cells in which the gages were located was converted to a daily mean discharge rate, in cubic feet per second, and compared to the recorded daily mean discharge rate.

Using a manual trial-and-error process, parameters defining the root-zone model were adjusted until a satisfactory fit between simulated and recorded daily mean discharge at all five gaging sites was obtained. The primary parameters adjusted were the thickness of the bedrock layer included in the root-zone for upland areas, the effective storage capacity of the bedrock layer available for evapotranspiration, and the root-zone density weighting parameters for all four root-zone layers. The root-zone weighting parameters mathematically represent the relative density of the roots for the root-zone layers. These are assumed values, and the bounds within which the densities could vary were also assumed. For wetter future climates, the parameters were adjusted to represent an assumed increase in root density and root zone depth with an increase in vegetation cover and a change in vegetation type that was, in turn, assumed to be representative of the predicted future climate conditions provided by USGS (2000b). The bounds assumed for the thickness of the bedrock layer included in the root-zone for upland areas is 0 to 2m, the effective storage capacity of the bedrock layer available for evapotranspiration ranges from 0.05 to 0.5, and the root-zone density weighting parameters for the four root-zone layers range from 0.01 to 0.6. The parameters were manually adjusted within these bounds until measured runoff could be reasonably matched by the simulation results simultaneously for all five calibration watersheds.

It was observed during model calibration that a sufficient bedrock storage term within the root-zone was needed to produce satisfactory model calibration results, given that the effective bedrock hydraulic conductivity and the soil depth parameters were held constant during model calibration. Another parameter that was adjusted during calibrations was effective surface-water flow area. This parameter had little effect on the resultant net infiltration. From field observations it was assumed that an initial area was about 1 to 99 percent of the grid block. If the stream discharge generated using this value did not match field observations then this value was changed during model calibration.

6.8.1 Climate Input Used for Model Calibration

The climate input file used for model calibration, MOD3-PPT.DAT (Attachment III, Yucca Mountain 1980-95 Developed Daily Precipitation Record), consists of daily precipitation estimates and was developed using an EXCEL worksheet (MOD3-PPT.XLS) and daily precipitation records from 1980 through 1995 at Yucca Mountain and from nearby locations (DTN: GS000200001221.002, GS000100001221.001, GS000208312111.001, GS000208312111.003, GS970108312111.001, GS960908312111.004). The developed record of daily precipitation is only an approximate representation of actual conditions over the general location and ground surface elevation of the potential repository area. Daily precipitation estimates for 1988 through 1995 were developed using the mean of the measured daily precipitation at USGS weather stations #1 and #3 located on Yucca Mountain (DTN: GS000208312111.001, GS000208312111.003, GS970108312111.001, GS960908312111.004). For 1980 through 1987, daily precipitation was estimated using a linear interpolation model and available precipitation records from six Nevada Test Site (NTS) monitoring sites (DTN: GS000200001221.002) and two National Weather Service (NWS) monitoring sites located near Yucca Mountain (DTN: GS000100001221.001). The linear interpolation model was developed using a weighted inverse-distance-squared estimation method. The weighting factors were calculated as the ratio of average annual precipitation for each of the eight stations over the mean calculated from the two USGS weather stations for the period July 17, 1987 through September 30, 1994 (this is the period for which the two sets of records overlapped). Table 6-1 provides a listing of all stations and corresponding precipitation records used to develop MOD3-PPT.DAT. Figure 6-18 shows the temporal distribution of daily precipitation amounts for the 1980-95 developed record.

Table 6-1. Stations and precipitation records used to develop the 1980-95 daily climate input files used for model calibration and for modern climate scenarios. (Attachment I)

Figure 6-18. Developed 1980–95 daily precipitation record used as input for model calibration. (Attachment II)

Daily air-temperature estimates used for model calibration were simulated internally in INFIL V2.0 using the sine wave function defined by Equation 2 in Section 6.4.2. The function coefficients are based on air temperature measurements (DTN: GS000208312111.002) and are described in Flint et al. (1996, eq. 20), where T1 = 17.3 degrees Celsius for mean annual temperature and T2 = 11.41 degrees Celsius for the half amplitude of the sine wave function defining the seasonal deviation from mean annual temperature.

6.8.2 Stream Flow Records Used for Model Calibration

The gage locations and records for the five stream gaging sites located on Yucca Mountain (Figure 6-19) (and within the area of the UZ flow and transport model) were obtained from stream gaging stations (DTN: GS941208312121.001, GS960908312121.001). The records consist of the estimated daily mean discharge, in cubic feet per second (ft^3/s or cfs), for each day of the period covered by the record.

Figure 6-19. Location of stream-gaging sites and calibration watersheds defined by the gaging sites. (Attachment II)

6.8.3 Model Calibration Results

The 1996 model was calibrated by comparing measured volumetric water contents using neutron moisture meters (DTN: GS940708312212.011, GS941208312212.017, GS950808312212.001, GS960108312212.001) and simulated water-content data using the 1996 version of the infiltration model (Flint et al., 1996) that did not include stream-routing. At selected neutron boreholes, water-content data were summed for the soil profile and compared to the model simulation for the same time period by using the developed site precipitation record (Attachment III, Yucca Mountain 1980-95 Developed Daily Precipitation Record). Two examples are presented: borehole USW UZ-N50, with soil 2.7 meters deep (Figure 6-20A) and borehole UE-25 UZN #63, with soil 1.7 meters deep (Figure 6-20B). The match of the simulated and measured volumetric water content was improved by varying the α and β values in the Priestley-Taylor equation, which adjusted the evapotranspiration calculations of the simulated water content to better match the measured water content. Simulated water content compared well with measured water content, which indicated that the water-balance technique used in the model to calculate simulated net infiltration could correctly maintain the proper soil moisture. This is important for accurate determination of when the water-storage capacity of the soil was exceeded and ponding at the soil/bedrock interface had occurred, which controls the calculation of net infiltration.

Figure 6-20. Graphs of comparisons of simulated net infiltration using water content in neutron boreholes (A) USW UZ-N50 and (B) UE-25 UZN #63. (Attachment II)

Using the 1996 model calibrated for evapotranspiration, it was then necessary to determine if simulations of net infiltration matched that calculated from the changes in water content in the neutron-borehole data. A direct comparison of measured neutron-borehole and simulated flux is difficult because the flux measured in the borehole occurs days to months following precipitation. However, annual comparisons between measured and simulated flux at the neutron boreholes can be used.

In order to simulate net infiltration for a comparison at neutron-borehole point locations, precipitation was required at those specific locations. This was done using the developed daily precipitation record described in Section 6.8.1 and spatially distributed to the neutron borehole locations (Flint and Flint, 1995) using Equation 3. Measured average annual precipitation is shown as the open squares in Figure 6-21 on a yearly basis, for the years 1985-95 for which neutron-borehole data is available. Some variation in average annual precipitation among

boreholes can be seen for any given year (the crosses in Figure 6-21) due to the differences in borehole elevation, especially for those years with higher average annual precipitation. To improve the model calibration, because the infiltration model neglects runoff in channels by not routing runoff between grid cells, precipitation was increased in grid cells where there were channels to simulate increases in water available for infiltration due to concentration of water in the channels. This is indicated by the open circles in Figure 6-21. A 30-percent enhancement factor was chosen on the basis of iterations simulating infiltration from the simulated precipitation as described in the following paragraph. Average annual precipitation simulated including the enhancement factor for neutron boreholes located in channels, increased the variability among boreholes.

Figure 6-21. Graph of average annual precipitation simulated at each borehole using precipitation record for 1980-95, and simulated with a 30-percent enhancement in the channel grid blocks only, compared to developed precipitation record distributed geostatistically to each borehole. (Attachment II)

These simulated precipitation data were then used to simulate net infiltration at each borehole using the model (Figure 6-22). The average annual precipitation described above and estimates of net infiltration based on neutron-borehole water-content data (DTN: GS960508312212.008) are again represented by the open squares. Models were fit to each data set, and the results indicated that the regression model of net infiltration simulated with the model, using the 30-percent increase in precipitation at boreholes located in channels, provides a reasonable match to the calculated yearly values of flux (DTN: GS960508312212.008). Net infiltration simulated without the 30-percent channel enhancement factor is slightly lower (Figure 6-22). The only support for using a 30-percent enhancement factor is the improved match to the neutron-hole flux data. Because average annual precipitation was distributed to each borehole instead of using measured precipitation data at each borehole, detailed statistical analysis of the match would not be appropriate. General trends are adequate to indicate that the model represents the influence of the site characteristics, such as precipitation, topography, and soil and rock properties, as well as they currently are known.

Figure 6-22. Graph of precipitation relative to infiltration simulated for each borehole with no channel-enhancement factor and with 30-percent channel-enhancement factor, and measured mean annual infiltration for all boreholes. (Attachment II)

The 1999 model was calibrated by using stream discharge data. Table 6.2 lists the measured versus simulated daily mean discharge values at the five gaging sites for the two recorded 1995 storm events of January 25–26 and March 11, 1995. The results were an acceptable overall fit of simulated to measured stream flow during the March 11,1995 event, which was approximately an order of magnitude greater than the January 25–26 event. The model correctly predicts a higher daily mean discharge at the upper Pagany Wash gage relative to the lower Pagany Wash gage. The total simulated daily mean discharge of 33.63 cfs for the five calibration watersheds provides a reasonable comparison with the total measured daily mean discharge of 31.20 cfs for the March 11,1995 stream flow event.

Comparison of model results with the January event indicates greater difficulty in matching the smaller stream flow events. This difficulty is associated with higher variability in predicting the

occurrence and magnitude of a small and barely initiated stream flow event versus a large and well-sustained flow event. The January 25–26 event did not include stream flow at the upper Drill Hole Wash gaging site, and only a barely measurable trace flow at the lower Pagany Wash gaging site. In addition, the January 25–26 event may have been affected by snowfall and subsequent snowmelt occurring at higher elevations within the calibration watersheds, which would help explain the one-day delay in the measured stream flow as compared to the simulated flow. The calibration simulations did not include a snowmelt simulation because the daily air temperature climate input for the 1980–95 calibration period was not completed at the time of model calibration.

The overall occurrence of stream flow at Yucca Mountain is still correctly predicted for the January 25–26 event, along with the minimal flow volumes and the much higher relative variability in flow across the five gaging sites. The two flow events were the only occurrences of stream flow observed for the entire 1994–95 recording period and this was correctly predicted by the model. The relative magnitude of the smaller January 25–26 event compared to the larger March 11 event was fairly well predicted by the model.

Table 6-2. Comparison of measured versus simulated daily mean discharge at stream-gaging sites for stream flow events in 1995. (Attachment I)

The parameter values used in calibrations discussed above varied during the calibration exercises over the bounds indicated. Selection of the final set of parameter values was based on the combination of values that provided the best match to the measured stream flow records. The final parameter values were consistent across the five watersheds and are as follows: maximum thickness of the bedrock layer is 2 meters, the effective storage capacity of the bedrock layer available for ET is 0.02, root-zone density weighting parameters for the upper soil depth zone is 1.0, second depth zone is 0.5, third depth zone is 0.2 and the bedrock zone is 0.01. The effective surface-water flow area parameter is 0.5. This is a non-unique solution because various different combinations of parameter values may provide similar or even identical results. The most important parameters adjusted during model calibration were the root zone weighting factors, the effective storage capacity of bedrock in the root zone (the product of the thickness of the root zone in bedrock x the effective bedrock porosity), and the scaling factor used to determine the effective surface-water flow area. Similar calibration results might have been achieved by adjusting the bulk saturated bedrock hydraulic conductivity, soil depth, field capacity, and soil saturated hydraulic conductivity, but a detailed parameter optimization exercise was not conducted.

6.9 REPRESENTATION OF CLIMATES FOR MODEL APPLICATION

The modern, monsoon, and glacial-transition climate stages are each represented with a drier lower bound, a wetter upper bound, and an intermediate mean climate scenario (DTN: GS000208311221.002). The lower and upper bound scenarios are developed to account for uncertainty and variability in the characteristics of precipitation and air temperature for each estimated future climate stage. The mean climate scenario is developed to represent average conditions within each stage. To develop a total of nine separate climate scenarios (three for each climate stage), separate INFIL V2.0 simulation results are averaged or sampled using the post-processing program MAPADD20 V1.0. The program MAPADD20 V1.0 also combines the

separate simulation results obtained for each of the 10 watershed modeling domains into a single result for the composite watershed model domain. Each individual simulation is defined by a unique combination of daily climate input and root-zone model coefficients (the coefficients are used to represent different vegetation characteristics). Characteristics of precipitation and air temperature for the estimated drier lower and wetter upper bound monsoon and glacial transition climate scenarios are defined in USGS (2000b). To define the mean net-infiltration values for the monsoon and glacial transition scenarios, the lower and upper bound net-infiltration estimates for each climate stage are averaged for each model grid cell. This implies that the distribution of net infiltration between the lower- and upper-bound scenarios for the monsoon and glacial transition climate stages is symmetric (e.g., normal or uniform).

To develop the daily climate input for INFIL V2.0 that is considered representative of the characteristics of the estimated upper bound monsoon, lower bound glacial transition, and upper bound glacial transition future climate scenario, available daily climate records at present-day analog sites were used. Selection of the representative analog sites is defined by USGS (2000b) and is based on a comparison of predicted versus measured Mean Annual Precipitation (MAP), Mean Annual Temperature (MAT), and the seasonal distribution of MAP and MAT. For each climate scenario, at least two analog sites were identified. Individual simulations were performed for each analog site, and the multiple simulations were averaged for all model grid cells to obtain a single net-infiltration estimate for each climate scenario.

6.9.1 Assumptions Concerning Future Climate Scenarios and Their Simulation with the Infiltration Model

Estimates of potential future climate conditions at Yucca Mountain for the next 10,000 years were taken directly from USGS (2000b). The scenarios define the timing, duration, and characteristics of three distinct potential future climate stages based on analysis and interpretations of periodic cycles identified in paleoclimate records. A general assumption is made that patterns in past climate cycles will be repeated in the future. The first climate stage is a continuation of current modern-day climate conditions from present day to approximately 600 years into the future. The second climate stage begins at approximately 600 years from present day and is characterized as a monsoon climate with wetter summers relative to modern climate. The third climate stage begins at approximately 2,000 years from present day and is characterized as a glacial transition climate with cooler air temperatures and on average higher annual precipitation relative to modern climate. The duration of the glacial transition climate is estimated to be 10,000 years, extending 2,000 years beyond the required 10,000-year estimation period.

Results from USGS (2000b) include the identification of a set of appropriate current climate analog sites for representing the estimated future climate stages in terms of MAP, MAT, and seasonal distributions of MAP and MAT. To incorporate uncertainty as variability in precipitation, and to a lesser degree air temperature characteristics, in the three estimated climate stages and corresponding estimates of net infiltration, results from USGS (2000b) define a lower and upper bound climate scenario within each climate stage. To reduce uncertainty in the selection of a single "best" analog site, the lower and upper bound climate scenarios are represented using a set of two or three analog sites identified by USGS (2000b). Net infiltration

is simulated using the climate input developed from the records at each analog site, and the results are averaged to obtain an estimate of net infiltration for a given climate scenario.

Assumptions and uncertainties regarding the estimated monsoon and glacial transition potential future climate scenarios, including the timing and duration of each estimated future climate stage, are documented by USGS (2000b). For model application using the developed daily climate input for each climate scenario, assumptions in defining the root-zone model coefficients are required. In developing the net-infiltration estimates for each climate scenario using a simple averaging of multiple simulation results, it is assumed that the length of the various simulation periods are adequate for characterizing a given climate scenario. To develop an estimate of net infiltration for the mean climate scenario within the monsoon and glacial transition climate stages, a uniform distribution of net-infiltration rates is assumed between the upper and lower bound estimates at each model grid cell. Net-infiltration estimates for the mean modern climate net-infiltration scenario were obtained by averaging simulations performed specifically for the mean modern climate and thus are not necessarily equivalent to the arithmetic mean of the estimates for the upper and lower bound modern climate scenarios.

6.9.2 Development of Results for the Modern Climate Scenarios

Net-infiltration estimates for the mean modern climate scenario (which is also used to define the lower bound glacial transition climate scenario) were calculated using MAPADD20 V1.0, the net-infiltration simulation results for the 1980–95 model calibration period, and results obtained using a 100-year stochastic simulation of daily precipitation modeled with the NTS station 4JA precipitation record (Attachment V, Development of Daily Climate Input using DAILY09 V1.0). A summary of the climate input used for the 1980-95 calibration period and the 100-year 4JA stochastic simulation is provided in Table 6-3. The length of the 1980-95 calibration period is short relative to the length of climate records considered adequate for characterizing climate conditions in the southern Nevada region, and the 4JA record provides a relatively long-term (longer than 30 years) record of precipitation near the potential repository site. The 100-year stochastic simulation provides an even longer-term representation of climatic conditions while incorporating the magnitudes and temporal distribution of the shorter-term measured record. In performing the INFIL V2.0 simulations, the daily precipitation amounts for the 4JA 100-year stochastic simulation are scaled using the ratio of mean annual precipitation between the Yucca Mountain (181 mm) and 4JA (140 mm) sites in order to account for orographic effects.

The stochastic precipitation model used to develop the 100-year simulation for 4JA consists of a pseudo-random number generator that provides a normalized uniform deviate for a two-step process of simulating daily precipitation. The first step uses a third-order two-state (precipitation either occurs or does not occur) Markov chain process to determine the occurrence of daily precipitation, and the second step uses a modified, exponential, cumulative-probability-distribution function to determine the magnitude of daily precipitation. The third-order Markov chain model defines the probability of precipitation for the fourth day of a sequence given the known sequence of precipitation occurrences for the preceding three days. The stochastic simulations are performed using the program PPTSIM V1.0 (STN: 10143-1.0-00), which requires a prime integer seed for the pseudo-random number generator and monthly model parameters for the Markov chain and the cumulative-probability-distribution function. The monthly model parameters are obtained using the program MARKOV V1.0 (STN 10142-1.0-00)

and available records of daily precipitation for the site or station being modeled. For this analysis, the monthly parameters for station 4JA were obtained using the daily precipitation record for 4JA through December 31,1993 (DTN: GS000200001221.002), and are identical to the parameters used in Flint et al. (1996, Table 6).

Mean net-infiltration estimates for the upper bound modern climate scenario were calculated using MAPADD20 V1.0, the net-infiltration simulation results for the 1980–95 model calibration period, and results obtained using a 100-year stochastic simulation of daily precipitation modeled using the NTS station Area 12 Mesa precipitation record (through December 31, 1993) and the programs MARKOV V1.0 and PPTSIM V1.0 . A summary of the Area 12 Mesa 100-year stochastic simulation of daily precipitation is provided in Table 6-3. For this analysis, the monthly parameters for station Area 12 Mesa are identical to the parameters used in Flint et al. (1996, Table 6). The upper bound modern climate scenario is used to represent wetter conditions from enhanced El Niño Southern Oscillation (ENSO) activity or other sources of present-day climate variability.

Net-infiltration estimates for the lower bound modern climate scenario were obtained using MAPADD20 V1.0 and sampling the 1980-95 simulation, the 4JA 100-year stochastic simulation, and the driest (in terms of net infiltration) 10-year period within the 4JA 100-year simulation for the lowest net infiltration rate at each grid cell. The lower bound modern climate scenario is considered to be representative of climate conditions resulting in minimum net infiltration, which may not necessarily be representative of the driest climate conditions in terms of mean annual precipitation.

Table 6-3. Summary of developed daily climate input files used for modern climate scenarios. (Attachment I)

6.9.3 Development of Results for the Monsoon Future Climate Scenarios

The lower bound monsoon climate scenario is defined by USGS (2000b) as being equivalent to the mean modern climate scenario. The upper bound monsoon climate is represented using daily climate records from two analog sites identified by USGS (2000b): Nogales, Arizona and Hobbs, New Mexico. A summary of the daily climate records, which were obtained as National Climatic Data Center/National Oceanic and Atmospheric Administration (NCDC/NOAA) records from the EARTHINFO database (DTN: GS000100001221.001), is provided in Table 6-4. The daily climate records from the two sites were exported from the EARTHINFO database (using the NCDC format option), and the exported files (Nogales.dat and Hobbs.dat) were provided as input to the program DAILY09 V1.0, which reformats the NCDC format into the xyz column format required by INFIL V2.0. In addition to reformatting, DAILY09 V1.0 also identifies gaps in the precipitation and the maximum and minimum air temperature records. Minor gaps (10 days or less for precipitation and 20 days or less for air temperature) are filled using an estimate of zero for precipitation and linear interpolation between the days having records on either side of the gap for air temperature. Years having major gaps in the record are identified and omitted from the reformatted output. Average daily air temperature is estimated as the mean of the recorded maximum and minimum daily air temperatures. Output from DAILY09 V1.0, which includes the average daily air temperature estimate, is provided directly as input to INFIL V2.0.

Table 6-4. Summary of analog climate records used to develop the daily climate input for the upper bound monsoon climate scenario. (Attachment I)

The upper bound monsoon climate net infiltration result is calculated as the arithmetic mean of the separate Nogales (MU1) and Hobbs (MU2) net infiltration simulations using the program MAPADD20 V1.0. The mean monsoon climate net infiltration result is calculated as the arithmetic mean of the lower and upper bound net infiltration results using MAPADD20 V1.0. This method assumes a normal, or symmetrical, distribution in net infiltration results between the lower and upper bound monsoon climate results[19]. The mean values were calculated using a set of two or more simulation results obtained from the daily climate input developed from the analog sites defined in USGS (2000b). The purpose of using multiple analog sites is to reduce the uncertainty involved in the selection of a single analog site as being representative of the predicted future climate conditions. The fact that unsaturated zone processes are non-linear is not relevant to the concept of reducing uncertainty in model results. Each individual simulation is in effect one realization of a set of possible results, based on the uncertainty in climate input as well as geospatial parameters, model coefficients, and material properties.

6.9.4 Development of Results for the Glacial Transition Future Climate Scenarios

The lower bound glacial transition climate is represented using daily climate records from two analog sites identified by USGS (2000b): Beowawe, Nevada and Delta, Utah. A summary of the daily climate records for the two lower bound glacial transition analog sites, which were obtained as NCDC/NOAA records from the EARTHINFO database (DTN: GS000100001221.001), is provided in Table 6-5. Following the methods described in Section 6.9.3., the routine DAILY09 V1.0 is applied to the NCDC format EARTHINFO exported files to develop the daily climate input files for INFIL V2.0 . The lower bound glacial transition net infiltration result is calculated as the arithmetic mean of the separate Beowawe (GL1) and Delta (GL2) net infiltration simulations using the program MAPADD20 V1.0. The upper bound glacial transition climate is represented using daily climate records from three analog sites identified by USGS (2000b): Rosalia, Washington; Spokane Washington; and St. John, Washington. A summary of the daily climate records for the three upper bound glacial transition analog sites, which were obtained as NCDC/NOAA records from the EARTHINFO database, is provided in Table 6-6. The routine DAILY09 V1.0 is applied to the exported EARTHINFO files for the three analog sites, and the upper bound glacial transition net infiltration result is calculated as the arithmetic mean of the separate Rosalia (GU1), Spokane (GU2), and Delta (GU3) net infiltration simulations using the program MAPADD20 V1.0. The upper bound glacial transition net infiltration result is calculated as the arithmetic mean of the separate Rosalia (GU1), Spokane (GU2), and Delta (GU3) net infiltration simulations using the program MAPADD20 V1.0. The mean glacial transition climate net infiltration result is calculated as the arithmetic mean of the lower and upper bound net infiltration results using MAPADD20 V1.0.

Table 6-5. Summary of analog climate records used to develop the daily climate input for the lower bound glacial transition climate scenario. (Attachment I)

[19] The net infiltration results include the calculated average annual rates for all components of the water balance (precipitation, snow fall, evapotranspiration, root-zone water content change, etc.). A symmetric distribution is assumed for all components of the water balance.

Table 6-6. Summary of analog climate records used to develop the daily climate input for the upper bound glacial transition climate scenario. (Attachment I)

In addition to the daily climate input files defined for the future climate scenarios, future climate conditions were also represented using root-zone parameters. Increases in vegetation density and changes in vegetation type were assumed for wetter and colder future climates. For the upper bound monsoon climate, the root-zone weighting parameters were adjusted to approximate a 40 percent vegetation cover (as compared to 20 percent for modern climate) and the maximum thickness of the bedrock root zone layer was increased from two meters to 2.5 meters. For the upper bound glacial transition climate, the root-zone weighting parameters were adjusted to approximate a 60 percent vegetation cover and the maximum thickness of the bedrock root zone layer was increased to three meters. All adjustments to root-zone parameters were based on assumed root-zone and vegetation characteristics for the future climate conditions. Calibration of the root-zone parameters to the future climate vegetation characteristics requires developing the net infiltration model for analog field site appropriate for each climate, and this was beyond the work scope of this analysis and modeling activity.

6.10 DEVELOPMENT OF INPUTS FOR UNCERTAINTY ANALYSIS

The purpose of the uncertainty analysis described in CRWMS M&O (2000b) is to provide an estimate of the uncertainty in infiltration rates over the footprint of the repository and to utilize the associated uncertainty distributions to provide input for calculations carried out in the Total-System-Performance Assessment. The uncertainty measure is provided by a complementary cumulative distribution function resulting from a set of 100 realizations (or vectors); each of which provides a unique representative infiltration rate. This representative rate, the metric in this analysis, is obtained by calculating the spatial average for the corresponding infiltration rate map, averaged over a rectangular region including the loaded footprint of the repository.

Within the scope of this AMR, the developed uncertainty parameters are available in the Technical Data Management System (TDMS) and only the methods used are described here. The application for the parameters for simulating flow and transport in the unsaturated zone at Yucca Mountain is described in CRWMS M&O (2000a). The results developed in this AMR and used for the Infiltration Uncertainty Analysis (CRWMS M&O 2000b) are listed in Table 7-1.

6.10.1 Sub-Watershed Models Developed for Uncertainty Analysis

In order to perform an uncertainty analysis (CRWMS M&O, 2000b) in a timely manner, sub-watersheds were identified that would be representative of the loaded potential repository area within the infiltration model domain. Using the procedure described in Section 6.5.3 of this AMR, a total of 7 sub-watersheds were extracted from the geospatial parameter base grid (using the WATSHD20 V1.0 software routine) for the modern climate uncertainty analysis and 17 sub-watersheds were extracted from the geospatial parameter base grid for the future climate uncertainty analysis. The additional sub-watersheds used for the future climate analysis were generated based on a need to increase the run-time efficiency of the sampling algorithm by using smaller modeling domains with fewer grid cells. The total area contained within the sub-

watersheds used for the modern and future climate uncertainty analysis is approximately 30 percent of the total net infiltration domain documented in this AMR.

A listing of the separate sub-watersheds generated specifically for the net infiltration uncertainty analysis is provided in Table 4-4 of CRWMS M&O (2000b).

6.10.2 Preliminary Input Distributions for Selected Parameters

The uncertainty analysis requires estimates of upper and lower bounds and corresponding distribution types for selected model input parameters considered potentially significant to model sensitivity for INFIL V2.0. The ideal approach would have been to include multiple input realizations distributed spatially across all grid cells. However, such an approach was not practical and thus only parameters which could be uniformly scaled using inputs included in the model control file were considered. A total of 12 parameters were identified for application in the net infiltration uncertainty analysis (CRWMS M&O, 2000b).

The parameters chosen for development of uncertainty distributions for modern climate were effective bedrock porosity (BRPOROS)[20], bedrock root zone thickness (BRZDEPTH), soil depth (SOILDEPM), precipitation (PRECIPM), potential evapotranspiration (POTETMUL), bulk bedrock saturated hydraulic conductivity (BRPERM), soil saturated hydraulic conductivity (SOILPERM), two parameters associated with bare soil evaporation (ETCOEFFA, ETCOEFFB) and effective surface-water flow area (FLAREA). Two additional parameters related to sublimation (SUBPAR1) and melting of snow cover (SNOPAR1) were considered for the estimated future climate simulations.

The upper and lower bounds for the parameters selected were determined using a combination of absolute bounds defined by physical limits of the parameter, e.g. porosity and the bedrock root-zone depth could not be negative, and reasonable limits. Reasonable limits are based on existing bounds within the available data. Distributions of the parameters were estimated as normal, lognormal or uniform. The lognormal distributions were assigned to conductivity parameters, and the uniform distribution was assigned to the snow cover parameters, with the remaining assumed normally distributed.

6.10.3 Preliminary Climate Input for Defining the Mean Glacial Transition Climate Scenario.

A requirement for the intended application of the net infiltration uncertainty analysis (CRWMS M&O, 2000b) is that the output distribution developed from the 100 realizations for a given climate stage can be used to define the uncertainty of the net infiltration model results around the mean climate scenario for that climate stage. As only upper and lower bounding future climate analogs were available from USGS (2000b), and the mean scenario was developed using an arithmetic mean without a distribution, a method to evaluate the uncertainty in the developed mean climate scenario was required. For the future climate uncertainty analysis, Tule Lake, CA, was selected as a mean future climate analog site on the basis of the daily climate record available for that location and the characteristics of precipitation and air temperature observed

[20] The parameter code names identified in brackets correspond to the IDPRAM parameter code names listed in Tables 4-1 and 4-2 in CRWMS M&O (2000b).

for that record. The record characteristics included MAP, MAT, and the seasonal distribution of precipitation and temperature as it compared to the upper and lower bounds defined in USGS (2000b) and also to the developed mean for the future climate estimates in Sections 6.9.3 and 6.9.4. To develop a daily climate input file based on the Tule Lake, CA record, the software routine DAILY09 V1.0 was applied to the NCDC format file exported from the EARTHINFO data base following the procedure described in Section 6.9.3. For the modern climate uncertainty analysis, a set of realizations were obtained separately for the 4JA 100-year stochastic simulation climate input and the 1980-95 model calibration climate input, and the distributions were averaged to provide a measure of uncertainty consistent with the methods used to obtain the mean modern climate net infiltration result. CRWMS M&O (2000b) should be consulted for discussion of the results and interpretations of these uncertainty analyses.

6.11 RESULTS OF NET-INFILTRATION ESTIMATES

Net infiltration modeling results for modern, monsoon and glacial transition climate scenarios can be located in data packages listed in Section 8.5.

6.11.1 Modern Climate

Table 6-7 lists the simulation results for the three model simulations (YM1-4ex, 4JA1-4ex, A121-4ex) used to develop net-infiltration estimates for the modern climate scenarios. Also listed is the simulation result for the 10-year period (1980-1990) within the 4JA1-4ex stochastic simulation that was used to develop the lower bound modern climate scenario. The results include an average net-infiltration rate of 5.1 mm/year over the area of the modeling domain for the 1980-95 calibration period, with a maximum rate of 1,486 mm/year obtained for a stream channel in the northern part of the Yucca Wash watershed. The 100-year 4JA simulation provided an average net-infiltration rate of 2.2 mm/year over the model domain, and a maximum rate of 574.4 mm/year. The wetter A121-4ex 100-year simulation provided an average net-infiltration rate of 14.0 mm/year, with a maximum rate of 4,354 mm/year for a stream channel location in Yucca Wash. The results indicate a good correlation between the maximum infiltrated surface-water run-on rates and the maximum net-infiltration rates, indicating the importance of surface-water flow in causing relatively high but localized net-infiltration rates.

Table 6-7. Summary of INFIL simulation results used to develop spatially distributed net-infiltration estimates for modern climate scenarios. (Attachment I)

Estimation results for the lower bound, mean, and upper bound modern climate scenarios obtained using the simulations presented in Table 6-7 and the post-processing methods discussed in Section 6 are tabulated for the areas of the net-infiltration model (Table 6-8), the UZ flow and transport model (Table 6-9), and the potential repository (Table 6-10). For the net-infiltration model domain, results for the mean modern climate scenario include an average precipitation rate of 188.5 mm/year, an average outflow rate of 0.2 mm/year (corresponding to an average stream discharge rate of 0.03 ft^3/second), and an average net-infiltration rate of 3.6 mm/year. In comparison, net infiltration is estimated to be 1.2 mm/year for the lower bound modern climate and 8.8 mm/year for the upper bound modern climate.

Table 6-8. Estimation results for modern climate scenarios over the 123.7-km^2 area of the infiltration model domain. (Attachment I)

For the area of the UZ flow and transport model, results for the mean modern climate scenario include an average precipitation rate of 190.6 mm/year, an average outflow rate of –0.2 mm/year, and an average net-infiltration rate of 4.6 mm/year (Table 6-9). The negative outflow rate indicates that more surface water flows into the UZ flow and transport model area than flows out (primarily due to inflow from Yucca Wash). For the lower bound modern climate, net infiltration is estimated to be 1.3 mm/year for the UZ flow and transport model area; for the upper bound modern climate, net infiltration is estimated to be 11.1 mm/year.

Table 6-9. Estimation results for modern climate scenarios over the 38.7-km^2 area of the 1999 UZ flow and transport model domain. (Attachment I)

For the area of the potential repository site, results for the mean modern climate scenario include an average precipitation rate of 196.9 mm/year, an average outflow rate of 1.4 mm/year, and an average net-infiltration rate of 4.7 mm/year (Table 6-10). For the lower bound modern climate, net infiltration is estimated to be 0.4 mm/year and outflow is estimated to be –0.3 mm/year. The negative outflow occurs because surface-water inflow from Drill Hole Wash exceeds outflow. For the upper bound modern climate, net infiltration is estimated to be 11.6 mm/year over the area of the potential repository.

Table 6-10. Estimation results for modern climate scenarios over the 4.7-km^2 area of the 1999 design potential repository area. (Attachment I)

The spatial distribution of estimated precipitation for the mean modern climate scenario indicates minimum estimates of 140 to 160 mm/year occurring along the southern and southeastern parts of the modeling domain, with maximum estimates of more than 260 mm/year occurring for the summit areas along the northern perimeter of the modeling domain (Figure 6-23).

Figure 6-23. Estimated precipitation (mm/year) for the mean modern climate scenario (DTN: GS000208311221.001). (Attachment II)

Estimated evapotranspiration rates in general reflect the distribution of precipitation but also reflect local terrain and surface-water flow effects (Figure 6-24). Minimum evapotranspiration rates of 140 to 160 mm/year occur along the southern and southeastern sections of the model domain, and maximum rates of 220 to 240 mm/year occur for higher elevations receiving greater precipitation amounts. Minimum evapotranspiration rates of less than 100 mm/year occur for steep north-facing sideslopes and areas with minimal soil cover, the west-facing slope of Solitario Canyon, and the rugged terrain in the northern part of Yucca Wash. Maximum evapotranspiration rates of 240 mm/year and higher, on the other hand, are indicative of locations subject to a high volume or frequency of infiltrated surface-water run-on, particularly when immediately downslope from areas receiving higher precipitation as well as rugged terrain conducive to runoff generation, such as the northern part of Yucca Wash.

Figure 6-24. Estimated evapotranspiration (mm/year) for the mean modern climate scenario. (Attachment II)

Infiltrated surface-water run-on indicates the contribution of surface-water flow to potential net infiltration and evapotranspiration (Figure 6-25). Maximum infiltrated surface-water run-on rates of more than 100 mm/year occur mostly along the Yucca Wash channel but also at more isolated locations in the upper sections of drainages such as Drill Hole Wash, Solitario Canyon, Pagany Wash, and Abandoned Wash. In general, the higher infiltrated run-on rates occur in the upstream and headwater sections of drainages, possibly indicating a greater contribution from smaller but higher frequency runoff events for the mean modern climate scenario.

Figure 6-25. Estimated surface-water run-on depth (mm/year) for the mean modern climate scenario. (Attachment II)

The spatial distribution of estimated net-infiltration rates for the mean modern climate indicates most net infiltration occurs in upland areas with thin soils (Figure 6-26). The spatial distribution also indicates a strong control of bedrock hydraulic conductivity on spatial distributions and magnitudes (Figure 6-26), in addition to the effects of thin soils and surface-water run-on. Relatively high net-infiltration rates of 100 mm/year and higher occur throughout the steep north, north-east facing slope of the Prow due to a combination of higher precipitation rates, reduced potential evapotranspiration, frequent surface-water run-on due to very thin soils, and high bedrock hydraulic conductivity associated with non-welded tuffs. Areas of relatively high net-infiltration rates also include the upper channel locations of Solitario Canyon, Drill Hole Wash, Pagany Wash, and Abandoned Wash. Variability in net infiltration caused by topographic effects on potential evapotranspiration are illustrated by the higher net-infiltration rates for the north slopes of washes compared to south facing slopes (this is well illustrated by the west-to-east drainages along the east slope of Yucca Mountain and bisected by the ESF main drift). Maximum net-infiltration rates of more than 100 mm/year occur within the UZ flow and transport model domain for isolated areas that include side-slope and channel locations with thin soils and high hydraulic conductivity bedrock. The contribution to the total net-infiltration volume over the area of the UZ flow and transport model is dominated, however, by the lower rates of 1 to 20 mm/year covering wider areas of sideslope and ridgetop locations because of a much greater total area of coverage.

Figure 6-26. Estimated net infiltration (mm/year) for the mean modern climate scenario. (Attachment II)

For the lower bound modern climate scenario, the total area with significant net infiltration is greatly reduced (Figure 6-27). Within the potential repository area, most areas, including the crest, have no net infiltration. Areas with net-infiltration rates greater than 5 mm/year are isolated to north-facing sideslopes and along the west-facing slope of Solitario Canyon. For the upper bound modern climate scenario, net infiltration along the crest of Yucca Mountain is more than 20 mm/year, and the relative contribution of net infiltration along channels to the total net-infiltration volume is greatly increased compared to the mean modern climate estimates (Figure 6-28). The maximum net-infiltration rate of almost 2,700 mm/year occurs for an active channel location in the northern part of Yucca Wash. Within the potential repository area, maximum net-infiltration estimates of between 100 and 500 mm/year occur in Drill Hole Wash and along the west-facing slope of Solitario Canyon.

Figure 6-27. Estimated net infiltration (mm/year) for the lower bound modern climate scenario. (Attachment II)

Figure 6-28. Estimated net infiltration (mm/year) for the upper bound modern climate scenario. (Attachment II)

In general, the maximum net-infiltration estimates for the three climate scenarios are more than two orders of magnitude higher than the spatially averaged net-infiltration rates for the three areas analyzed, indicating a high degree of spatial variability for the estimation results. In all cases, maximum net-infiltration rates occur at locations affected by surface-water run-on, and there is a strong correlation between the maximum infiltrated run-on rates with maximum net-infiltration rates for all areas and for all climate scenarios. However, because the areas with relatively high net-infiltration rates (greater than 100 mm/year) are small, most of the total net-infiltration volume occurs from upland areas with net-infiltration rates less than 20 mm/year.

6.11.2 Monsoon Climate

The lower bound monsoon climate scenario is defined using the mean modern day climate result (the lower bound monsoon climate result is equal to the modern day climate result). The simulation results used to develop the mean modern climate scenario are equivalent to the lower bound monsoon climate scenario. Net-infiltration estimates for the mean modern climate scenario were calculated using the net-infiltration simulation results for the 1980–95 model calibration period and results obtained using a 100-year stochastic simulation of daily precipitation modeled with the NTS station 4JA precipitation record. The simulation results for the two analog upper bound monsoon climate simulations (Nogales, Arizona and Hobbs, New Mexico) used to develop net-infiltration estimates for the mean and upper bound monsoon climate scenarios are provided in Table 6-11. The results indicate an average net-infiltration rate of 15.1 mm/year for the Nogales analog climate record and 12.1 mm/year for the Hobbs analog climate record, with maximum net-infiltration rates of 2,900 mm/year and 2,330 mm/year, respectively. As in the case of the modern climate simulations, the maximum net-infiltration rates occur in the active channel of Yucca Wash.

Table 6-11. Summary of INFIL simulation results used to develop spatially distributed net-infiltration estimates for the upper bound monsoon climate scenarios. (Attachment I)

Estimation results for the lower bound, mean, and upper bound monsoon climate scenarios are tabulated for the areas of the net-infiltration model (Table 6-12), the UZ flow and transport model (Table 6-13), and the potential repository (Table 6-14). The results for the mean monsoon climate scenario, which were calculated as the arithmetic mean of the lower bound and upper bound monsoon climate scenarios, include an average precipitation rate of 300.5 mm/year, an average outflow rate of 5.1 mm/year, and an average net-infiltration rate of 8.6 mm/year over the net-infiltration model domain. Results for the upper bound monsoon climate scenario, which were calculated as the arithmetic mean of net infiltration simulations for two analog sites (Nogales, AZ and Hobbs, NM) include an average precipitation rate of 412.5 mm/year, an average outflow rate of 10.0 mm/year, and an average net-infiltration rate of 13.6 mm/year over the net-infiltration model domain.

Table 6-12. Estimation results for the monsoon climate scenarios over the 123.7-km^2 area of the infiltration model domain. (Attachment I)

For the UZ flow and transport model area, results for the mean monsoon climate scenario include an average precipitation rate of 302.7 mm/year, an average outflow rate of 4.6 mm/year, and an average net-infiltration rate of 12.2 mm/year (Table 6-13). The maximum net-infiltration rate is 629 mm/year. For the lower bound monsoon climate scenario, average net infiltration is 4.6 mm/year for the UZ flow and transport model area (the mean modern climate result). Estimation results for the upper bound monsoon climate scenario include a precipitation rate of 414.8 mm/year, a snowfall rate of 6.8 mm/year, an average outflow rate of 9.5 mm/year, and a net-infiltration rate of 19.8 mm/year. The maximum net-infiltration rate for the upper bound monsoon climate scenario is 1,016.2 mm/year for the UZ flow and transport model area.

Table 6-13. Estimation results for the monsoon climate scenarios over the 38.7-km^2 area of the UZ flow and transport model domain. (Attachment I)

For the area of the potential repository site, results for the mean monsoon climate scenario include an average precipitation rate of 309.3 mm/year, an average outflow rate of 13.2 mm/year, and an average net-infiltration rate of 12.5 mm/year (Table 6-14). For the upper bound modern climate scenario, precipitation is estimated to be 421.6 mm/year, outflow is estimated to be 25.1 mm/year, and net infiltration is estimated to be 20.3 mm/year over the area of the potential repository.

Table 6-14. Estimation results for the monsoon climate scenarios over the 4.7-km^2 area of the 1999 design potential repository area. (Attachment I)

Figure 6-29 shows the spatial distribution of net-infiltration estimates for the mean monsoon climate scenario. Estimated net-infiltration rates along the crest of Yucca Mountain are in the range of 20 to 50 mm/year. Within the potential repository area, maximum net-infiltration rates of between 100 and 500 mm/year occur in the active channel of Drill Hole Wash and for outcrop locations of permeable, nonwelded tuffs in the middle section of the west-facing slope of Solitario Canyon. Relatively high net-infiltration rates of 100 to 500 mm/year also occur at many steep side-slope locations in the northern part of the UZ flow and transport model area. In contrast, net infiltration at upland locations with thin soils underlain by bedrock with low bulk hydraulic conductivity is less than 1 mm/year.

Figure 6-29. Estimated net infiltration (mm/year) for the mean monsoon climate scenario. (Attachment II)

The map of net-infiltration estimates for the upper bound monsoon climate scenario indicates a greater percentage of area affected by the relatively high net-infiltration rates of 100 to 500 mm/year, along with an increase in the moderately high net-infiltration rates along the crest of Yucca Mountain (Figure 6-30). In absolute terms, the increase in net infiltration for locations with bedrock having a high bulk hydraulic conductivity is much greater than the increase for locations with bedrock with a low bulk hydraulic conductivity, which remains less than 1 mm/year. The infiltrated run-on map indicates the importance of surface-water flow on net infiltration for the upper bound monsoon climate (Figure 6-31). Relatively high run-on

infiltration rates of 100 to 500 mm/year occur throughout the active channels of Drill Hole Wash, Pagany Wash, Solitario Canyon, Dune Wash, and Yucca Wash.

Figure 6-30. Estimated net infiltration (mm/year) for the upper bound monsoon climate scenario. (Attachment II)

Figure 6-31. Infiltrated surface-water run-on depth (mm/year) for the upper bound monsoon climate scenario. (Attachment II)

6.11.3 Glacial Transition Climate

Table 6-15 lists the simulation results for the two analog lower bound glacial transition climate simulations (Beowawe, Nevada and Delta, Utah) used to develop net-infiltration estimates for the lower bound and mean glacial transition climate scenarios. The results for the 32-year Beowawe simulation include a mean air temperature of 9.6 degrees Celsius, a precipitation rate of 208.4 mm/year, and a snowfall depth (water equivalent) of 30.7 mm/year. Net-infiltration estimation results for the Beowawe simulation include an average rate of 2.9 mm/year. The results for the 45-year Delta simulation include a mean air temperature of 10.8 degrees Celsius, a precipitation rate of 193.7 mm/year, and a snowfall depth (water equivalent) of 27.6 mm/year. Net-infiltration estimation results for the Delta simulation include an average rate of 1.4 mm/year.

Table 6-15. INFIL simulation results used to develop spatially distributed net-infiltration estimates for the lower bound glacial transition climate scenario. (Attachment I)

Table 6-16 lists the simulation results for the three analog upper bound glacial transition climate simulations (Rosalia, Washington; Spokane, Washington; and St. John, Washington) used to develop net-infiltration estimates for the upper and mean glacial transition climate scenarios. The results for the 44-year Rosalia simulation include a mean air temperature of 9.0 degrees Celsius, a precipitation rate of 454.9 mm/year, and a snowfall depth (water equivalent) of 67.5 mm/year. The results for the 50-year Spokane simulation include a mean air temperature of 9.2 degrees Celsius, a precipitation rate of 406.2 mm/year, and a snowfall depth (water equivalent) of 74.3 mm/year. For the 31-year St. John simulation, results include 9.9 degrees Celsius for mean air temperature, 432.1 mm/year for precipitation, and 44 mm/year for snowfall. Average net-infiltration rates for the three simulations are 29.7 mm/year for Rosalia, 21.2 mm/year for Spokane, and 23.0 mm/year for St. John. Maximum average annual net-infiltration rates are 9,126.2 mm/year for Rosalia, 7,033.7 mm/year for Spokane, and 6,308.1 mm/year for St. John.

Table 6-16. INFIL simulation results used to develop spatially distributed net-infiltration estimates for the upper bound glacial transition climate scenario. (Attachment I)

Estimation results for the lower bound, mean, and upper bound glacial transition climate scenarios obtained using the simulations presented in Tables 6-15 and 6-16 are tabulated for the areas of the net-infiltration model (Table 6-17), the UZ flow and transport model (Table 6-18), and the potential repository (Table 6-19). The results for the mean glacial transition climate scenario, which were calculated as the arithmetic mean of the results for the lower and upper bound glacial transition scenarios, include an average precipitation rate of 316.1 mm/year, an average snowfall depth of 45.5 mm/year, an average infiltrated surface-water run-on depth of

14.6 mm/ year, an average outflow rate of 1.5 mm/year, and an average net-infiltration rate of 13.4 mm/year for the net-infiltration model domain. In comparison, net infiltration is estimated to be 2.2 mm/year for the lower bound glacial transition scenario and 24.6 mm/year for the upper bound glacial transition scenario.

Table 6-17. Estimation results for the glacial transition climate scenarios over the 123.7-km^2 area of the infiltration model domain. (Attachment I)

For the area of the UZ flow and transport model, results for the mean glacial transition climate scenario include an average precipitation rate of 317.8 mm/year, an average annual infiltrated surface-water run-on depth of 15.6 mm/year, an average outflow rate of −0.2 mm/year, and an average net-infiltration rate of 17.8 mm/year (Table 6-18). For the lower bound glacial transition scenario, net infiltration is estimated to be 2.5 mm/year for the UZ flow and transport model area, while for the upper bound glacial transition scenario, net infiltration is estimated to be 33.0 mm/year. For the area of the potential repository site (Table 6-19), results for the mean glacial transition climate scenario include an average precipitation rate of 323.1 mm/year, an average annual infiltrated surface-water run-on depth of 12.0 mm/year, an average outflow rate of 8.0 mm/year, and an average net-infiltration rate of 19.8 mm/year. For the lower bound glacial transition scenario, net infiltration is estimated to be 2.2 mm/year and outflow is estimated to be 0.3 mm/year. For the upper bound glacial transition scenario, net infiltration is estimated to be 37.3 mm/year over the UZ flow and transport model area and outflow is estimated to be 15.6 mm/year.

Table 6-18. Estimation results for the glacial transition climate scenarios over the 38.7-km^2 area of the UZ flow and transport model domain. (Attachment I)

Table 6-19. Estimation results for the glacial transition climate scenarios for the 4.7-km^2 area of the 1999 design potential repository area. (Attachment I)

The spatial distribution of estimated precipitation for the mean glacial transition climate scenario indicates the reduced precipitation-elevation correlation specified in the model (relative to the modern climate correlation), with a minimum precipitation rate of approximately 280 mm/year and a maximum rate of almost 400 mm/year (Figure 6-32). The spatial distribution of snowfall depth indicates a stronger correlation with elevation because of the combined effects of the precipitation-elevation and the air temperature-elevation correlations (Figure 6-33). The minimum water-equivalent snowfall depth is less than 20 mm/year in the southern part of the modeling domain, and the maximum snowfall depth is more than 140 mm/year.

Figure 6-32. Precipitation (mm/year) for the mean glacial transition climate scenario. (Attachment II)

Figure 6-33. Water-equivalent snowfall depth (mm/year) for the mean glacial transition climate scenario. (Attachment II)

The spatial distribution of estimated evapotranspiration for the mean glacial transition scenario indicates, in the context of the model, the importance of precipitation, root-zone water-storage capacity, and infiltrated surface-water run-on in affecting the availability of water for

evapotranspiration (Figure 6-34). Minimum evapotranspiration rates are less than 100 mm/year on steep sideslopes with thin soil cover (Table 6-17), while maximum rates are close to 600 mm/year in active channel locations.

Figure 6-34. Evapotranspiration (mm/year) for the mean glacial transition climate scenario. (Attachment II)

Estimated infiltrated surface-water run-on rates exceed 100 mm/year throughout most of the upper channel locations, including Pagany Wash, Drill Hole Wash, Solitario Canyon, and sections of all washes draining the eastern slopes of Yucca Mountain (Figure 6-35). Within the net-infiltration model area, maximum infiltrated surface-water run-on rates of more than 3,000 mm/year occur along isolated sections of Yucca Wash (Table 6-17). The net-infiltration map for the mean glacial transition climate scenario indicates rates of 20 to 50 mm/year along the crest of Yucca Mountain, with isolated locations exceeding 50 mm/year along the crest (Figure 6-36). Within the potential repository area, a maximum net-infiltration rate exceeding 500 mm/year occurs in the channel of Drill Hole Wash.

Figure 6-35. Estimated infiltrated surface-water run-on (mm/year) for the mean glacial transition climate scenario. (Attachment II)

Figure 6-36. Estimated net infiltration (mm/year) for the mean glacial transition climate scenario. (Attachment II)

In comparison to net-infiltration estimates for the mean glacial transition climate scenario, net-infiltration rates for the lower bound glacial transition climate scenario are greatly reduced due to a more uniform seasonal distribution of precipitation characterized by a lack of severe storms or wetter than normal periods as compared to the upper bound glacial transition climate scenarios. The average intensity and frequency of precipitation events for the lower bound glacial transition climates is not sufficient to overcome evapotranspiration from the root zone. Maximum net-infiltration rates of 100 to 500 mm/year were obtained on the northeastern-facing slope of the Prow, along isolated sections of the west-facing slope of Solitario Canyon, and along isolated sections of upper Yucca Wash (Figure 6-37). Within the potential repository area, net infiltration does not occur in the channel of Drill Hole Wash and net infiltration along the crest of Yucca Mountain is only 1 to 5 mm/year. The map of infiltrated surface-water run-on for the lower bound glacial transition climate scenario indicates significantly less infiltration along channels than the other climate scenarios (Figure 6-38). Within the UZ flow and transport model area, maximum infiltrated surface-water run-on rates of more than 100 mm/year do not occur in channels but instead are limited to lower sideslopes.

Figure 6-37. Estimated net infiltration (mm/year) for the lower bound glacial transition climate scenario. (Attachment II)

Figure 6-38. Estimated infiltrated surface-water run-on depth (mm/year) for the lower bound glacial transition climate scenario. (Attachment II)

The map of estimated net infiltration for the upper bound glacial transition climate scenario indicates relatively high net-infiltration rates of 50 to 100 mm/year throughout the crest area of Yucca Mountain, and relatively high rates of 100 to 500 mm/year for most steep side-slope

locations in the northern part of the UZ flow and transport model domain (Figure 6-39). Maximum rates of more than 1,000 mm/year are common throughout the lower portions of the Yucca Wash channel. Within the potential repository area, maximum rates between 500 and 1,000 mm/year occur for isolated sections of the Drill Hole Wash channel.

The map of estimated infiltrated surface-water run-on indicates a maximum run-on infiltration rate of between 500 and 1,000 mm/year for an isolated section of Drill Hole Wash within the potential repository area (Figure 6-40). In general, the maximum net-infiltration rates occur at locations where the infiltrated run-on rates are high.

Figure 6-39. Estimated net infiltration (mm/year) for the upper bound glacial transition climate scenario. (Attachment II)

Figure 6-40. Estimated infiltrated surface-water run-on depth (mm/year) for the upper bound glacial transition climate scenario (DTN: GS000308311221.005). (Attachment II)

6.12 MODEL VALIDATION AND COMPARISON WITH ALTERNATIVE ESTIMATES OF NET INFILTRATION

Confidence in models representing natural systems with processes, such as net infiltration and recharge in arid environments, that cannot be directly measured can be developed by comparing model results with alternative and independent methods to estimate those processes. In particular, the comparison of the results from the net-infiltration model for the Yucca Mountain site area with various other methods of estimating net infiltration in the Yucca Mountain region provides confidence that the net-infiltration model is appropriate for its intended use in providing the upper boundary condition for the site-scale 3-dimensional UZ flow and transport model.

Net infiltration and recharge have been estimated for the areas within the Death Valley region using methods appropriate for arid environments, such as water-balance techniques (e.g., basinwide estimates of discharge or numerical models accounting for all significant components of the water balance), soil-physics techniques, geochemistry, and transfer equations based on other variables (such as precipitation). The net infiltration model INFIL V2.0 is a water-balance technique that can be compared to techniques using geochemistry and transfer functions.

Transfer functions relating recharge to precipitation have been widely used in the Death Valley region. Maxey and Eakin (1950) developed a method of estimating recharge to ground-water basins in Nevada, providing a baseline for the spatial distribution of recharge. This method uses average annual precipitation to classify areas of a basin into five recharge zones. Each zone uses a different percentage of average annual precipitation becoming recharge: zero percent recharge for less than 203 mm/yr average annual precipitation, 3 percent for 203 to 304 mm/yr, 7 percent for 305 to 380 mm/yr, 15 percent for 381 to 507 mm/yr, and 25 percent for 508 mm/yr or greater.

Net-infiltration and recharge estimates for basins in Nevada also have been obtained using chloride mass balance calculations. This method equates chloride in recharge water and runoff to chloride deposited in source areas by precipitation and dry fallout. Lichty and McKinley (1995) provided an analysis of recharge for two basins in central Nevada using a 6-yr measurement period and two independent modeling approaches: water balance and chloride mass balance.

Their results yielded recharge rates of 10 to 30 mm/yr for a drainage basin with an average annual precipitation of 270 mm, and 300 to 320 mm/yr for a drainage basin with an average annual precipitation of 640 mm. They determined that the chloride mass balance method was more viable for their study.

Net-infiltration estimates obtained for the nine climate scenarios over the net-infiltration model area, the UZ flow and transport model area, and the potential repository area were plotted against the corresponding average annual precipitation rates and compared with recharge and net-infiltration estimates obtained using the independent methods of Maxey and Eakin (1950, pp. 40-41) and Lichty and McKinley (1995, Table 15) (Figure 6-41). The qualitative comparison with the independent methods is based on the estimated average precipitation rate corresponding to a given recharge or net-infiltration estimate. An assumption is made that the spatially averaged net-infiltration estimates are approximately equivalent to recharge at Yucca Mountain for a given climate scenario (transient effects are ignored).

The net infiltration estimates were also compared against estimates of average recharge rates obtained using the chloride mass balance method for saturated zone boreholes at Yucca Mountain (CRWMS M&O, 2000c) (Figure 6-41). The recharge estimates were obtained using measurements of chloride concentrations from saturated-zone boreholes, and are based on an estimated long-term average annual precipitation rate of 170 mm/year (Hevesi et al., 1992), along with an estimated range of chloride concentrations in precipitation at Yucca Mountain of 0.3 to 0.6 mg/L (CRWMS M&O, 2000c). This results in an average recharge estimate ranging from 7 to 14 mm/year for the saturated zone underlying Yucca Mountain (CRWMS M&O, 2000d), and corresponds to an average Holocene precipitation rate of 170 mm/year at Yucca Mountain. The recharge estimates are higher than the spatially averaged mean modern climate net infiltration rate, but are in good general agreement with the upper bound modern climate, the mean monsoon climate, and the mean glacial transition climate net infiltration rates. The apparent discrepancy between the Holocene recharge estimates and the mean modern climate net infiltration estimate may be attributed to the saturated zone geochemistry being indicative of recharge from various different sources, including the higher recharge zones which are likely to exist to the north of Yucca Mountain (Pahute Mesa and Timber Mountain). In addition, the saturated zone geochemistry is representative of a longer-term Holocene climate period, and is likely to be indicative of recharge rates during wetter cycles within the Holocene. In comparison to chloride mass balance recharge estimates obtained for the saturated zone, chloride mass balance estimates from pore-water samples in the unsaturated zone indicate lower recharge rates, with an average rate of approximately 5 mm/year for Yucca Mountain (CRWMS M&O, 2000c). In general, the average unsaturated-zone chloride mass balance recharge estimate is consistent with the spatially averaged mean modern climate net infiltration estimate for Yucca Mountain, whereas the average saturated-zone chloride mass balance recharge estimate is more consistent with the longer-term mean monsoon and mean glacial transition climate net infiltration estimate.

Figure 6-41. Comparison of INFIL V2.0 simulated average net-infiltration rates (DTN: GS000308311221.005) at Yucca Mountain (upper bound, lower bound, and mean for three climates) with an estimate of the average Holocene recharge rate for the saturated zone at Yucca Mountain [CRWMS M&O, 2000c] and with estimates of recharge in the southern Great Basin obtained using alternative methods (Maxey and Eakin, 1950; Lichty and McKinley, 1995; Winograd, 1981). (Attachment II)

The graph of net infiltration and recharge versus precipitation indicates that the net-infiltration estimates for all lower and mean climate scenarios are in general agreement with independent recharge estimates for precipitation rates of less than approximately 350 mm/year. The net-infiltration estimates for the upper bound glacial transition and monsoon climates are low relative to the Maxey-Eakin recharge estimates obtained for precipitation rates of 400-450 mm/year. The higher Maxey-Eakin estimates are 15 percent of average annual precipitation, while the net-infiltration estimates are only 5-10 percent of average annual precipitation. For precipitation rates greater than 500 mm/year, Maxey-Eakin estimates are 25 percent of average annual precipitation. In the Maxey-Eakin method, the higher precipitation rates correspond to higher elevation basins in the central and southern Nevada region (Maxey and Eakin, 1950). Recharge estimates of approximately 300 mm/year obtained by Lichty and McKinley (1995) for a small, relatively high-elevation basin receiving approximately 600 mm/year precipitation (mostly as snow) indicate that recharge (and thus net infiltration) may be as high as 50 percent of precipitation at some locations in the Great Basin.

These methods have also been applied on a larger scale in the Great Basin and can also be compared to the INFIL results for net infiltration. The Maxey-Eakin method was applied to 167 basins in the Great Basin to estimate recharge for locations of MAP in excess of 8 in (203 mm/yr) (Harrill and Prudic, 1998) (Figure 6-42). The chloride mass balance method was used by Dettinger (1989) who applied it to 16 basins in Nevada; the estimates were close to those that they obtained using the Maxey-Eakin method and water-balance calculations. Values of recharge estimated for Dettinger's 16 basins, as well as the two points determined by Lichty and McKinley (1995) that are presented on Figure 6-41 are included on Figure 6-42.

The net infiltration for selected modeling domains (see Figure 6-12) and calibration watersheds (see Figure 6-19) at Yucca Mountain is shown on Figure 6-42. This figure shows recharge, or net infiltration, as a volume calculated per basin area as a function of average annual precipitation volume. The generally good agreement among the various methods for estimating net infiltration indicated by Figures 6-41 and 6-42, including the results from the net-infiltration model, supports the conclusion that the net-infiltration model is appropriate for estimating the spatial distribution of net infiltration within the Yucca Mountain site area.

Figure 6-42. Comparison of various methods to estimate recharge in the Death Valley region and Yucca Mountain with model results from INFIL V2.0 (DTN: GS000308311221.005), as a function of average annual precipitation. (Attachment II)

The empirical data with which the model results are compared in Figures 6-41 and 6-42 consist of a mixture of qualified and unqualified data. Because of the overall mutual consistency of these data and their general accordance with the net infiltration model results, the use of the unqualified data is appropriate for establishing confidence in the model and does not impact the validity of the model for its intended use.

7. CONCLUSIONS

This AMR describes enhancements made to the infiltration model documented in Flint et al. (1996) and documents an analysis using the model to generate spatial and temporal distributions over a model domain encompassing the Yucca Mountain site, Nevada. Net infiltration is the component of infiltrated precipitation, snowmelt, or surface water run-on that has percolated below the zone of evapotranspiration as defined by the depth of the effective root zone, the average depth below the ground surface (at a given location) from which water is removed by evapotranspiration. The estimates of net infiltration are used for defining the upper boundary condition for the site-scale 3-dimensional UZ flow and transport model and the Total System Performance Assessment model. Estimates of net infiltration are provided as raster-based, 2-dimensional grids of spatially distributed, time-averaged rates for three different climate stages estimated as likely conditions for the next 10,000 years beyond the present. Each climate stage is represented using a lower bound, a mean, and an upper bound climate and corresponding net-infiltration scenario for representing uncertainty in the characterization of daily climate conditions for each climate stage, as well as potential climate variability within each climate stage. The set of nine raster grid maps provide spatially detailed representations of the magnitude and distribution of net-infiltration rates that are used to define specified flux upper boundary conditions for the UZ flow and transport models.

All source data, references, models, routines and procedures are described, noted or referenced in this AMR for complete tracking of all analyses. All assumption used to obtain estimates of net infiltration are described. This analysis consists of (1) modifications to the 1996 model code INFIL V1.0 (Flint et al., 1996), (2) an updating of input parameters defining the new model INFIL V2.0 , (3) calibration of the new model using stream flow records, (4) the development of daily climate input representative of potential future climate stages, and (5) application of the model to provide net-infiltration estimates for a lower, mean, and upper bound climate scenario within each potential future climate stage. Developed output data are listed by Data Tracking Number (DTN) in Table 7-1.

Table 7-1. Output Data Sets Generated in the Development and Application of the Net Infiltration Model (Attachment I)

7.1 SUMMARY OF RESULTS

The net infiltration simulation results for the 1980-95 calibration period include an average net-infiltration rate of 5.1 mm/year over the area of the net infiltration model domain, with a maximum rate of 1,486 mm/year obtained for a stream channel location in the northern part of the Yucca Wash watershed. The 4JA current-climate 100-year simulation provided an average net-infiltration rate of 2.2 mm/year over the net infiltration model domain, and a maximum rate of 574.4 mm/year. The wetter Area 12 Mesa 100-year simulation provided an average net-infiltration rate of 14.0 mm/year over the net infiltration model domain, with a maximum rate of 4,354 mm/year for a stream channel location in Yucca Wash. The results indicate a good correlation between the maximum infiltrated surface-water run-on rates and the maximum net-

infiltration rates, indicating the importance of surface-water flow in causing relatively high but localized net-infiltration rates. The three separate net infiltration simulation results were integrated to provide spatially distributed net infiltration estimates for the lower bound, mean, and upper bound modern climate scenarios.

Results for the mean modern climate scenario include an average precipitation rate of 188.5 mm/year, an average outflow rate of 0.2 mm/year (corresponding to an average stream discharge rate of 0.03 ft^3/second), and an average net-infiltration rate of 3.6 mm/year for the area of the net infiltration model domain. In comparison, net infiltration is estimated to be 1.2 mm/year for the lower bound modern climate and 8.8 mm/year for the upper bound modern climate over the area of the net infiltration model domain. The spatial distribution of estimated precipitation for the mean modern climate scenario indicates minimum estimates of 140 to 160 mm/year occurring along the southern and southeastern parts of the modeling domain, with maximum estimates of more than 260 mm/year occurring for the summit areas along the northern perimeter of the modeling domain. The spatial distribution of estimated net-infiltration rates for the mean modern climate indicates most net infiltration occurs in upland areas with thin soils. The spatial distribution also indicates a strong control by bedrock hydraulic conductivity on spatial distributions and magnitudes, in addition to the effects of thin soils and surface-water run-on.

Variability in net infiltration caused by topographic effects on potential evapotranspiration are illustrated by the higher net-infiltration rates for the north-facing slopes of washes compared to south-facing slopes. Maximum net-infiltration rates of more than 100 mm/year occur within the UZ flow and transport model domain for isolated areas that include side-slope and channel locations with thin soils and high hydraulic conductivity bedrock. The contribution to the total net-infiltration volume over the area of the UZ flow and transport model is dominated, however, by the lower rates of one to 20 mm/year covering wider areas of sideslope and ridgetop locations because of a much greater total area of coverage.

In general, the maximum net-infiltration estimates for the three climate scenarios are more than two orders of magnitude higher than the spatially averaged net-infiltration rates for the three areas analyzed, indicating a high degree of spatial variability for the estimation results. In all cases, maximum net-infiltration rates occur at locations affected by surface-water run-on, and there is a strong correlation between the maximum infiltrated run-on rates with maximum net-infiltration rates for all areas and for all climate scenarios. However, because the areas with relatively high net-infiltration rates (greater than 100 mm/year) are small, most of the total net-infiltration volume occurs from upland areas with net-infiltration rates less than 20 mm/year.

The results for the mean monsoon climate scenario include an average precipitation rate of 300.5 mm/year, an average outflow rate of 5.1 mm/year, and an average net-infiltration rate of 8.6 mm/year over the net-infiltration model domain. Estimated net-infiltration rates along the crest of Yucca Mountain are in the range of 20 to 50 mm/year. Within the potential repository area, maximum net-infiltration rates of between 100 and 500 mm/year occur in the active channel of Drill Hole Wash and for outcrop locations of permeable, nonwelded tuffs in the middle section of the west-facing slope of Solitario Canyon. Relatively high net-infiltration rates of 100 to 500 mm/year also occur at many steep side-slope locations in the northern part of the UZ flow and transport model area. In contrast, net infiltration at upland locations with thin soils underlain by bedrock with low bulk hydraulic conductivity is less than 1 mm/year.

The results for the mean glacial transition climate scenario, which were calculated as the arithmetic mean of the results for the lower and upper bound glacial transition scenarios, include an average precipitation rate of 316.1 mm/year, an average snowfall depth of 45.5 mm/year, an average infiltrated surface-water run-on depth of 14.6 mm/ year, an average outflow rate of 1.5 mm/year, and an average net-infiltration rate of 13.4 mm/year for the net-infiltration model domain. In comparison, net infiltration is estimated to be 2.2 mm/year for the lower bound glacial transition scenario and 24.6 mm/year for the upper bound glacial transition scenario. The spatial distribution of estimated precipitation for the mean glacial transition climate scenario indicates the reduced precipitation-elevation correlation specified in the model (relative to the modern climate correlation), with a minimum precipitation rate of approximately 280 mm/year and a maximum rate of almost 400 mm/year.

Net-infiltration estimates for all lower and mean climate scenarios are in general agreement with independent recharge estimates for precipitation rates of less than approximately 350 mm/year. The net-infiltration estimates for the upper bound glacial transition and monsoon climates are low relative to the Maxey-Eakin recharge estimates (Maxey and Eakin, 1950) obtained for precipitation rates of 400- 450 mm/year.

Although the paleoclimates are not identical to the estimated monsoon and glacial transition future climates, results from the geochemistry analysis suggest that net-infiltration rates at Yucca Mountain are likely to be lower than the Maxey-Eakin recharge estimates for the higher elevation modern analogs corresponding to the estimated average annual precipitation rates for the upper bound monsoon and glacial transition future climates. Using the estimated duration of the modern and future climate stages, the weighted average simulated net infiltration rate for the next 10,000 years is 18 mm/year over the potential repository area and 16.4 mm/year over the area of the UZ flow and transport model. These results indicate that the simulated net infiltration rates are consistent with results obtained from chloride geochemistry analysis.

7.2 LIMITATIONS AND UNCERTAINTIES

Analysis of model sensitivity to uncertainty in input parameters and the impact of parameter accuracy on model results was not complete at the time of this analysis. Uncertainty in the precipitation and air-temperature characteristics of the estimated future climate stages were represented using lower and upper bound scenarios within each stage. Although a uniform distribution between the lower and upper bound monsoon and glacial transition climate scenarios was assumed at the time of this analysis for the development of the mean monsoon and glacial transition climate scenarios, the distribution of precipitation and air temperature characteristics between the upper and lower bound climate scenarios is not known. In addition to assumptions used in defining the daily climate input for the nine climate scenarios, an important source of uncertainty in the net-infiltration estimates for all climate scenarios is the assumptions used in defining root-zone model coefficients. Other sources of model uncertainty include input parameters such as bedrock hydraulic conductivity, soil depth, and soil hydrologic properties. A primary limitation of the model is that it cannot be used to extrapolate beyond the 10,000 years that was used for estimates of climate scenarios using analog sites.

A rigorous sensitivity analysis for net infiltration was addressed by CRWMS M&O (2000b) using 100 realizations (vectors) of a selected set of 12 uncertain input parameters for the glacial

transition climate stage considered in TSPA. The analysis resulted in a distribution of spatially averaged infiltration rates for the glacial transition climate stage over a rectangular region closely approximating what is referred to as the loaded repository footprint. A sensitivity analysis was performed using the results of the glacial transition climate to examine the importance of the sampled (uncertain) input parameters used for the uncertainty analysis. A histogram of average annual infiltration for the glacial transition climate scenario is shown in Figure 6-5 of CRWMS M&O (2000b). The four input parameters that were found to have significant effects on the infiltration rate uncertainty are soil depth, precipitation, potential evapotranspiration and bulk bedrock saturated hydraulic conductivity. These results and levels of uncertainty are consistent with the conceptual model of net infiltration presented in this AMR.

The results from the 100 realizations include a mean net infiltration rate of 25.5 mm/year, a median value of 20.6 mm/year, and a standard deviation of 19.2 mm/year (CRWMS M&O, 2000b). These results are consistent with the results presented in Table 6-19 for estimated net infiltration rates over the area of the potential repository. The coefficient of variation for the results obtained from the uncertainty analysis is much higher than the apparent coefficient of variation implied by the results obtained for the upper and lower bound climate scenarios. However, this is not an inconsistency because the net infiltration estimates presented in this AMR are only intended to be representative of uncertainty and variability in terms of climate input and to a lesser degree vegetation characteristics. The upper and lower bound net infiltration estimates are not necessarily representative of additional sources of model uncertainty, such as uncertainty in soil and bedrock properties.

The nearly lognormal output distribution obtained in the uncertainty analysis indicates a potential inconsistency with the uniform distributions assumed in this AMR for developing the results for the mean monsoon and glacial transition climate scenarios. As discussed in Section 6, the assumption of uniform distributions was preliminary because the results from the uncertainty analysis were not available at the time that the net infiltration estimates were required for the TSPA schedule. For the uncertainty analysis, the logarithms of the net infiltration rates were used to calculate appropriate weighting coefficients that will be applied to the net infiltration maps for the three climate scenarios in each climate stage of the RIP simulations for TSPA. The weighting factors were determined to be 0.17, 0.48, and 0.35 for the lower bound, mean, and upper bound climate scenarios in each climate stage (CRWMS M&O, 2000b). This result will cause an upward shift in mean net infiltration rates for the RIP simulations relative to the results presented in this AMR. This is considered only an apparent inconsistency because the nine developed net infiltration estimates were not originally intended to be representative of the additional sources of model uncertainty. A general conclusion that can be made is that the additional sources of model uncertainty, in particular soil and bedrock properties, tend to increase rather than decrease net infiltration estimates.

A more rigorous and physically based model of wind and terrain effects on snow redistribution and the snow pack energy balance was beyond the scope of this analysis.

It can be assumed based on the sources of model uncertainty described above and throughout the AMR document that the results presented in this AMR cannot be interpreted as being exact but instead should be interpreted as a single realization of an output distribution that has not yet been fully quantified. It can also be assumed based on knowledge of the sources of model uncertainty

that the output distribution obtained from multiple stochastic realizations would define a relatively wide output distribution. Thus, potential users of the results presented in this AMR need to be fully aware that the level of uncertainty associated with these results is relatively high and this must be considered in any application of these results.

7.3 RESTRICTIONS FOR SUBSEQUENT USE

There are no known restrictions for subsequent use.

7.4 IMPACT OF "TO BE VERIFIED" DESIGNATIONS

Several key inputs to this AMR have been designated To Be Verified (TBV); however, excluding these data would have prohibited construction of the net-infiltration model and performing the analyses documented in this AMR. Accordingly, data outputs from this AMR also are TBV. Those TBV data on which this AMR is based are being evaluated to determine their quality-assurance status. Data identified to be unqualified through this evaluation will be subject to an independent qualification process in accordance with AP-SIII.2Q, *Qualification of Unqualified Data and the Documentation of Rationale for Accepted Data,* to ensure that all data inputs are fully qualified.

This document may be affected by technical product input information that requires confirmation. Any changes to the document that may occur as a result of completing the confirmation activities will be reflected in subsequent revisions. The status of the input information quality may be confirmed by review of the Document Input Reference System database.

8. INPUTS AND REFERENCES

8.1 DOCUMENTS CITED

Altman, S.J.; Arnold, B.W.; Barnard, R.W.; Barr, G.E.; Ho, C.K.; McKenna, S.A.; and Eaton, R.R. 1996. *Flow Calculations for Yucca Mountain Groundwater Travel Time (GWTT-95).* SAND96-0819. Albuquerque, New Mexico: Sandia National Laboratories. ACC: MOL.19961209.0152.

Buesch, D.C.; Spengler, R.W.; Moyer, T.C.; and Geslin, J.K. 1996. *Proposed Stratigraphic Nomenclature and Macroscopic Identification of Lithostratigraphic Units of the Paintbrush Group Exposed at Yucca Mountain, Nevada.* Open-File Report 94-469. Denver, Colorado: U.S. Geological Survey. ACC: MOL.19970205.0061.

Campbell, G.S. 1977. *An Introduction to Environmental Biophysics.* New York, New York: Springer-Verlag. TIC: 238256.

Campbell, G.S. 1985. *Soil Physics with BASIC Transport Models for Soil-Plant Systems.* Developments in Soil Science 14. Amsterdam, The Netherlands: Elsevier Science B.V. TIC: 214477.

CRWMS M&O 1998. "Unsaturated Zone Hydrology Model." Chapter 2 of *Total System Performance Assessment-Viability Assessment (TSPA-VA) Analyses Technical Basis Document.* B00000000-01717-4301-00002 REV 01. Las Vegas, Nevada: CRWMS M&O. ACC: MOL.19981008.0002.

CRWMS M&O 2000a. *Unsaturated Zone Flow and Transport Model Process Model Report.* TDR-NBS-HS-000002 REV 00. Las Vegas, Nevada: CRWMS M&O. ACC: MOL.20000320.0400.

CRWMS M&O 2000b. *Analysis of Infiltration Uncertainty.* ANL-NBS-HS-000027 REV 00. Las Vegas, Nevada: CRWMS M&O. ACC: MOL.20000525.0377.

CRWMS M&O 2000c. *Analysis of Geochemical Data for the Unsaturated Zone.* ANL-NBS-HS-000017. Las Vegas, Nevada: CRWMS M&O. Submit to RPC URN-0048

CRWMS M&O 2000d. *Geochemical and Isotopic Constraints on Ground-Water Flow Directions, Mixing, and Recharge at Yucca Mountain, Nevada.* ANL-NBS-HS-000021 REV 00. Las Vegas, Nevada: CRWMS M&O. Submit to RPC URN-0060

Day, W.C.; Potter, C.J.; Sweetkind, D.S.; Dickerson, R.P.; and San Juan, C.A. 1998. *Bedrock Geologic Map of the Central Block Area, Yucca Mountain, Nye County, Nevada.* Map I-2601. Washington, D.C.: U.S. Geological Survey. TIC: 237019.

Dettinger, M.D. 1989. "Reconnaissance Estimates of Natural Recharge to Desert Basins in Nevada, U.S.A., by Using Chloride-Balance Calculations." *Journal of Hydrology, 106,* 55-78. Amsterdam, The Netherlands: Elsevier Science. TIC: 236967.

DOE (U.S. Department of Energy) 2000. *Quality Assurance Requirements and Description.* DOE/RW-0333P, Rev. 10. Washington, D.C.: U.S. Department of Energy, Office of Civilian Radioactive Waste Management. ACC: MOL.20000427.0422.

Dyer, J.R. 1999. "Revised Interim Guidance Pending Issuance of New U.S. Nuclear Regulatory Commission (NRC) Regulations (Revision 01, July 22, 1999), for Yucca Mountain, Nevada." Letter from J.R. Dyer (DOE/YMSCO) to D.R. Wilkins (CRWMS M&O), September 3, 1999, OL&RC:SB-1714, with enclosure, "Interim Guidance Pending Issuance of New NRC Regulations for Yucca Mountain (Revision 01)." ACC: MOL.19990910.0079.

Flint, A.L. and Childs, S.W. 1984. "Physical Properties of Rock Fragments and Their Effect on Available Water in Skeletal Soils." Chapter 10 of *Erosion and Productivity of Soils Containing Rock Fragments.* SSSA Special Publication #13. Madison, Wisconsin: Soil Science Society of America. TIC: 247223.

Flint, A.L. and Childs, S.W. 1987. "Calculation of Solar Radiation in Mountainous Terrain." *Agricultural and Forest Meteorology, 40,* (3), 233-249. Amsterdam, The Netherlands: Elsevier Science Publishers B.V. TIC: 225242.

Flint, A.L. and Childs, S.W. 1991. "Use of the Priestley-Taylor Evaporation Equation for Soil Water Limited Conditions in a Small Forest Clearcut." *Agricultural and Forest Meteorology, 56,* (3-4), 247-260. Amsterdam, The Netherlands: Elsevier. TIC: 241865.

Flint, A.L.; Hevesi, J.A.; and Flint, L.E. 1996. *Conceptual and Numerical Model of Infiltration for the Yucca Mountain Area, Nevada.* Milestone 3GUI623M. Denver, Colorado: U.S. Geological Survey. ACC: MOL.19970409.0087.

Flint, L.E. 1998. *Characterization of Hydrogeologic Units Using Matrix Properties, Yucca Mountain, Nevada.* Water-Resources Investigations Report 97-4243. Denver, Colorado: U.S. Geological Survey. ACC: MOL.19980429.0512.

Flint, L.E. and Flint, A.L. 1995. *Shallow Infiltration Processes at Yucca Mountain, Nevada—Neutron Logging Data 1984-93.* Water-Resources Investigations Report 95-4035. Denver, Colorado: U.S. Geological Survey. ACC: MOL.19960924.0577.

Freeze, R.A. and Cherry, J.A. 1979. *Groundwater.* Englewood Cliffs, New Jersey: Prentice-Hall. TIC: 217571.

French, R.H. 1983. "Precipitation in Southern Nevada." *Journal of Hydraulic Engineering, 109,* (7), 1023-1036. New York, New York: American Society of Civil Engineers. TIC: 238300.

Harrill, J.R. and Prudic, D.E. 1998. *Aquifer Systems in the Great Basin Region of Nevada, Utah, and Adjacent States - Summary Report.* USGS-PP-1409-A. Washington, D.C.: U.S. Government Printing Office. TIC: 247432.

Hatton, T. 1998. *Catchment Scale Recharge Modelling.* Part 4 of The Basics of Recharge and Discharge. Zhang, L., ed. Collingwood, Victoria, Australia: CSIRO Publishing. TIC: 247711.

Hevesi, J.A. and Flint, A.L. 1998. "Geostatistical Estimates of Future Recharge for the Death Valley Region." *High-Level Radioactive Waste Management, Proceedings of the Eighth International Conference, Las Vegas, Nevada, May 11-14, 1998.* Pages 173-177. La Grange Park, Illinois: American Nuclear Society. TIC: 237082.

Hevesi, J.A.; Ambos, D.S.; and Flint, A.L. 1994a. "A Preliminary Characterization of the Spatial Variability of Precipitation at Yucca Mountain, Nevada." *High-Level Radioactive Waste Management, Proceedings of the Fifth Annual International Conference, Las Vegas, Nevada, May 22-26, 1994. 4,* 2520-2529. La Grange Park, Illinois: American Nuclear Society. TIC: 210984.

Hevesi, J.A.; Flint, A.L.; and Flint, L.E. 1994b. "Verification of a One-Dimensional Model for Predicting Shallow Infiltration at Yucca Mountain." *High Level Radioactive Waste Management, Proceedings of the Fifth Annual International Conference, Las Vegas, Nevada, May 22-26, 1994. 4,* 2323-2332. La Grange Park, Illinois: American Nuclear Society. TIC: 210984.

Hevesi, J.A.; Flint, A.L.; and Istok, J.D. 1992. "Precipitation Estimation in Mountainous Terrain Using Multivariate Geostatistics. Part II: Isohyetal Maps." *Journal of Applied Meteorology, 31,* (7), 677-688. Boston, Massachusetts: American Meteorological Society. TIC: 225248.

Jury, W.A.; Gardner, W.R.; and Gardner, W.H. 1991. *Soil Physics.* 5th Edition. New York, New York: John Wiley & Sons. TIC: 241000.

Kwicklis, E.M.; Thamir, F.; Healy, R.W.; and Hampson, D. 1998. *Numerical Simulation of Air- and Water-Flow Experiments in a Block of Variably Saturated, Fractured Tuff from Yucca Mountain, Nevada.* Water-Resources Investigations Report 97-4274. Denver, Colorado: U.S. Geological Survey. ACC: MOL.19981215.0103.

Lichty, R.W. and McKinley, P.W. 1995. *Estimates of Ground-Water Recharge Rates for Two Small Basins in Central Nevada.* Water-Resources Investigations Report 94-4104. Denver, Colorado: U.S. Geological Survey. ACC: MOL.19960924.0524.

Liu, H.H.; Doughty, C.; and Bodvarsson, G.S. 1998. "An Active Fracture Model for Unsaturated Flow and Transport in Fractured Rocks." *Water Resources Research, 34,* (10), 2633-2646. Washington, D.C.: American Geophysical Union. TIC: 243012.

Maidment, D.R., ed. 1993. *Handbook of Hydrology.* New York, New York: McGraw-Hill. TIC: 236568.

Maxey, G.B. and Eakin, T.E. 1950. *Ground Water in White River Valley, White Pine, Nye, and Lincoln Counties, Nevada.* Water Resources Bulletin No. 8. Carson City, Nevada: State of Nevada, Office of the State Engineer. TIC: 216819.

McNaughton, K.G. and Spriggs, T.W. 1989. "An Evaluation of the Priestley and Taylor Equation and the Complementary Relationship Using Results from a Mixed-Layer Model of the Convective Boundary Layer." *Estimation of Areal Evapotranspiration, Proceedings of an International Workshop Held During the XIXth General Assembly of the International Union of Geodesy and Geophysics at Vancouver, British Columbia, Canada, 9-22 August, 1987. 177,* 89-104. Wallingford, United Kingdom: International Association of Hydrological Sciences. TIC: 245925.

Nichols, W.D. 1987. *Geohydrology of the Unsaturated Zone at the Burial Site for Low-Level Radioactive Waste Near Beatty, Nye County, Nevada.* Water-Supply Paper 2312. Denver, Colorado: U.S. Geological Survey. ACC: NNA.19920428.0023.

Priestley, C.H.B. and Taylor, R.J. 1972. "On the Assessment of Surface Heat Flux and Evaporation Using Large-Scale Parameters." *Monthly Weather Review, 100,* (2), 81-92. Washington, DC: U.S. Department of Commerce. TIC: 235941.

Savard, C.S. 1995. *Selected Hydrologic Data from Fortymile Wash in the Yucca Mountain Area, Nevada, Water Year 1992.* Open-File Report 94-317. Denver, Colorado: U.S. Geological Survey. ACC: MOL.19941208.0002.

Sawyer, D.A.; Wahl, R.R.; Cole, J.C.; Minor, S.A.; Laczniak, R.J.; Warren, R.G.; Engle, C.M.; and Vega, R.G. 1995. *Preliminary Digital Geological Map Database of the Nevada Test Site Area, Nevada.* Open-File Report 95-0567. Denver, Colorado: U.S. Geological Survey. TIC: 232986.

Scott, R.B. and Bonk, J. 1984. *Preliminary Geologic Map of Yucca Mountain, Nye County, Nevada, with Geologic Sections.* Open-File Report 84-494. Denver, Colorado: U.S. Geological Survey. TIC: 203162.

Thompson, R.S.; Anderson, K.H.; and Bartlein, P.J. 1999. *Quantitative Paleoclimatic Reconstructions from Late Pleistocene Plant Macrofossils of the Yucca Mountain Region.* Open-File Report 99-338. Denver, Colorado: U.S. Geological Survey. TIC: 245688.

USGS (U.S. Geological Survey). 2000a. *Simulation of Net Infiltration for Modern and Potential Future Climates AMR.* TDP-NBS-HS-000016, Rev. 01. Denver, Colorado: U.S. Geological Survey. ACC: MOL.2000516.0011.

USGS (U.S. Geological Survey). 2000b. *Future Climate Analysis.* ANL-NBS-GS-000008 REV 00. Denver, Colorado: U.S. Geological Survey. Submit to RPC URN-0004

Wemheuer, R.F. 1999. "First Issue of FY00 NEPO QAP-2-0 Activity Evaluations." Interoffice correspondence from R.F. Wemheuer (CRWMS M&O) to R.A. Morgan, October 1, 1999, LV.NEPO.RTPS.TAG.10/99-155, with enclosures. ACC: MOL.19991028.0162.

Winograd, I.J. 1981. "Radioactive Waste Disposal in Thick Unsaturated Zones." *Science, 212,* (4502), 1457-1464. Washington, D.C.: American Association for the Advancement of Science. TIC: 217258.

8.2 CODES, STANDARDS, REGULATIONS, AND PROCEDURES CITED

AP-2.13Q, Rev. 0, ICN 3. *Technical Product Development Planning.* Washington, D.C.: U.S. Department of Energy, Office of Civilian Radioactive Waste Management. ACC: MOL.20000504.0305

AP-3.10Q, Rev. 2, ICN 1. *Analysis and Models.* Washington, D.C.: U.S. Department of Energy, Office of Civilian Radioactive Waste Management. ACC: MOL.20000512.0066

AP-3.15Q, Rev. 1, ICN 1. *Managing Technical Product Inputs.* Washington, D.C.: U.S. Department of Energy. Office of Civilian Radioactive Waste Management. ACC: MOL.20000218.0069

AP-SI.1Q, Rev. 2, ICN 4. *Software Management.* Washington, D.C.: U.S. Department of Energy, Office of Civilian Radioactive Waste Management. ACC: MOL.20000223.0508

AP-SIII.2Q, Rev. 0, ICN 2. *Qualification of Unqualified Data and the Documentation of Rationale for Accepted Data.* Washington, D.C.: U.S. Department of Energy, Office of Civilian Radioactive Waste management. ACC: MOL.19991214.0625

AP-SV.1Q, Rev. 0, ICN 1. *Control of Electronic Management of Data.* Washington, D.C.: U.S. Department of Energy, Office of Civilian Radioactive Waste Management. ACC: MOL.20000512.0068

QAP-2-0, Rev. 5, ICN 1. *Conduct of Activities.* Las Vegas, Nevada: CRWMS M&O. ACC: MOL.19991109.0221

8.3 SOFTWARE USED

USGS (U.S. Geological Survey) 2000. *Software Code: ARCINFO V6.1.2.* STN: 10252-6.1.2-00. URN-0341

USGS (U.S. Geological Survey) 2000. *Software routine: BLOCKR7 V1.0.* ANL-NBS-HS-000032

USGS (U.S. Geological Survey) 2000. *Software routine: CHNNET16 V1.0.* ANL-NBS-HS-000032

USGS (U.S. Geological Survey) 2000. *Software routine: DAILY09 V1.0.* ANL-NBS-HS-000032

USGS (U.S. Geological Survey) 2000. *Software routine: GEOMAP7 V1.0.* ANL-NBS-HS-000032

USGS (U.S. Geological Survey) 2000. *Software routine: GEOMOD4 V1.0.* ANL-NBS-HS-000032

USGS (U.S. Geological Survey) 2000. *Software routine: MAPADD20 V1.0.* ANL-NBS-HS-000032

USGS (U.S. Geological Survey) 2000. *Software routine: MAPSUM01 V1.0.* ANL-NBS-HS-000032

USGS (U.S. Geological Survey) 1996. *Software Code: MARKOV V1.0.* STN: 10142-1.0-00.

USGS (U.S. Geological Survey) 1996. *Software Code: PPTSIM V1.0.* STN: 10143-1.0-00.

USGS (U.S. Geological Survey) 2000. *Software routine: SORTGRD1 V1.0.* ANL-NBS-HS-000032

USGS (U.S. Geological Survey) 2000. *Software routine: WATSHD20 V1.0.* ANL-NBS-HS-000032

USGS (U.S. Geological Survey) 2000. *Software routine: SOILMAP6 V1.0.* ANL-NBS-HS-000032

USGS (U.S. Geological Survey) 2000. *Software routine: VEGCOV01 V1.0.* ANL-NBS-HS-000032

USGS (U.S. Geological Survey) 2000. *Software Code: INFIL V2.0.* STN: 10307-2.0-00. URN-0349

8.4 DATA INPUTS, LISTED BY DATA TRACKING NUMBER (DTN)

GS000100001221.001. EarthInfo, Inc. Western US Meteorologic Station Weather Data - NCDC Summary of Day (West 1) and NCDC Summary of Day (West 2). Submittal date: 01/25/2000.

GS000200001221.002. Precipitation Data for Nevada Test Site, 1957-1994, from Air Resources Laboratory, from National Oceanographic and Atmospheric Administration (NOAA) Precipitation Data. Submittal date: 2/29/2000.

GS000200001221.003. NAD27 Datum of USGS Digital Elevation Model from Topopah Spring West and Busted Butte 7.5 Minute Quadrangles. Submittal date: 02/18/2000.

GS000208312111.001. Precipitation Data for May 3, 1989 through September 30, 1994 from Weather Stations 1 and 3, Yucca Mountain, Nevada. Submittal date: 02/22/2000.

GS000208312111.002. Air Temperature Data for Calendar Year 1992 from Weather Station 1 (Wx-1), Yucca Mountain, Nevada. Submittal date: 02/25/2000.

GS000208312111.003. Precipitation Data for July 17, 1987 through May 2, 1989 from Weather Stations 1 and 3, Yucca Mountain, Nevada. Submittal date: 03/01/2000.

GS000300001221.007. Empirical Equations from Campbell (1985) for Calculating Soil Properties from Texture Data. Submittal date: 03/02/2000.

GS000300001221.009. Evapotranspiration Coefficients. Submittal date: 03/02/2000.

GS000300001221.010. Preliminary Digital Geologic Map Database of the Nevada Test Site Area, Nevada by Sawyer and Wahl, 1995. Submittal date: 03/21/2000.

GS000308312231.001. Revised Physical Properties of Boreholes USW UZ-N17, USW UZ-N53, USW UZ-N55, USW SD-7, USW UZ-14, USW UZ-16. Submittal date: 03/01/2000.

GS000408312231.003. Relative Humidity Calculated Porosity Measurements on Samples From Borehole USW SD-9 Used For Saturated Hydraulic Conductivity. Submittal date: 04/10/2000. Submit to RPC URN-0378

GS000408312231.004. Data for Core Dried in RH Oven and 105C Oven for USW UZ-N31, UZ-N32, UZ-N33, UZ-N34, UZ-N35, UZ-N38, UZ-N58, UZ-N59, UE-25 UZN#63 and USW UZ-N64; Data for Core Dried in 105C Oven Only for USW UZ-N11, UZ-N15, UZ-N16, UZ-N17, UZ-N27, UZ-N36 and UZ-N37. Submittal date: 04/28/2000.

GS920508312231.012. USW UZ-N54 and USW UZ-N55 Core Analysis: Bulk Density, Porosity, Particle Density and In Situ Saturation for Core Dried in 105C Oven. Submittal date: 05/14/1992.

GS930108312231.006. USW UZ-N53 Core Analysis: Bulk Density, Porosity, Particle Density, and In-Situ Saturation for Core Dried in 105C Oven. Submittal date: 10/05/1992.

GS940408312231.004. Core Analysis of Bulk Density, Porosity, Particle Density, and In-Situ Saturation for 3 Neutron Boreholes, USW UZ-N57, UZ-N61, and UZ-N62. Submittal date: 04/01/1994.

GS940508312231.006. Core Analysis of Bulk Density, Porosity, Particle Density and In Situ Saturation for Borehole UE-25 UZ#16. Submittal date: 05/04/1994.

GS940708312212.011. Volumetric Water Content from Neutron Moisture Meter Counts for 99 Boreholes from 5/3/89 or from the Time They Were Drilled until 12/31/93. Submittal date: 07/13/1994.

GS941208312121.001. Surface-Water Discharge Data for the Yucca Mountain Area, Southern Nevada and Southern California, 1994 Water Year. Submittal date: 11/30/1994.

GS941208312212.017. Subsurface Water Content at Yucca Mountain, Nevada – Neutron Logging Data for 1/1/94 thru FY94. Submittal date: 12/02/1994.

GS950308312231.002. Laboratory Measurements of Bulk Density, Porosity, and Water Content for USW SD-12, from 19 Mar 94 to 11 Aug 94, and for Radial Boreholes from 11 Apr 94 to 6 Feb 95. Submittal date: 03/02/1995.

GS950308312231.003. UE-25 UZ#16 Pycnometer Data. Submittal date: 03/06/1995.

GS950408312231.004. Physical Properties and Water Potentials of Core from Borehole USW SD-9. Submittal date: 03/01/1995.

GS950408312231.005. Physical Properties and Water Potentials of Core from Borehole USW UZ-14. Submittal date: 03/09/1995.

GS950608312231.007. Physical Properties and Water Content from Borehole USW NRG-6, 19 Mar 94 to 27 Mar 95. Submittal date: 06/06/1995.

GS950608312231.008. Moisture Retention Data from Boreholes USW UZ-N27 and UE-25 UZ#16. Submittal date: 06/06/1995.

GS950708312211.002. FY94 and FY95 Laboratory Measurements of Physical Properties of Surficial Materials at Yucca Mountain, Nevada. Submittal date: 07/18/1995.

GS950708312211.003. Fracture/Fault Properties for Fast Pathways Model. Submittal date: 07/24/1995.

GS950808312212.001. Volumetric Water Content Calculated from Field Calibration Equations Using Neutron Counts from 97 Boreholes at Yucca Mountain from 1 Oct 94 to 31 May 95. Submittal date: 08/01/1995.

GS951108312231.009. Physical Properties, Water Content, and Water Potential for Borehole USW SD-7. Submittal date: 09/26/1995.

GS951108312231.010. Physical Properties and Water Content for Borehole USW NRG-7/7A. Submittal date: 09/26/1995.

GS951108312231.011. Physical Properties, Water Content, and Water Potential for Borehole USW UZ-7A. Submittal date: 09/26/1995.

GS960108312111.001. Geostatistical Model for Estimating Precipitation and Recharge in the Yucca Mountain Region, Nevada - California. Submittal date: 01/23/1996.

GS960108312211.001. FY95 Laboratory Measurements of Physical Properties of Surficial Material at Yucca Mountain, Part II. Submittal date: 01/04/1996.

GS960108312211.002. Gravimetric and Volumetric Water Content and Rock Fragment Content of 31 Selected Sites at Yucca Mountain, NV: FY95 Laboratory Measurements of Physical Properties of Surficial Material at Yucca Mountain, Part III. Submittal date: 01/08/1996.

GS960108312212.001. Volumetric Water Content Calculated from Field Calibration Equations Using Neutron Counts from 97 Boreholes at Yucca Mountain. Submittal date: 01/31/1996.

GS960508312212.007. Estimated Distribution of Geomorphic Surfaces and Depth to Bedrock for the Southern Half of the Topopah Spring NW 7.5 Minute Quadrangle and the Entire Busted Butte 7.5 Minute Quadrangle. Submittal date: 04/21/1996. Submit to RPC URN-0375

GS960508312212.008. Estimated Annual Shallow Infiltration at 84 Boreholes, Water Years 1990 to 1995. Submittal date: 05/17/1996. Submit to RPC URN-0374

GS960808312231.001. Water Permeability and Relative Humidity Calculated Porosity for Boreholes UE-25 UZ-16 and USW UZ-N27. Submittal date: 08/28/1996.

GS960808312231.003. Moisture Retention Data for Samples from Boreholes USW SD-7, USW SD-9, USW SD-12 and UE-25 UZ#16. Submittal date: 08/30/1996.

GS960808312231.004. Physical Properties, Water Content and Water Potential for Samples from Lower Depths in Boreholes USW SD- 7 and USW SD-12. Submittal date: 08/30/1996.

GS960808312231.005. Water Permeability and Relative Humidity Calculated Porosity for Samples from Boreholes USW SD-7, USW SD- 9, USW SD-12 AND USW UZ-14. Submittal date: 08/30/1996.

GS960908312111.004. Relative Humidity, Temperature, Wind Speed, Wind Direction, Net Solar Radiation and Precipitation Data from Five Weather Stations in the Yucca Mountain Area for 1995 Water Year. Submittal date: 09/12/96.

GS960908312121.001. Surface-Water Discharge Data for the Yucca Mountain Area, Southern Nevada and Southern California, 1995 Water Year. Submittal date: 10/10/1996.

GS960908312211.003. Conceptual and Numerical Model of Infiltration at Yucca Mountain, Nevada. Submittal date: 09/12/1996.

GS960908312211.004. Heat Dissipation Probe Data: Bleach Bone Ridge 3/95 - 11/95. Submittal date: 09/19/1996.

GS970108312111.001. FY96 Site Meteorology Data: Relative Humidity, Temperature, Wind Speed, Wind Direction, Net Solar Radiation and Barometric Pressure from Two Weather Stations in the Yucca Mountain Area, Oct. 1 - Dec. 3, 1995. Submittal date: 01/15/1997.

GS971208314221.003. Revised Bedrock Geologic Map of the Central Block Area, Yucca Mountain, Nevada. Submittal date: 12/30/1997.

GS980708312242.011. Physical Properties and Hydraulic Conductivity Measurements of Lexan-Sealed Samples from USW WT-24. Submittal date: 07/30/1998.

GS980808312242.012. Unsaturated Hydraulic Properties of Lexan-Sealed Samples From USW WT-24, Measured Using a Centrifuge. Submittal date: 08/05/1998.

GS980908312242.038. Physical Properties and Saturated Hydraulic Conductivity Measurements of Lexan-Sealed Samples from USW SD-6. Submittal date: 09/22/1998.

GS980908312242.039. Unsaturated Water Retention Data for Lexan-Sealed Samples from USW SD-6 Measured Using a Centrifuge. Submittal date: 09/22/1998.

GS990408312231.001. Saturated Hydraulic Conductivity of Core from SD-9, 2/27 - 3/27/95. Submittal date: 04/27/1999.

MO0003COV00095.000. Coverage: Scotbons. Submittal date: 03/01/2000. Submit to RPC

SNSAND96081900.000. Flow Calculations for Yucca Mountain Groundwater Travel Time (GWTT-95). Submittal date: 12/17/1996.

8.5 OUTPUT DATA, LISTED BY DATA TRACKING NUMBER (DTN)

GS000308311221.005 Net Infiltration Modeling Results for 3 Climate Scenarios FY99. Submittal date: 03/01/2000.

GS000308311221.011. Template Files for Uncertainty Analyses. Submitttal date: 03/13/2000.

GS000308311221.010. Preliminary Developed Daily Climate Data From Tule Lake, California Used for Infiltration Uncertainty Analysis. Submittal date: 03/07/2000.

GS000308311221.008. Preliminary Estimates of Input Parameter Distributions Used for Infiltration Uncertainty Analysis. Submittal date: 03/13/2000.

GS000399991221.002 Rainfall Runoff/Run-on 1999 Simulations. Submittal date: 03/10/2000.

GS000208311221.001. Yucca Mountain 1980-1995 Developed Daily Precipitation Record. Submittal date: 02/28/2000.

GS000208311221.002. Preliminary Developed Daily Climate Data for Potential Future Monsoon and Glacial Transition Climates Using Records from Selected Analog Sites. Submittal date: 02/28/2000.

GS000308311221.004. Preliminary Geospatial Input Data for Infil V2.0 FY99. Submittal date: 03/01/2000.

GS000308311221.006. Merged USGS Digital Elevation Model from Topopah Spring West and Busted Butte 7.5' DEMS. Submittal date: 03/02/2000.

GS000308312231.002. Developed Matrix Hydrologic Properties Information. Submittal date: 03/01/2000.

9. ATTACHMENTS

ATTACHMENT I **Tables**

ATTACHMENT II: **Figures**

ATTACHMENT III: **Yucca Mountain 1980-95 Developed Daily Precipitation Record**

ATTACHMENT IV: **Geospatial Input Data for INFIL V2.0 FY99**

ATTACHMENT V: **Development of Daily Climate Input using DAILY09 V1.0**

ATTACHMENT VI: **Calculation of Blocking Ridges using BLOCKR7 V1.0**

ATTACHMENT VII: **Inclusion of Updated Bedrock Geology using GEOMAP7 V1.0**

ATTACHMENT VIII: **Adjustment of the Soil Depth Class Map using GEOMOD4 V1.0**

ATTACHMENT IX: **Estimation of Soil Depth using SOILMAP6 V1.0**

ATTACHMENT X: **Development of Flow Routing Parameters using SORTGRD1 V1.0**

ATTACHMENT XI: **Calculation of Flow Routing Parameters using CHNNET16 V1.0**

ATTACHMENT XII: **Development of Geospatial Input Parameters using VEGCOV01 V1.0**

ATTACHMENT XIII: **Extraction of Watershed Modeling Domains using WATSHED20 V1.0**

ATTACHMENT XIV: **Post-processing of model results using MAPADD20 V1.0**

ATTACHMENT XV: **Post-processing of model results using MAPSUM01 V1.0**

ATTACHMENT I

TABLES

TOTAL PAGES: 26

Table 3-1 Computer Software Used to Develop Estimates of Net Infiltration.

Item No.	Software Name	Version	Software Tracking Number	Computer Type Used	Description
1	MARKOV	1.0	10142-1.0-00	Pentium Pro PC, Windows NT 4.0	Calculates monthly Markov chain probabilities for occurrence of daily precipitation and fits monthly exponential distribution coefficients to define the cumulative probability distribution function for the magnitude of daily precipitation. Uses daily precipitation records for input.
2	PPTSIM	1.0	10143-1.0-00	Pentium Pro PC, Windows NT 4.0	Performs a stochastic simulation of daily precipitation using input probabilities and coefficients provided as output from MARKOV and a user defined prime seed.
3	BLOCKR7	1.0	Attachment VI	Pentium Pro PC, Windows NT 4.0 FORTRAN77	Combines ARCINFO raster-grid export files (30mlat.asc, 30mlong.asc, 30mslope.asc, 30maspct.asc, 30melev.asc, 30msoil.asc, 30mdpth.asc, 30mrock.asc, and 30mtopo.asc) into a single column-formatted ASCII text file. Calculates 36 blocking ridge parameters for all grid locations using the raster-grid elevation data and adds the 36 columns to the output file (30msite.inp).
4	GEOMAP7	1.0	Attachment VII	Pentium Pro PC, Windows NT 4.0 FORTRAN77	Updates the 1996 INFIL V1.0 geospatial input file (30msite.inp) to include the Day and others (1998) central block geology map.
5	VEGCOV01	1.0	Attachment XII	Pentium Pro PC, Windows NT 4.0 FORTRAN77	Performs a modification to bedrock saturated hydraulic conductivity provided as input to account for a north-south gradation in bedrock hydraulic conductivity.
6	GEOMOD4	1.0	Attachment VIII	Pentium Pro PC, Windows NT 4.0 FORTRAN77	Defines an intermediate soil depth buffer zone between thin upland soils and thick alluvium using the mapped alluvium boundary and estimates the bedrock geology type underlying the buffer zone. Uses output from GEOMAP7 as input.
7	SOILMAP6	1.0	Attachment IX	Pentium Pro PC, Windows NT 4.0 FORTRAN77	Estimates soil depths based on mapped soil depth classes and calculated ground surface slope included as input parameters in the geospatial parameter input file created as output from GEOMOD4.

Item No.	Software Name	Version	Software Tracking Number	Computer Type Used	Description
8	SORTGRD1	1.0	Attachment X	Pentium Pro PC, Windows NT 4.0 FORTRAN77	Performs a bubble sort on the geospatial parameter input file based on elevation (sorts elevation from highest to lowest). The sorted file increases the efficiency of channel routing. Input is provided by SOILMAP6.
9	CHNNET16	1.0	Attachment XI	Pentium Pro PC, Windows NT 4.0 FORTRAN77	Establishes the numerical channel network using elevations from the output file generated by SORTGRD1. Outputs a new file containing flow routing parameters for all grid cells. The new output file is used as input to WATSHD20.
10	WATSHD20	1.0	Attachment XIII	Pentium Pro PC, Windows NT 4.0 FORTRAN77	Extracts the watershed modeling domains based on a user defined watershed outflow point and input supplied form SORTGRD1 and CHNNET16. The output file is supplied directly as input to INFIL V2.0.
11	INFIL	2.0	10307-2.0-00	Pentium Pro PC, Windows NT 4.0 FORTRAN77	Simulates components of the water balance for watershed input domains supplied by WATSHD20, daily climate input, and model parameters included in the model control file. Outputs average annual rates for all components of the water balance, including net infiltration rates, for all grid cells located within the watershed-modeling domain.
12	DAILY09	1.0	Attachment V	Pentium Pro PC, Windows NT 4.0 FORTRAN77	Reformats daily climate records exported from the EarthInfo database. Checks for data gaps and interpolates missing data if gaps are small or discards annual records if gaps are large.
13	MAPADD20	1.0	Attachment XIV	Pentium Pro PC, Windows NT 4.0 FORTRAN77	Compiles results obtained for individual watersheds into a single composite watershed-modeling domain, and calculates statistics for the composite watershed-modeling domain.

Item No.	Software Name	Version	Software Tracking Number	Computer Type Used	Description
14	MAPSUM01	1.0	Attachment XV	Pentium Pro PC, Windows NT 4.0 FORTRAN77	Calculates statistics for sub-areas within the composite watershed model domain. Uses results from MAPADD20 and a blanked SURFER grid as input. The blanked SURFER grid is created using the output from MAPADD20 and the boundary line of the sub-area.
15	ARCINFO	6.1.2	10252-6.1.2-00	Pentium Pro PC, windows NT 4.0	Performs GIS applications (vector data to raster data conversions, coordinate transformations, and slope and aspect calculations).

Table 4-1. Data Sets Used for Model Development, Calibration, and Application.

Description	Data Tracking Number
EarthInfo, Inc. Western US Meteorologic Station Weather Data - NCDC Summary of Day (West 1) and NCDC Summary of Day (West 2). Submittal date: 01/25/2000.	GS000100001221.001.
Precipitation Data for Nevada Test Site, 1957-1994, from Air Resources Laboratory, from National Oceanographic and Atmospheric Administration (NOAA) Precipitation Data. Submittal date: 2/29/2000.	GS000200001221.002
NAD27 Datum of USGS Digital Elevation Model from Topopah Spring West and Busted Butte 7.5 Minute Quadrangles. Submittal date: 02/18/2000.	GS000200001221.003
Precipitation Data for May 3, 1989 through September 30, 1994 from Weather Stations 1 and 3, Yucca Mountain, Nevada. Submittal date: 02/22/2000.	GS000208312111.001
Air Temperature Data for Calendar Year 1992 from Weather Station 1 (Wx-1), Yucca Mountain, Nevada. Submittal date: 02/25/2000.	GS000208312111.002
Precipitation Data for July 17; 1987 through May 2, 1989 from Weather Stations 1 and 3, Yucca Mountain, Nevada. Submittal date: 03/01/2000.	GS000208312111.003
Empirical Equations from Campbell (1985) for Calculating Soil Properties from Texture Data. Submittal date: 03/02/2000.	GS000300001221.007
Evapotranspiration Coefficients. Submittal date: 03/02/2000.	GS000300001221.009
Preliminary Digital Geologic Map Database of the Nevada Test Site Area, Nevada by Sawyer and Wahl, 1995. Submittal date: 03/21/2000.	GS000300001221.010
Revised Physical Properties of Boreholes USW UZ-N17, USW UZ-N53, USW UZ-N55, USW SD-7, USW UZ-14, USW UZ-16. Submittal date: 03/01/2000.	GS000308312231.001
Relative Humidity Calculated Porosity Measurements on Samples From Borehole USW SD-9 Used For Saturated Hydraulic Conductivity. Submittal date: 04/10/2000.	GS000408312231.003
USW UZ-N54 and USW UZ-N55 Core Analysis: Bulk Density, Porosity, Particle Density and In Situ Saturation for Core Dried in 105C Oven. Submittal date: 05/14/1992.	GS920508312231.012
USW UZ-N53 Core Analysis: Bulk Density, Porosity, Particle Density, and In-Situ Saturation for Core Dried in 105C Oven. Submittal date: 10/05/1992.	GS930108312231.006
Data For Core Dried in RH Oven and 105C Oven for USW UZ-N31, UZ-N32, UZ-N33, UZ-N34, UZ-N35, UZ-N38, UZ-N58, UZ-N59, UE-25 UZN#63, and USW UZ-N64; Data for Core Dried in 105C Oven only for USW UZ-N11, UZ-N15, UZ-N16, UZ-N17, UZ-N27, UZ-N36, and UZ-N37. Submittal date: 04/28/2000.	GS000408312231.004
Core Analysis for bulk density, porosity, particle density and in situ saturation for 17 Neutron Boreholes: Data for Core Dried in RH Oven and 105C Oven for USW UZ-N31, UZ-N32, UZ-N33, UZ-N34, UZ-N35, UZ-N38, UZ-N58, UZ-N59, UE-25 UZN#63 and USW UZ-N64; Data for Core Dried in 105C Oven Only for USW UZ-N11, UZ-N15, UZ-N16, UZ-N17, UZ-N27, UZ-N36 and UZ-N37.	GS000408312231.004
Core Analysis of Bulk Density, Porosity, Particle Density, and In-Situ Saturation for 3 Neutron Boreholes, USW UZ-N57, UZ-N61, and UZ-N62. Submittal date: 04/01/1994.	GS940408312231.004
Core Analysis of Bulk Density, Porosity, Particle Density and In Situ Saturation for Borehole UE-25 UZ#16. Submittal date: 05/04/1994.	GS940508312231.006
Volumetric Water Content from Neutron Moisture Meter Counts for 99 Boreholes from 5/3/89 or from the Time They Were Drilled until 12/31/93. Submittal date: 07/13/1994.	GS940708312212.011
Surface-Water Discharge Data for the Yucca Mountain Area, Southern Nevada and Southern California, 1994 Water Year. Submittal date: 11/30/1994.	GS941208312121.001
Subsurface Water Content at Yucca Mountain, Nevada – Neutron Logging Data for 1/1/94 thru FY94. Submittal date: 12/02/1994.	GS941208312212.017
Laboratory Measurements of Bulk Density, Porosity, and Water Content for USW SD-12, from 19 Mar 94 to 11 Aug 94, and for Radial Boreholes from 11 Apr 94 to 6 Feb 95. Submittal date: 03/02/1995.	GS950308312231.002
UE-25 UZ#16 Pycnometer Data. Submittal date: 03/06/1995.	GS950308312231.003
Physical Properties and Water Potentials of Core from Borehole USW SD-9. Submittal date: 03/01/1995.	GS950408312231.004

Description	Data Tracking Number
Physical Properties and Water Potentials of Core from Borehole USW UZ-14. Submittal date: 03/09/1995.	GS950408312231.005
Physical Properties and Water Content from Borehole USW NRG-6, 19 Mar 94 to 27 Mar 95. Submittal date: 06/06/1995.	GS950608312231.007
Moisture Retention Data from Boreholes USW UZ-N27 and UE-25 UZ#16. Submittal date: 06/06/1995.	GS950608312231.008
FY94 and FY95 Laboratory Measurements of Physical Properties of Surficial Materials at Yucca Mountain, Nevada. Submittal date: 07/18/1995.	GS950708312211.002
Fracture/Fault Properties for Fast Pathways Model. Submittal date: 07/24/1995.	GS950708312211.003
Volumetric Water Content Calculated from Field Calibration Equations Using Neutron Counts from 97 Boreholes at Yucca Mountain from 1 Oct 94 to 31 May 95. Submittal date: 08/01/1995.	GS950808312212.001
Physical Properties, Water Content, and Water Potential for Borehole USW SD-7. Submittal date: 09/26/1995.	GS951108312231.009
Physical Properties and Water Content for Borehole USW NRG-7/7A. Submittal date: 09/26/1995.	GS951108312231.010
Physical Properties, Water Content, and Water Potential for Borehole USW UZ-7A. Submittal date: 09/26/1995.	GS951108312231.011
Geostatistical Model for Estimating Precipitation and Recharge in the Yucca Mountain Region, Nevada - California. Submittal date: 01/23/1996.	GS960108312111.001
Volumetric Water Content Calculated from Field Calibration Equations Using Neutron Counts from 97 Boreholes at Yucca Mountain. Submittal date: 01/31/1996.	GS960108312212.001
Estimated Distribution of Geomorphic Surfaces and Depth to Bedrock for the Southern Half of the Topopah Spring NW 7.5 Minute Quadrangle and the Entire Busted Butte 7.5 Minute Quadrangle. Submittal date: 04/21/1996. Submit to RPC	GS960508312212.007
Estimated Annual Shallow Infiltration at 84 Boreholes, Water Years 1990 to 1995. Submittal date: 05/17/1996. Submit to RPC	GS960508312212.008
Water Permeability and Relative Humidity Calculated Porosity for Boreholes UE-25 UZ-16 and USW UZ-N27. Submittal date: 08/28/1996.	GS960808312231.001
Moisture Retention Data for Samples from Boreholes USW SD-7, USW SD-9, USW SD-12 and UE-25 UZ#16. Submittal date: 08/30/1996.	GS960808312231.003
Physical Properties, Water Content and Water Potential for Samples from Lower Depths in Boreholes USW SD- 7 and USW SD-12. Submittal date: 08/30/1996.	GS960808312231.004
Water Permeability and Relative Humidity Calculated Porosity for Samples from Boreholes USW SD-7, USW SD- 9, USW SD-12 AND USW UZ-14. Submittal date: 08/30/1996.	GS960808312231.005
Relative Humidity, Temperature, Wind Speed, Wind Direction, Net Solar Radiation and Precipitation Data from Five Weather Stations in the Yucca Mountain Area for 1995 Water Year. Submittal date: 09/12/96.	GS960908312111.004
Surface-Water Discharge Data for the Yucca Mountain Area, Southern Nevada and Southern California, 1995 Water Year. Submittal date: 10/10/1996.	GS960908312121.001
FY95 Laboratory Measurements of Physical Properties of Surficial Material at Yucca Mountain, Part II. Submittal date: 01/04/1996.	GS960108312211.001
Gravimetric and Volumetric Water Content and Rock Fragment Content of 31 Selected Sites at Yucca Mountain, Part III. Submittal date: 01/08/1996	GS960108312211.002
Conceptual and Numerical Model of Infiltration at Yucca Mountain, Nevada. Submittal date: 09/12/1996.	GS960908312211.003
Heat Dissipation Probe Data: Bleach Bone Ridge 3/95 - 11/95. Submittal date: 09/19/1996.	GS960908312211.004
FY96 Site Meteorology Data: Relative Humidity, Temperature, Wind Speed, Wind Direction, Net Solar Radiation and Barometric Pressure from Two Weather Stations in the Yucca Mountain Area, Oct. 1 - Dec. 3, 1995. Submittal date: 01/15/1997.	GS970108312111.001
Revised Bedrock Geologic Map of the Central Block Area, Yucca Mountain, Nevada. Submittal date: 12/30/1997.	GS971208314221.003

Description	Data Tracking Number
Physical Properties and Hydraulic Conductivity Measurements of Lexan-Sealed Samples from USW WT-24. Submittal date: 07/30/1998.	GS980708312242.011
Unsaturated Hydraulic Properties of Lexan-Sealed Samples From USW WT-24, Measured Using a Centrifuge. Submittal date: 08/05/1998.	GS980808312242.012
Physical Properties and Saturated Hydraulic Conductivity Measurements of Lexan-Sealed Samples from USW SD-6. Submittal date: 09/22/1998.	GS980908312242.038
Unsaturated Water Retention Data for Lexan-Sealed Samples from USW SD-6. Submittal date: 09/22/1998.	GS980908312242.039
Saturated Hydraulic Conductivity of Core from SD-9, 2/27 - 3/27/95. Submittal date: 04/27/1999.	GS990408312231.001
Coverage: Scotbons. Submittal date: 03/01/2000. Submit to RPC	MO0003COV00095.000
Flow Calculations for Yucca Mountain Groundwater Travel Time (GWTT-95). Submittal date: 12/17/1996.	SNSAND96081900.000.

Table 6-1. Stations And Precipitation Records Used to Develop the 1980–95 Daily Climate Input Files Used for Model Calibration and for Modern Climate Scenarios
[UTM, Universal Transverse Mercator; m, meters; mm, millimeters]

Precipitation records used for developing 1980–95 daily climate input used for model calibration							
Station name	**Data source**	**UTM easting (m)**	**UTM northing (m)**	**Station elevation (m)**	**Record starting date**	**Record ending date**	**07/17/87–09/30/94 Average annual Precipitation (mm)**
Beatty 8 N	NCDC: GS000100001221.001	525,211	4,094,707	1,082	12/01/72	12/31/94	133
Amargosa Farms	NCDC: GS000100001221.001	547,723	4,046,733	747	12/01/65	12/31/94	107
4JA	NTS: GS000200001221.002	563,949	4,070,874	1,043	12/01/57	09/30/94	154
40MN	NTS: GS000200001221.002	563,726	4,100,456	1,469	02/15/60	09/30/94	201
Rock Valley	NTS: GS000200001221.002	571,477	4,059,840	1,036	02/01/63	09/30/94	155
Cane Spring	NTS: GS000200001221.002	580,273	4,074,710	1,219	09/01/64	09/30/94	202
Mid Valley	NTS: GS000200001221.002	574,182	4,091,296	1,420	09/01/64	09/30/94	195
Tippipah Spring #2	NTS: GS000200001221.002	572,619	4,100,528	1,518	09/01/64	09/30/94	206
Weather station #1	USGS GS000208312111.001 GS000208312111.003	550,424	4,071,986	1,163	04/27/87	09/30/95	157
Weather station #3	USGS GS000208312111.001 GS000208312111.003	548,038	4,080,316	1,351	06/06/87	09/30/95	179

Precipitation records used for developing 100-year stochastic models of daily climate input

Station name	**Data source**	**UTM easting (m)**	**UTM northing (m)**	**Station elevation (m)**	**Record starting date**	**Record ending date**	**Complete Record Average annual precipitation (mm)**
4JA	NTS: GS000200001221.002	563,949	4,070,874	1,043	12/01/57	09/30/94	131
Area 12 Mesa	NTS: GS000200001221.002	569,533	4,115,294	2,283	03/11/59	10/04/94	315

Table 6-2. Comparison of measured versus simulated daily mean discharge at stream-gaging sites for streamflow events in 1995 [cfs, cubic feet per second] (data source:GS941208312121.001; GS960908312121.001)

		1995 Stream flow events (Daily Mean Discharge, in cfs) NWIS Database ATS#YD-200000269			
Calibration watershed	**Date**	**01/25/95**	**01/26/95**	**03/10/95**	**03/11/95**
Lower Pagany Wash	Measured	0.00	0.01	0.00	8.60
	Simulated	0.00	0.00	0.00	7.23
Upper Pagany Wash	Measured	0.00	1.70	0.00	12.00
	Simulated	0.34	0.00	0.13	9.46
Upper Drillhole Wash	Measured	0.00	0.00	0.00	5.00
	Simulated	1.55	0.00	0.00	9.33
Upper Split Wash	Measured	0.10	1.50	0.00	3.00
	Simulated	0.07	0.02	0.28	3.69
Wren Wash	Measured	0.66	0.96	0.00	2.60
	Simulated	0.71	0.19	0.70	3.92

Table 6-3. Summary of developed daily climate input files used for modern climate scenarios [mm, millimeters] (data source: GS000208311221.001)

	Yucca Mountain calibration daily climate input	**4JA stochastic simulation**	**Area 12 Mesa Stochastic simulation**
Filename	Mod3-ppt.dat	4JA.s01	Area12.s01
Beginning of record	01/01/1980	n/a	n/a
Ending of record	10/01/1995	n/a	n/a
Total number of years for simulation	15.75	100	100
Mean annual precipitation (mm)	181	140	328
Maximum daily precipitation (mm)	58	82	76

Table 6-4. Summary of analog climate records used to develop the daily climate input for the upper bound monsoon climate scenario (data source: GS000100001221.001).

	Monsoon upper bound #1 (MU1)	**Monsoon upper bound #2 (MU2)**
Source filename	Nogales.dat	Hobbs.dat
Approximate Station Location	Nogales, AZ	Hobbs, NM
NCDC Station Code	AZ 5921	NM 4026
Elevation (m)	1162	1102
Latitude (deg, min, sec)	31, 21, 00	32, 42, 00
Longitude (deg, min, sec)	110, 55, 00	103, 08, 00
Beginning of record	July, 1948	January, 1948
Ending of record	June, 1983	December, 1997
Number of complete years of record	33	50
Mean annual precip. (mm)	414.0	417.6
Mean January - March precip. (mm)	70.6	36.8
Mean April - June precip. (mm)	20.3	120.9
Mean July - September precip. (mm)	251.5	191.3
Mean October - December precip. (mm)	78.5	140.2
Maximum daily precip. (mm)	77.7	190.5
Mean annual snow (mm)	7.5	13.2
Mean October - March snow fall (mm)	6.8	13.1
Mean April - September snow fall (mm)	0.6	0.6
Maximum daily snow fall (mm)	30.5	25.4
Mean daily air temperature (Celsius)	15.8	16.8
Mean October - March daily air temperature (Celsius)	10.5	10.2
Mean April - September daily air temperature (Celsius)	21.2	23.2

Table 6-5. Summary of analog climate records used to develop the daily climate input for the lower bound glacial transition climate scenario (data source: GS000100001221.001).

	Glacial transition lower bound #1 (GL1)	Glacial transition lower bound #2 (GL2)
Source filename	Beowawe.dat	Delta.dat
Approximate Station Location	Beowawe, Nevada	Delta, Utah
NCDC Station Code	NV 795	UT 2090
Elevation (m)	1432	1409
Latitude (deg, min, sec)	40, 35, 25	39, 20, 22
Longitude (deg, min, sec)	116, 28, 29	112, 35, 45
Beginning of record	July, 1949	June, 1938
Ending of record	December, 1997	December, 1997
Number of complete years of record	42	52
Mean annual precip. (mm)	219.5	197.9
Mean January - March precip. (mm)	53.6	50.3
Mean April - June precip. (mm)	71.9	55.6
Mean July - September precip. (mm)	31.0	40.4
Mean October - December precip. (mm)	70.1	67.8
Maximum daily precip. (mm)	43.2	65.8
Mean annual snow fall (mm)	36.6	63.9
Mean October - March snow fall (mm)	29.7	57.3
Mean April - September snow fall (mm)	1.7	5.2
Maximum daily snow fall (mm)	25.4	40.6
Mean air temperature (Celsius)	8.8	10.1
Mean October - March air temperature (Celsius)	1.9	2.1
Mean April - September air temperature (Celsius)	15.7	18.0

Table 6-6. Summary of analog climate records used to develop the daily climate input for the upper bound glacial transition climate scenario (data source: GS000100001221.001).

	Glacial transition upper bound #1 (GU1)	Glacial transition upper bound #2 (GU2)	Glacial transition upper bound #2 (GU3)
Source filename	Rosalia.dat	Spokane.dat	Stjohn.dat
Approximate Station Location	Rosalia, WA	Spokane, WA	St John, WA
NCDC Station Code	WA 7180	WA 7938	WA 7267
Elevation (m)	731	718	593
Latitude (deg, min, sec)	47, 14, 00	47, 38, 00	47, 06, 00
Longitude (deg, min, sec)	117, 22, 00	117, 32, 00	117, 35, 00
Beginning of record	06/1948	08/1889	08/1963
Ending of record	12/1997	12/1997	12/1997
Number of complete years of record	43	108	33
Mean annual precip. (mm)	459.7	410.2	433.3
Mean January - March precip. (mm)	138.7	125.5	125.2
Mean April - June precip. (mm)	109.7	94.0	104.6
Mean July - September precip. (mm)	56.9	51.3	56.1
Mean October - December precip. (mm)	172.7	160.0	165.4
Maximum daily precip. (mm)	36.8	42.2	41.1
Mean annual snow fall (mm)	61.8	107.0	65.5
Mean October - March snow fall (mm)	60.9	105.7	59.8
Mean April - September snow fall (mm)	0.5	1.4	0.8
Maximum daily snow fall (mm)	27.9	32.3	30.2
Mean daily air temperature (Celsius)	8.4	8.9	9.1
Mean October - March daily air temperature (Celsius)	2.0	1.9	2.9
Mean April - September daily air temperature (Celsius)	14.5	15.8	15.1

Table 6-7. Summary of INFIL simulation results used to develop spatially distributed net-infiltration estimates for modern climate scenarios [mm, millimeters] (GS000308311221.005)

		INFIL simulation results for the 123.7-km^2 area of the net infiltration model domain			
INFIL simulation ID used for developing the modern climate scenario		YM1-4ex	4JA1-4ex	4JA1-4ex	A121-4ex
Daily climate input filename		Mod3-ppt.dat	4JA.s01	4JA.s01	Area12.s01
Simulation period (year number)		1980 – 1995	0 - 100	80 - 90	0 - 100
Simulation time (years)		16	100	10	100
Average annual precipitation (mm/year)	Mean	189.3	187.7	182.8	342.8
	Maximum	282.9	280.6	273.3	512.4
	Minimum	148.0	146.8	143.0	268.1
Average annual evapotranspiration (mm/year)	Mean	182.7	185.5	181.8	326.8
	Maximum	571.9	652.3	689.1	788.8
	Minimum	61.9	51.1	50.6	83.4
Average annual infiltrated surface water run-on (mm/year)	Mean	6.0	2.7	1.6	15.1
	Maximum	1,514.4	669.6	599.7	4,343.8
	Minimum	0.0	0.0	0.0	0.0
Average annual outflow (mm/year)		0.3	0.1	0.0	1.5
Average annual net infiltration (mm/year)	Mean	5.1	2.2	1.3	14.0
	Maximum	1,486.2	574.4	252.0	4,354.3
	Minimum	0.0	0.0	0.0	0.0

Table 6-8. Estimation results for modern climate scenarios over the 123.7- km^2 area of the infiltration model domain [mm, millimeters] [GS000308311221.005]

		Estimation results for modern climate scenarios for total area of infiltration model domain		
Modern climate scenario		Lower bound	Mean	Upper bound
Filename for spatial distribution results		Modernl.dat	Modernm.dat	Modernu.dat
Average annual precipitation (mm/year)	Mean	185.8	188.5	265.6
	Maximum	282.2	281.8	397.1
	Minimum	148.0	147.4	207.8
Average annual evapotranspiration (mm/year)	Mean	184.8	184.1	255.5
	Maximum	571.9	612.1	700.5
	Minimum	54.7	56.5	71.5
Average annual infiltrated surface water run-on (mm/year)	Mean	2.1	4.4	9.7
	Maximum	474.2	994.1	2,669.0
	Minimum	0.0	0.0	0.0
Average annual outflow (mm/year)		0.2	0.2	0.9
Average annual net infiltration (mm/year)	Mean	1.2	3.6	8.8
	Maximum	252.0	958.9	2,656.6
	Minimum	0.0	0.0	0.0

Table 6-9. Estimation results for modern climate scenarios over the 38.7- km^2 area of the 1999 UZ flow and transport model domain [mm, millimeters] [GS000308311221.005]

		Estimation results for modern climate scenarios for area of UZ flow and transport model domain		
Modern climate scenario		Lower bound	Mean	Upper bound
Filename for spatial distribution results		Modernl.dat	Modernm.dat	Modernu.dat
Average annual precipitation (mm/year)	Mean	186.8	190.6	268.6
	Maximum	246.3	246.5	347.4
	Minimum	162.7	167.1	235.5
Average annual evapotranspiration (mm/year)	Mean	186.2	185.3	257.1
	Maximum	367.9	348.2	485.6
	Minimum	62.2	59.7	77.2
Average annual infiltrated surface water run-on (mm/year)	Mean	1.9	4.1	10.1
	Maximum	194.9	277.0	802.9
	Minimum	0.0	0.0	0.0
Average annual outflow (mm/year)		-0.7	-0.2	-0.3
Average annual net infiltration (mm/year)	Mean	1.3	4.6	11.1
	Maximum	218.8	263.6	784.9
	Minimum	0.0	0.0	0.0

Table 6-10. Estimation results for modern climate scenarios over the 4.7- km^2 area of the 1999 design potential repository area [mm, millimeters] [GS000308311221.005]

		Estimation results for modern climate scenarios for area of potential repository		
Modern climate scenario		Lower bound	Mean	Upper bound
Filename for spatial distribution results		Modernl.dat	Modernm.dat	Modernu.dat
Average annual precipitation (mm/year)	Mean	191.6	196.9	277.5
	Maximum	204.1	209.9	295.8
	Minimum	178.2	183.4	258.5
Average annual evapotranspiration (mm/year)	Mean	191.7	189.9	260.4
	Maximum	252.9	273.3	423.0
	Minimum	155.0	154.7	203.0
Average annual infiltrated surface water run-on (mm/year)	Mean	1.0	3.4	8.1
	Maximum	59.8	161.1	454.8
	Minimum	0.0	0.0	0.0
Average annual outflow (mm/year)		-0.3	1.4	4.9
Average annual net infiltration (mm/year)	Mean	0.4	4.7	11.6
	Maximum	26.6	120.1	387.4
	Minimum	0.0	0.0	0.0

Table 6-11. Summary of INFIL simulation results used to develop spatially distributed net-infiltration estimates for the upper bound monsoon climate scenarios [mm, millimeters] [GS000308311221.005]

		INFIL simulation results for the 123.7-km^2 area of the net infiltration model domain	
INFIL simulation ID used for developing the upper bound monsoon climate scenario		MU1-5oh	MU2-5oh
Daily climate input filename		Nogales.inp	Hobbs.inp
Simulation period (begin date – end date)		1/1/49 - 12/31/82	1/1/48 - 12/31/97
Air temperature (Celsius)	Mean annual	16.6	17.5
	Maximum daily	33.2	34.0
	Minimum daily	-8.5	-13.7
Average annual precipitation (mm/year)	Mean	410.5	414.4
	Maximum	511.2	516.0
	Minimum	366.2	369.7
Average annual snow fall (mm/year)	Mean	1.3	12.2
	Maximum	33.7	44.9
	Minimum	0.0	2.4
Average annual evapotranspiration (mm/year)	Mean	386.3	386.3
	Maximum	814.7	818.8
	Minimum	107.9	90.8
Average annual infiltrated surface water run-on (mm/year)	Mean	19.9	16.3
	Maximum	2,884.9	2,306.4
	Minimum	0.0	0.0
Average annual outflow (mm/year)		5.8	14.3
Average annual net infiltration (mm/year)	Mean	15.1	12.1
	Maximum	2,900.6	2,330.0
	Minimum	0.0	0.0

Table 6-12. Estimation results for the monsoon climate scenarios over the 123.7- km^2 area of the infiltration model domain [mm, millimeters] [GS000308311221.005]

		Estimation results for monsoon climate scenarios for total area of infiltration model domain		
Monsoon climate scenario		Lower bound	Mean	Upper bound
Filename for spatial distribution results		Monsoonl.dat	Monsoonm.dat	Monsoonu.dat
Mean annual air temperature (Celsius)		17.3	17.2	17.0
Average annual precipitation (mm/year)	Mean	188.5	300.5	412.5
	Maximum	281.8	397.7	513.6
	Minimum	147.4	257.7	368.0
Average annual snow fall (mm/year)	Mean	n/a	n/a	6.8
	Maximum	n/a	n/a	39.3
	Minimum	n/a	n/a	1.2
Average annual evapotranspiration (mm/year)	Mean	184.1	285.2	386.3
	Maximum	612.1	714.4	816.7
	Minimum	56.5	77.9	99.3
Average annual infiltrated surface-water run-on (mm/year)	Mean	4.4	11.2	18.1
	Maximum	994.1	1,794.9	2,595.7
	Minimum	0.0	0.0	0.0
Average annual outflow (mm/year)		0.2	5.1	10.0
Average annual net infiltration (mm/year)	Mean	3.6	8.6	13.6
	Maximum	958.9	1,787.1	2,615.3
	Minimum	0.0	0.0	0.0

Table 6-13. Estimation results for the monsoon climate scenarios over the 38.7-km^2 area of the UZ flow and transport model domain [mm, millimeters] [GS000308311221.005]

		Estimation results for monsoon climate scenarios for area of UZ flow and transport model		
Monsoon climate scenario		Lower bound	Mean	Upper bound
Filename for spatial distribution results		Monsoonl.dat	Monsoonm.dat	Monsoonu.dat
Average annual precipitation (mm/year)	Mean	190.6	302.7	414.8
	Maximum	246.5	360.9	475.4
	Minimum	167.1	278.2	389.3
Average annual snow fall (mm/year)	Mean	n/a	n/a	6.8
	Maximum	n/a	n/a	18.8
	Minimum	n/a	n/a	3.0
Average annual evapotranspiration (mm/year)	Mean	185.3	284.0	382.8
	Maximum	348.2	509.9	684.7
	Minimum	59.7	81.7	103.7
Average annual infiltrated surface-water run-on (mm/year)	Mean	4.1	12.2	20.4
	Maximum	277.0	642.7	1,018.2
	Minimum	0.0	0.0	0.0
Average annual outflow (mm/year)		-0.2	4.6	9.5
Average annual net infiltration (mm/year)	Mean	4.6	12.2	19.8
	Maximum	263.6	629.0	1,016.2
	Minimum	0.0	0.0	0.0

Table 6-14. Estimation results for the monsoon climate scenarios over the 4.7-km^2 area of the 1999 design potential repository area [mm, millimeters] [GS000308311221.005]

		Estimation results for monsoon climate scenarios for area of potential repository		
Monsoon climate scenario		Lower bound	Mean	Upper bound
Filename for spatial distribution results		Monsoonl.dat	Monsoonm.dat	Monsoonu.dat
Average annual precipitation (mm/year)	Mean	196.9	309.3	421.6
	Maximum	209.9	322.8	435.7
	Minimum	183.4	295.2	407.0
Average annual snow fall (mm/year)	Mean	n/a	n/a	7.7
	Maximum	n/a	n/a	10.9
	Minimum	n/a	n/a	5.3
Average annual evapotranspiration (mm/year)	Mean	189.9	281.7	373.5
	Maximum	273.3	466.4	666.0
	Minimum	154.7	217.8	277.1
Average annual infiltrated surface-water run-on (mm/year)	Mean	3.4	9.1	14.8
	Maximum	161.1	348.6	536.1
	Minimum	0.0	0.0	0.0
Average annual outflow (mm/year)		1.4	13.2	25.1
Average annual net infiltration (mm/year)	Mean	4.7	12.5	20.3
	Maximum	120.1	267.0	413.8
	Minimum	0.0	0.0	0.0

Table 6-15. INFIL simulation results used to develop spatially distributed net-infiltration estimates for the lower bound glacial transition climate scenario [mm, millimeters] [GS000308311221.005]

		INFIL simulation results for the 123.7-km^2 area of the net infiltration model domain	
INFIL simulation ID used for developing the lower bound glacial transition climate scenario		GL1-5od	GL2-5od
Daily climate input filename		Beowawe.inp	Delta.inp
Simulation period (begin date – end date)		01/1/51 - 12/31/97	01/1/48 - 12/31/97
Air temperature (Celsius)	Mean annual	9.6	10.8
	Maximum daily	31.0	31.5
	Minimum daily	-31.2	-24.9
Average annual precipitation (mm/year)	Mean	208.4	193.7
	Maximum	259.5	241.1
	Minimum	185.9	172.8
Average annual snow fall (mm/year)	Mean	30.7	27.6
	Maximum	118.8	100.0
	Minimum	8.5	9.9
Average annual evapotranspiration (mm/year)	Mean	201.1	188.1
	Maximum	542.6	508.9
	Minimum	68.1	79.0
Average annual infiltrated surface-water run-on (mm/year)	Mean	2.9	1.4
	Maximum	735.4	351.2
	Minimum	0.0	0.0
Average annual mean outflow (mm/year)		0.0	0.0
Average annual net infiltration (mm/year)	Mean	2.9	1.4
	Maximum	559.7	228.0
	Minimum	0.0	0.0

Table 6-16. INFIL simulation results used to develop spatially distributed net-infiltration estimates for the upper bound glacial transition climate scenario [mm, millimeters] [GS000308311221.005]

		INFIL simulation results for the 123.7-km^2 area of the net infiltration model domain		
INFIL simulation ID used for developing the upper bound glacial transition climate scenario		Gu1-5os	Gu2-5os	Gu3-5os
Daily climate input filename		Rosalia.inp	Spokane.inp	Stjohn.inp
Simulation period (begin date – end date)		01/1/51-12/31/97	01/1/48-12/31/97	01/1/64-12/31/97
Air temperature (Celsius)	Mean annual	9.0	9.2	9.9
	Maximum daily	33.5	31.8	30.1
	Minimum daily	-25.4	-26.2	-26.0
Average annual precipitation (mm/year)	Mean	454.9	406.2	432.1
	Maximum	566.4	505.8	538.0
	Minimum	405.8	362.4	385.5
Average annual snow fall (mm/year)	Mean	67.5	74.3	44.0
	Maximum	288.0	265.9	209.5
	Minimum	19.1	25.6	13.7
Average annual evapotranspiration (mm/year)	Mean	411.5	374.4	399.0
	Maximum	773.8	770.4	751.0
	Minimum	122.2	113.8	112.9
Average annual infiltrated surface-water run-on (mm/year)	Mean	31.4	24.2	25.3
	Maximum	9,092.6	7,044.8	6,308.7
	Minimum	0.0	0.0	0.0
Average annual mean outflow (mm/year)		3.7	1.8	3.2
Average annual net infiltration (mm/year)	Mean	29.7	21.2	23.0
	Maximum	9,126.2	7,033.7	6,308.1
	Minimum	0.0	0.0	0.0

Table 6-17. Estimation results for the glacial transition climate scenarios over the 123.7-km^2 area of the infiltration model domain [mm, millimeters] [GS000308311221.005]

		Estimation results for glacial transition climate scenarios for total area of infiltration model domain		
Glacial transition climate scenario		Lower bound	Mean	Upper bound
Filename for spatial distribution results		GlacialII.dat	Glacialm.dat	Glacialu.dat
Mean annual air temperature (Celsius)		10.2	9.8	9.4
Average annual precipitation (mm/year)	Mean	201.0	316.1	431.1
	Maximum	250.3	393.5	536.8
	Minimum	179.4	282.0	384.6
Average annual snow fall (mm/year)	Mean	29.1	45.5	61.9
	Maximum	109.4	181.9	254.5
	Minimum	9.2	14.3	19.5
Average annual evapotranspiration (mm/year)	Mean	194.6	294.8	395.0
	Maximum	525.7	600.7	751.2
	Minimum	73.6	94.9	116.3
Average annual infiltrated surface-water run-on (mm/year)	Mean	2.2	14.6	27.0
	Maximum	524.3	3,913.2	7,482.0
	Minimum	0.0	0.0	0.0
Average annual outflow (mm/year)		0.0	1.5	2.9
Average annual net infiltration (mm/year)	Mean	2.2	13.4	24.6
	Maximum	370.3	3,902.5	7,489.3
	Minimum	0.0	0.0	0.0

Table 6-18. Estimation results for the glacial transition climate scenarios over the 38.7-km^2 area of the UZ flow and transport model domain [mm, millimeters] [GS000308311221.005]

		Estimation results for glacial transition climate scenarios for area of UZ flow and transport model domain		
Glacial transition climate scenario		Lower bound	Mean	Upper bound
Filename for spatial distribution results		GlacialII.dat	GlacialM.dat	GlacialU.dat
Average annual precipitation (mm/year)	Mean	202.2	317.8	433.5
	Maximum	231.7	364.3	496.8
	Minimum	189.8	298.3	406.9
Average annual snow fall (mm/year)	Mean	29.1	45.1	61.1
	Maximum	75.1	122.0	168.9
	Minimum	16.3	25.3	34.2
Average annual evapotranspiration (mm/year)	Mean	195.2	293.5	391.8
	Maximum	343.3	502.3	733.9
	Minimum	76.9	99.4	121.9
Average annual infiltrated surface-water run-on (mm/year)	Mean	1.7	15.6	29.6
	Maximum	193.1	1,301.1	2,586.2
	Minimum	0.0	0.0	0.0
Average annual outflow (mm/year)		-0.1	-0.2	-0.3
Average annual net infiltration (mm/year)	Mean	2.5	17.8	33.0
	Maximum	219.2	1,282.9	2,555.0
	Minimum	0.0	0.0	0.0

Table 6-19. Estimation results for the glacial transition climate scenarios for the 4.7-km^2 area of the 1999 design potential repository area [mm, millimeters] [GS000308311221.005]

		Estimation results for glacial transition climate scenarios for area of potential repository		
Glacial transition climate scenario		Lower bound	Mean	Upper bound
Filename for spatial distribution results		GlacialII.dat	Glacialm.dat	Glacialu.dat
Average annual precipitation (mm/year)	Mean	205.5	323.1	440.6
	Maximum	212.4	333.8	455.3
	Minimum	198.4	311.8	425.3
Average annual snow fall (mm/year)	Mean	32.5	50.3	68.1
	Maximum	42.0	65.2	88.3
	Minimum	24.9	37.8	50.7
Average annual evapotranspiration (mm/year)	Mean	197.5	287.8	378.1
	Maximum	279.4	477.8	688.6
	Minimum	171.0	219.3	265.3
Average annual infiltrated surface-water run-on (mm/year)	Mean	1.4	12.0	22.5
	Maximum	100.5	676.6	1,334.8
	Minimum	0.0	0.0	0.0
Average annual outflow (mm/year)		0.3	8.0	15.6
Average annual net infiltration (mm/year)	Mean	2.2	19.8	37.3
	Maximum	116.3	591.0	1,181.4
	Minimum	0.0	0.0	0.0

Table 7-1. Output Data Sets Generated in the Development and Application of the Net Infiltration Model

Description	Data Tracking Number
Preliminary Estimates of Input Parameter Distributions Used for Infiltration Uncertainty Analysis	GS000308311221.008
Preliminary Net Infiltration Modeling Results for 3 Climate Scenarios for FY99	GS000308311221.005
Template files for Uncertainty Analysis	GS000308311221.011
Preliminary Developed Daily Climate Data from Tule Lake, California, Used for Infiltration Uncertainty Analysis	GS000308311221.010
Rainfall/Runoff/Run-on 1999 Simulations	GS000399991221.002
Preliminary Geospatial Input Data for INFIL V2.0 FY99	GS000308311221.004
Merged USGS Digital Elevation Model from Topopah Spring West and Busted Butte 7.5' DEMs	GS000308311221.006
Yucca Mountain 1980-1995 Developed Daily Precipitation Record	GS000208311221.001
Preliminary Developed Daily Climate Data for Potential Future Monsoon and Glacial Transition Climates Using Records from Selected Analog Sites.	GS000208311221.002
Developed Matrix Hydrologic Properties Information	GS000308312231.002

ATTACHMENT II

FIGURES

TOTAL PAGES: 43

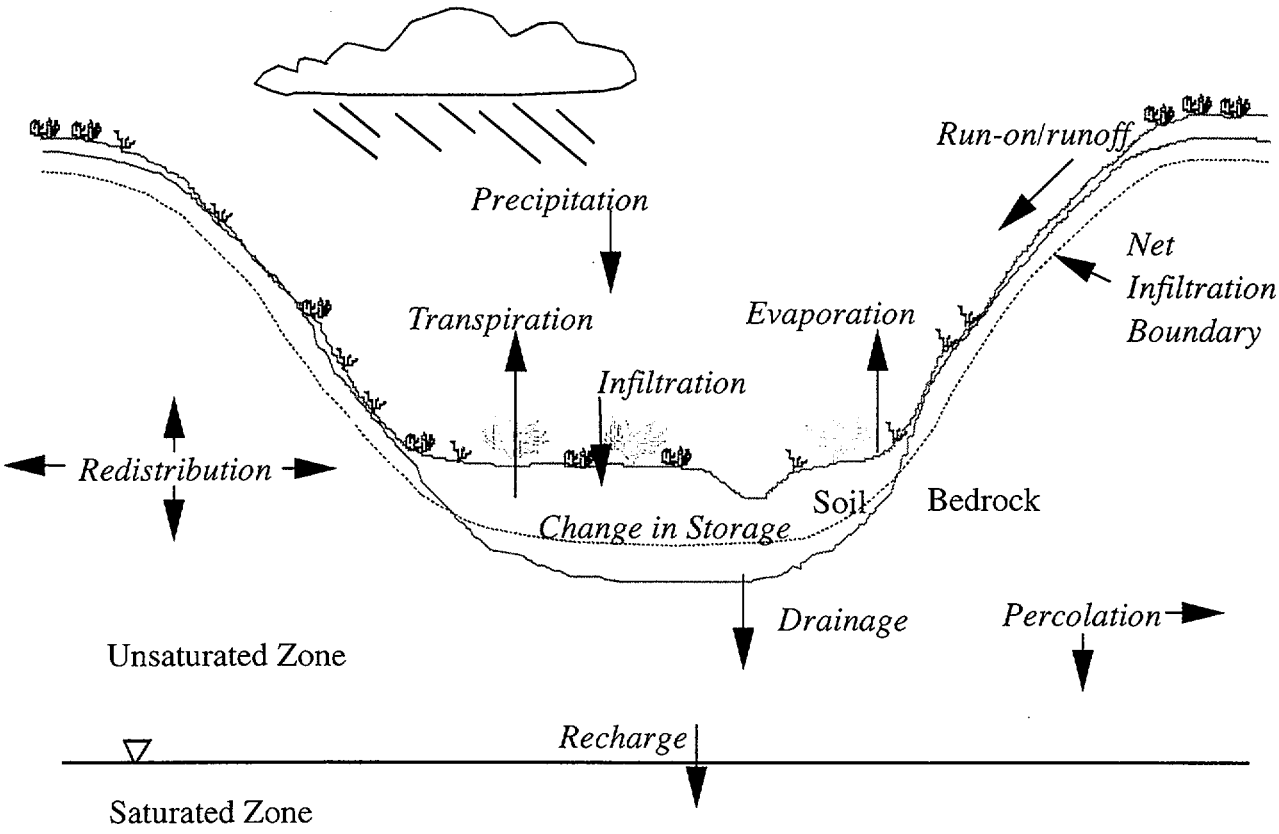

Figure 6-1. Field-scale water balance and processes controlling net infiltration (from Flint et al., 1996, Figure 3).

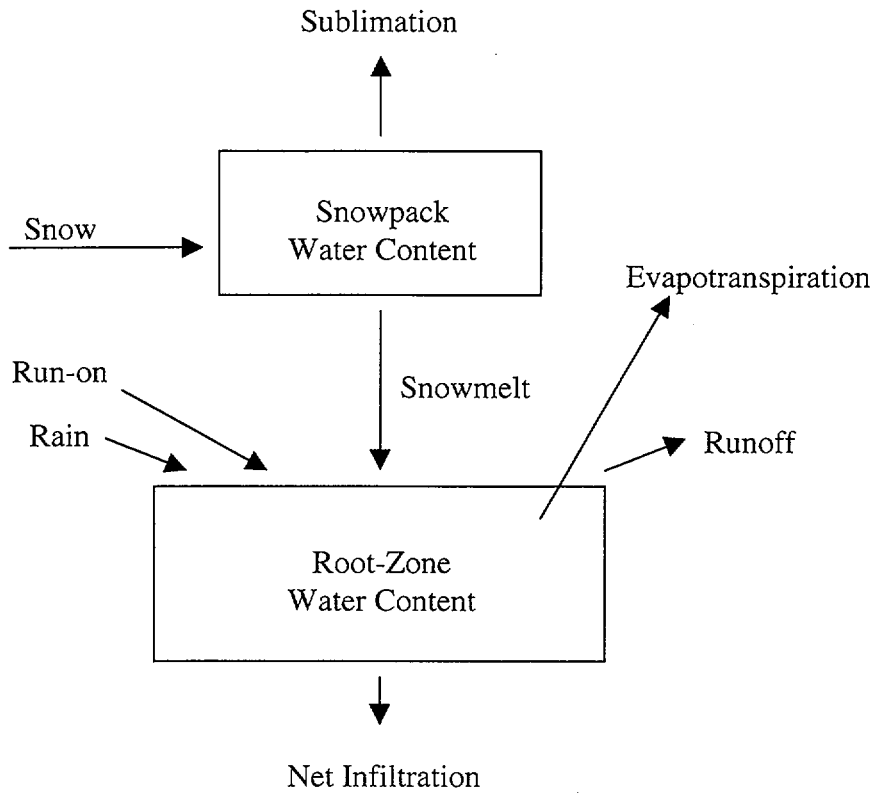

Change in Root-Zone Water Content:
If water content < water content at field capacity,
change in water content = Rain + Run-on + Snowmelt - Evapotranspiration
If water content < porosity > water content at field capacity,
change in water content = Rain + Run-on + Snowmelt – Evapotranspiration
- Net Infiltration

Figure 6-2. The daily root-zone water-balance used to model net infiltration.

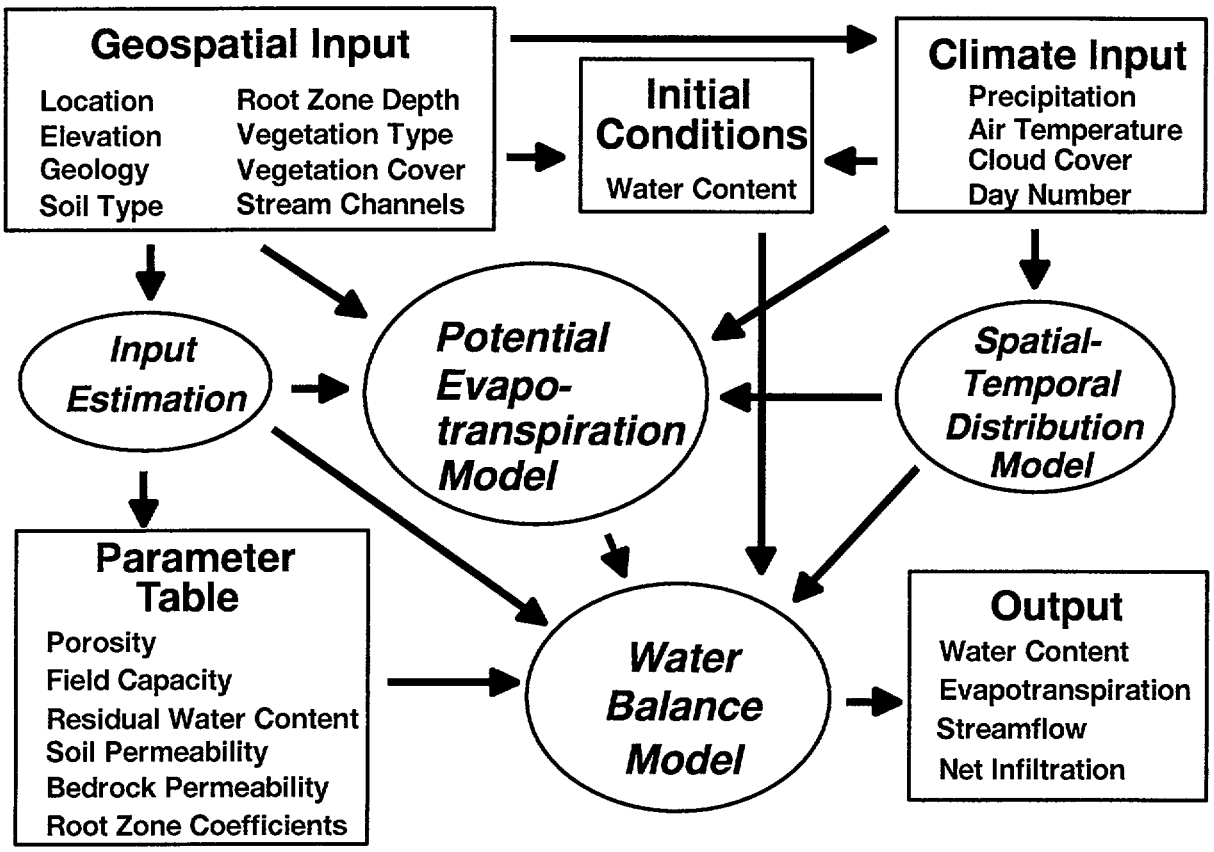

Figure 6-3. Major components of the net-infiltration modeling process.

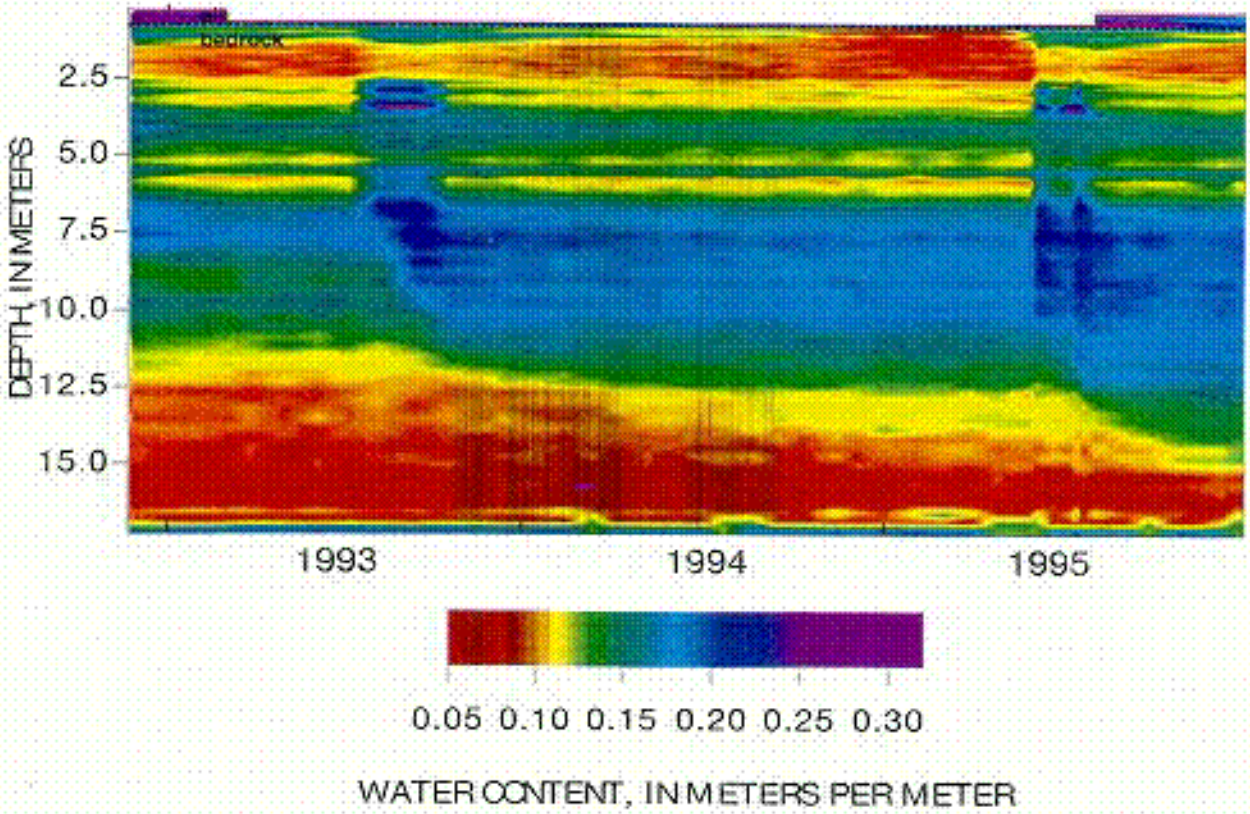

Figure 6-4. Measured water-content profiles at borehole UZN-15 for 1993-95 (DTN: GS940708312212.011, GS941208312212.017, GS950808312212.001, GS960108312212.001).

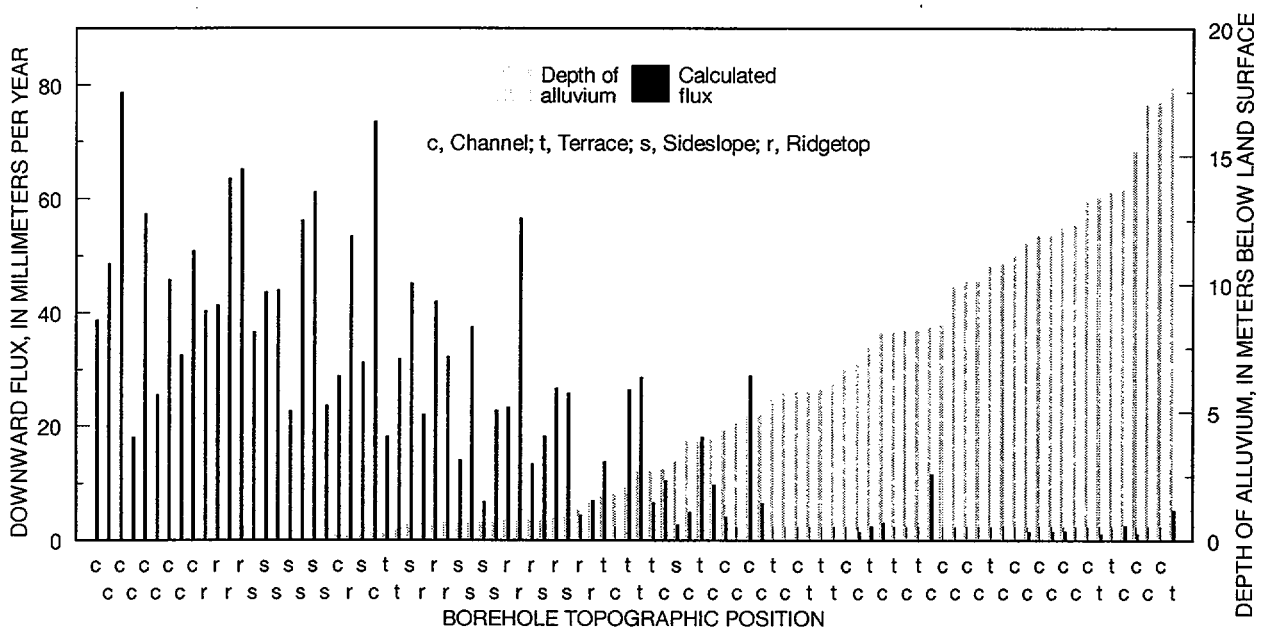

Figure 6-5. Estimates of average net-infiltration rates at Yucca Mountain calculated using changes in measured water-content profiles obtained for the period 1989–95 from a network of monitoring boreholes (DTN: GS960508312212.008), compared to depth of alluvium at each borehole (DTN: GS960508312212.007).

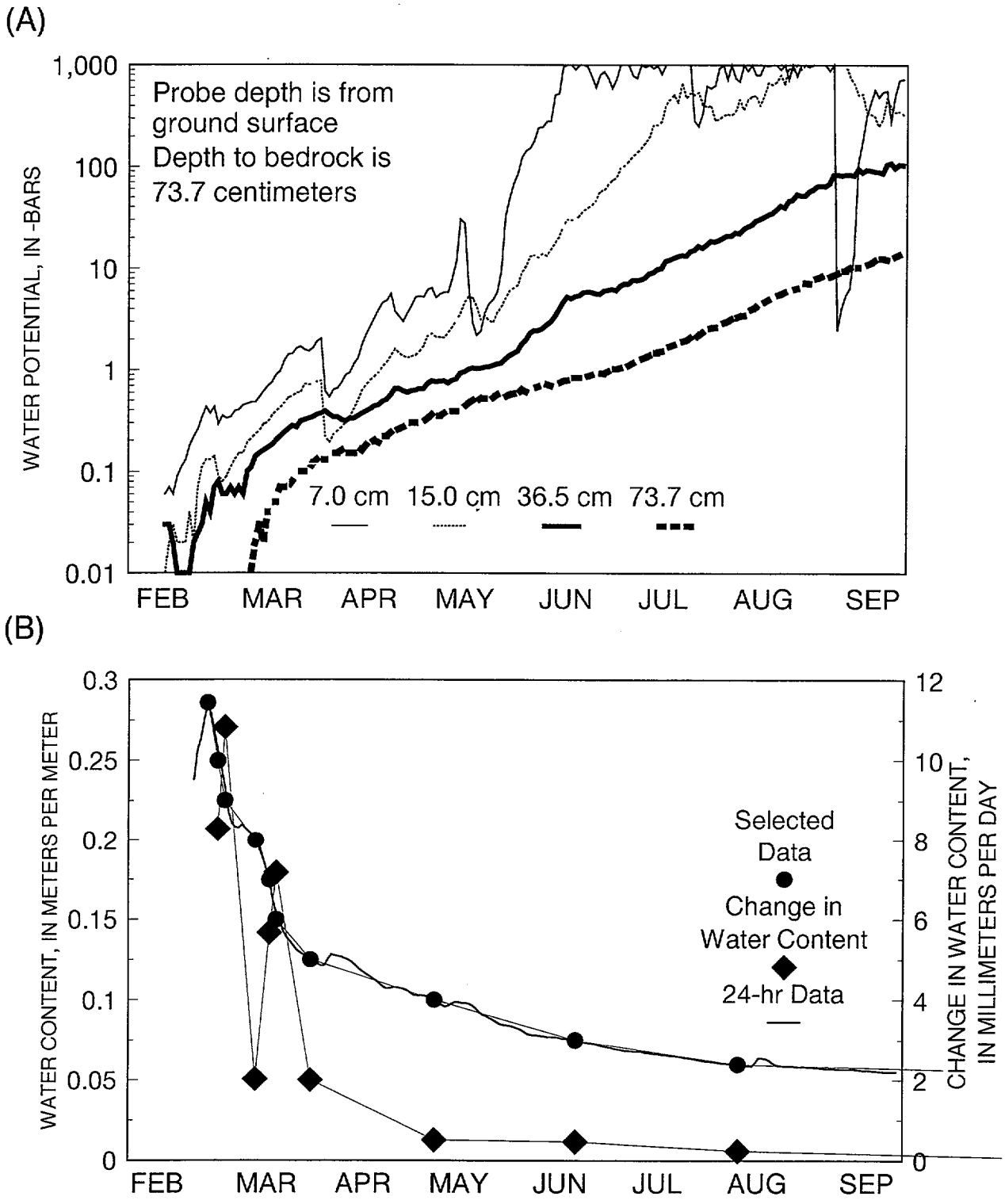

Figure 6-6. Graphs of water-potential measurements near borehole USW UZ-N15 using heat dissipation probes, (DTN: GS960908312211.004), (A) measured at four depths for 1995 and (B) used to calculate flux.

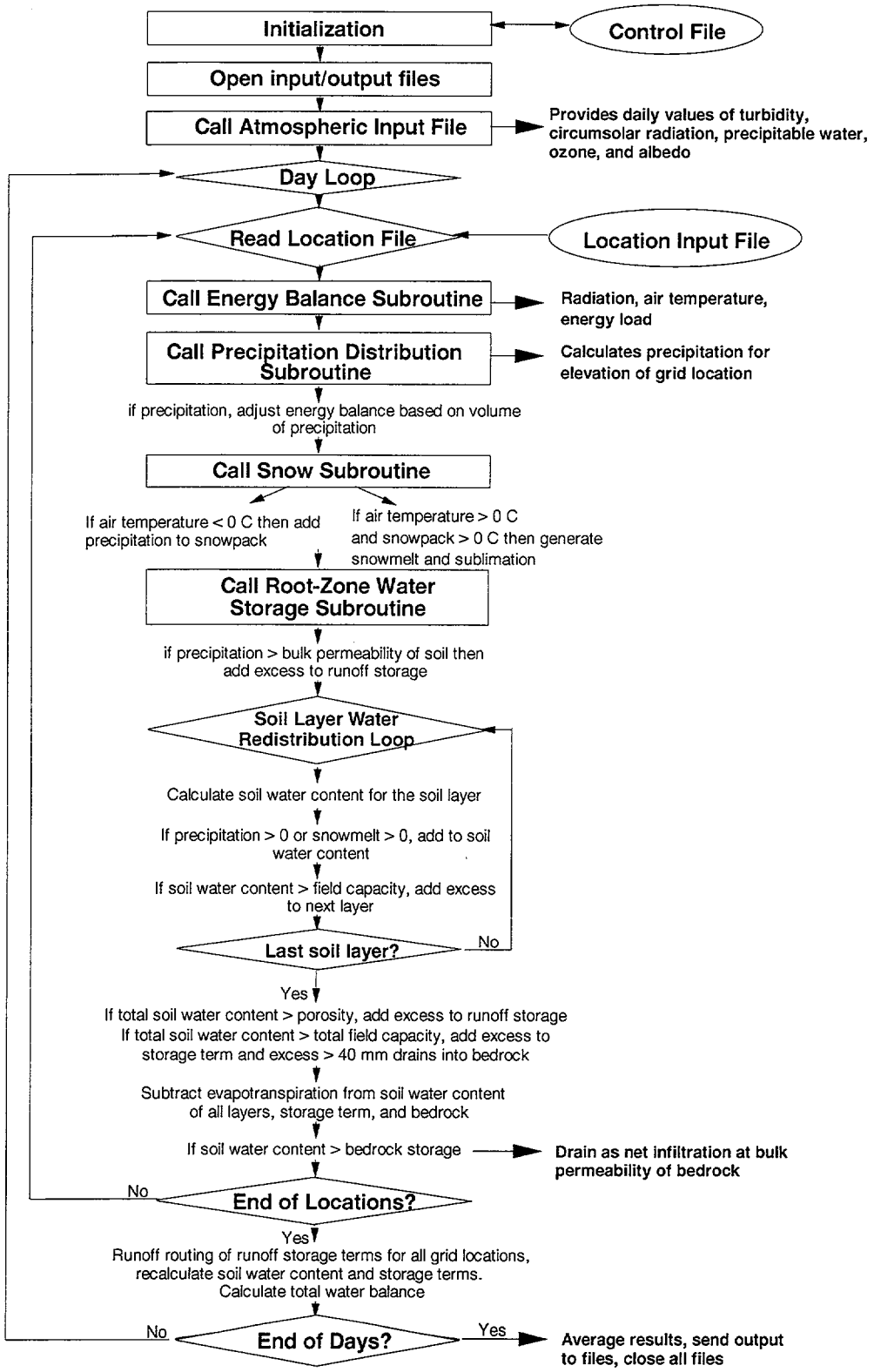

Figure 6-7. Flow chart of the model algorithm used for simulating net infiltration.

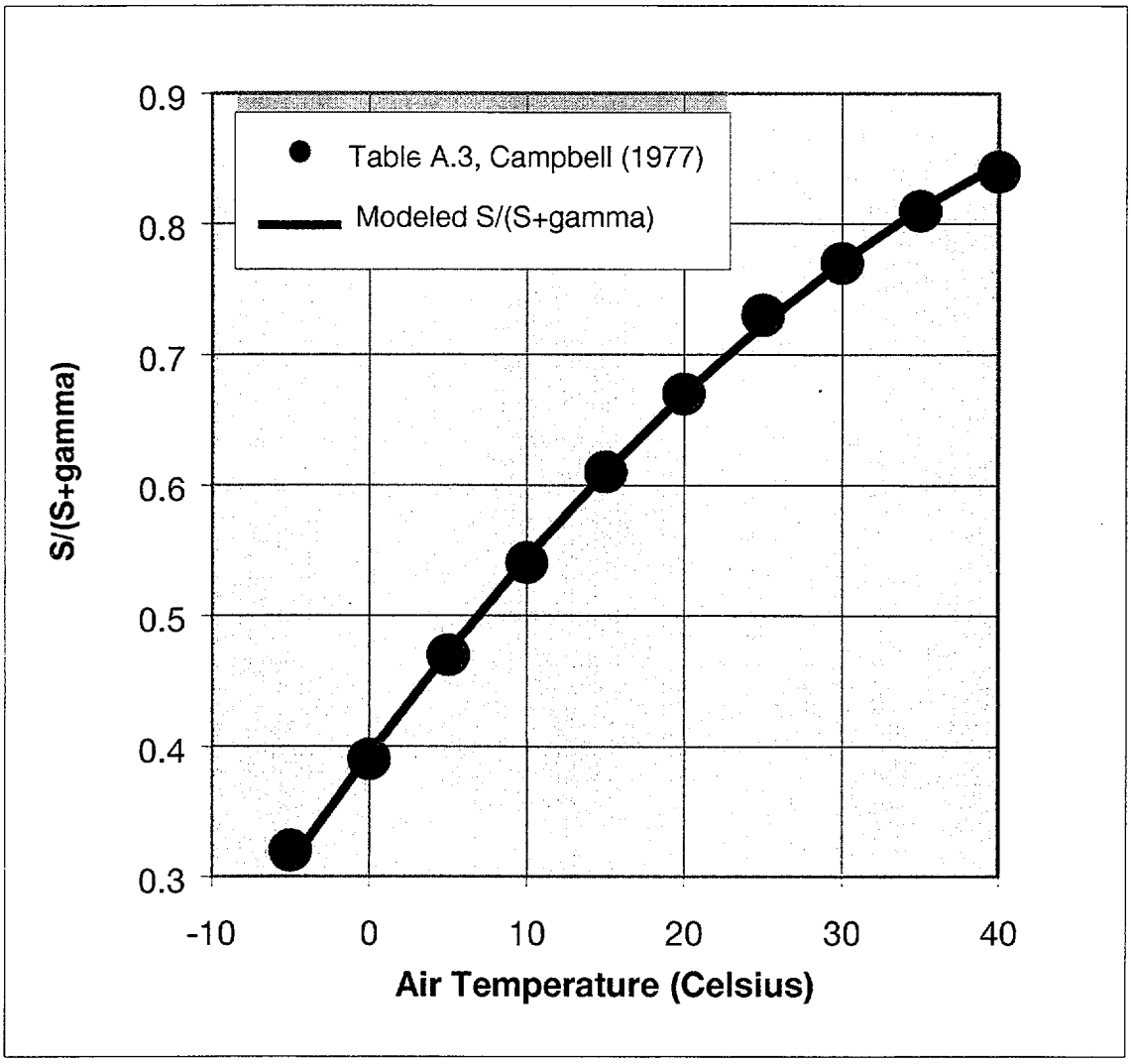

Figure 6-8. Relative effect of air temperature change on the modeled S/(S+γ) term of the Priestley-Taylor equation used for estimating potential evapotranspiration. (DTN: GS000300001221.009)

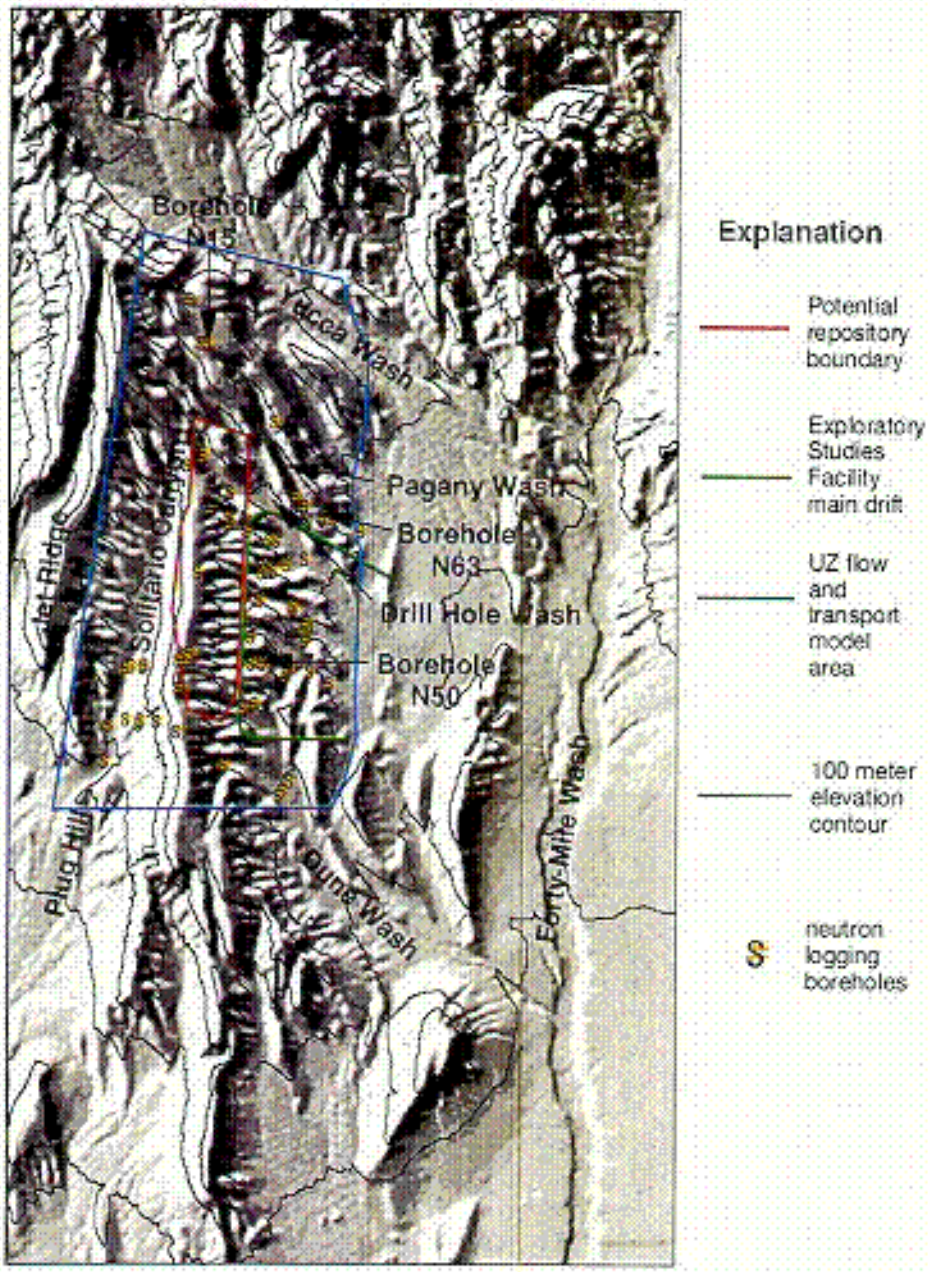

Figure 6-9. Yucca Mountain DEM used to define the geospatial-input parameters and watershed modeling domains (DTN: GS000308311221.006).

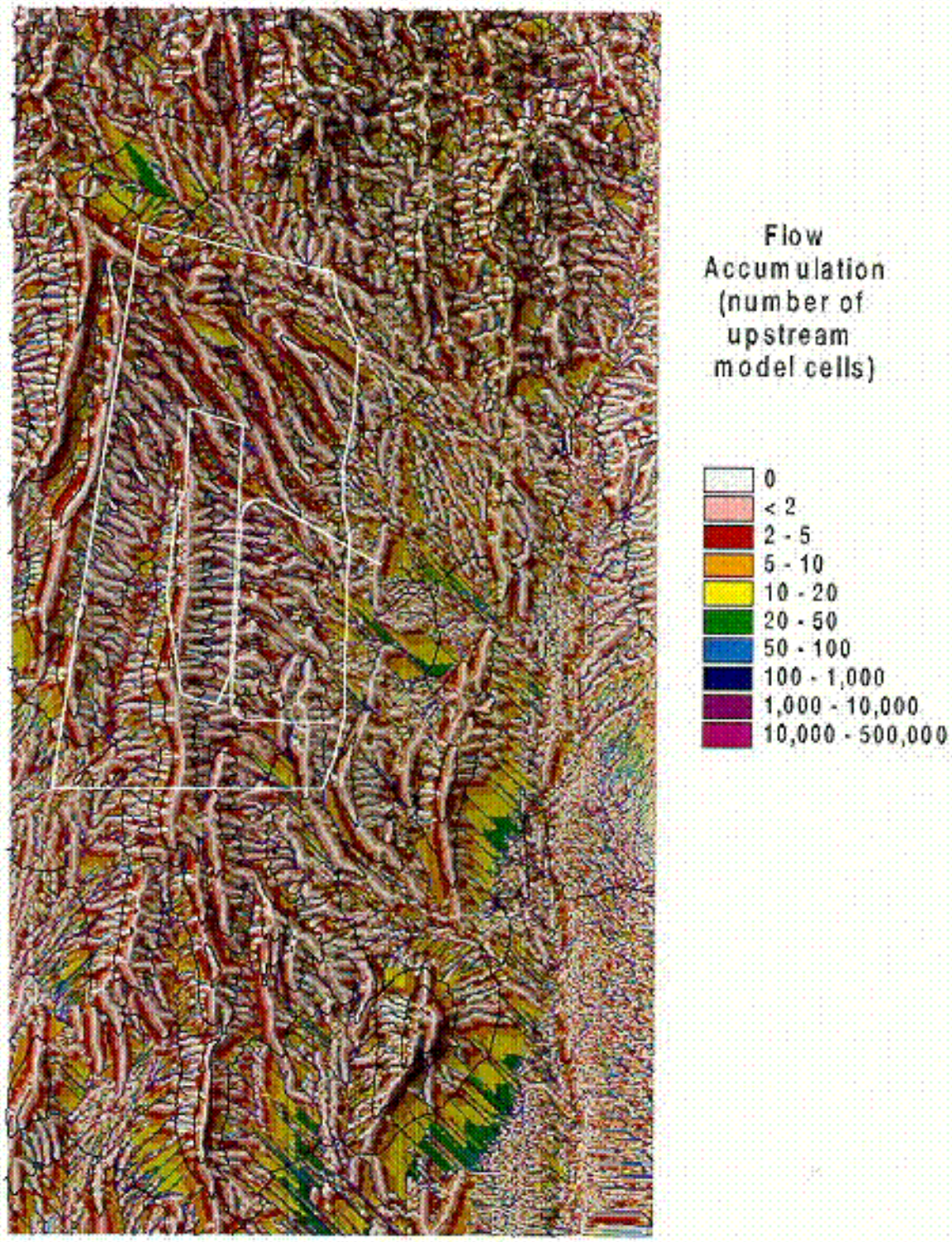

Figure 6-10. Number of upstream cells indicating the numerical channel network. (see Attachment XI)

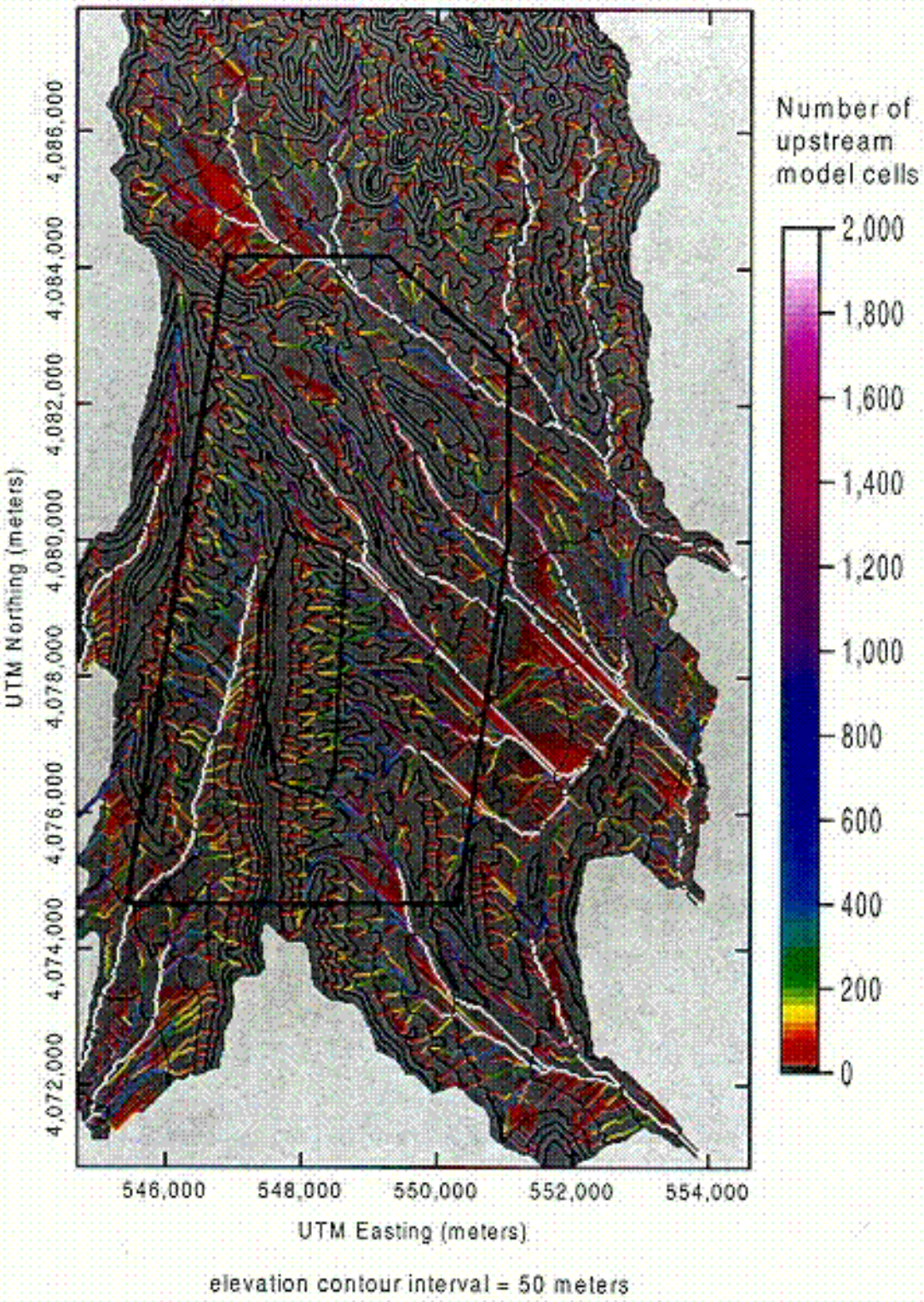

Figure 6-11. Isolation of the drainage networks overlying the area of the UZ flow and transport model. (see Attachment XI)

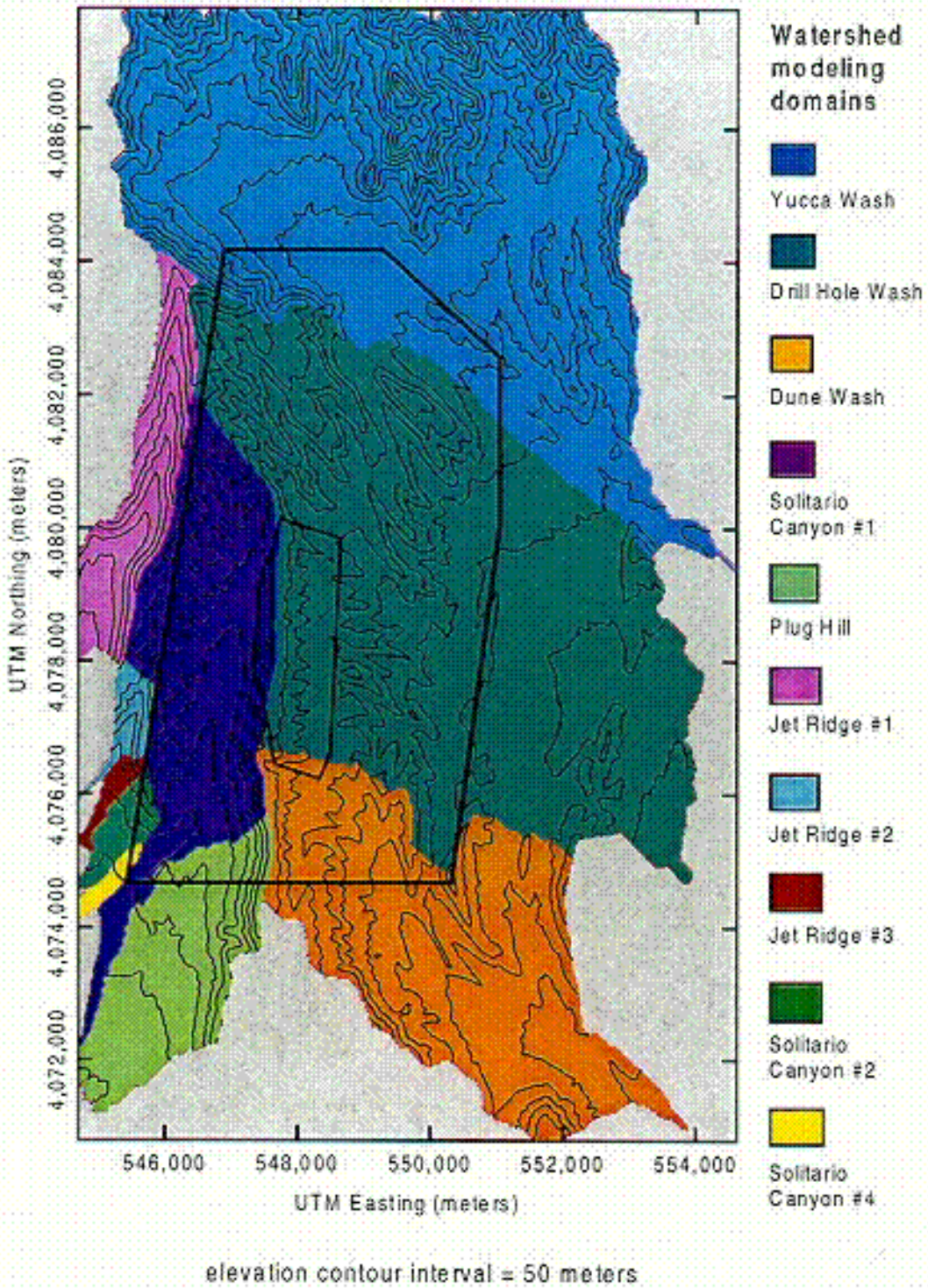

Figure 6-12. Location of 10 watershed model domains included in the composite watershed model area overlying the area of the UZ flow and transport model. (see Attachment XIII)

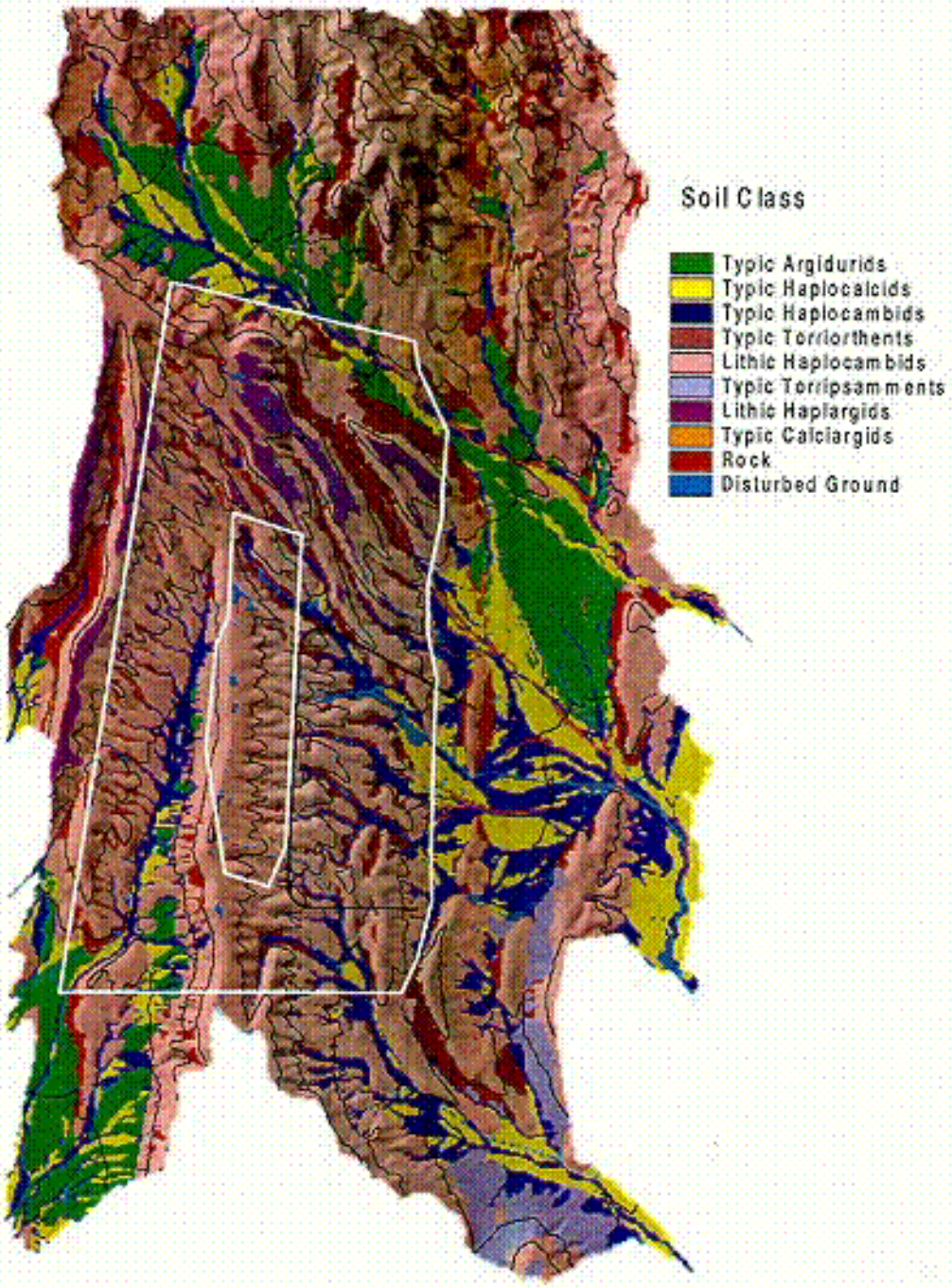

Figure 6-13. Recombined soil classes used in the 1996 net-infiltration model (from Flint et al., 1996, Figure 14; DTN: GS000308311221.004).

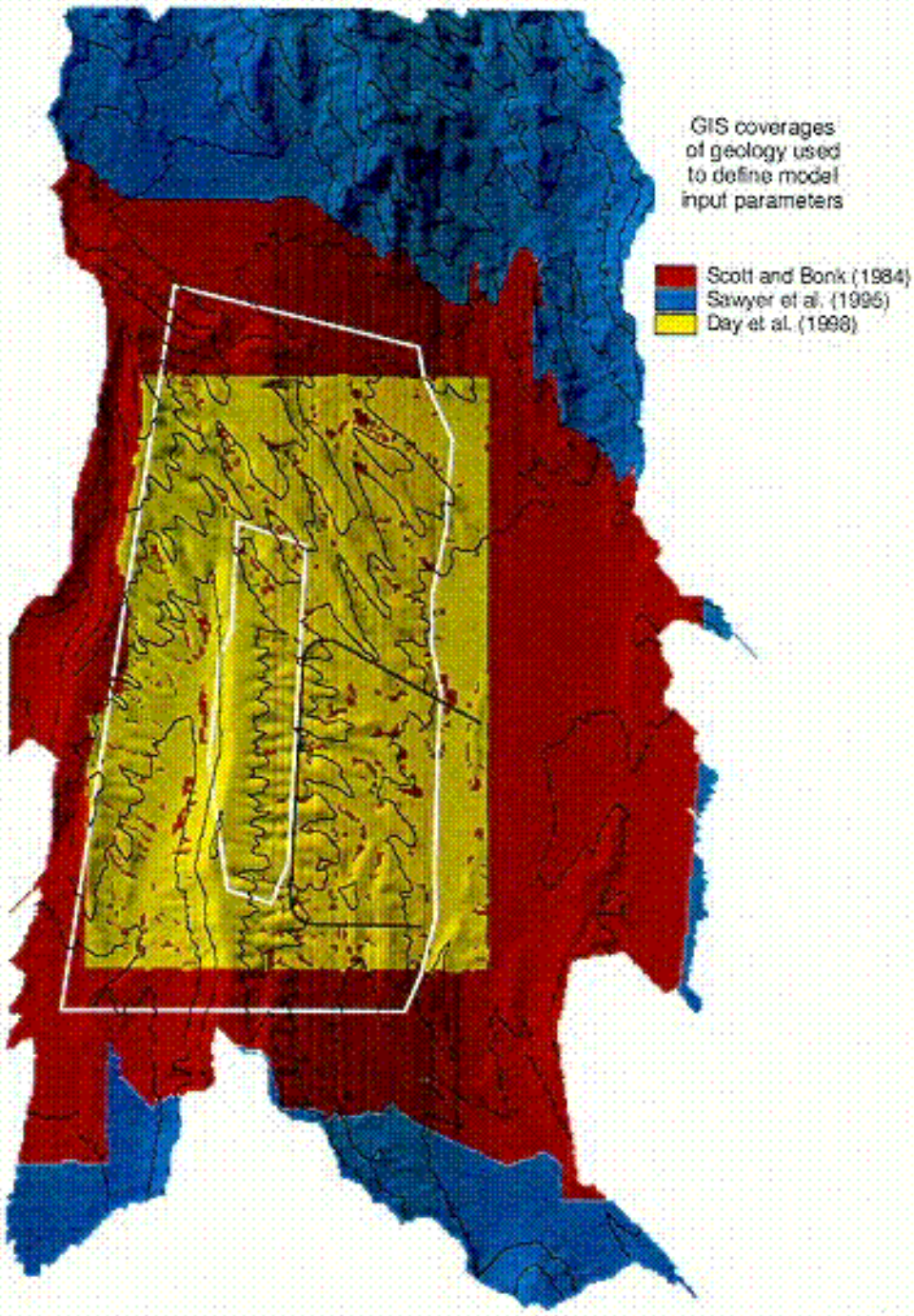

Figure 6-14. Overlay of the three geologic maps used to define rock types underlying the root zone and included in the bottom root-zone layer (Day et al., 1998, DTN: GS971208314221.003; Scott and Bonk, 1984, DTN: MO0003COV00095.000; Sawyer et al., 1995, DTN: GS000300001221.010)

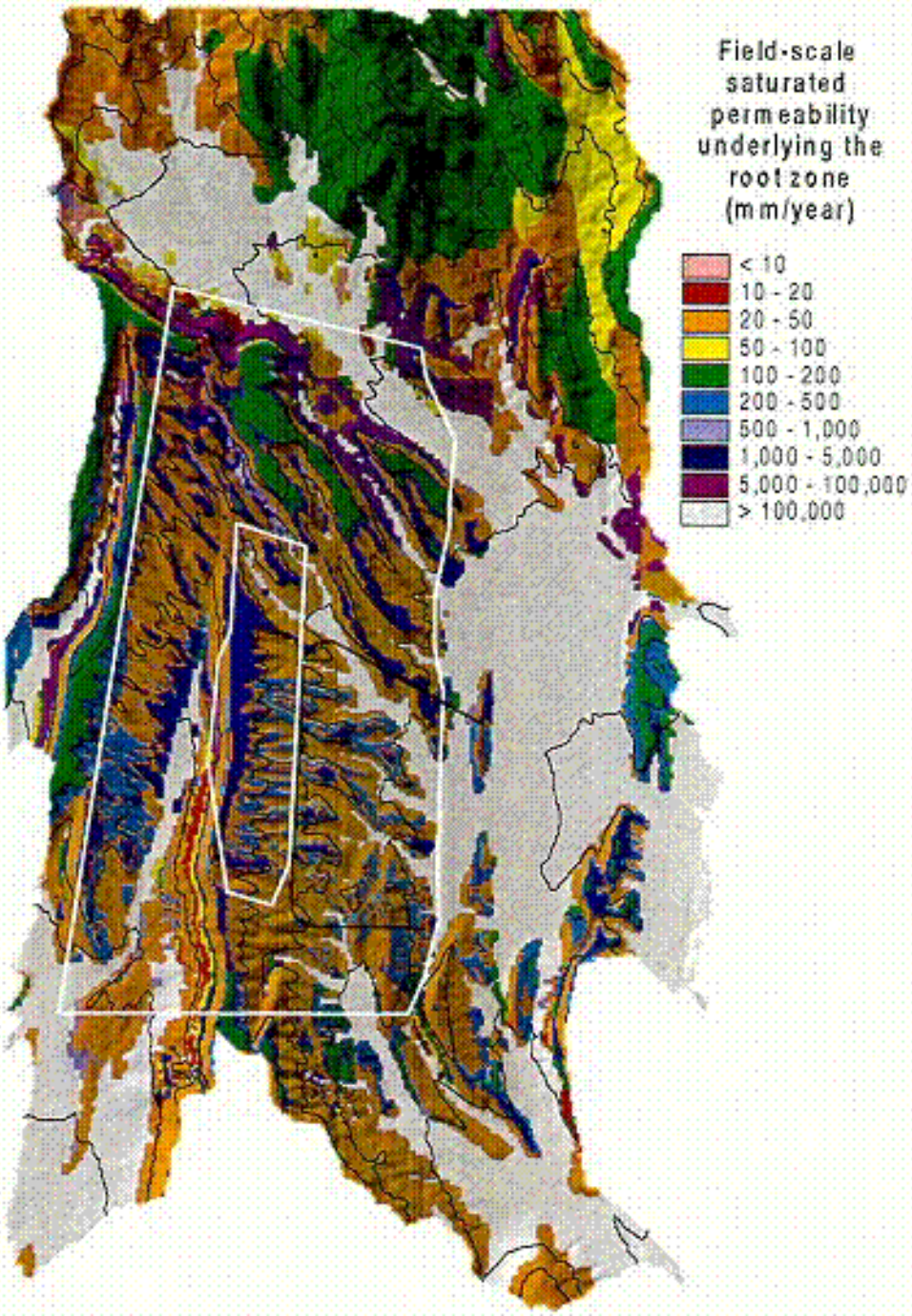

Figure 6-15. Estimated field-scale saturated hydraulic conductivity of bedrock or soils underlying the root zone (DTN: GS000308312231.002).

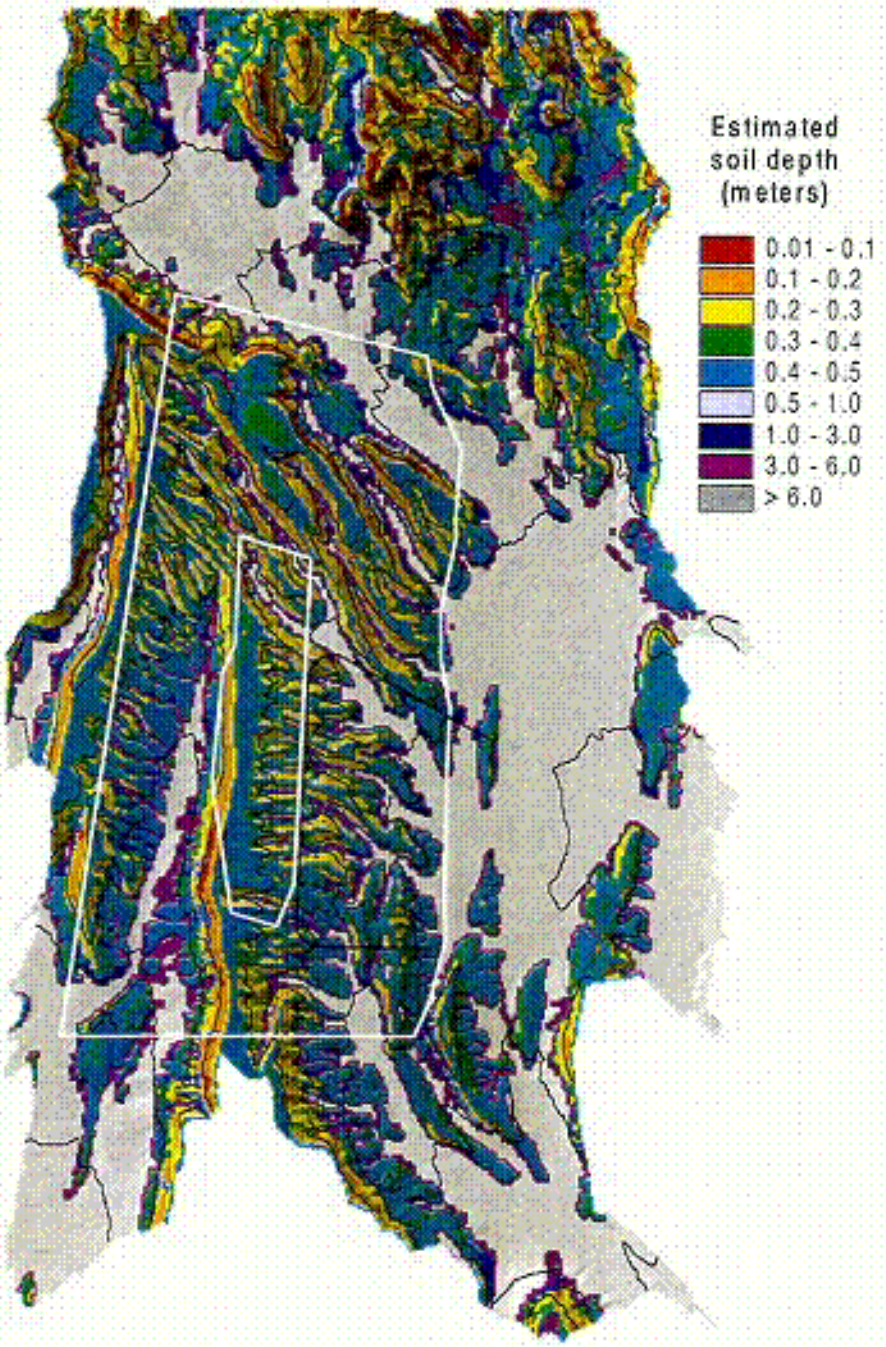

Figure 6-16. Estimated soil depth (DTN: GS960508312212.007) using the 1996 soil-depth class map and calculated land-surface slope (DTN: GS000308311221.004).

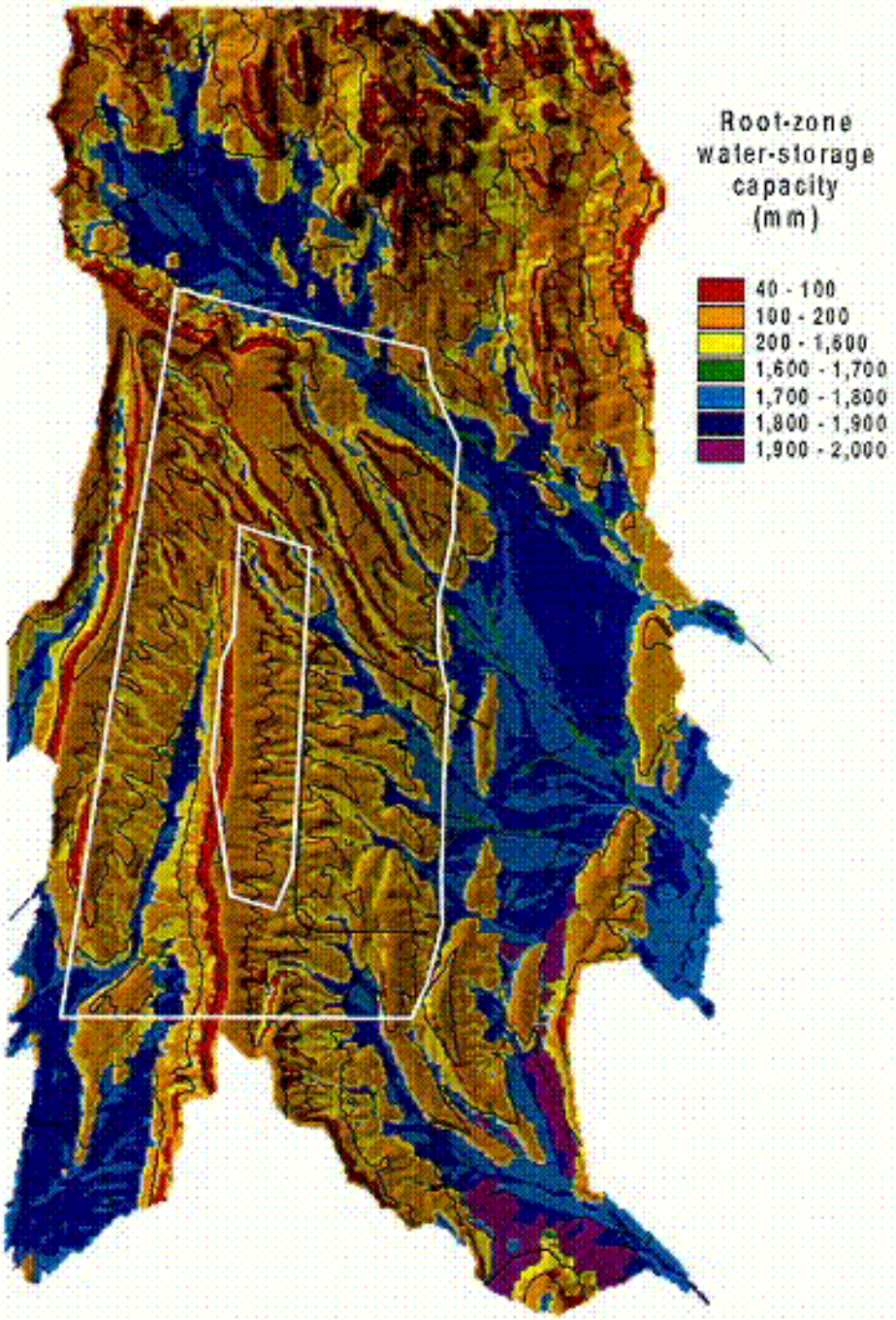

Figure 6-17. Total water-storage capacity of the modeled root zone, including bedrock and soil layers (DTN: GS000308311221.004).

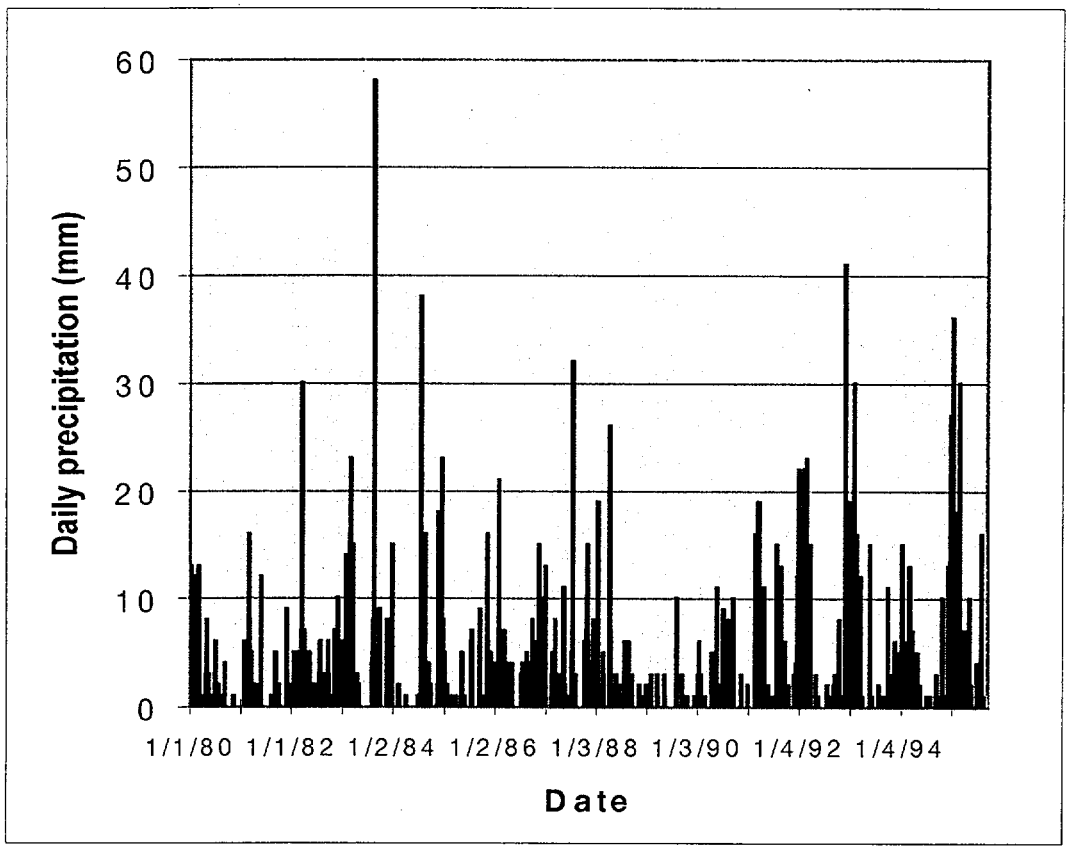

Figure 6-18. Developed 1980–95 daily precipitation record used as input for model calibration (DTN: GS000208311221.001).

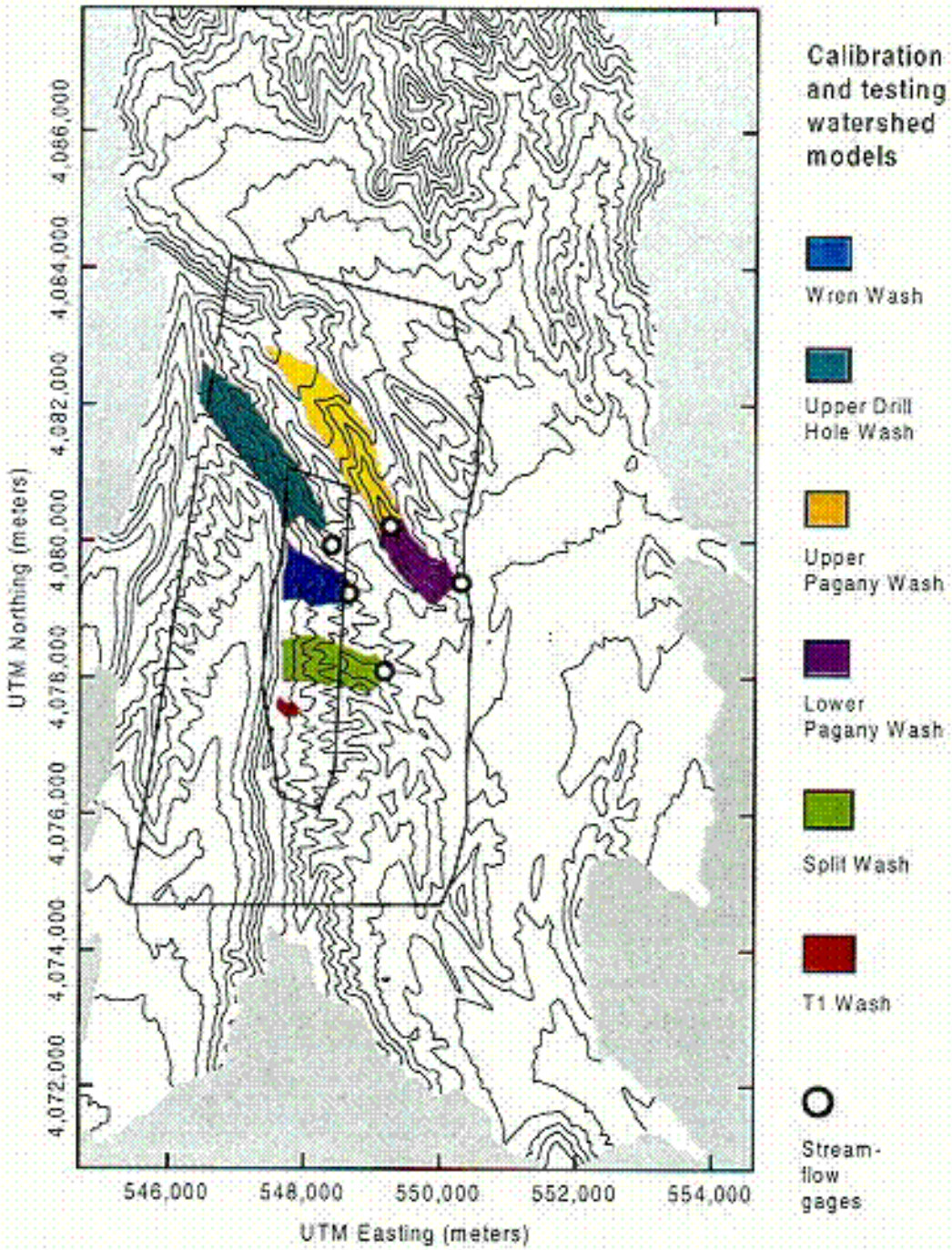

Figure 6-19. Location of stream-gaging sites and calibration watersheds defined by the gaging sites (DTN: GS960908312121.001, GS941208312121.001).

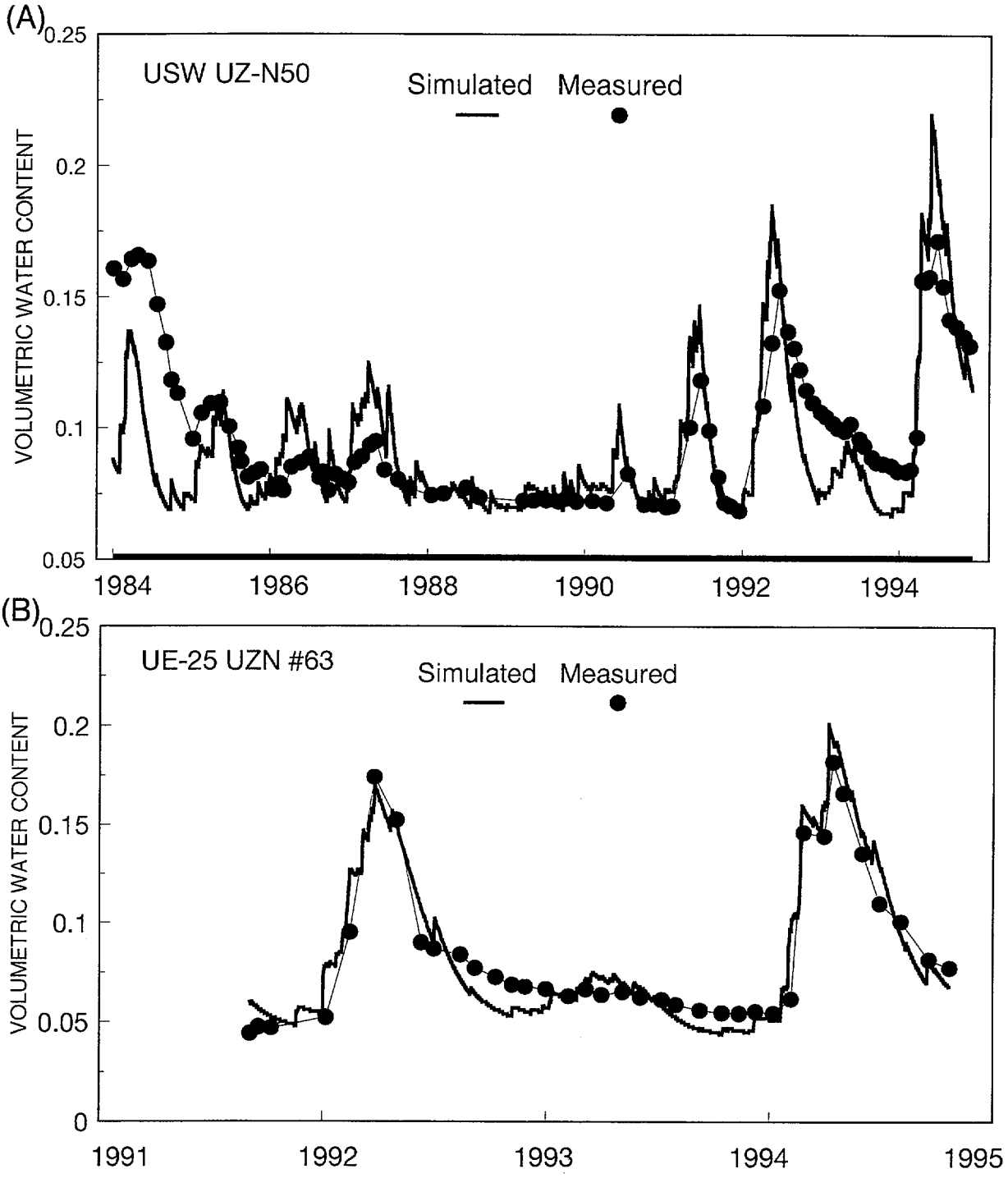

Figure 6-20. Graphs of comparisons of simulated net infiltration using water content in neutron boreholes (A) USW UZ-N50 and (B) UE-25 UZN #63 (DTN: GS940708312212.011, GS941208312212.017, GS950808312212.001, GS960108312212.001).

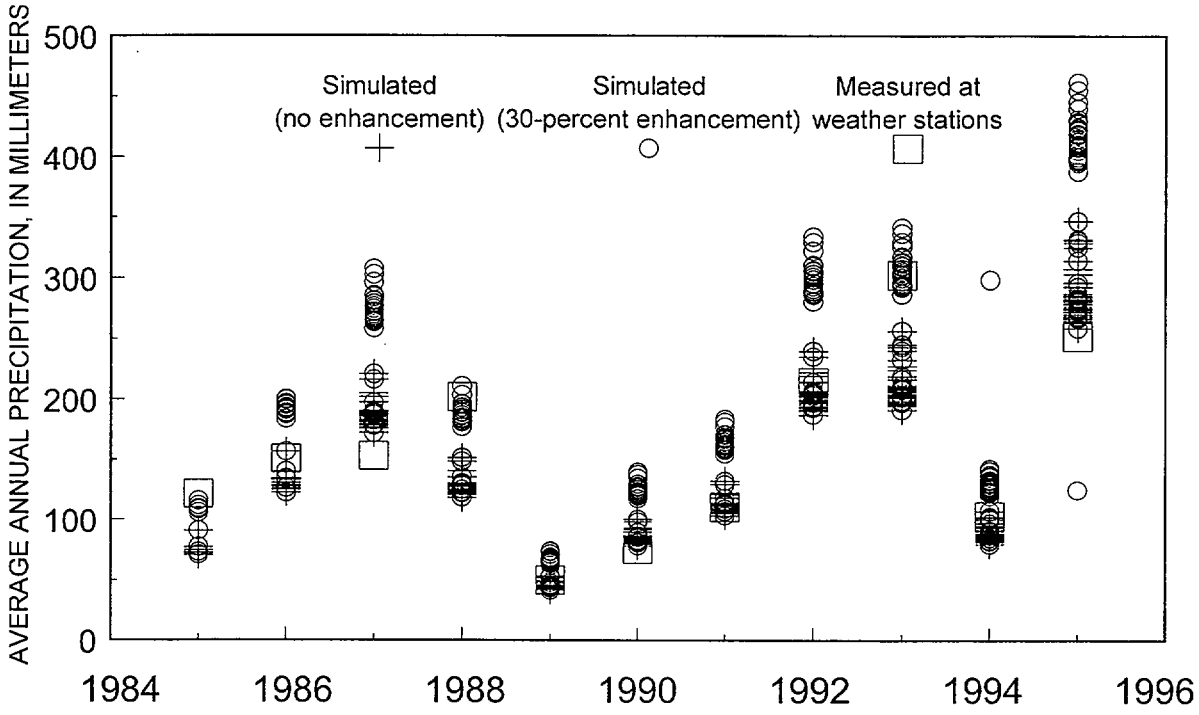

Figure 6-21. Graph of average annual precipitation simulated at each borehole using precipitation record for 1980-95 (DTN: GS000208311221.001), and simulated with a 30-percent enhancement in the channel grid blocks only, compared to developed precipitation record distributed geostatistically to each borehole.

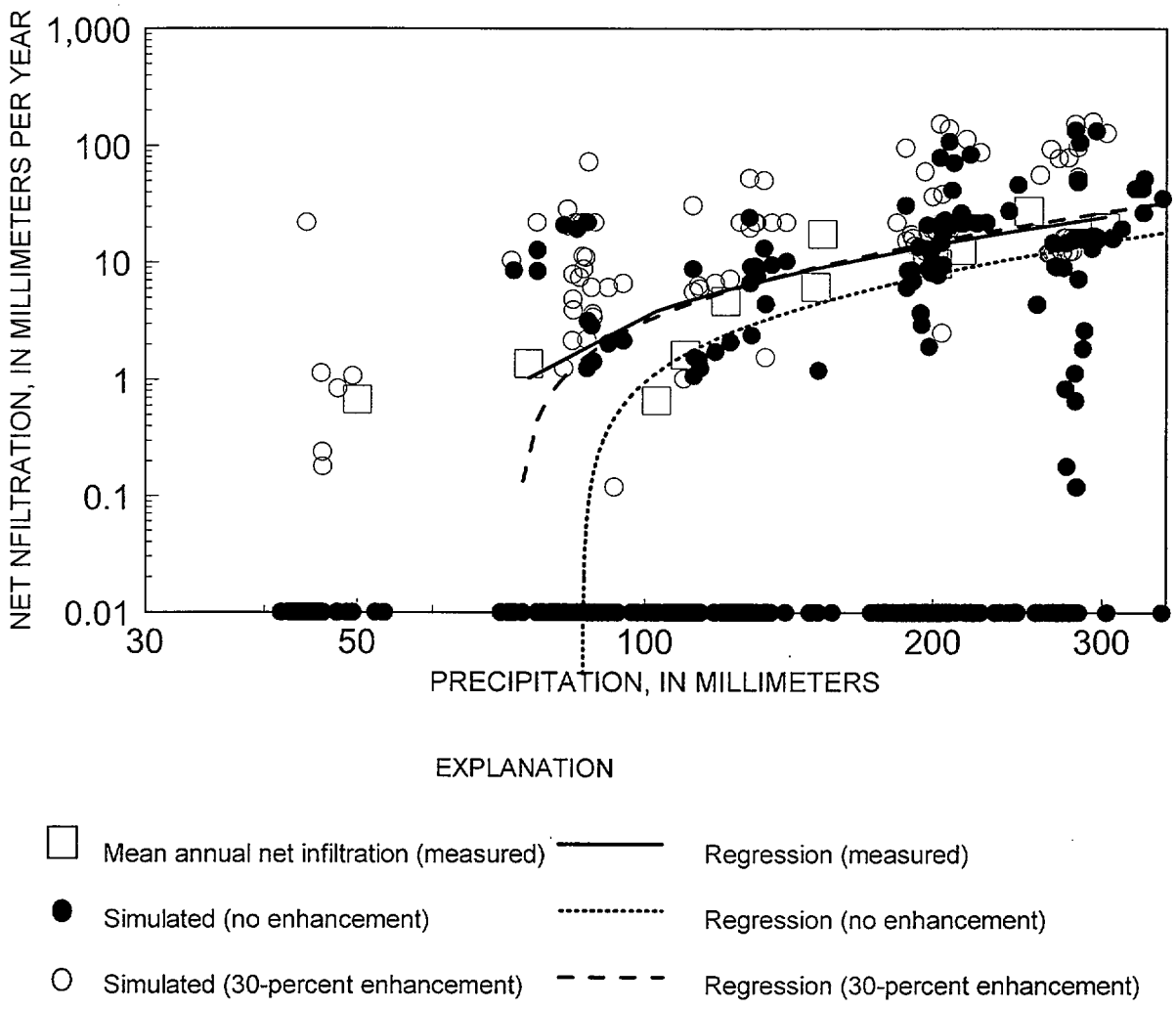

Figure 6-22. Graph of precipitation (DTN: GS000208311221.002) relative to infiltration simulated for each borehole with no channel-enhancement factor and with 30-percent channel-enhancement factor, and mean annual infiltration (DTN: GS960508312212.008) for all boreholes.

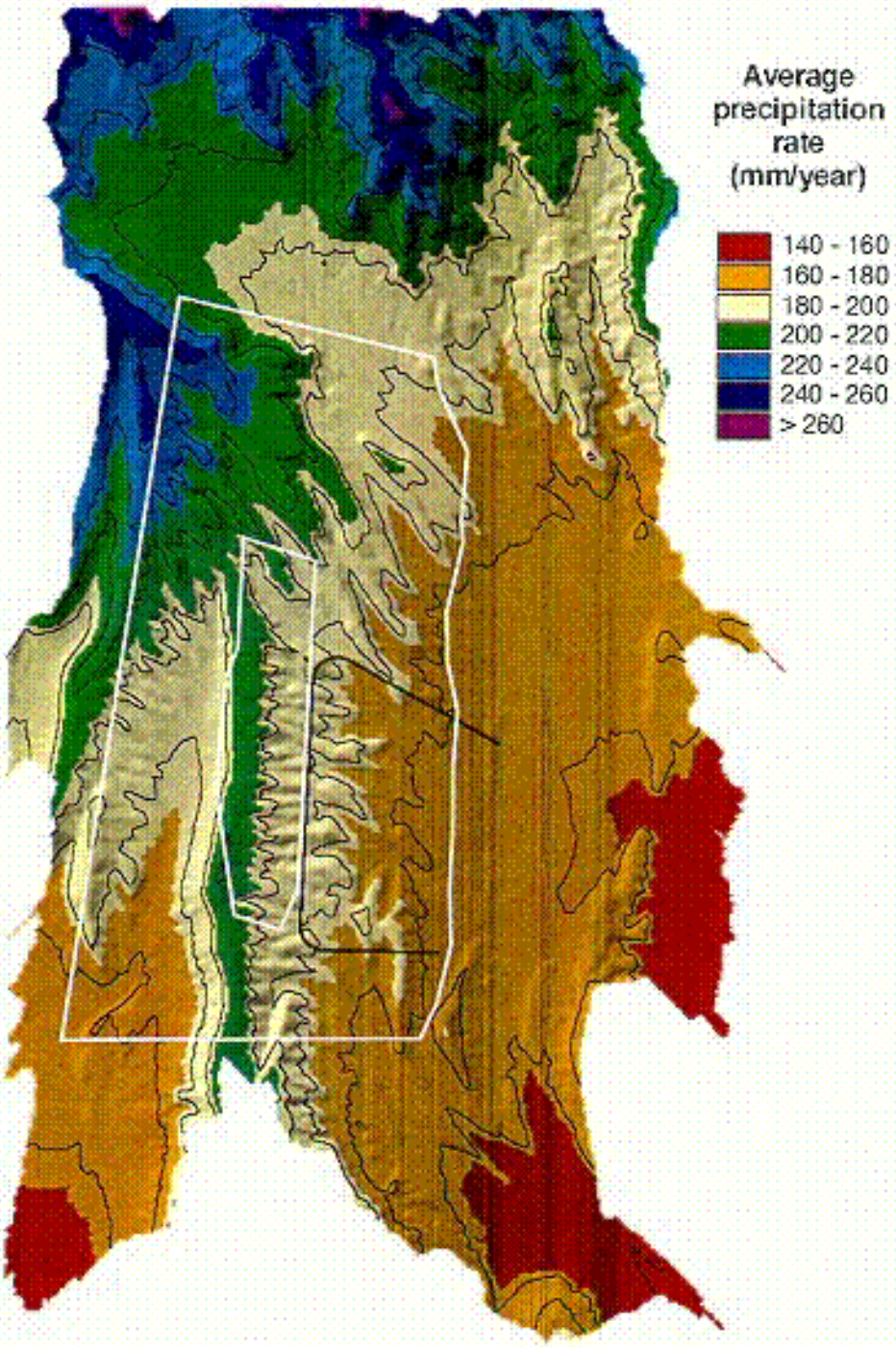

Figure 6-23. Estimated precipitation (mm/year) for the mean modern climate scenario (DTN: GS000208311221.001).

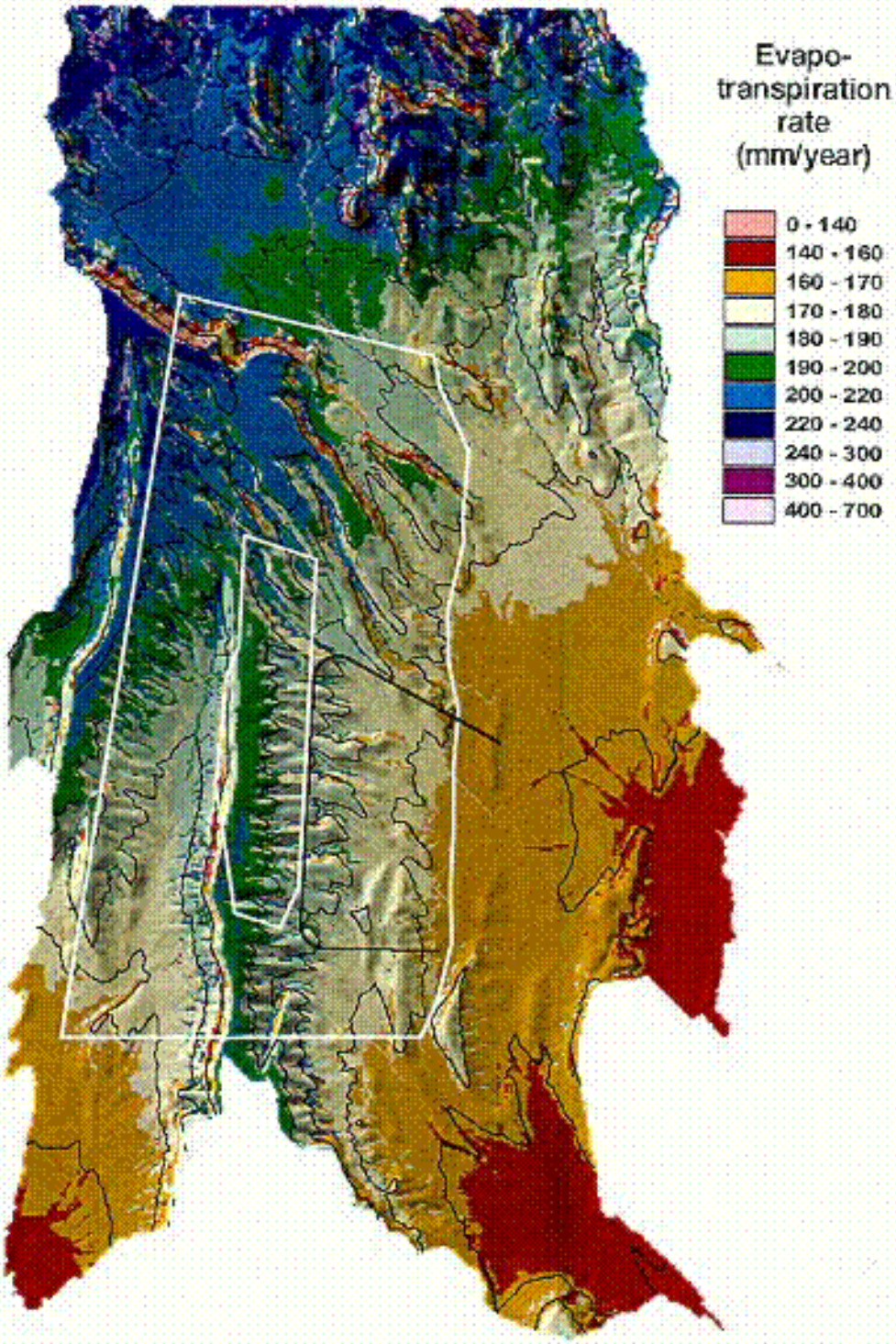

Figure 6-24. Estimated evapotranspiration (mm/year) for the mean modern climate scenario (DTN: GS000308311221.005).

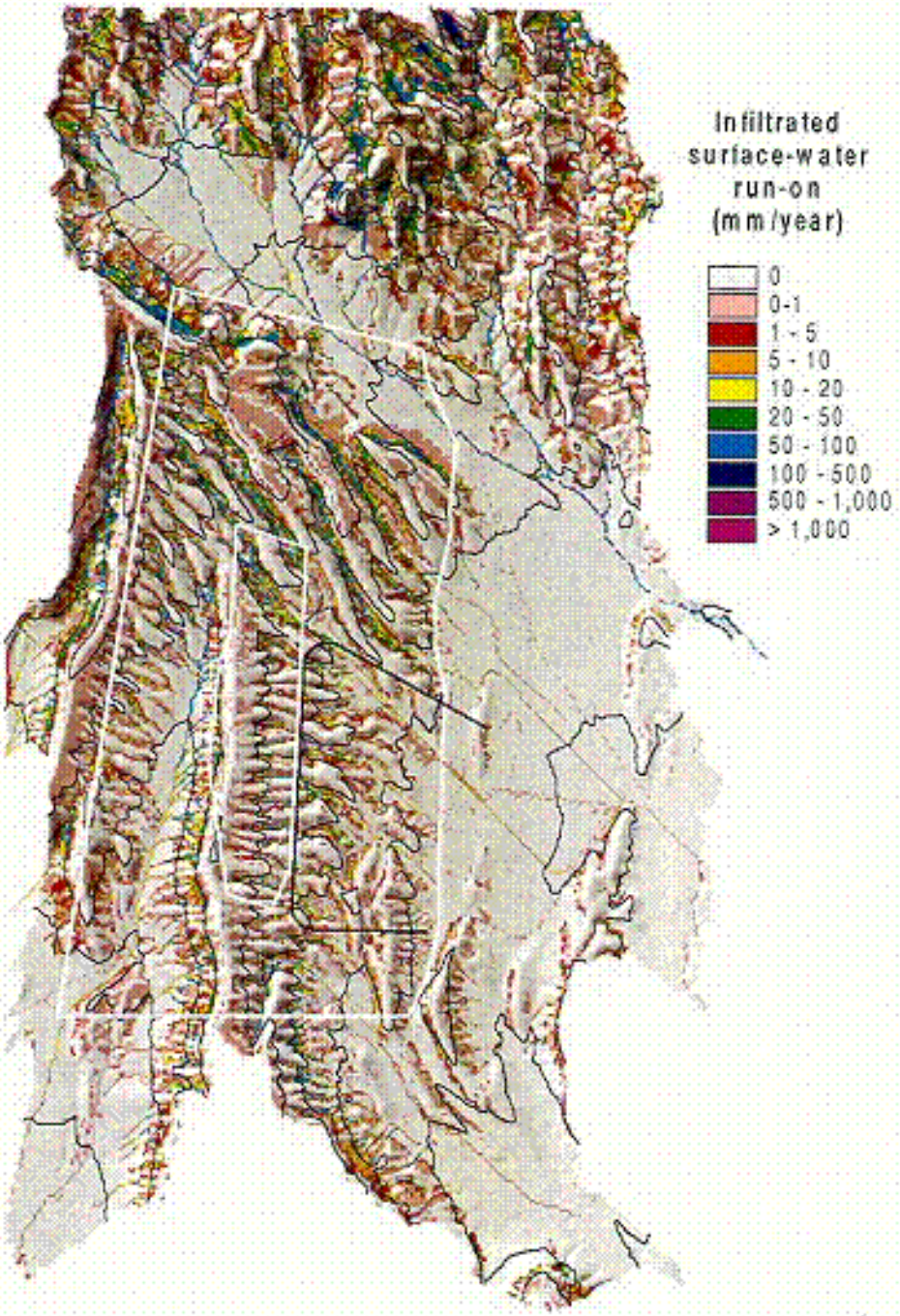

Figure 6-25. Estimated surface-water run-on depth (mm/year) for the mean modern climate scenario (DTN: GS000308311221.005).

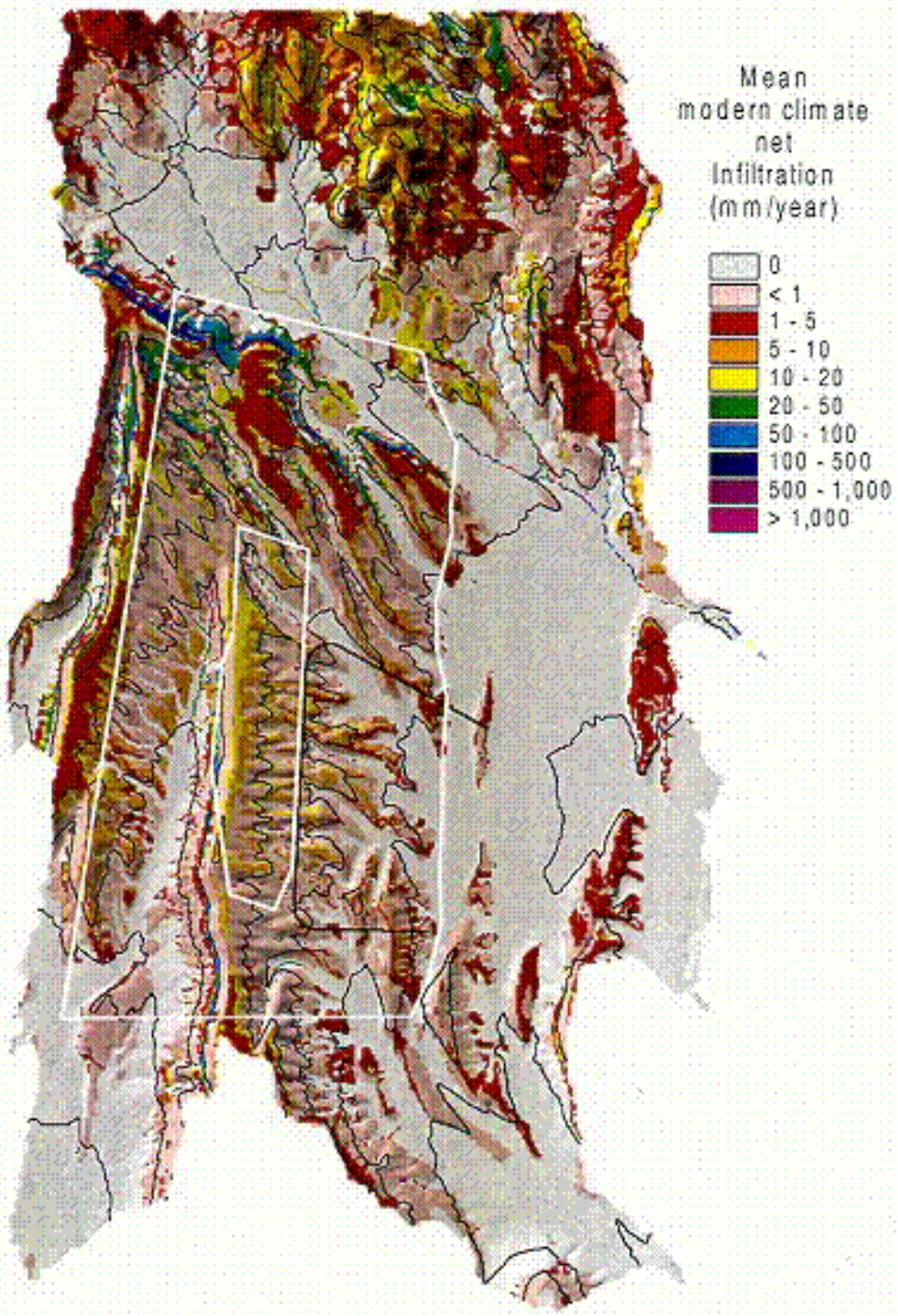

Figure 6-26. Estimated net infiltration (mm/year) for the mean modern climate scenario (DTN: GS000308311221.005).

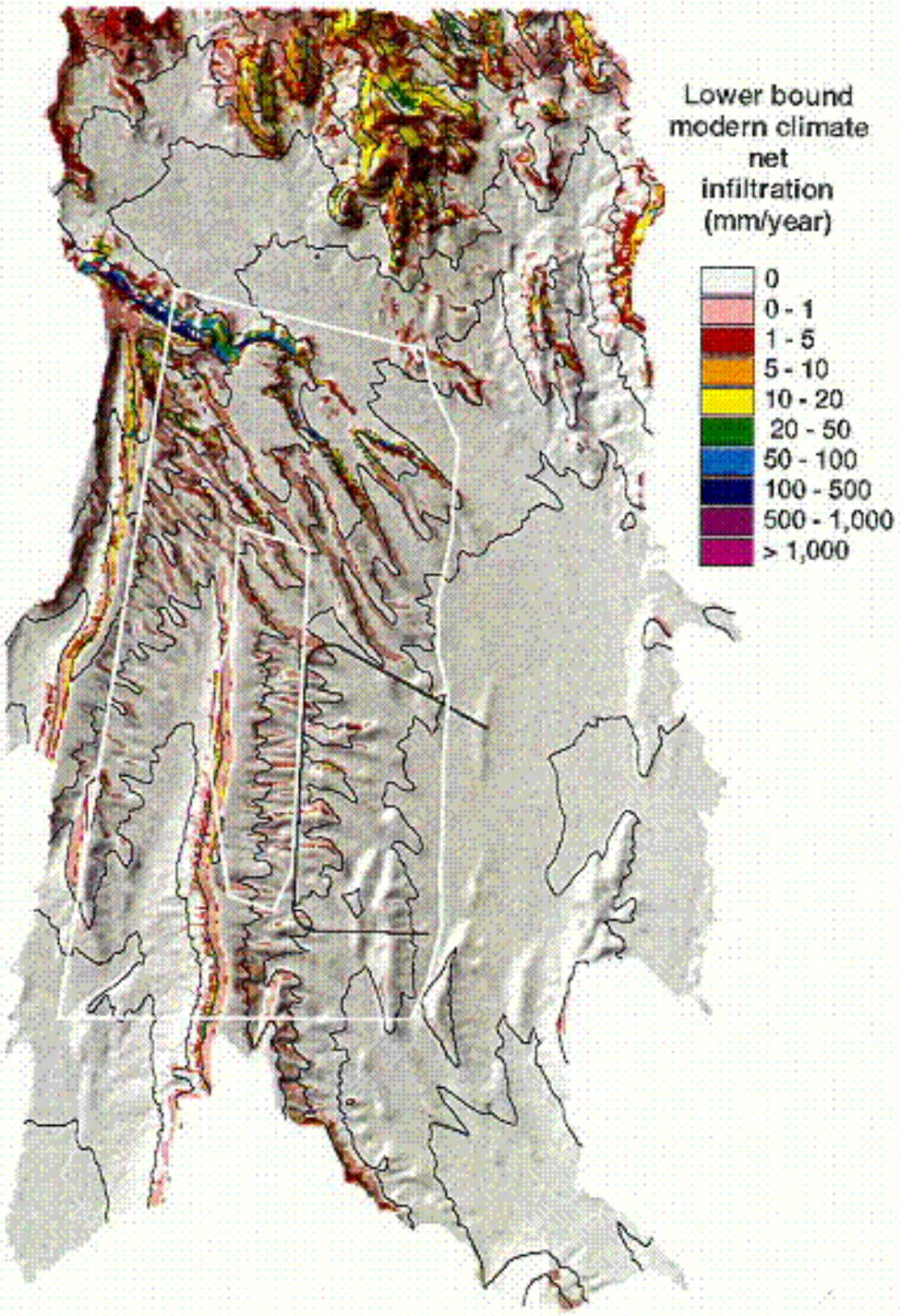

Figure 6-27. Estimated net infiltration (mm/year) for the lower bound modern climate scenario (DTN: GS000308311221.005).

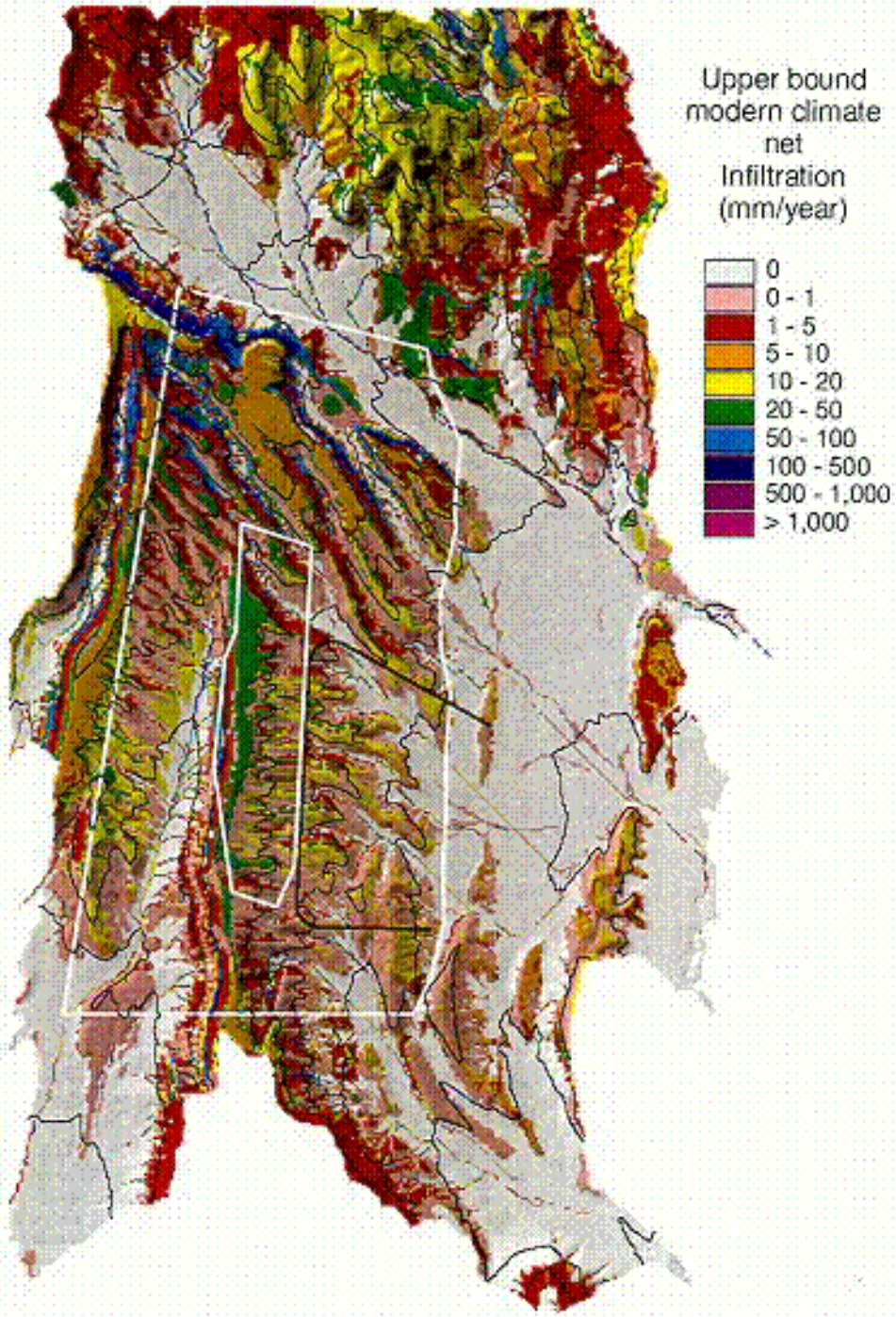

Figure 6-28. Estimated net infiltration (mm/year) for the upper bound modern climate scenario (DTN: GS000308311221.005).

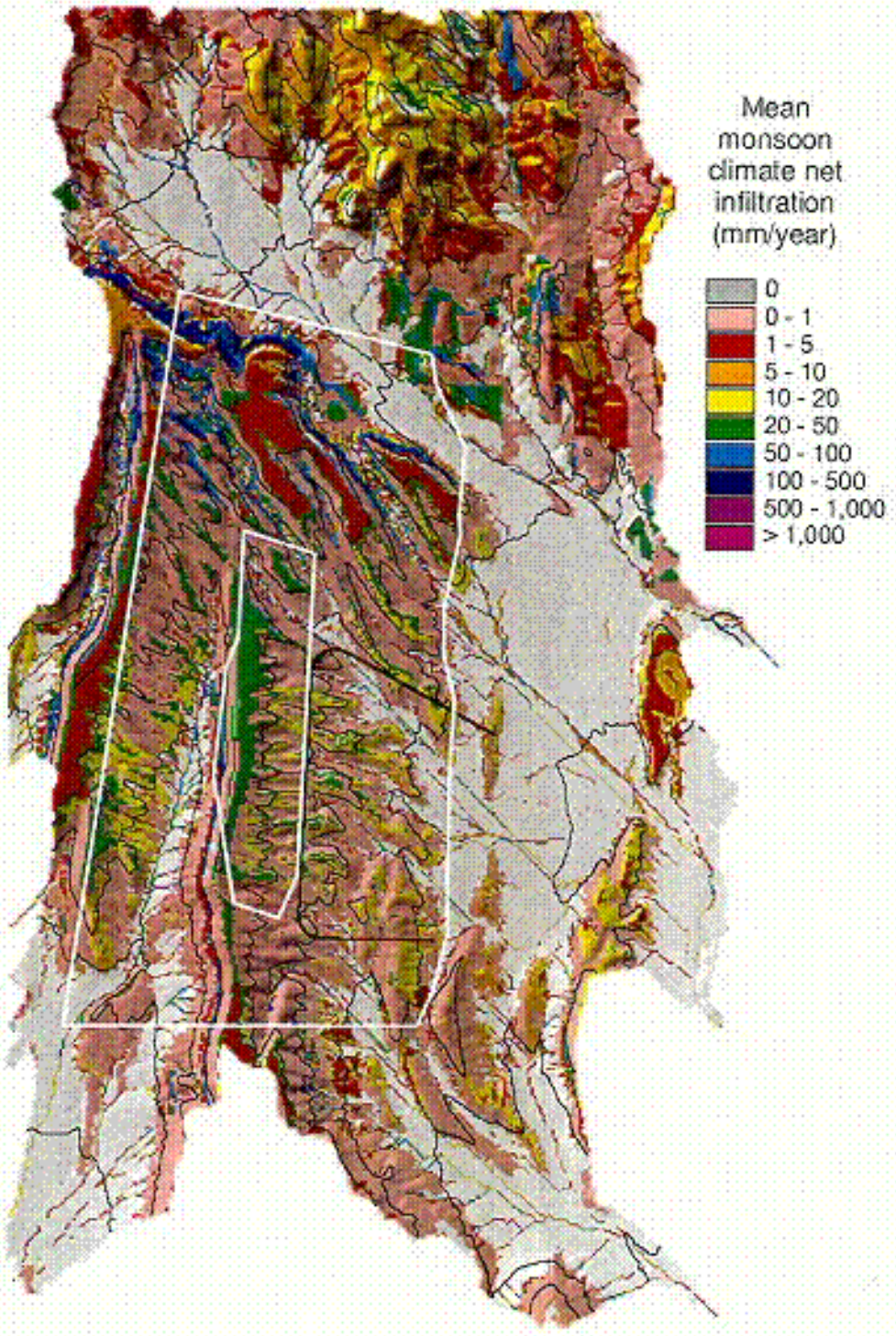

Figure 6-29. Estimated net infiltration (mm/year) for the mean monsoon climate scenario (DTN: GS000308311221.005).

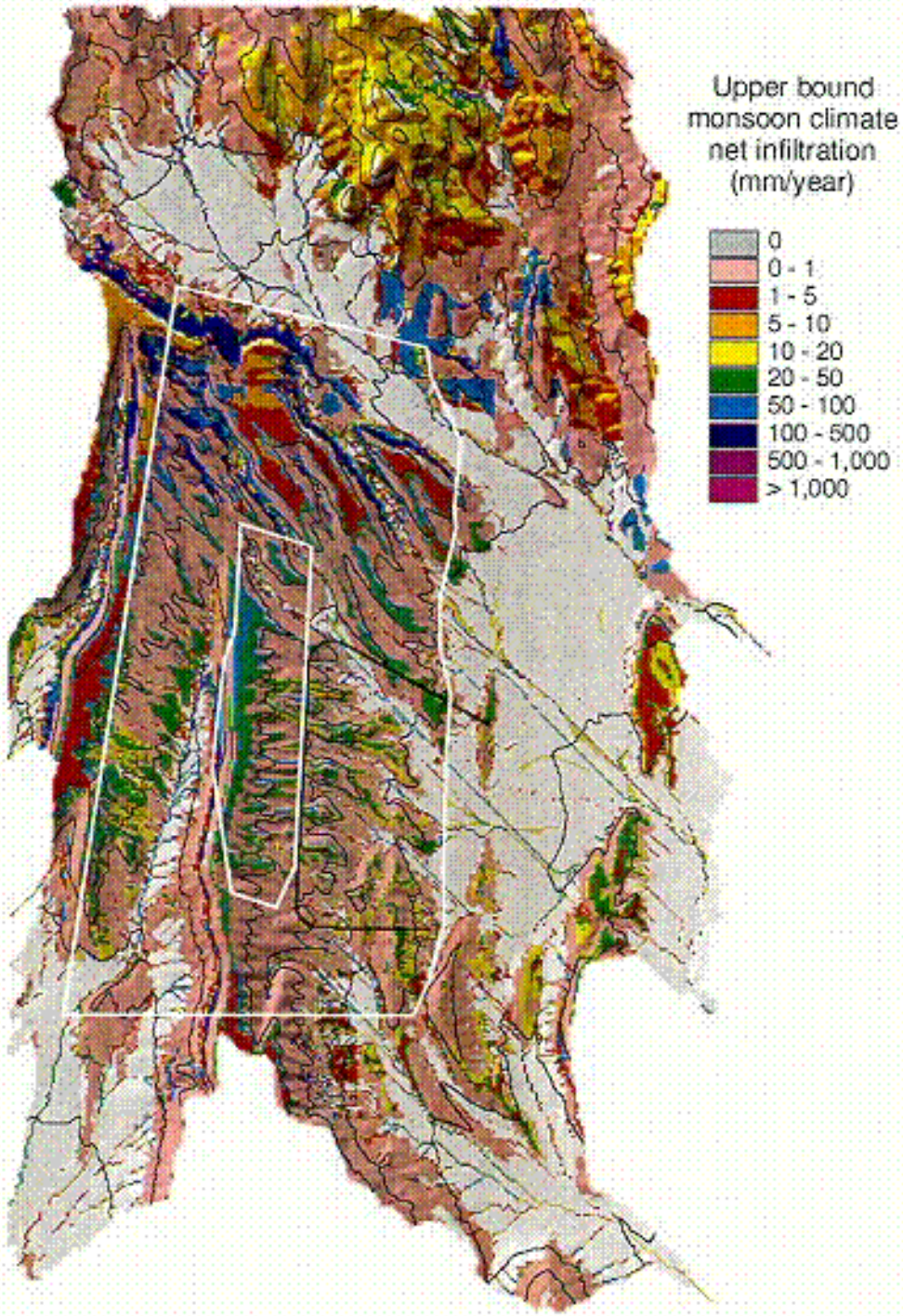

Figure 6-30. Estimated net infiltration (mm/year) for the upper bound monsoon climate scenario (DTN: GS000308311221.005).

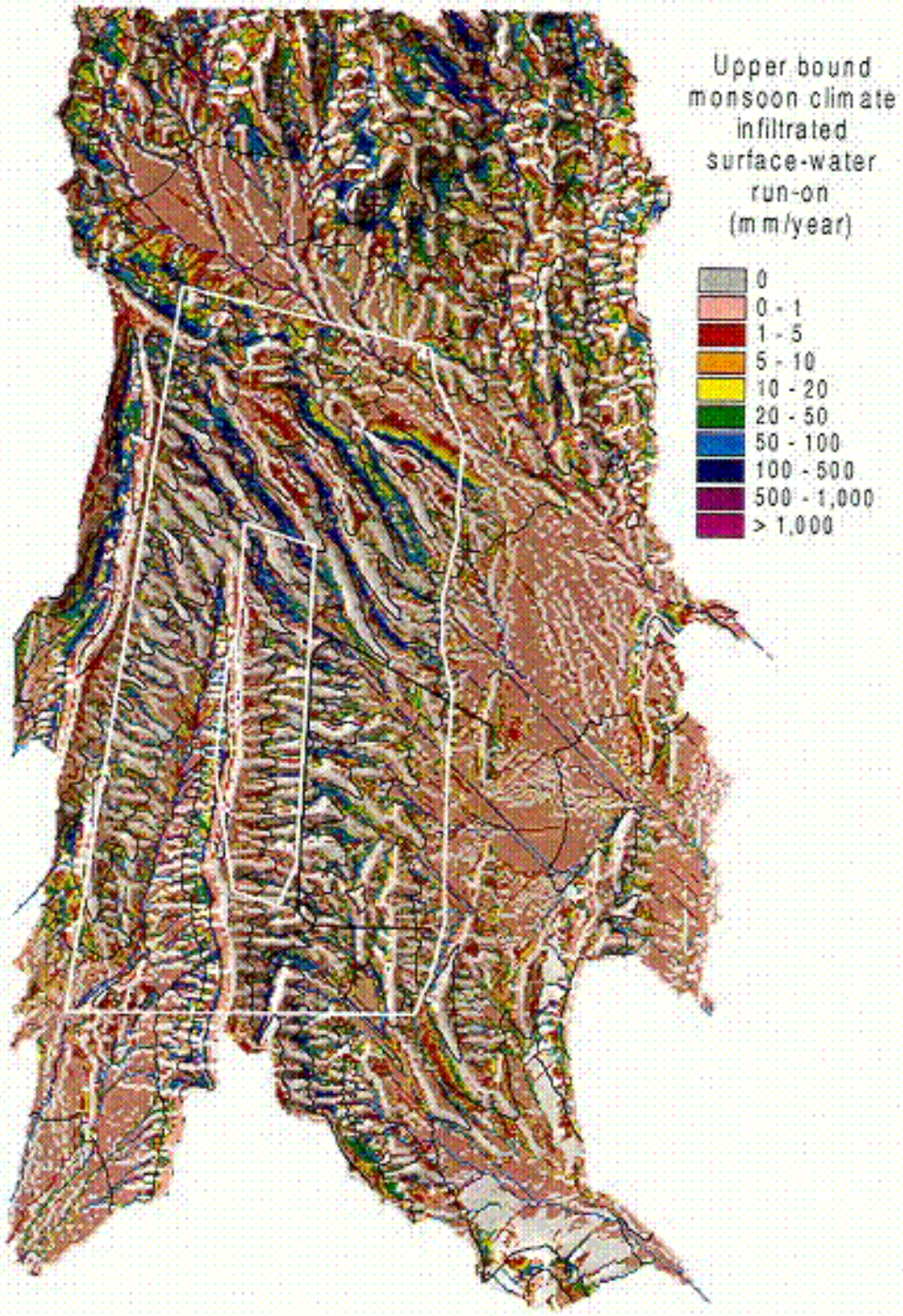

Figure 6-31. Infiltrated surface-water run-on depth (mm/year) for the upper bound monsoon climate scenario (DTN: GS000308311221.005).

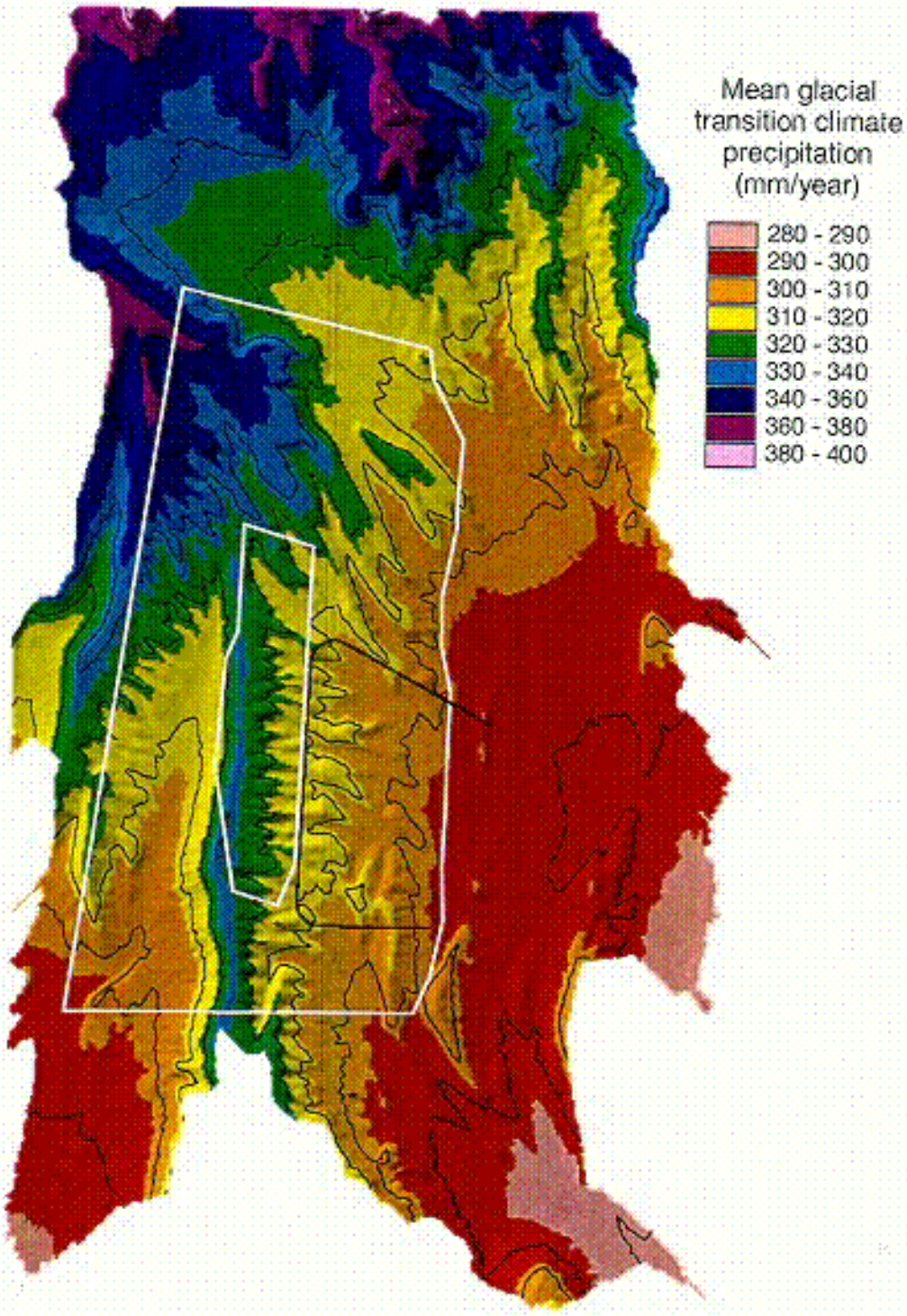

Figure 6-32. Precipitation (mm/year) for the mean glacial transition climate scenario (DTN: GS000208311221.002).

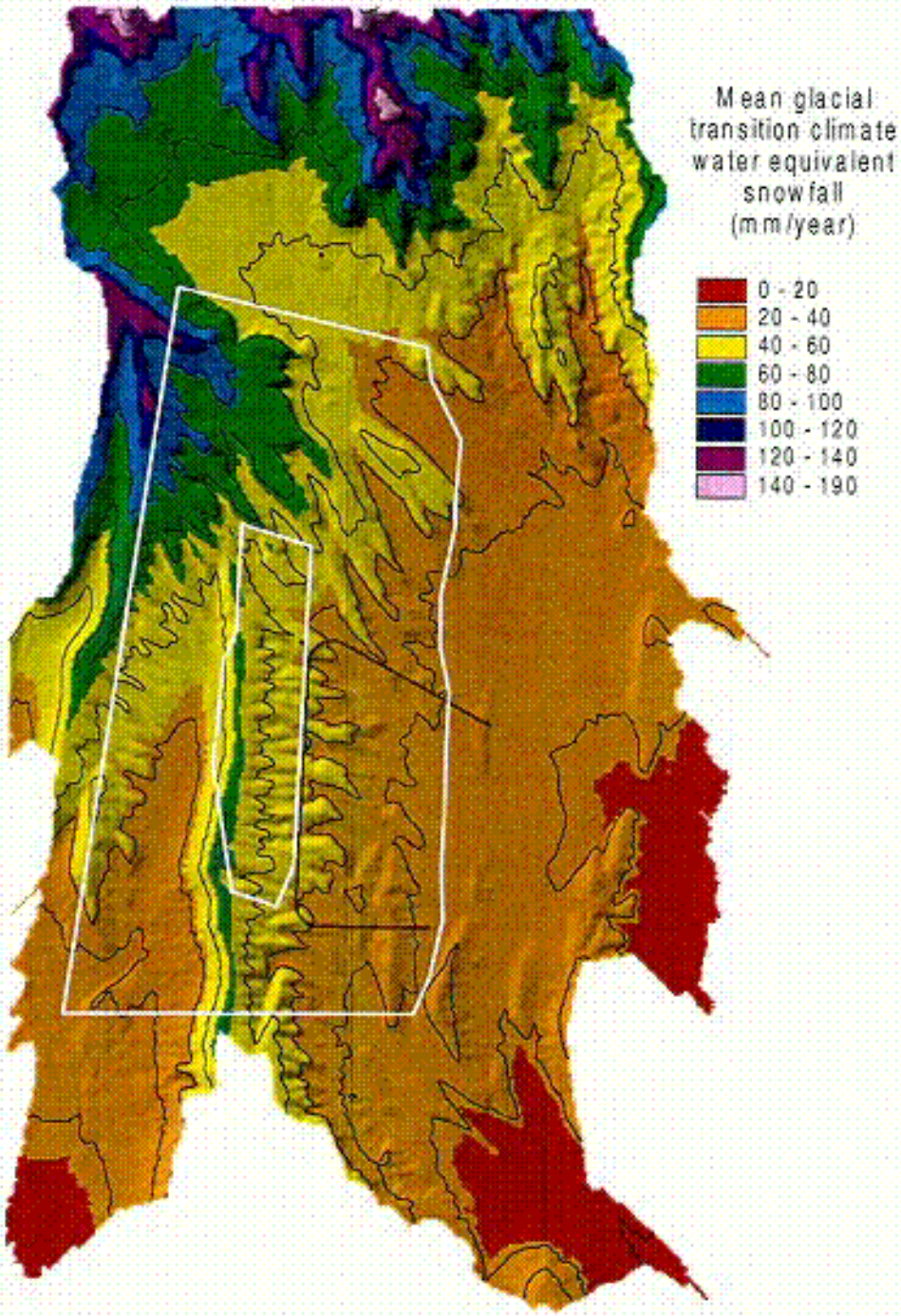

Figure 6-33. Water-equivalent snowfall depth (mm/year) for the mean glacial transition climate scenario (DTN: GS000308311221.005).

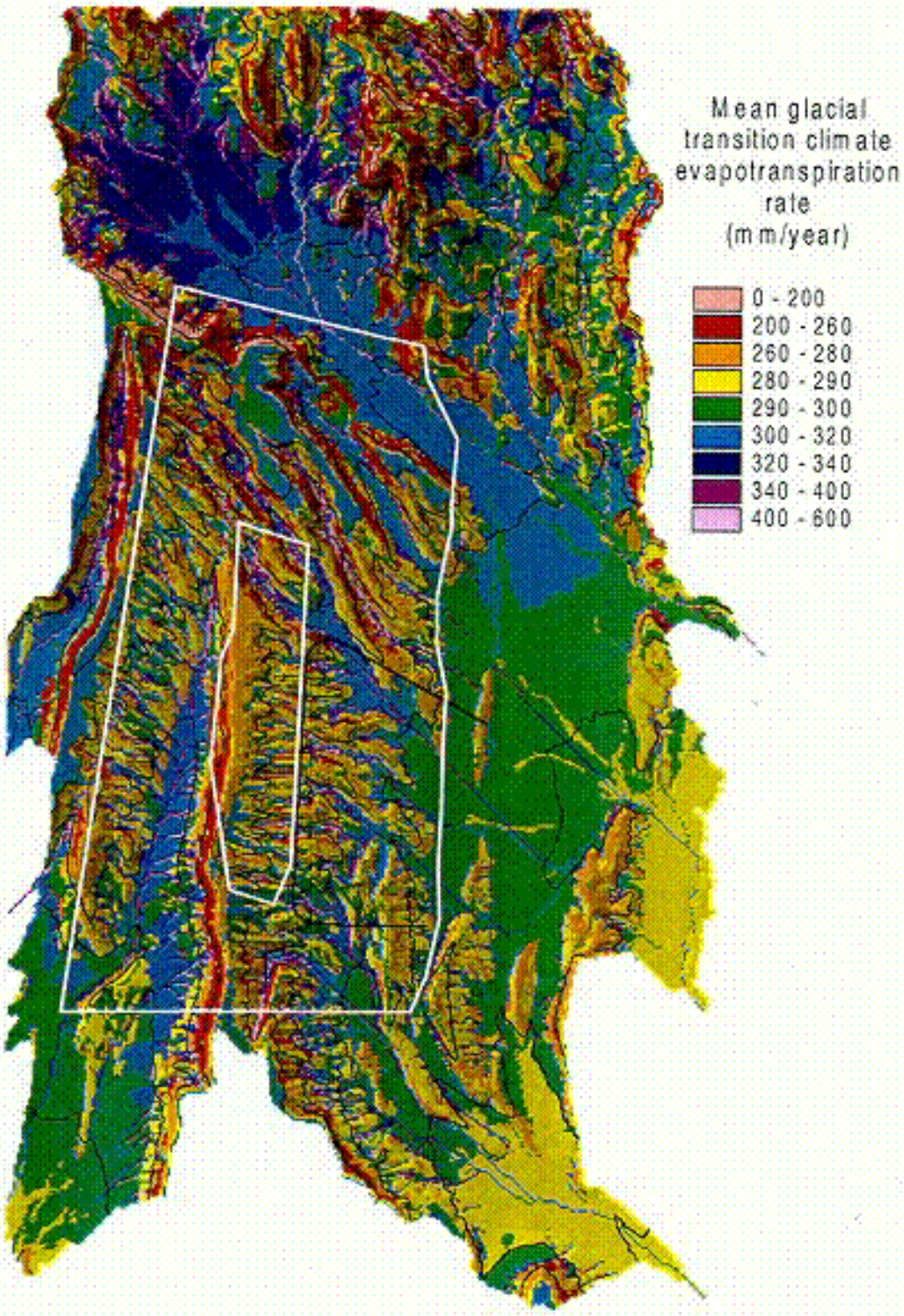

Figure 6-34. Evapotranspiration (mm/year) for the mean glacial transition climate scenario (DTN: GS000308311221.005).

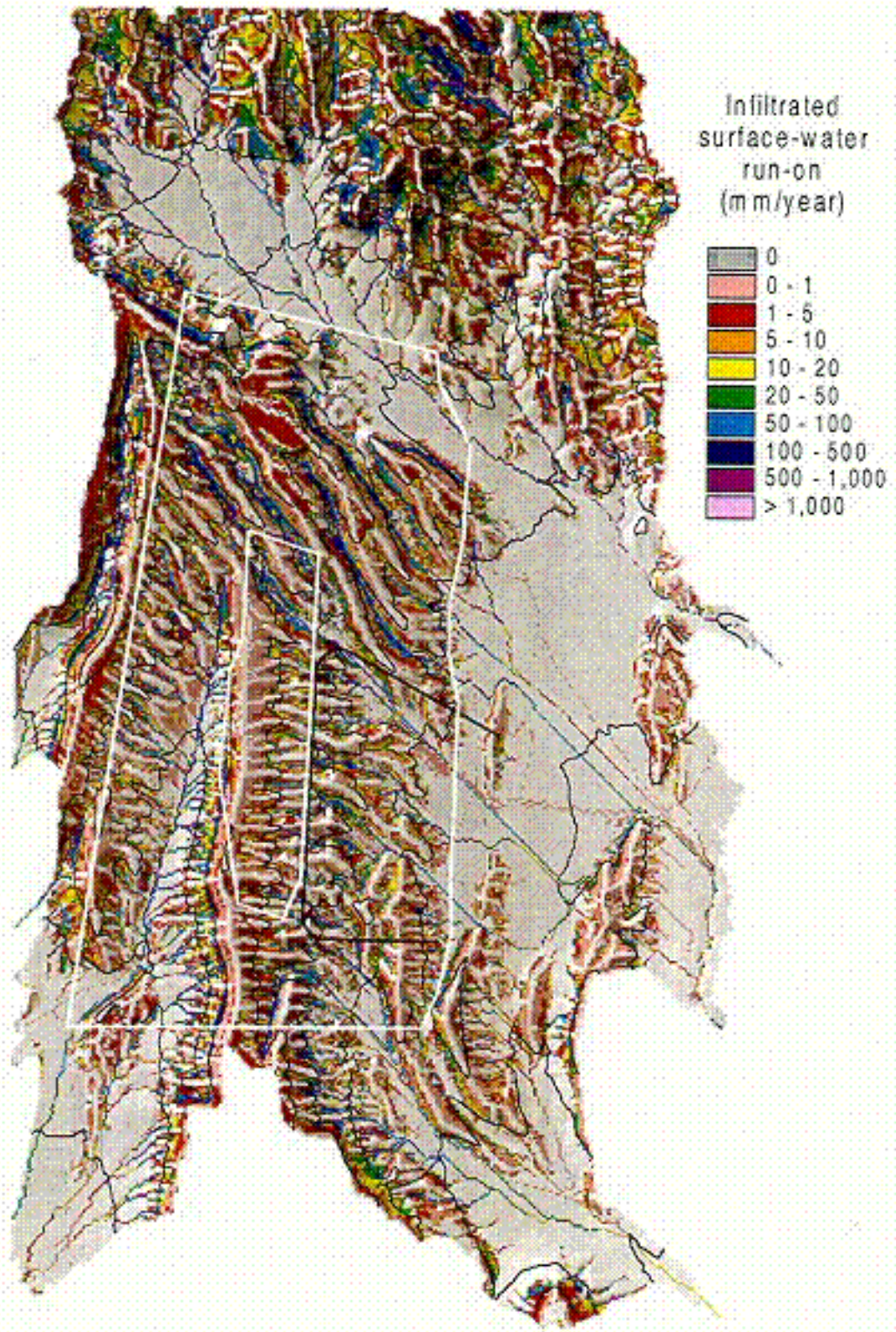

Figure 6-35. Estimated infiltrated surface-water run-on depth (mm/year) for the mean glacial transition climate scenario (DTN: GS000308311221.005).

C24

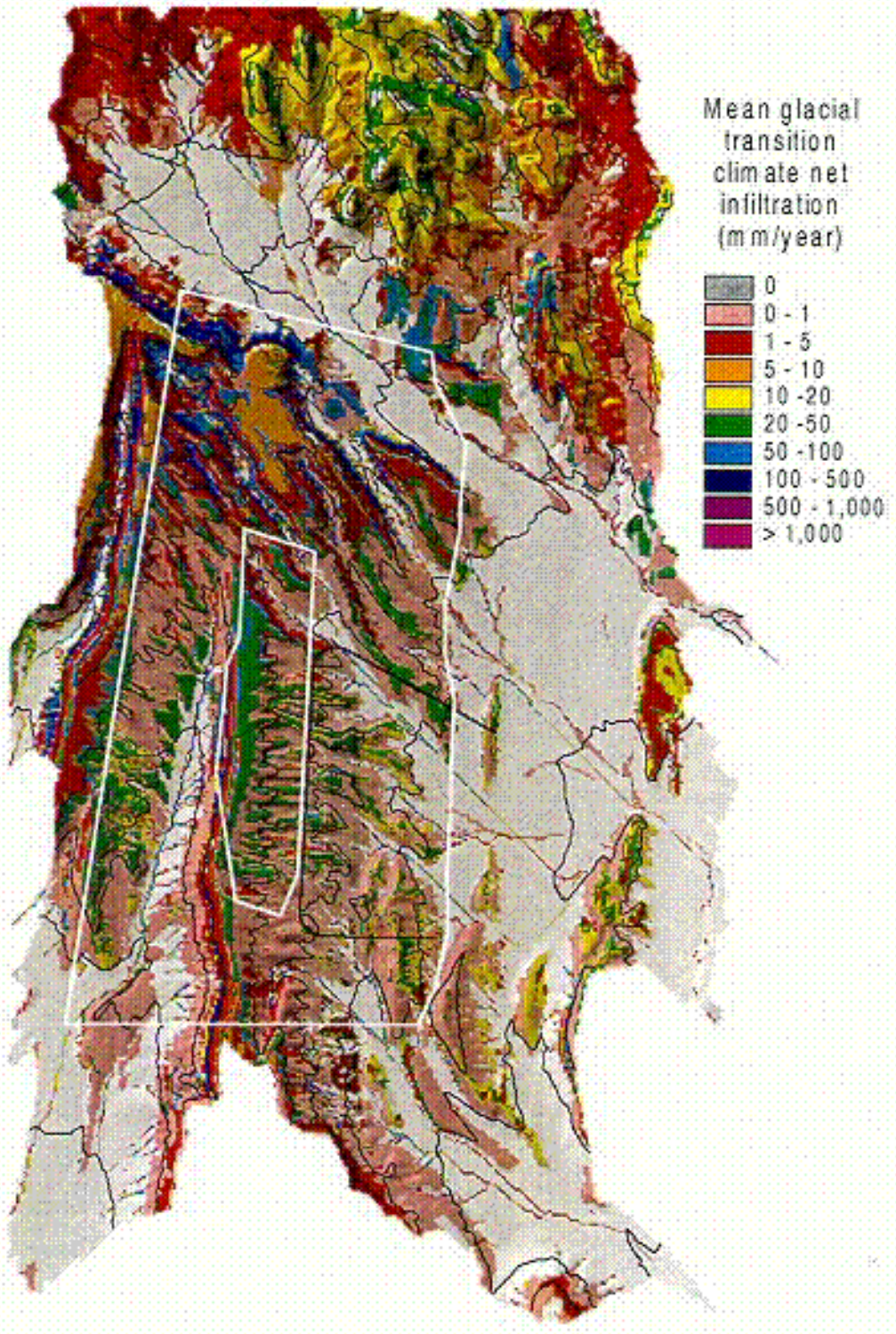

Figure 6-36. Estimated net infiltration (mm/year) for the mean glacial transition climate scenario (DTN: GS000308311221.005).

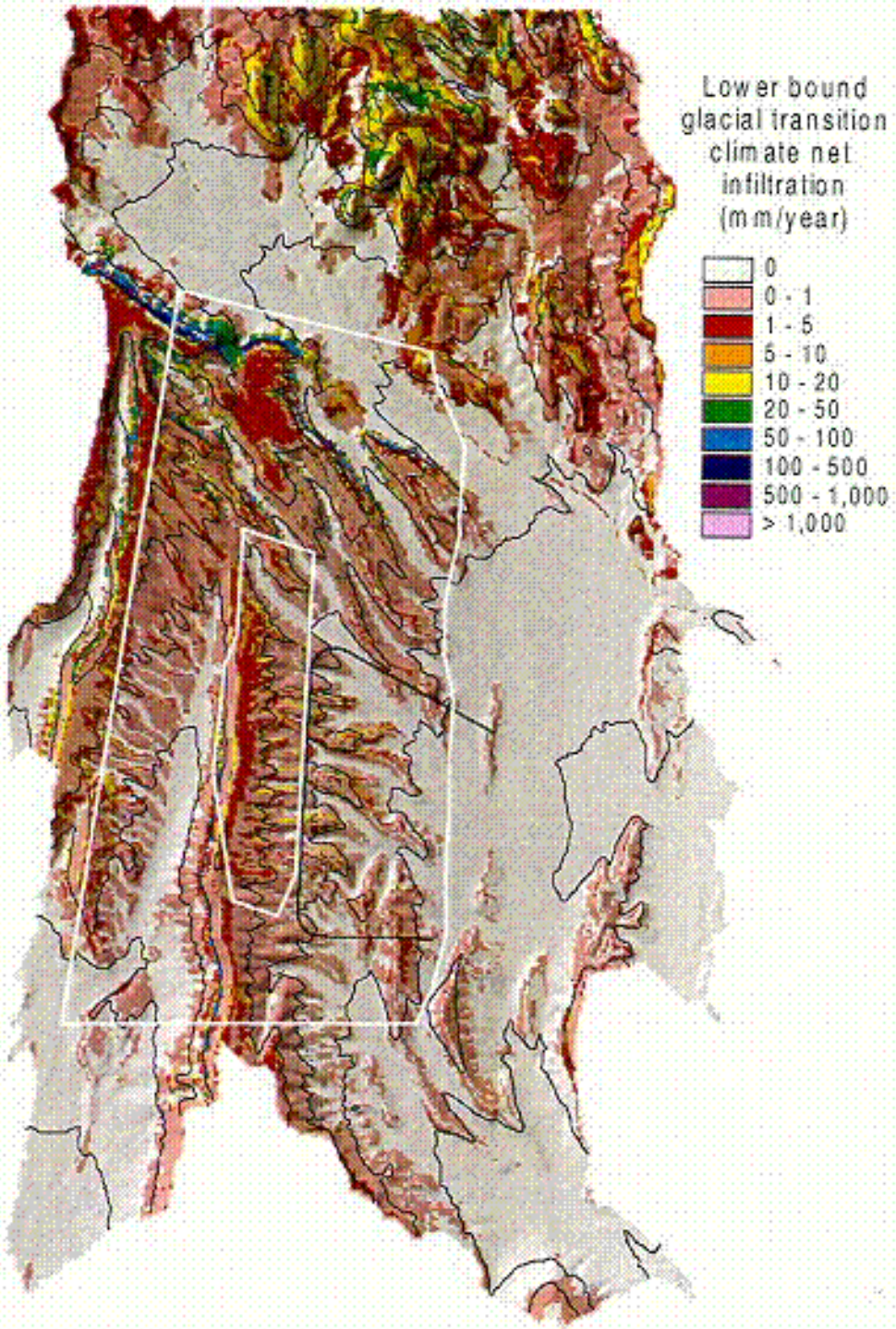

Figure 6-37. Estimated net infiltration (mm/year) for the lower bound glacial transition climate scenario (DTN: GS000308311221.005).

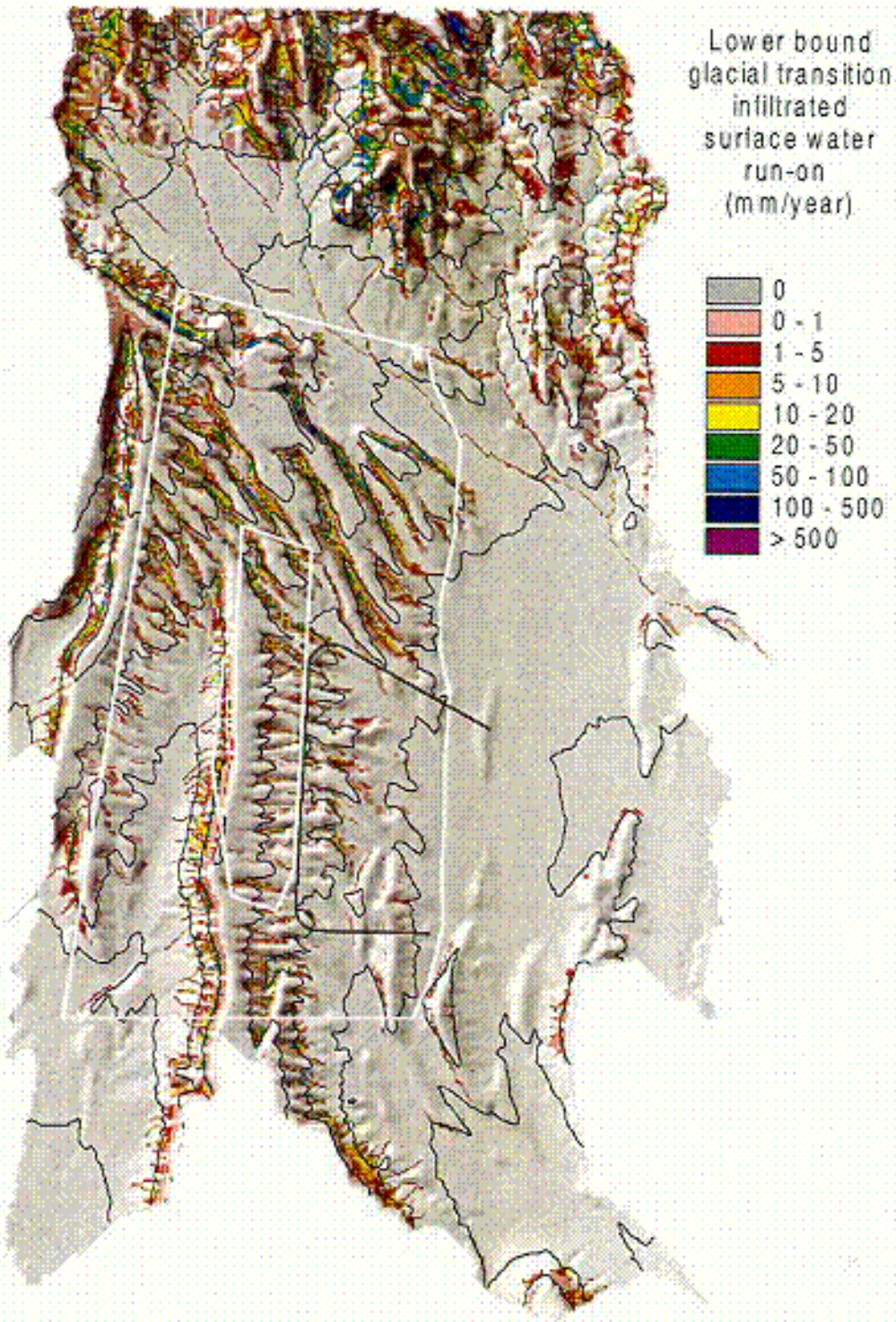

Figure 6-38. Estimated infiltrated surface-water run-on depth (mm/year) for the lower bound glacial transition climate scenario (DTN: GS000308311221.005).

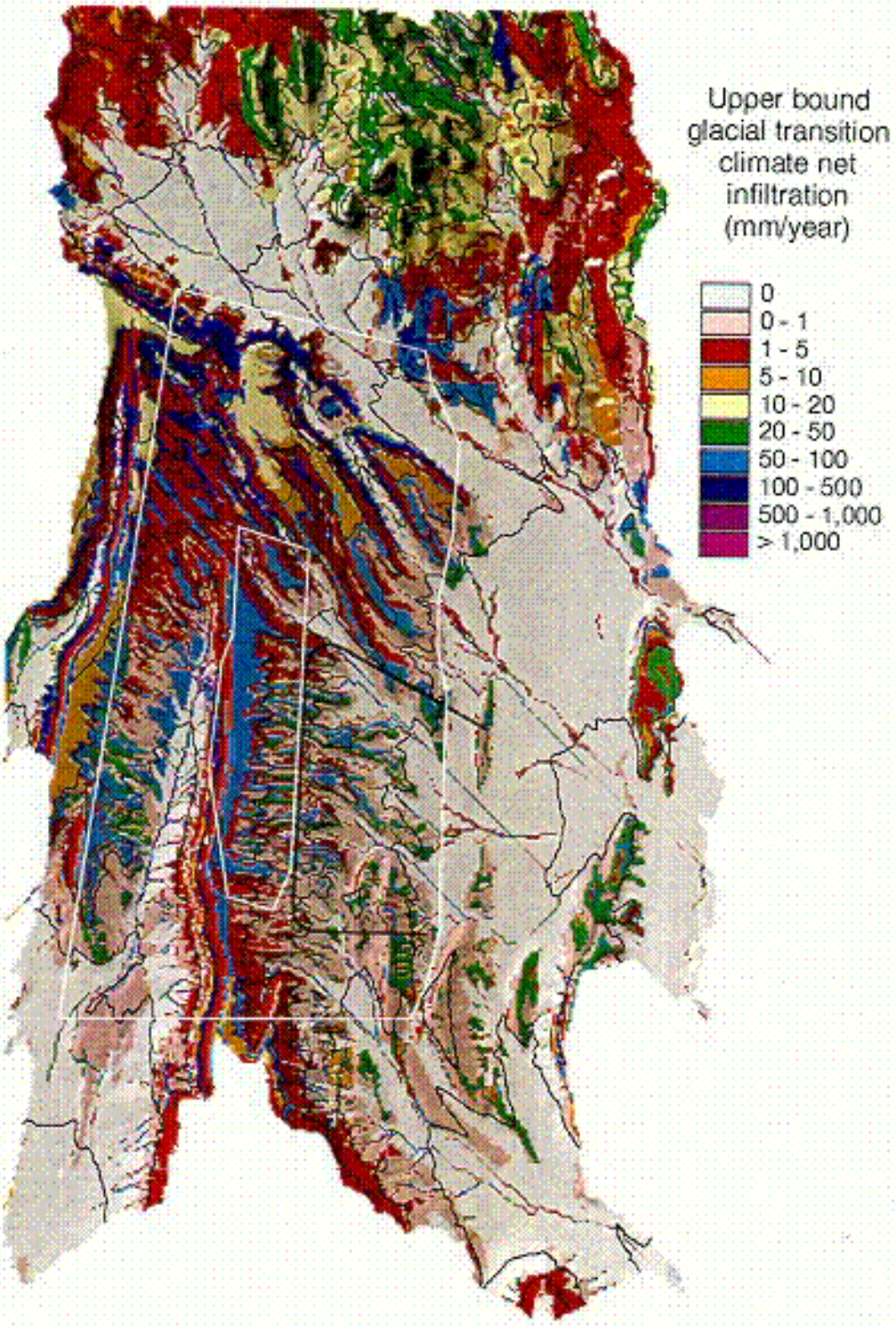

Figure 6-39. Estimated net infiltration (mm/year) for the upper bound glacial transition climate scenario (DTN: GS000308311221.005).

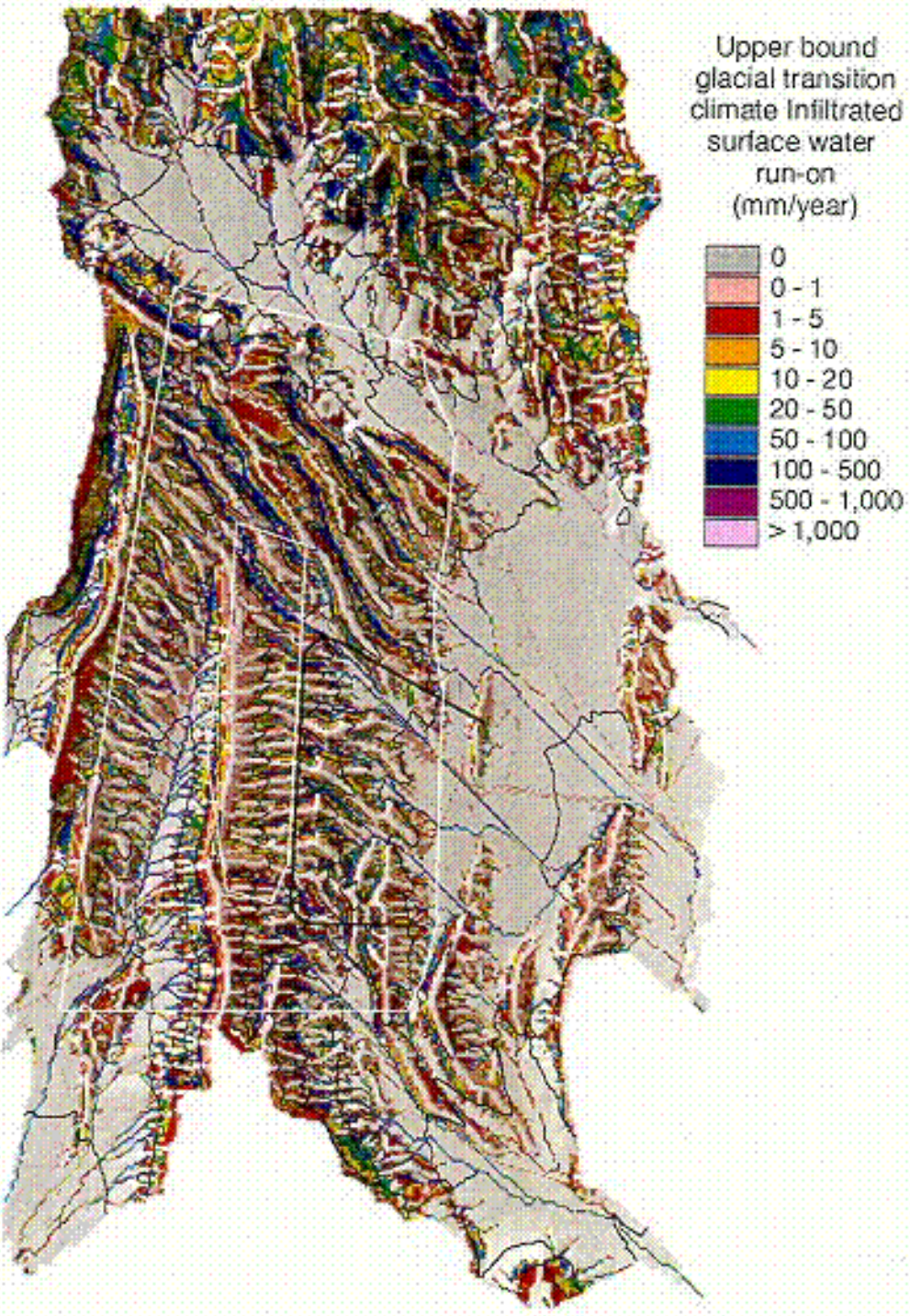

Figure 6-40. Estimated infiltrated surface-water run-on depth (mm/year) for the upper bound glacial transition climate scenario (DTN: GS000308311221.005).

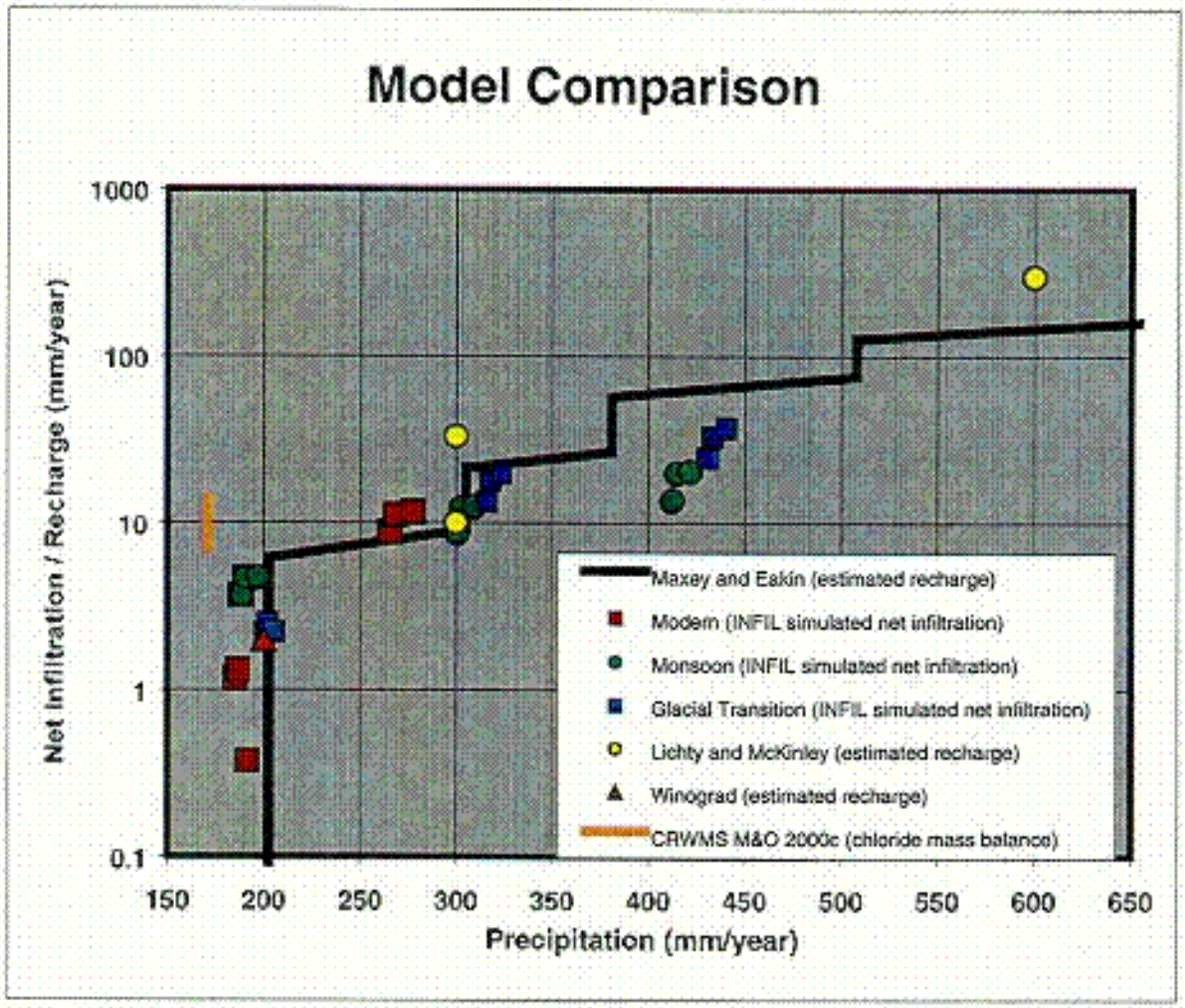

Figure 6-41. Comparison of INFIL V2.0 simulated average net-infiltration rates (DTN: GS000308311221.005) at Yucca Mountain (upper bound, lower bound, and mean for three climates) with an estimate of the average Holocene recharge rate for the saturated zone at Yucca Mountain [CRWMS M&O, 2000c] and with estimates of recharge in the southern Great Basin obtained using alternative methods (Maxey and Eakin, 1950; Lichty and McKinley, 1995; Winograd, 1981).

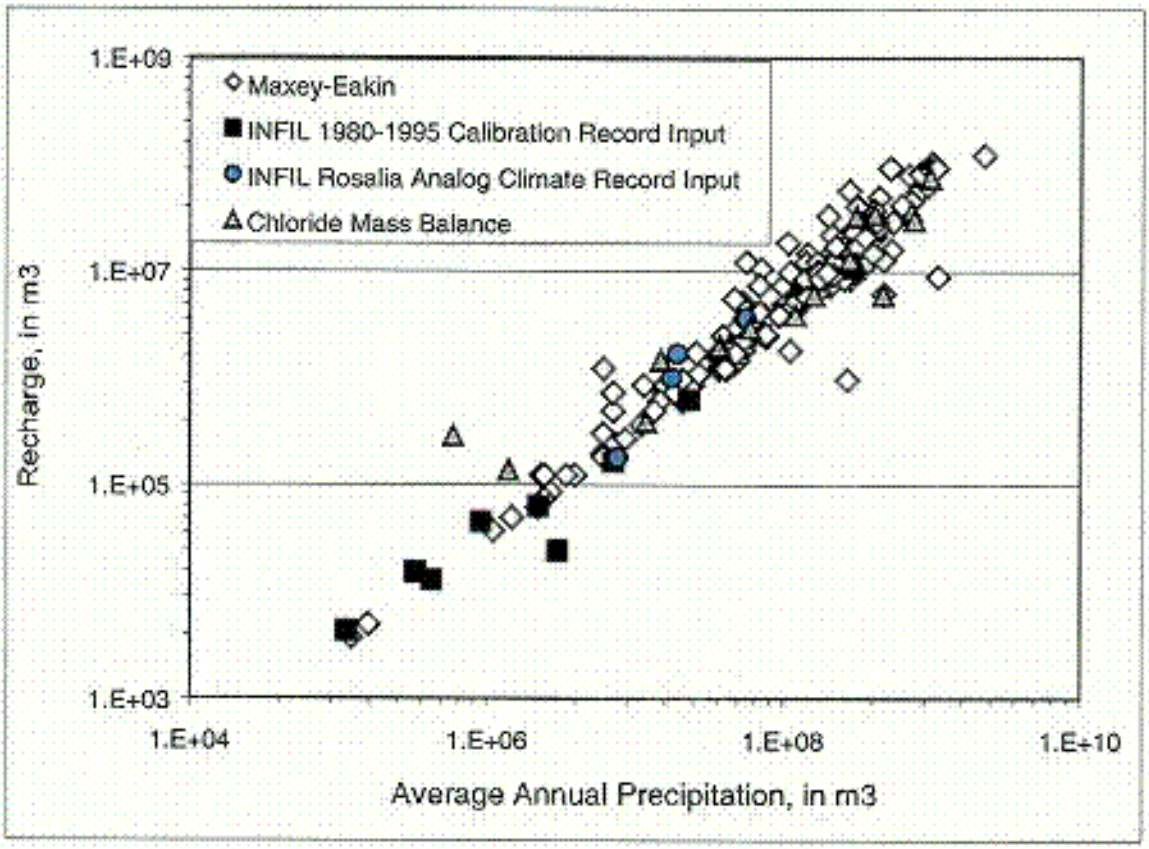

Figure 6-42. Comparison of various methods to estimate recharge in the Death Valley region and Yucca Mountain with model results from INFIL V2.0 (DTN: GS000308311221.005), as a function of average annual precipitation.

ATTACHMENT III

YUCCA MOUNTAIN 1980-95 DEVELOPED DAILY PRECIPITATION RECORD

TOTAL PAGES: 30

Yucca Mountain 1980-95 Developed Daily Precipitation Record

1. Statement of Intended Use for the Data

The purpose of these data is to provide a temporal record of precipitation at one point on Yucca Mountain for the time period 1980 through 1995. These data represent a point near the center of Yucca Mountain approximately 1400 m in elevation and will be used to spatially distribute precipitation over the site area using correlations with elevation in order to (1) calibrate the net infiltration model, and (2) develop net infiltration results for the modern climate scenarios, which are used as input for UZ ground-water flow and transport models for TSPA.

2. General Information Pertaining to the Data Set

The climate input file used for model calibration, MOD3-PPT.DAT, is the same developed daily precipitation record that was used for calibration of the original 1996 (INFIL V1.0) net infiltration model for Yucca Mountain (Flint et al., 1996, Figure 19, DTN: GS960908312211.003). The file MOD3-PPT.DAT consists of daily precipitation estimates only and was developed using source data of daily precipitation records from 1980 through 1995.

A. Source data (all data used is shown in Excel file MOD3-PPT.xls)

USGS Yucca Mountain precipitation data from weatherstations WX1 and WX3.
GS960908312111.004 (1995 water year)
GS970108312111.001 (Oct. 1- Dec. 3, 1995)
GS000208312111.003 (1987-1989, non-Q)
GS000208312111.001 (1989-1994)

Nevada Test Site (NTS) precipitation data for stations 4JA, 40MN, Rock Valley, Cane Spring, Mid Valley and Tippipah Spring #2. These data are accepted data and available in DTN: GS000200001221.002.

National Weather Service (NWS) stations at Beatty 8N and Amargosa Farms, from the National Climate Data Center and available through EarthInfo, accepted data, DTN: GS000100001221.001, MO9811NC (TIC: 245534).

B. Development of daily precipitation record

The developed record of daily precipitation is only an approximate representation of actual conditions over the general location and ground surface elevation of the potential repository area. Daily precipitation estimates for 1988 through 1995 were developed using the mean of the data from the Yucca Mountain weatherstations. For 1980 through 1987, daily precipitation was estimated using a linear interpolation model and available precipitation records from the six Nevada Test Site (NTS) monitoring sites and the two National Weather Service (NWS) monitoring sites located near Yucca Mountain. The model was developed using linear regression of a weighted mean daily precipitation calculated from the eight

stations against the mean calculated from the two USGS weather stations for the period July 17, 1987 through September 30, 1994 (this is the period for which the two sets of records overlapped).

Table III-1 is the developed data precipitation record for Yucca Mountain that was used directly as input for INFIL V2.0. There is an EXCEL spreadsheet used to generate the developed data that is available in DTN: GS000208311221.001, and an identical spreadsheet formatted to display the formulas that can be printed out as hard copies.

Mod3-ppt1.xls: EXCEL spreadsheet used to perform calculations for developing mod3-ppt.dat, with values in cells shown.

Mod3-ppt2.xls: EXCEL spreadsheet used to perform calculations for developing mod3-ppt.dat, with formulas in cells shown.

3. Spreadsheet calculations

Calculations in the spreadsheet MOD3-PPT.xls are done following a series of steps outlined in the first sheet of the file, and reiterated here.

Step 1: average daily precipitation is calculated for USGS weather stations WX1 and WX3 for the period July 17, 1987 through September 30, 1994. For gaps in the record, a value of zero is estimated.

Step 2: Average annual precipitation is calculated for the six NTS stations and two NWS stations for all records beginning on July 17, 1987 and ending on September 30, 1994. This period of time coincides with the period for which precipitation data is available for USGS weather stations WX1 and WX3 (either stations). For all eight stations, the ratio $B_i = AAP_o/AAP_i$ is calculated, where AAP_i = average annual precipitation for the period July 17, 1987 – July 30, 1994 for station i, and AAP_o = mean average annual precipitation for USGS weather stations WX1 and WX3 (calculated in step 1), rounded to the nearest millimeter. The ratio is then used to scale the daily precipitation records for all eight stations using $PPT_i^* = B_i(PPT_i)$, where B_i is the scaling factor, PPT_i is the original daily precipitation record for station i, and PPT_i is the adjusted daily precipitation record. The scaling function is applied to all eight stations for 1/1/80 through 12/31/94.

Step 3: An inverse-distance-squared interpolation is performed to estimate the mean daily precipitation for WX1 and WX3 for the period July 17, 1987 – July 30, 1994. The inverse distance squared interpolation involves the calculation of a linear weighting factor based on the distance between locations. A central location on Yucca Mountain used with UTM coordinates of 548,553 m easting, 4,078,230 m northing. The equation is:

$$\text{Weighting factor}_i = (1/d_i^2)/(\Sigma_i\,(1/(di\,_i^2))$$

where d_i is the distance of station i from the central location having the indicated coordinates. Station coordinates, calculated distances, and calculated weighting factors are listed in the spreadsheet.

Step 4: The inverse distance squared model defined in step 3 is used to calculate the daily precipitation for the location defined in step 3.

Step 5: A linear model, based on a regression of measured precipitation vs. the adjusted daily precipitation record (the inverse-distance-squared interpolated precipitation), is applied to the results of the inverse-distance-squared interpolation for the period January 1, 1980 through September 30, 1994 using:

$$PPT_{YM} = 0.946546 * ([(1/d_i^2)/\Sigma_i (1/(d_i^2))] PPT_i^*)+0.0821$$

where PPT_{YM} is the estimated daily precipitation amount (to the nearest millimeter only) for the central location defined by the coordinates in step 3, and PPT_i^* is the scaled daily precipitation amount for station i. The results of the linear model are used to define the Yucca Mountain daily precipitation estimates for January 1, 1980 through May 11, 1989 (file mod3-ppt.day). The results of step 1 (to the nearest millimeter only) are used to define the Yucca Mountain daily precipitation estimates for May 11, 1989 through October 1, 1995 (file mod3-ppt.dat).

Table III-1. Developed data precipitation record for Yucca Mountain that was used directly as input for INFIL V2.0. (data source: GS000208311221.001)

Year	Day of Year	Daily Precip-itation (mm)	Year	Day of Year	Daily Precip-itation (mm)	Year	Day of Year	Daily Precip-itation (mm)	Year	Day of Year	Daily Precip-itation (mm)	Year	Day of Year	Daily Precip-itation (mm)
80	1	0	80	74	0	80	147	0	80	220	0	80	293	0
80	2	0	80	75	0	80	148	0	80	221	0	80	294	0
80	3	0	80	76	0	80	149	0	80	222	0	80	295	0
80	4	0	80	77	0	80	150	0	80	223	0	80	296	0
80	5	0	80	78	0	80	151	0	80	224	0	80	297	0
80	6	0	80	79	0	80	152	0	80	225	0	80	298	0
80	7	0	80	80	0	80	153	0	80	226	0	80	299	0
80	8	0	80	81	0	80	154	0	80	227	0	80	300	0
80	9	13	80	82	0	80	155	0	80	228	0	80	301	0
80	10	0	80	83	0	80	156	0	80	229	0	80	302	0
80	11	8	80	84	1	80	157	0	80	230	0	80	303	0
80	12	0	80	85	0	80	158	0	80	231	0	80	304	0
80	13	1	80	86	0	80	159	0	80	232	0	80	305	0
80	14	0	80	87	0	80	160	0	80	233	0	80	306	0
80	15	0	80	88	0	80	161	0	80	234	0	80	307	0
80	16	0	80	89	0	80	162	0	80	235	0	80	308	0
80	17	0	80	90	0	80	163	0	80	236	0	80	309	0
80	18	6	80	91	0	80	164	0	80	237	0	80	310	0
80	19	2	80	92	0	80	165	0	80	238	1	80	311	0
80	20	0	80	93	0	80	166	0	80	239	0	80	312	0
80	21	0	80	94	0	80	167	0	80	240	0	80	313	0
80	22	0	80	95	0	80	168	0	80	241	0	80	314	0
80	23	0	80	96	0	80	169	0	80	242	0	80	315	0
80	24	0	80	97	0	80	170	0	80	243	0	80	316	0
80	25	0	80	98	0	80	171	0	80	244	0	80	317	1
80	26	0	80	99	0	80	172	0	80	245	0	80	318	0
80	27	0	80	100	0	80	173	0	80	246	0	80	319	0
80	28	2	80	101	0	80	174	0	80	247	0	80	320	0
80	29	11	80	102	0	80	175	0	80	248	0	80	321	0
80	30	1	80	103	0	80	176	0	80	249	0	80	322	0
80	31	0	80	104	0	80	177	0	80	250	0	80	323	0
80	32	0	80	105	0	80	178	0	80	251	3	80	324	0
80	33	0	80	106	0	80	179	0	80	252	4	80	325	0
80	34	0	80	107	0	80	180	0	80	253	3	80	326	0
80	35	0	80	108	0	80	181	0	80	254	0	80	327	0
80	36	0	80	109	0	80	182	3	80	255	0	80	328	0
80	37	0	80	110	0	80	183	6	80	256	0	80	329	0
80	38	0	80	111	0	80	184	0	80	257	0	80	330	0
80	39	0	80	112	0	80	185	0	80	258	0	80	331	0
80	40	0	80	113	0	80	186	0	80	259	0	80	332	0
80	41	0	80	114	1	80	187	0	80	260	0	80	333	0
80	42	0	80	115	0	80	188	0	80	261	0	80	334	0
80	43	0	80	116	0	80	189	0	80	262	0	80	335	0
80	44	2	80	117	0	80	190	0	80	263	0	80	336	0

Year	Day of Year	Daily Precip-itation (mm)	Year	Day of Year	Daily Precip-itation (mm)	Year	Day of Year	Daily Precip-itation (mm)	Year	Day of Year	Daily Precip-itation (mm)	Year	Day of Year	Daily Precip-itation (mm)
80	45	12	80	118	0	80	191	0	80	264	0	80	337	0
80	46	0	80	119	1	80	192	0	80	265	0	80	338	0
80	47	8	80	120	3	80	193	0	80	266	0	80	339	0
80	48	5	80	121	3	80	194	0	80	267	0	80	340	0
80	49	1	80	122	8	80	195	0	80	268	0	80	341	0
80	50	7	80	123	0	80	196	0	80	269	0	80	342	0
80	51	0	80	124	0	80	197	0	80	270	0	80	343	0
80	52	0	80	125	0	80	198	0	80	271	0	80	344	0
80	53	0	80	126	0	80	199	0	80	272	0	80	345	0
80	54	0	80	127	0	80	200	0	80	273	0	80	346	0
80	55	0	80	128	0	80	201	0	80	274	0	80	347	0
80	56	0	80	129	0	80	202	0	80	275	0	80	348	0
80	57	0	80	130	0	80	203	0	80	276	0	80	349	0
80	58	0	80	131	0	80	204	0	80	277	0	80	350	0
80	59	0	80	132	0	80	205	2	80	278	0	80	351	0
80	60	0	80	133	0	80	206	0	80	279	0	80	352	0
80	61	0	80	134	0	80	207	0	80	280	0	80	353	0
80	62	13	80	135	3	80	208	1	80	281	0	80	354	0
80	63	10	80	136	0	80	209	0	80	282	0	80	355	0
80	64	0	80	137	0	80	210	0	80	283	0	80	356	0
80	65	2	80	138	0	80	211	0	80	284	0	80	357	0
80	66	8	80	139	0	80	212	1	80	285	0	80	358	0
80	67	5	80	140	0	80	213	0	80	286	0	80	359	0
80	68	0	80	141	0	80	214	0	80	287	0	80	360	0
80	69	0	80	142	0	80	215	0	80	288	0	80	361	0
80	70	0	80	143	0	80	216	0	80	289	0	80	362	0
80	71	0	80	144	1	80	217	0	80	290	0	80	363	0
80	72	0	80	145	0	80	218	0	80	291	0	80	364	0
80	73	0	80	146	0	80	219	0	80	292	0	80	365	0
												80	366	0

Table III-1. Developed data precipitation record for Yucca Mountain that was used directly as input for INFIL V2.0 (cont.)

ear	Day of Year	Daily recip-itation (mm)	ear	Day of ear	Daily recip-itation (mm)	ear	Day of ear	Daily recip-itation (mm)	ear	Day of ear	Daily recip-itation (mm)	ear	Day of ear	Daily recip-itation (mm)
81	1	0	81	74	0	81	147	12	81	220	0	81	293	0
81	2	0	81	75	0	81	148	0	81	221	0	81	294	0
81	3	0	81	76	0	81	149	0	81	222	0	81	295	0
81	4	0	81	77	0	81	150	0	81	223	1	81	296	0
81	5	0	81	78	5	81	151	0	81	224	1	81	297	0
81	6	0	81	79	2	81	152	0	81	225	0	81	298	0
81	7	0	81	80	0	81	153	0	81	226	1	81	299	0
81	8	0	81	81	0	81	154	0	81	227	0	81	300	0
81	9	0	81	82	0	81	155	0	81	228	0	81	301	0
81	10	0	81	83	0	81	156	0	81	229	0	81	302	0
81	11	0	81	84	0	81	157	0	81	230	0	81	303	0
81	12	0	81	85	2	81	158	0	81	231	0	81	304	0
81	13	0	81	86	0	81	159	0	81	232	0	81	305	0
81	14	0	81	87	0	81	160	0	81	233	0	81	306	0
81	15	0	81	88	0	81	161	0	81	234	0	81	307	0
81	16	0	81	89	0	81	162	0	81	235	0	81	308	0
81	17	0	81	90	0	81	163	0	81	236	0	81	309	0
81	18	0	81	91	0	81	164	0	81	237	0	81	310	0
81	19	0	81	92	0	81	165	0	81	238	0	81	311	0
81	20	0	81	93	0	81	166	0	81	239	0	81	312	0
81	21	0	81	94	0	81	167	0	81	240	0	81	313	0
81	22	0	81	95	0	81	168	0	81	241	0	81	314	0
81	23	0	81	96	0	81	169	0	81	242	0	81	315	0
81	24	0	81	97	0	81	170	0	81	243	0	81	316	0
81	25	0	81	98	0	81	171	0	81	244	0	81	317	0
81	26	0	81	99	0	81	172	0	81	245	0	81	318	0
81	27	0	81	100	0	81	173	0	81	246	0	81	319	0
81	28	5	81	101	0	81	174	0	81	247	0	81	320	0
81	29	6	81	102	0	81	175	0	81	248	0	81	321	0
81	30	0	81	103	0	81	176	0	81	249	1	81	322	0
81	31	0	81	104	0	81	177	0	81	250	2	81	323	0
81	32	0	81	105	0	81	178	0	81	251	5	81	324	0
81	33	0	81	106	0	81	179	0	81	252	2	81	325	0
81	34	0	81	107	0	81	180	0	81	253	0	81	326	0
81	35	0	81	108	2	81	181	0	81	254	0	81	327	0
81	36	0	81	109	0	81	182	0	81	255	1	81	328	0
81	37	0	81	110	0	81	183	0	81	256	0	81	329	0
81	38	0	81	111	0	81	184	0	81	257	0	81	330	2
81	39	1	81	112	0	81	185	0	81	258	0	81	331	2
81	40	1	81	113	0	81	186	0	81	259	0	81	332	9
81	41	0	81	114	0	81	187	0	81	260	0	81	333	3
81	42	0	81	115	0	81	188	0	81	261	0	81	334	0
81	43	0	81	116	0	81	189	0	81	262	0	81	335	0
81	44	0	81	117	0	81	190	0	81	263	0	81	336	0
81	45	0	81	118	0	81	191	0	81	264	0	81	337	0

ear	Day of Year	Daily recip-itation (mm)	ear	Day of ear	Daily recip-itation (mm)	ear	Day of ear	Daily recip-itation (mm)	ear	Day of ear	Daily recip-itation (mm)	ear	Day of ear	Daily recip-itation (mm)
81	46	0	81	119	0	81	192	0	81	265	0	81	338	0
81	47	0	81	120	0	81	193	0	81	266	0	81	339	0
81	48	0	81	121	0	81	194	0	81	267	0	81	340	0
81	49	0	81	122	0	81	195	0	81	268	0	81	341	0
81	50	0	81	123	0	81	196	0	81	269	0	81	342	0
81	51	0	81	124	0	81	197	0	81	270	0	81	343	0
81	52	0	81	125	0	81	198	0	81	271	0	81	344	0
81	53	0	81	126	0	81	199	0	81	272	0	81	345	0
81	54	0	81	127	0	81	200	0	81	273	0	81	346	0
81	55	0	81	128	0	81	201	0	81	274	0	81	347	0
81	56	0	81	129	0	81	202	0	81	275	2	81	348	0
81	57	2	81	130	0	81	203	0	81	276	0	81	349	0
81	58	0	81	131	0	81	204	0	81	277	0	81	350	0
81	59	0	81	132	0	81	205	0	81	278	0	81	351	0
81	60	16	81	133	0	81	206	0	81	279	0	81	352	0
81	61	5	81	134	1	81	207	0	81	280	0	81	353	0
81	62	0	81	135	1	81	208	0	81	281	0	81	354	0
81	63	0	81	136	0	81	209	0	81	282	0	81	355	0
81	64	8	81	137	0	81	210	0	81	283	0	81	356	0
81	65	2	81	138	0	81	211	0	81	284	0	81	357	0
81	66	0	81	139	0	81	212	0	81	285	0	81	358	0
81	67	0	81	140	0	81	213	0	81	286	0	81	359	0
81	68	0	81	141	0	81	214	0	81	287	0	81	360	0
81	69	0	81	142	0	81	215	0	81	288	0	81	361	0
81	70	0	81	143	0	81	216	0	81	289	0	81	362	0
81	71	0	81	144	0	81	217	0	81	290	0	81	363	0
81	72	0	81	145	0	81	218	0	81	291	0	81	364	0
81	73	0	81	146	1	81	219	0	81	292	0	81	365	0

Table III-1. Developed data precipitation record for Yucca Mountain that was used directly as input for INFIL V2.0 (cont.)

ear	Day of Year	Daily recip-itation (mm)	ear	Day of ear	Daily recip-itation (mm)	ear	Day of ear	Daily recip-itation (mm)	ear	Day of ear	Daily recip-itation (mm)	ear	Day of ear	Daily recip-itation (mm)
82	1	1	82	74	2	82	147	0	82	220	0	82	293	0
82	2	0	82	75	0	82	148	0	82	221	0	82	294	0
82	3	0	82	76	30	82	149	0	82	222	0	82	295	0
82	4	0	82	77	7	82	150	0	82	223	0	82	296	0
82	5	2	82	78	1	82	151	0	82	224	2	82	297	0
82	6	0	82	79	0	82	152	0	82	225	0	82	298	0
82	7	0	82	80	0	82	153	0	82	226	0	82	299	1
82	8	0	82	81	0	82	154	0	82	227	0	82	300	0
82	9	0	82	82	0	82	155	0	82	228	0	82	301	0
82	10	0	82	83	0	82	156	0	82	229	0	82	302	0
82	11	0	82	84	0	82	157	0	82	230	2	82	303	1
82	12	0	82	85	1	82	158	0	82	231	0	82	304	0
82	13	0	82	86	0	82	159	0	82	232	0	82	305	0
82	14	0	82	87	0	82	160	0	82	233	0	82	306	0
82	15	0	82	88	0	82	161	0	82	234	3	82	307	0
82	16	0	82	89	0	82	162	0	82	235	3	82	308	0
82	17	0	82	90	0	82	163	0	82	236	1	82	309	0
82	18	0	82	91	7	82	164	0	82	237	0	82	310	0
82	19	0	82	92	0	82	165	0	82	238	0	82	311	0
82	20	5	82	93	0	82	166	0	82	239	0	82	312	0
82	21	1	82	94	0	82	167	0	82	240	0	82	313	7
82	22	0	82	95	0	82	168	0	82	241	0	82	314	6
82	23	0	82	96	0	82	169	2	82	242	0	82	315	0
82	24	0	82	97	0	82	170	0	82	243	0	82	316	0
82	25	0	82	98	0	82	171	0	82	244	0	82	317	0
82	26	0	82	99	0	82	172	0	82	245	0	82	318	0
82	27	0	82	100	0	82	173	0	82	246	0	82	319	0
82	28	0	82	101	3	82	174	0	82	247	0	82	320	0
82	29	0	82	102	0	82	175	0	82	248	0	82	321	0
82	30	0	82	103	0	82	176	0	82	249	0	82	322	0
82	31	0	82	104	0	82	177	0	82	250	0	82	323	0
82	32	0	82	105	0	82	178	0	82	251	0	82	324	0
82	33	0	82	106	0	82	179	0	82	252	1	82	325	0
82	34	0	82	107	0	82	180	0	82	253	3	82	326	1
82	35	0	82	108	0	82	181	0	82	254	1	82	327	1
82	36	0	82	109	0	82	182	0	82	255	0	82	328	0
82	37	0	82	110	0	82	183	0	82	256	0	82	329	0
82	38	0	82	111	0	82	184	0	82	257	0	82	330	0
82	39	0	82	112	0	82	185	0	82	258	0	82	331	0
82	40	0	82	113	0	82	186	0	82	259	0	82	332	0
82	41	5	82	114	0	82	187	0	82	260	0	82	333	0
82	42	1	82	115	0	82	188	0	82	261	0	82	334	10
82	43	0	82	116	0	82	189	0	82	262	0	82	335	0
82	44	0	82	117	0	82	190	0	82	263	0	82	336	0
82	45	0	82	118	0	82	191	0	82	264	0	82	337	0

ear	Day of Year	Daily recip-itation (mm)	ear	Day of ear	Daily recip-itation (mm)	ear	Day of ear	Daily recip-itation (mm)	ear	Day of ear	Daily recip-itation (mm)	ear	Day of ear	Daily recip-itation (mm)
82	46	0	82	119	0	82	192	0	82	265	0	82	338	0
82	47	0	82	120	0	82	193	0	82	266	0	82	339	0
82	48	0	82	121	0	82	194	0	82	267	3	82	340	0
82	49	0	82	122	3	82	195	0	82	268	6	82	341	0
82	50	0	82	123	2	82	196	0	82	269	2	82	342	0
82	51	0	82	124	2	82	197	0	82	270	3	82	343	2
82	52	0	82	125	0	82	198	0	82	271	0	82	344	1
82	53	0	82	126	0	82	199	0	82	272	1	82	345	0
82	54	0	82	127	0	82	200	0	82	273	0	82	346	0
82	55	0	82	128	0	82	201	0	82	274	0	82	347	0
82	56	0	82	129	5	82	202	0	82	275	0	82	348	0
82	57	0	82	130	1	82	203	0	82	276	0	82	349	0
82	58	0	82	131	0	82	204	0	82	277	0	82	350	0
82	59	0	82	132	0	82	205	3	82	278	0	82	351	0
82	60	0	82	133	0	82	206	0	82	279	0	82	352	0
82	61	1	82	134	0	82	207	2	82	280	0	82	353	0
82	62	0	82	135	0	82	208	6	82	281	0	82	354	0
82	63	0	82	136	0	82	209	0	82	282	0	82	355	0
82	64	0	82	137	0	82	210	0	82	283	0	82	356	6
82	65	0	82	138	0	82	211	0	82	284	0	82	357	2
82	66	0	82	139	0	82	212	0	82	285	0	82	358	0
82	67	0	82	140	0	82	213	0	82	286	0	82	359	0
82	68	0	82	141	0	82	214	0	82	287	0	82	360	0
82	69	0	82	142	0	82	215	0	82	288	0	82	361	0
82	70	0	82	143	0	82	216	0	82	289	0	82	362	0
82	71	0	82	144	0	82	217	0	82	290	0	82	363	0
82	72	0	82	145	0	82	218	0	82	291	0	82	364	0
82	73	7	82	146	0	82	219	0	82	292	0	82	365	0

Table III-1. Developed data precipitation record for Yucca Mountain that was used directly as input for INFIL V2.0 (cont.)

ear	Day of Year	Daily recip-itation (mm)	ear	Day of ear	Daily recip-itation (mm)	ear	Day of ear	Daily recip-itation (mm)	ear	Day of ear	Daily recip-itation (mm)	ear	Day of ear	Daily recip-itation (mm)
83	1	0	83	74	0	83	147	0	83	220	0	83	293	0
83	2	0	83	75	0	83	148	0	83	221	3	83	294	0
83	3	0	83	76	0	83	149	0	83	222	5	83	295	0
83	4	0	83	77	6	83	150	0	83	223	0	83	296	0
83	5	0	83	78	0	83	151	0	83	224	0	83	297	0
83	6	0	83	79	0	83	152	0	83	225	0	83	298	0
83	7	0	83	80	15	83	153	0	83	226	0	83	299	0
83	8	0	83	81	0	83	154	0	83	227	3	83	300	0
83	9	0	83	82	0	83	155	0	83	228	8	83	301	0
83	10	0	83	83	2	83	156	0	83	229	4	83	302	0
83	11	0	83	84	0	83	157	0	83	230	58	83	303	0
83	12	0	83	85	0	83	158	0	83	231	5	83	304	0
83	13	0	83	86	0	83	159	0	83	232	0	83	305	0
83	14	0	83	87	0	83	160	0	83	233	0	83	306	0
83	15	0	83	88	0	83	161	0	83	234	0	83	307	0
83	16	2	83	89	0	83	162	0	83	235	0	83	308	0
83	17	1	83	90	0	83	163	0	83	236	0	83	309	0
83	18	0	83	91	0	83	164	0	83	237	0	83	310	0
83	19	3	83	92	2	83	165	0	83	238	0	83	311	0
83	20	0	83	93	2	83	166	0	83	239	0	83	312	0
83	21	0	83	94	2	83	167	0	83	240	0	83	313	0
83	22	2	83	95	0	83	168	0	83	241	0	83	314	0
83	23	1	83	96	0	83	169	0	83	242	0	83	315	0
83	24	6	83	97	0	83	170	0	83	243	0	83	316	0
83	25	0	83	98	0	83	171	0	83	244	0	83	317	0
83	26	0	83	99	0	83	172	0	83	245	0	83	318	0
83	27	6	83	100	0	83	173	0	83	246	0	83	319	0
83	28	0	83	101	3	83	174	0	83	247	0	83	320	0
83	29	14	83	102	2	83	175	0	83	248	0	83	321	0
83	30	0	83	103	0	83	176	0	83	249	0	83	322	0
83	31	0	83	104	0	83	177	0	83	250	0	83	323	0
83	32	0	83	105	0	83	178	0	83	251	0	83	324	1
83	33	0	83	106	0	83	179	0	83	252	0	83	325	0
83	34	1	83	107	0	83	180	0	83	253	0	83	326	0
83	35	0	83	108	3	83	181	0	83	254	0	83	327	0
83	36	3	83	109	0	83	182	0	83	255	0	83	328	8
83	37	3	83	110	0	83	183	0	83	256	0	83	329	5
83	38	1	83	111	1	83	184	0	83	257	0	83	330	0
83	39	2	83	112	0	83	185	0	83	258	0	83	331	0
83	40	0	83	113	0	83	186	0	83	259	0	83	332	0
83	41	0	83	114	0	83	187	0	83	260	0	83	333	0
83	42	0	83	115	0	83	188	0	83	261	0	83	334	0
83	43	0	83	116	0	83	189	0	83	262	0	83	335	0
83	44	1	83	117	0	83	190	0	83	263	0	83	336	0
83	45	0	83	118	0	83	191	0	83	264	0	83	337	3

ear	Day of Year	Daily recip-itation (mm)	ear	Day of ear	Daily recip-itation (mm)	ear	Day of ear	Daily recip-itation (mm)	ear	Day of ear	Daily recip-itation (mm)	ear	Day of ear	Daily recip-itation (mm)
83	46	0	83	119	0	83	192	0	83	265	0	83	338	0
83	47	0	83	120	1	83	193	0	83	266	0	83	339	0
83	48	0	83	121	2	83	194	0	83	267	0	83	340	0
83	49	0	83	122	0	83	195	0	83	268	1	83	341	0
83	50	0	83	123	0	83	196	0	83	269	9	83	342	0
83	51	0	83	124	0	83	197	0	83	270	1	83	343	0
83	52	0	83	125	0	83	198	0	83	271	0	83	344	0
83	53	0	83	126	0	83	199	0	83	272	0	83	345	0
83	54	0	83	127	0	83	200	0	83	273	1	83	346	0
83	55	1	83	128	0	83	201	0	83	274	4	83	347	0
83	56	1	83	129	0	83	202	0	83	275	0	83	348	0
83	57	0	83	130	0	83	203	0	83	276	0	83	349	0
83	58	5	83	131	0	83	204	0	83	277	0	83	350	0
83	59	0	83	132	0	83	205	0	83	278	0	83	351	0
83	60	16	83	133	0	83	206	0	83	279	0	83	352	0
83	61	14	83	134	0	83	207	0	83	280	0	83	353	0
83	62	23	83	135	0	83	208	0	83	281	0	83	354	0
83	63	0	83	136	0	83	209	0	83	282	0	83	355	0
83	64	0	83	137	0	83	210	0	83	283	0	83	356	0
83	65	0	83	138	0	83	211	0	83	284	0	83	357	0
83	66	0	83	139	0	83	212	0	83	285	0	83	358	6
83	67	0	83	140	0	83	213	0	83	286	0	83	359	15
83	68	0	83	141	0	83	214	0	83	287	0	83	360	1
83	69	0	83	142	0	83	215	0	83	288	0	83	361	0
83	70	0	83	143	0	83	216	0	83	289	0	83	362	0
83	71	0	83	144	0	83	217	0	83	290	0	83	363	0
83	72	0	83	145	0	83	218	4	83	291	0	83	364	0
83	73	0	83	146	0	83	219	2	83	292	0	83	365	0

Table III-1. Developed data precipitation record for Yucca Mountain that was used directly as input for INFIL V2.0 (cont.)

ear	Day of Year	Daily recip-itation (mm)	ear	Day of ear	Daily recip-itation (mm)	ear	Day of ear	Daily recip-itation (mm)	ear	Day of ear	Daily recip-itation (mm)	ear	Day of ear	Daily recip-itation (mm)
84	1	0	84	74	0	84	147	0	84	220	0	84	293	0
84	2	0	84	75	0	84	148	0	84	221	0	84	294	0
84	3	0	84	76	0	84	149	0	84	222	0	84	295	0
84	4	0	84	77	0	84	150	0	84	223	0	84	296	0
84	5	0	84	78	0	84	151	0	84	224	0	84	297	0
84	6	0	84	79	0	84	152	0	84	225	0	84	298	0
84	7	0	84	80	0	84	153	0	84	226	0	84	299	0
84	8	0	84	81	0	84	154	0	84	227	15	84	300	0
84	9	0	84	82	0	84	155	0	84	228	8	84	301	0
84	10	0	84	83	0	84	156	0	84	229	0	84	302	0
84	11	0	84	84	0	84	157	0	84	230	0	84	303	0
84	12	0	84	85	0	84	158	0	84	231	5	84	304	0
84	13	0	84	86	0	84	159	0	84	232	16	84	305	0
84	14	0	84	87	0	84	160	0	84	233	0	84	306	0
84	15	0	84	88	0	84	161	0	84	234	0	84	307	0
84	16	0	84	89	0	84	162	0	84	235	0	84	308	0
84	17	0	84	90	0	84	163	0	84	236	0	84	309	0
84	18	0	84	91	0	84	164	0	84	237	0	84	310	0
84	19	0	84	92	0	84	165	0	84	238	0	84	311	0
84	20	0	84	93	0	84	166	0	84	239	0	84	312	0
84	21	0	84	94	0	84	167	0	84	240	0	84	313	0
84	22	0	84	95	0	84	168	0	84	241	0	84	314	0
84	23	0	84	96	0	84	169	0	84	242	0	84	315	0
84	24	0	84	97	1	84	170	0	84	243	0	84	316	0
84	25	0	84	98	0	84	171	0	84	244	0	84	317	0
84	26	0	84	99	0	84	172	0	84	245	0	84	318	0
84	27	0	84	100	0	84	173	0	84	246	0	84	319	0
84	28	0	84	101	0	84	174	0	84	247	0	84	320	0
84	29	0	84	102	0	84	175	0	84	248	0	84	321	0
84	30	0	84	103	0	84	176	0	84	249	0	84	322	0
84	31	0	84	104	0	84	177	0	84	250	0	84	323	0
84	32	0	84	105	0	84	178	0	84	251	0	84	324	0
84	33	0	84	106	0	84	179	0	84	252	0	84	325	0
84	34	0	84	107	0	84	180	0	84	253	0	84	326	2
84	35	0	84	108	0	84	181	0	84	254	0	84	327	18
84	36	0	84	109	0	84	182	0	84	255	0	84	328	4
84	37	0	84	110	0	84	183	0	84	256	0	84	329	3
84	38	0	84	111	0	84	184	0	84	257	0	84	330	0
84	39	0	84	112	0	84	185	1	84	258	0	84	331	0
84	40	0	84	113	0	84	186	0	84	259	0	84	332	0
84	41	2	84	114	0	84	187	0	84	260	4	84	333	0
84	42	0	84	115	0	84	188	0	84	261	1	84	334	0
84	43	0	84	116	0	84	189	0	84	262	0	84	335	0
84	44	0	84	117	0	84	190	0	84	263	0	84	336	0
84	45	1	84	118	0	84	191	0	84	264	1	84	337	0

ear	Day of Year	Daily recip-itation (mm)	ear	Day of ear	Daily recip-itation (mm)	ear	Day of ear	Daily recip-itation (mm)	ear	Day of ear	Daily recip-itation (mm)	ear	Day of ear	Daily recip-itation (mm)
84	46	0	84	119	0	84	192	0	84	265	0	84	338	0
84	47	0	84	120	0	84	193	0	84	266	0	84	339	0
84	48	0	84	121	0	84	194	1	84	267	0	84	340	0
84	49	0	84	122	0	84	195	1	84	268	0	84	341	0
84	50	0	84	123	0	84	196	0	84	269	0	84	342	0
84	51	0	84	124	0	84	197	0	84	270	0	84	343	2
84	52	0	84	125	0	84	198	0	84	271	0	84	344	0
84	53	0	84	126	0	84	199	0	84	272	0	84	345	1
84	54	0	84	127	0	84	200	0	84	273	0	84	346	2
84	55	0	84	128	0	84	201	1	84	274	0	84	347	1
84	56	0	84	129	0	84	202	0	84	275	1	84	348	0
84	57	0	84	130	0	84	203	11	84	276	2	84	349	0
84	58	0	84	131	0	84	204	38	84	277	0	84	350	1
84	59	0	84	132	0	84	205	1	84	278	0	84	351	6
84	60	0	84	133	0	84	206	0	84	279	0	84	352	0
84	61	0	84	134	0	84	207	0	84	280	0	84	353	10
84	62	0	84	135	0	84	208	0	84	281	0	84	354	23
84	63	0	84	136	0	84	209	1	84	282	0	84	355	1
84	64	0	84	137	0	84	210	3	84	283	0	84	356	0
84	65	0	84	138	0	84	211	2	84	284	0	84	357	0
84	66	0	84	139	0	84	212	1	84	285	0	84	358	0
84	67	0	84	140	0	84	213	11	84	286	0	84	359	0
84	68	0	84	141	0	84	214	0	84	287	0	84	360	0
84	69	0	84	142	0	84	215	0	84	288	0	84	361	3
84	70	0	84	143	0	84	216	0	84	289	0	84	362	8
84	71	0	84	144	0	84	217	0	84	290	0	84	363	5
84	72	0	84	145	0	84	218	0	84	291	0	84	364	0
84	73	0	84	146	0	84	219	0	84	292	0	84	365	0
												84	366	0

Table III-1. Developed data precipitation record for Yucca Mountain that was used directly as input for INFIL V2.0 (cont.)

ear	Day of Year	Daily recip-itation (mm)	ear	Day of ear	Daily recip-itation (mm)	ear	Day of ear	Daily recip-itation (mm)	ear	Day of ear	Daily recip-itation (mm)	ear	Day of ear	Daily recip-itation (mm)
85	1	0	85	74	0	85	147	0	85	220	0	85	293	0
85	2	0	85	75	0	85	148	0	85	221	0	85	294	0
85	3	0	85	76	0	85	149	0	85	222	0	85	295	0
85	4	0	85	77	1	85	150	0	85	223	0	85	296	0
85	5	0	85	78	0	85	151	0	85	224	0	85	297	0
85	6	0	85	79	0	85	152	0	85	225	0	85	298	0
85	7	5	85	80	0	85	153	0	85	226	0	85	299	0
85	8	2	85	81	0	85	154	1	85	227	0	85	300	0
85	9	0	85	82	0	85	155	0	85	228	0	85	301	0
85	10	0	85	83	0	85	156	0	85	229	0	85	302	0
85	11	0	85	84	0	85	157	0	85	230	0	85	303	0
85	12	0	85	85	0	85	158	0	85	231	0	85	304	0
85	13	0	85	86	0	85	159	0	85	232	0	85	305	0
85	14	0	85	87	1	85	160	0	85	233	0	85	306	0
85	15	0	85	88	0	85	161	0	85	234	0	85	307	0
85	16	0	85	89	0	85	162	0	85	235	0	85	308	0
85	17	0	85	90	0	85	163	0	85	236	0	85	309	0
85	18	0	85	91	0	85	164	0	85	237	0	85	310	0
85	19	0	85	92	0	85	165	0	85	238	0	85	311	0
85	20	0	85	93	0	85	166	0	85	239	0	85	312	0
85	21	0	85	94	0	85	167	0	85	240	0	85	313	0
85	22	0	85	95	0	85	168	0	85	241	0	85	314	0
85	23	0	85	96	0	85	169	0	85	242	0	85	315	16
85	24	0	85	97	0	85	170	0	85	243	0	85	316	6
85	25	0	85	98	0	85	171	0	85	244	0	85	317	0
85	26	2	85	99	0	85	172	0	85	245	0	85	318	0
85	27	1	85	100	0	85	173	0	85	246	0	85	319	0
85	28	0	85	101	0	85	174	0	85	247	0	85	320	0
85	29	0	85	102	0	85	175	0	85	248	0	85	321	0
85	30	0	85	103	0	85	176	0	85	249	0	85	322	0
85	31	0	85	104	0	85	177	0	85	250	0	85	323	0
85	32	0	85	105	0	85	178	0	85	251	0	85	324	0
85	33	0	85	106	0	85	179	0	85	252	0	85	325	0
85	34	0	85	107	0	85	180	0	85	253	0	85	326	0
85	35	0	85	108	0	85	181	0	85	254	0	85	327	0
85	36	0	85	109	0	85	182	0	85	255	0	85	328	2
85	37	0	85	110	0	85	183	0	85	256	0	85	329	2
85	38	0	85	111	0	85	184	0	85	257	0	85	330	0
85	39	0	85	112	0	85	185	0	85	258	0	85	331	0
85	40	1	85	113	0	85	186	0	85	259	0	85	332	0
85	41	1	85	114	0	85	187	0	85	260	0	85	333	4
85	42	0	85	115	0	85	188	0	85	261	9	85	334	0
85	43	0	85	116	0	85	189	0	85	262	0	85	335	0
85	44	0	85	117	0	85	190	0	85	263	0	85	336	5
85	45	0	85	118	0	85	191	0	85	264	0	85	337	0

ear	Day of Year	Daily recip-itation (mm)	ear	Day of ear	Daily recip-itation (mm)	ear	Day of ear	Daily recip-itation (mm)	ear	Day of ear	Daily recip-itation (mm)	ear	Day of ear	Daily recip-itation (mm)
85	46	0	85	119	0	85	192	0	85	265	0	85	338	0
85	47	0	85	120	0	85	193	0	85	266	0	85	339	0
85	48	0	85	121	0	85	194	0	85	267	0	85	340	0
85	49	0	85	122	0	85	195	0	85	268	0	85	341	0
85	50	0	85	123	0	85	196	0	85	269	0	85	342	0
85	51	0	85	124	0	85	197	0	85	270	1	85	343	0
85	52	0	85	125	0	85	198	1	85	271	0	85	344	0
85	53	0	85	126	0	85	199	6	85	272	0	85	345	0
85	54	0	85	127	0	85	200	2	85	273	0	85	346	0
85	55	0	85	128	0	85	201	7	85	274	0	85	347	0
85	56	0	85	129	1	85	202	1	85	275	0	85	348	0
85	57	0	85	130	5	85	203	0	85	276	0	85	349	0
85	58	0	85	131	0	85	204	0	85	277	0	85	350	0
85	59	0	85	132	0	85	205	0	85	278	0	85	351	0
85	60	0	85	133	0	85	206	0	85	279	0	85	352	0
85	61	0	85	134	0	85	207	0	85	280	1	85	353	0
85	62	0	85	135	0	85	208	0	85	281	1	85	354	0
85	63	0	85	136	0	85	209	0	85	282	0	85	355	0
85	64	0	85	137	0	85	210	0	85	283	0	85	356	0
85	65	0	85	138	0	85	211	0	85	284	0	85	357	0
85	66	0	85	139	0	85	212	0	85	285	0	85	358	0
85	67	0	85	140	0	85	213	0	85	286	0	85	359	0
85	68	0	85	141	0	85	214	0	85	287	0	85	360	0
85	69	0	85	142	0	85	215	0	85	288	0	85	361	0
85	70	0	85	143	0	85	216	0	85	289	0	85	362	0
85	71	0	85	144	0	85	217	0	85	290	0	85	363	0
85	72	0	85	145	0	85	218	0	85	291	0	85	364	0
85	73	0	85	146	0	85	219	0	85	292	0	85	365	0

Table III-1. Developed data precipitation record for Yucca Mountain that was used directly as input for INFIL V2.0 (cont.)

ear	Day of Year	Daily recip-itation (mm)	ear	Day of ear	Daily recip-itation (mm)	ear	Day of ear	Daily recip-itation (mm)	ear	Day of ear	Daily recip-itation (mm)	ear	Day of ear	Daily recip-itation (mm)
86	1	0	86	74	4	86	147	0	86	220	0	86	293	2
86	2	0	86	75	1	86	148	0	86	221	0	86	294	0
86	3	0	86	76	0	86	149	0	86	222	2	86	295	0
86	4	0	86	77	0	86	150	0	86	223	0	86	296	0
86	5	4	86	78	0	86	151	0	86	224	0	86	297	0
86	6	0	86	79	0	86	152	0	86	225	0	86	298	0
86	7	0	86	80	0	86	153	0	86	226	0	86	299	0
86	8	0	86	81	0	86	154	0	86	227	0	86	300	0
86	9	0	86	82	0	86	155	0	86	228	0	86	301	0
86	10	0	86	83	0	86	156	0	86	229	0	86	302	0
86	11	0	86	84	0	86	157	0	86	230	1	86	303	0
86	12	0	86	85	0	86	158	0	86	231	0	86	304	0
86	13	0	86	86	0	86	159	0	86	232	0	86	305	0
86	14	0	86	87	0	86	160	0	86	233	0	86	306	0
86	15	0	86	88	0	86	161	0	86	234	0	86	307	0
86	16	0	86	89	0	86	162	0	86	235	0	86	308	0
86	17	0	86	90	0	86	163	0	86	236	0	86	309	0
86	18	0	86	91	0	86	164	0	86	237	5	86	310	0
86	19	0	86	92	0	86	165	0	86	238	3	86	311	0
86	20	0	86	93	0	86	166	0	86	239	4	86	312	0
86	21	0	86	94	0	86	167	0	86	240	0	86	313	0
86	22	0	86	95	1	86	168	0	86	241	0	86	314	0
86	23	0	86	96	4	86	169	0	86	242	0	86	315	0
86	24	0	86	97	0	86	170	0	86	243	0	86	316	0
86	25	0	86	98	0	86	171	0	86	244	0	86	317	0
86	26	0	86	99	0	86	172	0	86	245	0	86	318	0
86	27	0	86	100	0	86	173	0	86	246	0	86	319	0
86	28	0	86	101	0	86	174	0	86	247	0	86	320	0
86	29	0	86	102	0	86	175	0	86	248	0	86	321	0
86	30	21	86	103	0	86	176	0	86	249	0	86	322	15
86	31	2	86	104	0	86	177	0	86	250	0	86	323	0
86	32	0	86	105	0	86	178	0	86	251	0	86	324	0
86	33	0	86	106	0	86	179	0	86	252	0	86	325	0
86	34	0	86	107	0	86	180	0	86	253	0	86	326	0
86	35	1	86	108	0	86	181	0	86	254	0	86	327	0
86	36	0	86	109	0	86	182	0	86	255	0	86	328	0
86	37	0	86	110	0	86	183	0	86	256	0	86	329	0
86	38	0	86	111	0	86	184	0	86	257	0	86	330	0
86	39	0	86	112	0	86	185	0	86	258	0	86	331	0
86	40	0	86	113	0	86	186	0	86	259	0	86	332	0
86	41	0	86	114	0	86	187	0	86	260	0	86	333	0
86	42	0	86	115	0	86	188	0	86	261	0	86	334	0
86	43	0	86	116	0	86	189	0	86	262	0	86	335	0
86	44	1	86	117	0	86	190	0	86	263	0	86	336	0
86	45	7	86	118	0	86	191	0	86	264	0	86	337	0

ear	Day of Year	Daily recip-itation (mm)	ear	Day of ear	Daily recip-itation (mm)	ear	Day of ear	Daily recip-itation (mm)	ear	Day of ear	Daily recip-itation (mm)	ear	Day of ear	Daily recip-itation (mm)
86	46	6	86	119	0	86	192	0	86	265	0	86	338	0
86	47	0	86	120	0	86	193	0	86	266	1	86	339	0
86	48	0	86	121	0	86	194	0	86	267	0	86	340	4
86	49	0	86	122	0	86	195	0	86	268	0	86	341	2
86	50	0	86	123	0	86	196	3	86	269	0	86	342	0
86	51	0	86	124	0	86	197	0	86	270	0	86	343	0
86	52	0	86	125	0	86	198	0	86	271	0	86	344	0
86	53	0	86	126	4	86	199	0	86	272	0	86	345	0
86	54	0	86	127	0	86	200	0	86	273	0	86	346	0
86	55	0	86	128	0	86	201	0	86	274	1	86	347	0
86	56	0	86	129	0	86	202	4	86	275	8	86	348	0
86	57	0	86	130	0	86	203	0	86	276	0	86	349	0
86	58	0	86	131	0	86	204	2	86	277	0	86	350	0
86	59	0	86	132	0	86	205	0	86	278	0	86	351	0
86	60	0	86	133	0	86	206	0	86	279	0	86	352	0
86	61	0	86	134	0	86	207	0	86	280	0	86	353	2
86	62	0	86	135	0	86	208	0	86	281	0	86	354	10
86	63	0	86	136	0	86	209	0	86	282	0	86	355	0
86	64	0	86	137	0	86	210	0	86	283	0	86	356	0
86	65	0	86	138	0	86	211	0	86	284	0	86	357	0
86	66	0	86	139	0	86	212	0	86	285	0	86	358	0
86	67	2	86	140	0	86	213	0	86	286	0	86	359	0
86	68	0	86	141	0	86	214	0	86	287	0	86	360	0
86	69	7	86	142	0	86	215	0	86	288	0	86	361	0
86	70	0	86	143	0	86	216	0	86	289	0	86	362	0
86	71	1	86	144	0	86	217	0	86	290	0	86	363	0
86	72	4	86	145	0	86	218	0	86	291	0	86	364	0
86	73	2	86	146	0	86	219	0	86	292	6	86	365	0

Table III-1. Developed data precipitation record for Yucca Mountain that was used directly as input for INFIL V2.0 (cont.)

Year	Day of Year	Daily recip-itation (mm)	Year	Day of Year	Daily recip-itation (mm)	Year	Day of Year	Daily recip-itation (mm)	Year	Day of Year	Daily recip-itation (mm)	Year	Day of Year	Daily recip-itation (mm)
87	1	0	87	74	8	87	147	0	87	220	0	87	293	0
87	2	0	87	75	0	87	148	2	87	221	0	87	294	0
87	3	0	87	76	0	87	149	0	87	222	0	87	295	4
87	4	13	87	77	0	87	150	0	87	223	0	87	296	0
87	5	7	87	78	0	87	151	0	87	224	0	87	297	7
87	6	2	87	79	0	87	152	0	87	225	0	87	298	0
87	7	2	87	80	2	87	153	0	87	226	0	87	299	0
87	8	0	87	81	1	87	154	0	87	227	0	87	300	0
87	9	0	87	82	0	87	155	0	87	228	0	87	301	0
87	10	0	87	83	0	87	156	0	87	229	0	87	302	2
87	11	0	87	84	0	87	157	1	87	230	0	87	303	0
87	12	0	87	85	0	87	158	0	87	231	0	87	304	10
87	13	0	87	86	0	87	159	1	87	232	0	87	305	6
87	14	0	87	87	0	87	160	0	87	233	0	87	306	1
87	15	0	87	88	0	87	161	0	87	234	0	87	307	0
87	16	0	87	89	0	87	162	0	87	235	0	87	308	0
87	17	0	87	90	0	87	163	0	87	236	0	87	309	15
87	18	0	87	91	0	87	164	0	87	237	0	87	310	6
87	19	0	87	92	0	87	165	0	87	238	0	87	311	0
87	20	0	87	93	0	87	166	0	87	239	0	87	312	0
87	21	0	87	94	3	87	167	0	87	240	0	87	313	0
87	22	0	87	95	0	87	168	0	87	241	0	87	314	0
87	23	0	87	96	0	87	169	0	87	242	0	87	315	0
87	24	0	87	97	0	87	170	0	87	243	0	87	316	0
87	25	0	87	98	0	87	171	0	87	244	0	87	317	0
87	26	0	87	99	0	87	172	0	87	245	0	87	318	0
87	27	0	87	100	0	87	173	0	87	246	0	87	319	0
87	28	0	87	101	0	87	174	0	87	247	0	87	320	0
87	29	0	87	102	0	87	175	0	87	248	0	87	321	0
87	30	0	87	103	0	87	176	0	87	249	0	87	322	0
87	31	0	87	104	0	87	177	0	87	250	0	87	323	0
87	32	0	87	105	0	87	178	0	87	251	0	87	324	0
87	33	0	87	106	0	87	179	0	87	252	0	87	325	0
87	34	0	87	107	0	87	180	0	87	253	0	87	326	0
87	35	0	87	108	0	87	181	0	87	254	0	87	327	0
87	36	0	87	109	0	87	182	0	87	255	0	87	328	0
87	37	0	87	110	0	87	183	0	87	256	0	87	329	0
87	38	0	87	111	0	87	184	0	87	257	0	87	330	0
87	39	0	87	112	0	87	185	0	87	258	0	87	331	0
87	40	0	87	113	0	87	186	0	87	259	0	87	332	0
87	41	0	87	114	0	87	187	0	87	260	0	87	333	0
87	42	0	87	115	0	87	188	0	87	261	0	87	334	0
87	43	0	87	116	0	87	189	0	87	262	0	87	335	0
87	44	0	87	117	0	87	190	0	87	263	0	87	336	0
87	45	0	87	118	0	87	191	0	87	264	0	87	337	0

ear	Day of Year	Daily recip-itation (mm)	ear	Day of ear	Daily recip-itation (mm)	ear	Day of ear	Daily recip-itation (mm)	ear	Day of ear	Daily recip-itation (mm)	ear	Day of ear	Daily recip-itation (mm)
87	46	1	87	119	3	87	192	0	87	265	0	87	338	4
87	47	0	87	120	0	87	193	0	87	266	0	87	339	2
87	48	0	87	121	0	87	194	0	87	267	0	87	340	0
87	49	0	87	122	0	87	195	0	87	268	0	87	341	0
87	50	0	87	123	0	87	196	0	87	269	0	87	342	0
87	51	0	87	124	0	87	197	5	87	270	0	87	343	0
87	52	0	87	125	0	87	198	0	87	271	0	87	344	0
87	53	0	87	126	0	87	199	0	87	272	0	87	345	0
87	54	3	87	127	2	87	200	0	87	273	0	87	346	0
87	55	1	87	128	1	87	201	32	87	274	0	87	347	0
87	56	5	87	129	0	87	202	5	87	275	0	87	348	0
87	57	0	87	130	0	87	203	0	87	276	0	87	349	0
87	58	0	87	131	0	87	204	0	87	277	0	87	350	0
87	59	0	87	132	2	87	205	0	87	278	0	87	351	8
87	60	0	87	133	0	87	206	0	87	279	0	87	352	0
87	61	0	87	134	0	87	207	0	87	280	0	87	353	1
87	62	0	87	135	2	87	208	0	87	281	0	87	354	0
87	63	0	87	136	11	87	209	0	87	282	0	87	355	0
87	64	3	87	137	1	87	210	0	87	283	0	87	356	2
87	65	5	87	138	0	87	211	0	87	284	0	87	357	1
87	66	2	87	139	0	87	212	0	87	285	2	87	358	0
87	67	0	87	140	0	87	213	0	87	286	6	87	359	0
87	68	0	87	141	0	87	214	0	87	287	0	87	360	0
87	69	0	87	142	0	87	215	0	87	288	0	87	361	0
87	70	0	87	143	0	87	216	1	87	289	0	87	362	0
87	71	0	87	144	0	87	217	3	87	290	0	87	363	0
87	72	0	87	145	0	87	218	0	87	291	0	87	364	0
87	73	0	87	146	0	87	219	0	87	292	0	87	365	0

Table III-1. Developed data precipitation record for Yucca Mountain that was used directly as input for INFIL V2.0 (cont.)

ear	Day of Year	Daily recip-itation (mm)	ear	Day of ear	Daily recip-itation (mm)	ear	Day of ear	Daily recip-itation (mm)	ear	Day of ear	Daily recip-itation (mm)	ear	Day of ear	Daily recip-itation (mm)
88	1	0	88	74	0	88	147	0	88	220	0	88	293	0
88	2	0	88	75	0	88	148	0	88	221	0	88	294	0
88	3	0	88	76	0	88	149	0	88	222	0	88	295	0
88	4	1	88	77	0	88	150	3	88	223	0	88	296	0
88	5	6	88	78	0	88	151	0	88	224	0	88	297	0
88	6	0	88	79	0	88	152	0	88	225	0	88	298	0
88	7	0	88	80	0	88	153	0	88	226	0	88	299	0
88	8	0	88	81	0	88	154	0	88	227	0	88	300	0
88	9	0	88	82	0	88	155	0	88	228	0	88	301	0
88	10	0	88	83	0	88	156	0	88	229	0	88	302	0
88	11	0	88	84	0	88	157	0	88	230	0	88	303	0
88	12	0	88	85	0	88	158	0	88	231	0	88	304	0
88	13	0	88	86	0	88	159	0	88	232	0	88	305	0
88	14	0	88	87	0	88	160	0	88	233	0	88	306	0
88	15	0	88	88	0	88	161	0	88	234	0	88	307	0
88	16	0	88	89	0	88	162	0	88	235	0	88	308	0
88	17	19	88	90	0	88	163	0	88	236	3	88	309	0
88	18	4	88	91	0	88	164	0	88	237	1	88	310	0
88	19	0	88	92	0	88	165	0	88	238	3	88	311	0
88	20	0	88	93	0	88	166	0	88	239	6	88	312	0
88	21	0	88	94	0	88	167	0	88	240	2	88	313	0
88	22	0	88	95	0	88	168	0	88	241	4	88	314	0
88	23	0	88	96	0	88	169	0	88	242	0	88	315	0
88	24	0	88	97	0	88	170	0	88	243	1	88	316	0
88	25	0	88	98	0	88	171	0	88	244	0	88	317	0
88	26	0	88	99	0	88	172	1	88	245	0	88	318	0
88	27	0	88	100	0	88	173	1	88	246	0	88	319	2
88	28	0	88	101	0	88	174	2	88	247	0	88	320	0
88	29	0	88	102	0	88	175	0	88	248	0	88	321	0
88	30	0	88	103	0	88	176	0	88	249	0	88	322	0
88	31	0	88	104	1	88	177	0	88	250	0	88	323	0
88	32	0	88	105	7	88	178	0	88	251	0	88	324	0
88	33	2	88	106	26	88	179	0	88	252	0	88	325	0
88	34	0	88	107	1	88	180	0	88	253	0	88	326	0
88	35	0	88	108	0	88	181	0	88	254	0	88	327	0
88	36	0	88	109	0	88	182	0	88	255	0	88	328	0
88	37	0	88	110	0	88	183	0	88	256	0	88	329	0
88	38	0	88	111	7	88	184	0	88	257	0	88	330	0
88	39	0	88	112	2	88	185	0	88	258	0	88	331	0
88	40	0	88	113	1	88	186	0	88	259	0	88	332	0
88	41	0	88	114	0	88	187	0	88	260	0	88	333	0
88	42	0	88	115	0	88	188	0	88	261	0	88	334	0
88	43	0	88	116	0	88	189	0	88	262	0	88	335	0
88	44	0	88	117	0	88	190	0	88	263	0	88	336	0
88	45	0	88	118	0	88	191	0	88	264	1	88	337	0

ear	Day of Year	Daily recip-itation (mm)	ear	Day of ear	Daily recip-itation (mm)	ear	Day of ear	Daily recip-itation (mm)	ear	Day of ear	Daily recip-itation (mm)	ear	Day of ear	Daily recip-itation (mm)
88	46	0	88	119	0	88	192	0	88	265	3	88	338	0
88	47	0	88	120	0	88	193	0	88	266	1	88	339	0
88	48	0	88	121	0	88	194	0	88	267	0	88	340	0
88	49	0	88	122	0	88	195	0	88	268	0	88	341	0
88	50	0	88	123	0	88	196	0	88	269	0	88	342	0
88	51	0	88	124	0	88	197	0	88	270	0	88	343	0
88	52	0	88	125	0	88	198	0	88	271	0	88	344	0
88	53	0	88	126	1	88	199	0	88	272	0	88	345	0
88	54	0	88	127	2	88	200	0	88	273	0	88	346	0
88	55	0	88	128	0	88	201	0	88	274	0	88	347	0
88	56	0	88	129	0	88	202	0	88	275	0	88	348	0
88	57	0	88	130	0	88	203	0	88	276	0	88	349	0
88	58	5	88	131	0	88	204	1	88	277	0	88	350	0
88	59	1	88	132	0	88	205	0	88	278	0	88	351	0
88	60	3	88	133	0	88	206	0	88	279	0	88	352	0
88	61	2	88	134	0	88	207	0	88	280	0	88	353	1
88	62	0	88	135	0	88	208	0	88	281	0	88	354	0
88	63	0	88	136	0	88	209	0	88	282	0	88	355	0
88	64	0	88	137	0	88	210	0	88	283	0	88	356	1
88	65	0	88	138	0	88	211	2	88	284	0	88	357	0
88	66	0	88	139	0	88	212	6	88	285	0	88	358	0
88	67	0	88	140	0	88	213	1	88	286	0	88	359	0
88	68	0	88	141	0	88	214	5	88	287	0	88	360	0
88	69	0	88	142	0	88	215	0	88	288	0	88	361	0
88	70	0	88	143	0	88	216	0	88	289	0	88	362	0
88	71	0	88	144	0	88	217	0	88	290	0	88	363	0
88	72	0	88	145	0	88	218	0	88	291	0	88	364	0
88	73	0	88	146	0	88	219	0	88	292	0	88	365	0
												88	366	0

Table III-1. Developed data precipitation record for Yucca Mountain that was used directly as input for INFIL V2.0 (cont.)

ear	Day of Year	Daily recip-itation (mm)	ear	Day of ear	Daily recip-itation (mm)	ear	Day of ear	Daily recip-itation (mm)	ear	Day of ear	Daily recip-itation (mm)	ear	Day of ear	Daily recip-itation (mm)
89	1	0	89	74	0	89	147	0	89	220	2	89	293	0
89	2	0	89	75	0	89	148	0	89	221	1	89	294	0
89	3	0	89	76	0	89	149	0	89	222	0	89	295	0
89	4	2	89	77	0	89	150	0	89	223	10	89	296	0
89	5	0	89	78	0	89	151	0	89	224	0	89	297	0
89	6	0	89	79	0	89	152	0	89	225	0	89	298	1
89	7	0	89	80	0	89	153	0	89	226	0	89	299	0
89	8	0	89	81	0	89	154	0	89	227	0	89	300	0
89	9	0	89	82	0	89	155	0	89	228	0	89	301	0
89	10	0	89	83	0	89	156	0	89	229	0	89	302	0
89	11	0	89	84	3	89	157	0	89	230	0	89	303	0
89	12	0	89	85	1	89	158	0	89	231	0	89	304	0
89	13	0	89	86	0	89	159	0	89	232	0	89	305	0
89	14	0	89	87	0	89	160	0	89	233	0	89	306	0
89	15	0	89	88	0	89	161	0	89	234	0	89	307	0
89	16	0	89	89	0	89	162	0	89	235	0	89	308	0
89	17	0	89	90	0	89	163	0	89	236	0	89	309	0
89	18	0	89	91	0	89	164	0	89	237	0	89	310	0
89	19	0	89	92	0	89	165	0	89	238	0	89	311	0
89	20	0	89	93	0	89	166	0	89	239	0	89	312	0
89	21	0	89	94	0	89	167	0	89	240	0	89	313	0
89	22	0	89	95	0	89	168	0	89	241	0	89	314	0
89	23	0	89	96	0	89	169	0	89	242	0	89	315	0
89	24	0	89	97	0	89	170	0	89	243	0	89	316	0
89	25	0	89	98	0	89	171	0	89	244	0	89	317	0
89	26	0	89	99	0	89	172	0	89	245	0	89	318	0
89	27	0	89	100	0	89	173	0	89	246	0	89	319	0
89	28	0	89	101	0	89	174	0	89	247	0	89	320	0
89	29	0	89	102	0	89	175	0	89	248	0	89	321	0
89	30	0	89	103	0	89	176	0	89	249	0	89	322	0
89	31	0	89	104	0	89	177	0	89	250	0	89	323	0
89	32	0	89	105	0	89	178	0	89	251	0	89	324	0
89	33	0	89	106	0	89	179	0	89	252	0	89	325	0
89	34	0	89	107	0	89	180	0	89	253	0	89	326	0
89	35	2	89	108	0	89	181	0	89	254	0	89	327	0
89	36	0	89	109	0	89	182	0	89	255	0	89	328	0
89	37	0	89	110	0	89	183	0	89	256	0	89	329	0
89	38	0	89	111	0	89	184	0	89	257	0	89	330	0
89	39	1	89	112	0	89	185	0	89	258	0	89	331	0
89	40	3	89	113	0	89	186	0	89	259	0	89	332	0
89	41	1	89	114	0	89	187	0	89	260	0	89	333	0
89	42	0	89	115	0	89	188	0	89	261	0	89	334	0
89	43	0	89	116	0	89	189	0	89	262	3	89	335	0
89	44	0	89	117	0	89	190	0	89	263	0	89	336	0
89	45	0	89	118	0	89	191	0	89	264	0	89	337	0

ear	Day of Year	Daily recip-itation (mm)	ear	Day of ear	Daily recip-itation (mm)	ear	Day of ear	Daily recip-itation (mm)	ear	Day of ear	Daily recip-itation (mm)	ear	Day of ear	Daily recip-itation (mm)
89	46	0	89	119	0	89	192	0	89	265	0	89	338	0
89	47	0	89	120	0	89	193	0	89	266	0	89	339	0
89	48	0	89	121	0	89	194	0	89	267	0	89	340	0
89	49	0	89	122	0	89	195	0	89	268	0	89	341	0
89	50	0	89	123	0	89	196	0	89	269	0	89	342	0
89	51	0	89	124	0	89	197	0	89	270	0	89	343	0
89	52	0	89	125	0	89	198	0	89	271	0	89	344	0
89	53	0	89	126	0	89	199	0	89	272	0	89	345	0
89	54	0	89	127	0	89	200	0	89	273	0	89	346	0
89	55	0	89	128	0	89	201	0	89	274	0	89	347	0
89	56	0	89	129	0	89	202	0	89	275	0	89	348	0
89	57	0	89	130	0	89	203	0	89	276	0	89	349	0
89	58	0	89	131	3	89	204	0	89	277	0	89	350	0
89	59	0	89	132	0	89	205	0	89	278	0	89	351	0
89	60	0	89	133	1	89	206	0	89	279	0	89	352	0
89	61	0	89	134	0	89	207	0	89	280	0	89	353	0
89	62	0	89	135	1	89	208	0	89	281	0	89	354	0
89	63	0	89	136	0	89	209	0	89	282	0	89	355	1
89	64	0	89	137	0	89	210	0	89	283	0	89	356	0
89	65	0	89	138	0	89	211	0	89	284	0	89	357	0
89	66	0	89	139	0	89	212	0	89	285	0	89	358	0
89	67	0	89	140	0	89	213	0	89	286	0	89	359	0
89	68	0	89	141	0	89	214	0	89	287	0	89	360	0
89	69	0	89	142	0	89	215	0	89	288	0	89	361	0
89	70	0	89	143	0	89	216	0	89	289	0	89	362	0
89	71	0	89	144	0	89	217	0	89	290	0	89	363	0
89	72	0	89	145	0	89	218	0	89	291	0	89	364	0
89	73	0	89	146	0	89	219	1	89	292	0	89	365	0

Table III-1. Developed data precipitation record for Yucca Mountain that was used directly as input for INFIL V2.0 (cont.)

ear	Day of Year	Daily recip-itation (mm)	ear	Day of ear	Daily recip-itation (mm)	ear	Day of ear	Daily recip-itation (mm)	ear	Day of ear	Daily recip-itation (mm)	ear	Day of ear	Daily recip-itation (mm)
90	1	0	90	74	0	90	147	3	90	220	0	90	293	0
90	2	1	90	75	0	90	148	11	90	221	0	90	294	0
90	3	0	90	76	0	90	149	0	90	222	0	90	295	0
90	4	0	90	77	0	90	150	0	90	223	0	90	296	0
90	5	0	90	78	0	90	151	0	90	224	1	90	297	0
90	6	0	90	79	0	90	152	0	90	225	0	90	298	0
90	7	0	90	80	0	90	153	0	90	226	0	90	299	0
90	8	0	90	81	0	90	154	0	90	227	8	90	300	0
90	9	0	90	82	0	90	155	0	90	228	0	90	301	0
90	10	0	90	83	0	90	156	0	90	229	0	90	302	0
90	11	0	90	84	0	90	157	0	90	230	0	90	303	0
90	12	0	90	85	0	90	158	0	90	231	0	90	304	0
90	13	0	90	86	0	90	159	0	90	232	0	90	305	0
90	14	3	90	87	0	90	160	1	90	233	0	90	306	0
90	15	0	90	88	0	90	161	2	90	234	0	90	307	0
90	16	2	90	89	0	90	162	0	90	235	0	90	308	0
90	17	6	90	90	0	90	163	0	90	236	0	90	309	0
90	18	0	90	91	0	90	164	0	90	237	0	90	310	0
90	19	0	90	92	0	90	165	0	90	238	0	90	311	0
90	20	0	90	93	0	90	166	0	90	239	0	90	312	0
90	21	0	90	94	0	90	167	0	90	240	0	90	313	0
90	22	0	90	95	0	90	168	0	90	241	0	90	314	0
90	23	0	90	96	0	90	169	0	90	242	0	90	315	0
90	24	0	90	97	0	90	170	0	90	243	0	90	316	0
90	25	0	90	98	0	90	171	0	90	244	0	90	317	0
90	26	0	90	99	0	90	172	0	90	245	0	90	318	0
90	27	0	90	100	0	90	173	0	90	246	0	90	319	0
90	28	0	90	101	0	90	174	0	90	247	0	90	320	0
90	29	0	90	102	0	90	175	0	90	248	0	90	321	0
90	30	0	90	103	0	90	176	0	90	249	0	90	322	0
90	31	0	90	104	0	90	177	0	90	250	0	90	323	1
90	32	3	90	105	0	90	178	0	90	251	0	90	324	3
90	33	0	90	106	0	90	179	0	90	252	0	90	325	0
90	34	0	90	107	0	90	180	0	90	253	0	90	326	0
90	35	0	90	108	0	90	181	0	90	254	0	90	327	0
90	36	0	90	109	0	90	182	0	90	255	0	90	328	0
90	37	0	90	110	5	90	183	0	90	256	0	90	329	0
90	38	0	90	111	0	90	184	0	90	257	0	90	330	0
90	39	0	90	112	0	90	185	0	90	258	0	90	331	0
90	40	0	90	113	1	90	186	0	90	259	0	90	332	0
90	41	0	90	114	0	90	187	0	90	260	0	90	333	0
90	42	0	90	115	0	90	188	0	90	261	0	90	334	0
90	43	0	90	116	0	90	189	0	90	262	0	90	335	0
90	44	0	90	117	0	90	190	0	90	263	0	90	336	0
90	45	0	90	118	0	90	191	0	90	264	0	90	337	0

ear	Day of Year	Daily recip-itation (mm)	ear	Day of ear	Daily recip-itation (mm)	ear	Day of ear	Daily recip-itation (mm)	ear	Day of ear	Daily recip-itation (mm)	ear	Day of ear	Daily recip-itation (mm)
90	46	0	90	119	0	90	192	0	90	265	0	90	338	0
90	47	0	90	120	0	90	193	0	90	266	10	90	339	0
90	48	0	90	121	0	90	194	0	90	267	0	90	340	0
90	49	0	90	122	0	90	195	9	90	268	0	90	341	0
90	50	0	90	123	0	90	196	0	90	269	0	90	342	0
90	51	0	90	124	0	90	197	7	90	270	0	90	343	0
90	52	0	90	125	0	90	198	0	90	271	1	90	344	0
90	53	0	90	126	0	90	199	0	90	272	0	90	345	0
90	54	0	90	127	0	90	200	0	90	273	0	90	346	0
90	55	0	90	128	0	90	201	0	90	274	0	90	347	0
90	56	0	90	129	0	90	202	0	90	275	0	90	348	0
90	57	0	90	130	0	90	203	0	90	276	0	90	349	0
90	58	0	90	131	0	90	204	0	90	277	0	90	350	0
90	59	0	90	132	0	90	205	0	90	278	0	90	351	0
90	60	0	90	133	0	90	206	0	90	279	0	90	352	0
90	61	0	90	134	0	90	207	0	90	280	0	90	353	0
90	62	0	90	135	0	90	208	0	90	281	0	90	354	0
90	63	0	90	136	0	90	209	0	90	282	0	90	355	0
90	64	1	90	137	0	90	210	0	90	283	0	90	356	0
90	65	0	90	138	0	90	211	0	90	284	0	90	357	0
90	66	0	90	139	0	90	212	0	90	285	0	90	358	0
90	67	0	90	140	0	90	213	0	90	286	0	90	359	0
90	68	0	90	141	0	90	214	0	90	287	0	90	360	0
90	69	0	90	142	0	90	215	0	90	288	0	90	361	0
90	70	0	90	143	0	90	216	0	90	289	0	90	362	0
90	71	0	90	144	0	90	217	0	90	290	0	90	363	0
90	72	0	90	145	0	90	218	0	90	291	0	90	364	0
90	73	0	90	146	0	90	219	0	90	292	0	90	365	0

Table III-1. Developed data precipitation record for Yucca Mountain that was used directly as input for INFIL V2.0 (cont.)

ear	Day of Year	Daily recip-itation (mm)	ear	Day of ear	Daily recip-itation (mm)	ear	Day of ear	Daily recip-itation (mm)	ear	Day of ear	Daily recip-itation (mm)	ear	Day of ear	Daily recip-itation (mm)
91	1	0	91	74	0	91	147	0	91	220	0	91	293	0
91	2	0	91	75	0	91	148	0	91	221	0	91	294	0
91	3	2	91	76	0	91	149	0	91	222	4	91	295	0
91	4	1	91	77	0	91	150	0	91	223	1	91	296	0
91	5	0	91	78	11	91	151	0	91	224	9	91	297	0
91	6	0	91	79	4	91	152	2	91	225	0	91	298	0
91	7	0	91	80	19	91	153	0	91	226	0	91	299	2
91	8	0	91	81	1	91	154	0	91	227	0	91	300	0
91	9	0	91	82	0	91	155	0	91	228	0	91	301	0
91	10	0	91	83	0	91	156	0	91	229	0	91	302	0
91	11	0	91	84	0	91	157	0	91	230	0	91	303	0
91	12	0	91	85	3	91	158	0	91	231	0	91	304	0
91	13	0	91	86	19	91	159	0	91	232	0	91	305	0
91	14	0	91	87	0	91	160	0	91	233	0	91	306	0
91	15	0	91	88	0	91	161	0	91	234	0	91	307	0
91	16	0	91	89	0	91	162	0	91	235	0	91	308	0
91	17	0	91	90	0	91	163	0	91	236	0	91	309	0
91	18	0	91	91	0	91	164	0	91	237	0	91	310	0
91	19	0	91	92	0	91	165	0	91	238	0	91	311	0
91	20	0	91	93	0	91	166	0	91	239	0	91	312	0
91	21	0	91	94	0	91	167	0	91	240	0	91	313	0
91	22	0	91	95	0	91	168	0	91	241	0	91	314	0
91	23	0	91	96	0	91	169	0	91	242	0	91	315	0
91	24	0	91	97	0	91	170	0	91	243	13	91	316	0
91	25	0	91	98	0	91	171	0	91	244	0	91	317	0
91	26	0	91	99	0	91	172	0	91	245	0	91	318	0
91	27	0	91	100	0	91	173	0	91	246	0	91	319	0
91	28	0	91	101	0	91	174	0	91	247	0	91	320	0
91	29	0	91	102	0	91	175	0	91	248	2	91	321	0
91	30	0	91	103	0	91	176	0	91	249	2	91	322	0
91	31	0	91	104	0	91	177	0	91	250	0	91	323	0
91	32	0	91	105	0	91	178	0	91	251	0	91	324	0
91	33	0	91	106	0	91	179	0	91	252	0	91	325	0
91	34	0	91	107	0	91	180	0	91	253	0	91	326	0
91	35	0	91	108	0	91	181	0	91	254	0	91	327	0
91	36	0	91	109	0	91	182	0	91	255	0	91	328	0
91	37	0	91	110	0	91	183	0	91	256	0	91	329	0
91	38	0	91	111	0	91	184	0	91	257	0	91	330	0
91	39	0	91	112	0	91	185	0	91	258	0	91	331	0
91	40	0	91	113	0	91	186	0	91	259	0	91	332	0
91	41	0	91	114	0	91	187	0	91	260	0	91	333	0
91	42	0	91	115	0	91	188	1	91	261	0	91	334	0
91	43	0	91	116	0	91	189	0	91	262	0	91	335	0
91	44	0	91	117	0	91	190	0	91	263	0	91	336	0
91	45	0	91	118	0	91	191	0	91	264	0	91	337	0

ear	Day of Year	Daily recip-itation (mm)	ear	Day of ear	Daily recip-itation (mm)	ear	Day of ear	Daily recip-itation (mm)	ear	Day of ear	Daily recip-itation (mm)	ear	Day of ear	Daily recip-itation (mm)
91	46	0	91	119	0	91	192	0	91	265	0	91	338	0
91	47	0	91	120	0	91	193	0	91	266	0	91	339	0
91	48	0	91	121	0	91	194	0	91	267	0	91	340	0
91	49	0	91	122	11	91	195	0	91	268	0	91	341	2
91	50	0	91	123	1	91	196	0	91	269	0	91	342	3
91	51	0	91	124	0	91	197	0	91	270	0	91	343	0
91	52	0	91	125	0	91	198	0	91	271	6	91	344	1
91	53	0	91	126	0	91	199	0	91	272	0	91	345	0
91	54	0	91	127	0	91	200	0	91	273	0	91	346	0
91	55	0	91	128	0	91	201	0	91	274	0	91	347	0
91	56	0	91	129	0	91	202	0	91	275	0	91	348	0
91	57	0	91	130	0	91	203	0	91	276	0	91	349	0
91	58	8	91	131	0	91	204	0	91	277	0	91	350	0
91	59	16	91	132	0	91	205	0	91	278	0	91	351	0
91	60	9	91	133	1	91	206	0	91	279	0	91	352	0
91	61	0	91	134	0	91	207	0	91	280	0	91	353	4
91	62	0	91	135	0	91	208	0	91	281	0	91	354	0
91	63	0	91	136	0	91	209	0	91	282	0	91	355	0
91	64	0	91	137	0	91	210	0	91	283	0	91	356	0
91	65	0	91	138	0	91	211	0	91	284	0	91	357	0
91	66	0	91	139	0	91	212	0	91	285	0	91	358	0
91	67	0	91	140	0	91	213	15	91	286	0	91	359	0
91	68	0	91	141	0	91	214	1	91	287	0	91	360	0
91	69	0	91	142	0	91	215	0	91	288	0	91	361	0
91	70	0	91	143	0	91	216	0	91	289	0	91	362	0
91	71	0	91	144	0	91	217	0	91	290	0	91	363	5
91	72	1	91	145	0	91	218	0	91	291	0	91	364	12
91	73	2	91	146	0	91	219	0	91	292	0	91	365	0

Table III-1. Developed data precipitation record for Yucca Mountain that was used directly as input for INFIL V2.0 (cont.)

ear	Day of Year	Daily recip-itation (mm)	ear	Day of ear	Daily recip-itation (mm)	ear	Day of ear	Daily recip-itation (mm)	ear	Day of ear	Daily recip-itation (mm)	ear	Day of ear	Daily recip-itation (mm)
92	1	0	92	74	0	92	147	0	92	220	0	92	293	0
92	2	0	92	75	0	92	148	0	92	221	0	92	294	0
92	3	3	92	76	0	92	149	0	92	222	0	92	295	0
92	4	5	92	77	0	92	150	1	92	223	0	92	296	0
92	5	22	92	78	0	92	151	0	92	224	1	92	297	0
92	6	8	92	79	0	92	152	0	92	225	0	92	298	8
92	7	0	92	80	4	92	153	0	92	226	0	92	299	0
92	8	0	92	81	10	92	154	0	92	227	0	92	300	0
92	9	0	92	82	2	92	155	0	92	228	0	92	301	7
92	10	0	92	83	3	92	156	0	92	229	0	92	302	0
92	11	0	92	84	0	92	157	0	92	230	0	92	303	0
92	12	0	92	85	0	92	158	0	92	231	0	92	304	1
92	13	0	92	86	0	92	159	0	92	232	0	92	305	0
92	14	0	92	87	5	92	160	0	92	233	0	92	306	0
92	15	0	92	88	0	92	161	0	92	234	0	92	307	0
92	16	0	92	89	5	92	162	0	92	235	0	92	308	0
92	17	0	92	90	15	92	163	0	92	236	0	92	309	0
92	18	0	92	91	6	92	164	0	92	237	0	92	310	0
92	19	0	92	92	0	92	165	0	92	238	0	92	311	0
92	20	0	92	93	0	92	166	0	92	239	0	92	312	0
92	21	0	92	94	0	92	167	0	92	240	0	92	313	0
92	22	0	92	95	0	92	168	0	92	241	0	92	314	0
92	23	0	92	96	0	92	169	0	92	242	0	92	315	0
92	24	0	92	97	0	92	170	0	92	243	0	92	316	0
92	25	0	92	98	0	92	171	0	92	244	0	92	317	0
92	26	0	92	99	0	92	172	0	92	245	0	92	318	0
92	27	0	92	100	0	92	173	0	92	246	0	92	319	0
92	28	0	92	101	0	92	174	0	92	247	0	92	320	0
92	29	0	92	102	0	92	175	0	92	248	0	92	321	0
92	30	0	92	103	0	92	176	0	92	249	0	92	322	0
92	31	0	92	104	0	92	177	0	92	250	0	92	323	0
92	32	0	92	105	0	92	178	0	92	251	0	92	324	0
92	33	0	92	106	0	92	179	0	92	252	0	92	325	0
92	34	0	92	107	0	92	180	0	92	253	0	92	326	0
92	35	0	92	108	0	92	181	0	92	254	0	92	327	0
92	36	0	92	109	0	92	182	0	92	255	0	92	328	0
92	37	15	92	110	0	92	183	0	92	256	0	92	329	0
92	38	12	92	111	0	92	184	0	92	257	0	92	330	0
92	39	0	92	112	0	92	185	0	92	258	0	92	331	0
92	40	3	92	113	0	92	186	0	92	259	0	92	332	0
92	41	17	92	114	0	92	187	0	92	260	2	92	333	0
92	42	7	92	115	0	92	188	0	92	261	0	92	334	0
92	43	22	92	116	0	92	189	0	92	262	2	92	335	0
92	44	9	92	117	0	92	190	0	92	263	0	92	336	0
92	45	0	92	118	0	92	191	0	92	264	0	92	337	0

ear	Day of Year	Daily recip-itation (mm)	ear	Day of ear	Daily recip-itation (mm)	ear	Day of ear	Daily recip-itation (mm)	ear	Day of ear	Daily recip-itation (mm)	ear	Day of ear	Daily recip-itation (mm)
92	46	9	92	119	0	92	192	0	92	265	0	92	338	0
92	47	0	92	120	0	92	193	0	92	266	1	92	339	0
92	48	0	92	121	0	92	194	0	92	267	0	92	340	1
92	49	0	92	122	0	92	195	0	92	268	2	92	341	0
92	50	0	92	123	0	92	196	0	92	269	0	92	342	41
92	51	0	92	124	0	92	197	0	92	270	0	92	343	19
92	52	0	92	125	0	92	198	0	92	271	3	92	344	0
92	53	0	92	126	0	92	199	0	92	272	0	92	345	0
92	54	0	92	127	0	92	200	0	92	273	0	92	346	2
92	55	0	92	128	0	92	201	0	92	274	0	92	347	0
92	56	0	92	129	3	92	202	0	92	275	0	92	348	0
92	57	0	92	130	0	92	203	0	92	276	0	92	349	0
92	58	0	92	131	0	92	204	0	92	277	0	92	350	0
92	59	0	92	132	0	92	205	0	92	278	0	92	351	0
92	60	0	92	133	0	92	206	0	92	279	0	92	352	0
92	61	0	92	134	0	92	207	0	92	280	0	92	353	1
92	62	23	92	135	0	92	208	0	92	281	0	92	354	0
92	63	3	92	136	0	92	209	0	92	282	0	92	355	0
92	64	0	92	137	0	92	210	0	92	283	0	92	356	0
92	65	0	92	138	0	92	211	0	92	284	0	92	357	1
92	66	2	92	139	0	92	212	0	92	285	0	92	358	1
92	67	5	92	140	0	92	213	2	92	286	0	92	359	0
92	68	1	92	141	0	92	214	0	92	287	0	92	360	0
92	69	0	92	142	1	92	215	0	92	288	0	92	361	0
92	70	0	92	143	0	92	216	0	92	289	0	92	362	1
92	71	0	92	144	0	92	217	0	92	290	0	92	363	7
92	72	0	92	145	0	92	218	0	92	291	0	92	364	1
92	73	0	92	146	0	92	219	0	92	292	0	92	365	0
												92	366	0

ATTACHMENT IV

GEOSPATIAL INPUT DATA FOR INFIL V2.0 FY99

TOTAL PAGES: 16

Geospatial Input Data for INFIL V2.0 FY99

1. Statement of Intended Use for the Data

The purpose of these data is to provide spatial information and properties for each grid block necessary to calculate net infiltration at each location for the Yucca Mountain site using the model INFIL V2.0.

2. General Information Pertaining to the Data Set

Source data software used for development of geospatial input data are as follows:

(1) Elevation, northing and easting: USGS Digital Elevation Model (DEM) from Topopah Spring West and Busted Butte 7.5-minute quadrangles: DTN: GS000308311221.006, ARCINFO, to produce ASCII file 30MSITE.INP (DTN: GS000308311221.006)
(2) Downstream grid cell: 30MSITE.INP, SORTGRD1 V1.0, CHNNET16 V1.0 (DTN: GS000308311221.006)
(3) Number of upstream cells: 30MSITE.INP, SORTGRD1 V1.0, CHNNET16 V1.0 (DTN: GS000308311221.006)
(4) Slope: 30MSITE.INP, ARCINFO (DTN: GS000308311221.006)
(5) Aspect: 30MSITE.INP, ARCINFO (DTN: GS000308311221.006)
(6) Soil-type: INFIL V2.0 control file INFILS5o.CTL and 30MSITE.INF (DTN: GS960508312212.007, GS000308311221.006)
(7) Soil depth class: soil depth map (DTN: GS960508312212.007), INFIL V2.0 control file INFILS5o.CTL, and 30MSITE.INP (DTN: GS000308311221.006)
(8) Modeled soil depth: soil depth class (DTN: GS960508312212.007), GEOMAP7 V1.0, GEOMOD4 V1.0, and SOILMAP6 V1.0
(9) Rock type: INFIL V2.0 control file INFILS5o.CTL, and README2.DAY [coverage explanations for Day et al. (1998)], (DTN: GS971208314221.003)
(10) Topographic position: INFIL V2.0 control file INFILS5o.CTL
(11) Blocking ridges: 30MSITE.INP (DTN: GS000308311221.006), BLOCKR7 V1.0

This data set consists of three parts. One is a set of 10 files consisting of grid blocks within individual watershed modeling domains and all associated geospatial input listed above. The 10 modeling domains are illustrated in Figure 6-12 (Attachment II). These files are in EXCEL worksheets formatted with descriptive column headers and are available in DTN: GS000308311221.004:

YuccaWash.xls
DuneWash.xls
DrillHole.xls
Solitario1.xls
Solitario2.xls
Solitario4.xls
PlugHill.xls
JetRidge1.xls
JetRidge2.xls

JetRidge3.xls.

The parameters included in each file are grid cell identifier number, UTM easting, UTM northing (m), latitude, longitude (decimal degrees), grid cell row index, grid cell column index, downstream grid cell identifier (used for surface water routing), number of upstream grid cells, elevation (m), slope (degrees inclination from horizontal), aspect (degrees from north), soil-type identifier, soil depth class identifier, modeled soil depth (m), rock-type identifier, topographic position, 36 blocking ridge angles (decimal degrees, inclination above horizontal) (see Table IV-1). An abbreviated example of the files is shown in Table IV-2.

The second part is the lookup table providing properties for each grid. It consists of a spreadsheet called GeoK.xls and consists of rock-type identifier, source, geologic description, hydrogeologic identifier, and bulk bedrock permeability (Table IV-3).

Part 3 is the soil properties (Table IV-4). These are measured and calculated properties. Measured properties are bulk density, porosity, and rock fragment content. Saturated hydraulic conductivity, moisture retention curve fit parameters alpha and n, water content at –0.1 bar water potential, and water content at –60 bars water potential were estimated using empirical equations) from Campbell (1985, DTN: GS000300001221.007).

Part 1: Geospatial input for each of 10 drainages

This input is primarily based on the USGS Digital Elevation Model (DEM) from Topopah Spring West and Busted Butte 7.5-minute quadrangles. The base grid (DTN: GS000308311221.006) was used to define location coordinates for the geospatial parameter input files for the 1996 version of the net infiltration model (Flint et al., 1996). The DEM is a regular 2-dimensional grid of 253,597 cells having dimensions of 30 x 30 meters and elevations to the nearest meter. The 30-meter grid is based on a Universal Transverse Mercator (UTM), zone 11, NAD 1927 projection, consists of 691 northing "rows" (grid cell row index) and 367 easting "columns" (grid cell column index) aligned orthogonal to the UTM coordinate axis, and has a lower left corner coordinate of 544,661 meters easting and 4,067,133 meters northing. Grid locations are also defined using geographic coordinates, latitude and longitude in decimal degrees, which were calculated in ARCINFO and used as input for the SOLRAD sub-model in INFIL V2.0. The row and column location indices are used in the flow routing module in INFIL in the calculation of the surface water run-on term.

Downstream grid cell identifer is the flow routing parameter and determines which of eight surrounding grid cells is the lowest in elevation. A value of –3 indicates the downstream grid cell is a drainage boundary. Flow directions were calculated for each grid cell using a two-step process. For the first step, the entire base-grid is sorted by elevation using the routine SORTGRD V1.0. In the second step, flow routing directions are calculated based on a standard D8 routing algorithm using the routine CHNNET16 V1.0. CHNNET16 V1.0 is a convergent flow routing algorithm; multiple cells are allowed to route to a single cell, but any given cell can route to only one downstream grid cell (as opposed to two in cases of flow dispersion). The CHNNET16 V1.0 algorithm provides a method for routing through surface depressions in the DEM. The number of upstream grid cells is included in each file.

Elevation from mean sea level in meters is included in each file.

Slope is a required input parameter for estimating soil depths. Slope and aspect were calculated for the net infiltration model from the DEM (DTN: GS000308311221.006) using standard GIS applications in ARCINFO.

Soil type is indicated by values of between 1 and 10 (Flint et al., 1996, Table 3, DTN: GS960908312211.003). When encountered in INFIL it uses a lookup table (INFILS5o.CTL) that has all hydrologic parameters for each soil type as listed in Flint et al. (1996). Depth class identifier is a value between 1 and 6 and is used in the preprocessing routine SOILMAP6 V1.0 with depth to bedrock map (DTN: GS960508312212.007, Estimated distribution of geomorphic surfaces and depth to bedrock for the southern half of the Topopah Spring NW 7.5 minute quadrangle and the entire Busted Butte 7.5 minute quadrangle), and slope to calculate soil depth at all grid block locations. Soil depth is estimated using a combination of the soil depth class map and an estimated linear relation between soil depth and slope within each depth class (GEOMAP7 V1.0 and GEOMOD4 V1.0). Soil depth classes represent different ranges in actual soil depths that were estimated using a combination of Quaternary geologic maps, field observations, and soil depth recorded at borehole sites (Flint and Flint, 1995, Table 2). Depth class #1 identifies locations with soil depths ranging from 0 to 0.5 meters and primarily occurs in rugged upland areas. Depth class #2 identifies deeper soils ranging from 0.5 to 3.0 meters occurring at mid to lower side-slope locations in upland areas affected by slumps, slides, and other mass-wasting processes. Depth class #3 identifies locations in the transition zone between upland areas and alluvial fans or basins with intermediate soil depths ranging from 3 to 6 meters. Depth class #4 identifies deep soils with depths of 6 meters or greater. Depth class #5 is an intermediate depth zone equivalent to Depth class #3, however #3 did not represent field conditions well when the Day et al. (1998) map was incorporated into the model. Depth class #5 is therefore an adjusted version of Depth class #3 where the geology is represented by Day et al. (1998) . Depth class #6 occurs where Scott and Bonk (1984) mapped bedrock and Day et al. (1998) mapped deep alluvium. A compromise for this depth class was chosen as 3-6 m. The soil depth classes were used to estimate soil depths based on calculated slope and an empirical soil-depth model (modeled soil depth, in meters). This model is based on an assumed soil depth – slope correlation within the soil depth classes defined for the 1996 version of the net infiltration model (Flint et al., 1996). The conceptual soil depth model for depth class 1 assumes that soils are thinnest at summit and ridge-crest areas as well as steep side slopes. Deeper soils are assumed to occur at the relatively gently sloping shoulder areas that define the transition between summit or ridge crest areas and steep side slope areas. Deeper soils are also assumed to occur for more gently sloping foot-slope locations. The model for soil depth class 1 is defined by:

$$D = 0.03 * S + 0.1, \quad S \leq 10$$
$$D = 0.013 * (10 - S) + 0.4, \quad 10 < S < 40$$
$$D = 0.01, \quad S \geq 40$$

where D = soil depth (in meters), and S = slope (degrees). The model for depth class #2 is defined by:

$$D = 2 - (0.05 * S), \quad S < 32$$
$$D = 0.4, \quad S \geq 32$$

and the model for depth class # 3 is defined by:

$$D = 6 - (0.16 * S), \qquad S \leq 25$$
$$D = 2.0$$

For depth class #4, soil depth is set to a uniform depth of 6 meters.

Rock-type identifier defines the rock type for each grid cell so that the corresponding bulk bedrock permeability can be found in the look up table shown in Table IV-3. Bedrock geology was defined for each grid element using three ARCINFO map coverages and a vector to raster conversion performed by ARCINFO. The three maps used for the bedrock determinations are the 1:6000 scale Bedrock Geologic Map of the Central block area by Day et al. (1998), the Preliminary Geologic Map of Yucca Mountain by Scott and Bonk (1984), and the Geologic Map of the Topopah Spring Northwest Quadrangle by Sawyer et al. (1995) . Within the UZ flow and transport model area, bedrock geology for the net infiltration model (which is defined as a unique integer identifier for each rock-type in the geospatial parameter input file) is primarily defined by Day et al. (1998). Bedrock geology for the northern and southern perimeter sections of the UZ flow and transport model area is defined by Scott and Bonk (1984). Bedrock geology is represented in the geospatial parameter input file using a unique integer identifier for each rock-type. The identifier is linked to a bulk (field-scale) saturated permeability in the model control file (represented in GeoK.xls). Multiple rock-types can be assigned the same bulk permeability value in the model control file.

Topographic position is indicated by values ranging from 1 to 4, corresponding to the classification ridgetop, sideslope, alluvial terrace, and channel discussed in Section 6.1.2 of this AMR. This information was used in INFIL V1.0 to identify channel locations, but as routing is done in version 2.0 this parameter is not used. It is however maintained as a placeholder.

The 36 blocking ridge angles (degrees inclination above horizontal) are calculated at each 10-degree horizontal arc (with the azimuth aligned in the UTM northing direction) for each grid cell using the routine BLOCKR7. Calculations were performed using the DEM as input and a technique for approximating the 10-degree horizontal angles based on grid cell distances. The blocking ridge parameters cannot account for topographic influences outside of the DEM, and thus the blocking ridge effect is only partly accounted for along the perimeter of the DEM.

Part 2: Geologic unit identifier and associated bulk bedrock saturated hydraulic conductivity

The second part includes only the file GeoK.xls (Table IV-3). The geologic identifier in the first column is a value that allows each grid cell to use this file as a lookup table to identify rock type. The source is the map the rock type was taken from using ARCINFO coverages. The next two columns are geologic descriptions extracted from the sources that, when combined with map location, allow for the interpretation of corresponding lithostratigraphic unit shown in the next column which is represented by nomenclature from Buesch et al. (1996). The determination of corresponding lithostratigraphic unit is typically straightforward based on description. The column with corresponding hydrogeologic unit is based on Flint (1998 Table 1 and DTN: GS000308312231.002) and incorporates data from analyses of samples of most of the rock types for saturated hydraulic conductivity (DTN: GS000308312231.002). Saturated hydraulic conductivity (K_s) on individual core samples was determined on subsamples from several boreholes

(DTN: GS990408312231.001, GS960808312231.001, GS960808312231.005). Cores were vacuum saturated, and K_s was measured using a steady-state permeameter that forces water through the core at a measured pressure while weighing the outflow over time. K_s was calculated using Darcy's law. Mean values of saturated hydraulic conductivity for each hydrogeologic unit were determined by using a geometric mean calculation (DTN: GS000308312231.002). The bulk bedrock hydraulic conductivity represents the combined matrix and fracture saturated hydraulic conductivity of each rock-type. Bulk bedrock hydraulic conductivity was calculated using measured saturated hydraulic conductivity of fracture fill material. A value of 43.2 mm/day was selected and used as a preliminary value. However, a value of 46.7 mm/day is the average value calculated from all measurements in DTN: GS950708312211.003, Fracture/Fault Properties For Fast Pathways Model; the difference in calculated bulk hydraulic conductivity between these values is insignificant and results in bulk hydraulic conductivities that are less than 1% different. Additional values used to calculate bulk bedrock hydraulic conductivity included an estimate of the percent area occupied by 250 micron fractures (the assumption of this size fracture is discussed in Flint et al., 1996) and the mean saturated hydraulic conductivity of the bedrock matrix for that rock type (Flint, 1998, Table 7; DTN: GS000308312231.002). The percent area occupied by fractures of 250-microns aperture is equal to 250 microns divided by 1,000,000 microns per meter, multiplied by the fracture densities in fractures per meter. The fracture desities for each rock type that were used to calculate the bulk bedrock hydraulic conductivities were estimated from field observations and, subsequently, were corroborated by the fracture density data from boreholes NRG-4, NRG-5, NRG-6, NRG-7, SD-9 and SD-12 reported in Altman et al. (1996, Table 3-6, DTN: SNSAND96081900.000).

For the development of hydrogeologic units, the data originally collected from laboratory measurements on all samples from 31 surface-based boreholes drilled from 1995 through 1997, were analysed and data were submitted in the following data packages: DTN: GS920508312231.012, GS930108312231.006, GS940408312231.004, GS000408312231.004, GS940508312231.006, GS950608312231.007, GS950308312231.004, GS950608312231.005, GS950308312231.003, GS951108312231.009, GS951108312231.011, GS951108312231.010, GS950308312231.002, GS960808312231.004, GS950608312231.006, GS960808312231.002, GS960808312231.001, GS950608312231.008, GS960808312231.005, GS960808312231.003, GS000308312231.001, and GS000308312231.002. These are also included in Section 8.4. Outliers and inappropriate data have been removed to allow for a better representation of the hydrogeologic units. Physical properties of bulk density, porosity, and particle density; flow properties of saturated hydraulic conductivity and moisture-retention characteristics; and the state variables (variables describing the current state of field conditions) of saturation and water potential were determined for each unit. Units were defined using the data base of physical and hydrologic properties, described lithostratigraphic boundaries and corresponding relations to porosity, recognition of transition zones with pronounced changes in properties over short vertical distances, characterization of the influence of mineral alteration on hydrologic properties such as permeability and moisture-retention characteristics, and a statistical analysis to evaluate where boundaries should be adjusted to minimize the variance within layers. Additional data packages referred to in this attachment pertaining to the development of parameters for geospatial input for the net-infiltration model are also included in Section 8.4.

Part 3: Properties for 10 soil units

The properties in Table IV-4 represent soils located around Yucca Mountain, Nevada. Bulk density, porosity, and rock fragment content were measured using laboratory analyses described in Flint and others (1996, p. 41). The source data for these measured properties were submitted under the following DTNs:

GS950708312211.002 - "FY94 and FY95 Laboratory Measurements of Physical Properties of Surficial Materials at Yucca Mountain, Nevada."
GS960108312211.001 - "FY95 Lab Measurements of Physical Properties of Surficial Material, at Yucca Mountain, NV PART II"
GS960108312211.002 - "Gravimetric and Volumetric Water Content and Rock Fragment Content of 31 Selected Sites at Yucca Mountain, NV: FY95 Laboratory Measurements of Physical Properties of Surficial Material at Yucca Mountain, Part III"

Field and laboratory analyses were conducted on the soils around Yucca Mountain. Large-volume, field bulk-density samples were collected from the surface to 0.3 m by using an irregular-hole, bulk-density device called a bead cone. Bulk density, porosity, rock fragment content, and sand, silt, and clay percentages were determined. Saturated hydraulic conductivity was measured using a double-ring infiltrometer on soils in locations where it could be measured and then compared to conductivity simulated using textural data for the fine-soil fraction (<2 mm) by using Equation 6.12 of Campbell (1985, DTN: GS000300001221.007). Log-log water-characteristic curves were determined using Equations 2.15, 2.16, 2.17, 2.18, 5.10, and 5.11 of Campbell (1985, DTN: GS000300001221.007) and were converted to van Genuchten curves in Excel. Soil-water contents at -0.1 bar and -60 bars water potential were used as field capacity and residual water content, the difference of which is plant available water content. The soil properties are summarized in Table IV-4, where the parameters defining the van Genuchten curves (conductivity, alpha, and n) are simulated from texture, rock fragment content, and bulk density measured in the field. Also listed in Table IV-4 are the soil-water contents corresponding to -0.1 and -60 bars water potential for each soil type, calculated using the fitted water-retention van Genuchten curve for each soil type.

To test the validity of using textural analysis as a surrogate for measurements of soil properties, field-measured hydraulic conductivities were compared with the geometric-mean particle diameter using a method discussed in Campbell (1985, eq. 2.15, DTN: GS000300001221.007) and with the model predictions of hydraulic properties made using Campbell (1985, eqs. 5.10 and 5.11, DTN: GS000300001221.007), which is developed for <2-mm particle sizes. The results indicated an adequate correlation to use textural data for particle sizes < 0.3 mm; however, the presence of rock fragments has a substantial effect on soil properties. To account for the presence of rock fragments, the log of simulated hydraulic conductivity from Campbell (1985, DTN: GS000300001221.007) and the gravimetric rock-fragment content were regressed against the log of the measured values of hydraulic conductivity to produce a modified Campbell equation with an r^2 of 0.85. The equation was then applied to each unit in Table IV-4 to determine the saturated hydraulic conductivity. This analysis assumes that textural changes with depth are insignificant and that properties determined from textural sampling from the top 0.3 m of soil represents the entire soil profile. A large percentage of the surficial deposits in the study area are < 0.5 m deep (Flint et al., 1996, Figure 13) and the application of these data for these shallow soils is considered appropriate.

Textural data also were used for the calculation of moisture-retention curves for the surficial soils using Campbell (1985, DTN: GS000300001221.007). Six moisture-retention curves were measured in the laboratory on soil units 1, 2, and 4 using tempe cells, pressure pots, and chilled-mirror psychrometers to measure water potential over a full range of saturations (Flint et al., 1996, Figures 16A, 16B, and 16C). Curves were fit to the combined data sets for each soil unit. Curves calculated from the average textural data for the soil units are very similar to the curves from the measured data for the three units. It was considered, therefore, that texture could be used to calculate curves and associated parameters for the remaining five soil units, and all curves are illustrated in Flint et al. (1996, Figure 16D). These parameters are those listed in Table IV-4.

Table IV-1. Description of columns in output files with geospatial input for INFIL V2.0.

Column	Description
1	Grid cell identifier number
2	UTM easting (m)
3	UTM northing (m)
4	Latitude (decimal degrees)
5	Longitude (decimal degrees)
6	Grid cell row index
7	Grid cell column index
8	Downstream grid cell identifier number (used for surface water routing)
9	Number of upstream grid cells
10	Elevation (m)
11	Slope (degrees inclination from horizontal)
12	Aspect (degrees azimuth from the UTM northing axis, in the horizontal plane)
13	Soil type identifier
14	Depth class identifier
15	Modeled soil depth (m)
16	Rock type identifier
17	Topographic position
18	1st of 36 blocking ridge angles (inclination above horizontal, decimal degrees)
	-
	-
	-
	-
54	Last of 36 blocking ridge angles

Table IV-2. Example of output found in files used as geospatial input for INFIL V2.0. (DTN: GS000308311221.004)

Grid cell identifier	UTM Easting (m)	UTM Northing (m)	Latitude (degrees)	Longitude (degrees)	Grid cell row index	Grid cell column index	Downstream grid cell identifier	Number of upstream grid cells	Elevation (m)
59985	545681	4076613	36.8361	116.4877	375	35	-3	0	1393
60288	545681	4076583	36.8359	116.4877	376	35	62707	0	1392
60879	545681	4076553	36.8356	116.4877	377	35	63010	0	1390
61172	545711	4076613	36.8361	116.4874	375	36	-3	0	1389
61179	545681	4076523	36.8353	116.4877	378	35	63573	0	1389
61794	545651	4076613	36.8361	116.488	375	34	-3	0	1387
61795	545711	4076583	36.8359	116.4874	376	36	-3	0	1387
62076	545711	4076553	36.8356	116.4874	377	36	-3	0	1386
62077	545681	4076493	36.835	116.4877	379	35	65103	0	1386
62706	545651	4076583	36.8359	116.488	376	34	-3	1	1384
62707	545651	4076553	36.8356	116.488	377	34	66960	1	1384
62708	545711	4076523	36.8353	116.4874	378	36	-3	0	1384
62711	545681	4076463	36.8348	116.4877	380	35	67273	0	1384
63010	545651	4076523	36.8353	116.4881	378	34	67584	1	1383
63011	545711	4076493	36.835	116.4874	379	36	-3	0	1383
63573	545651	4076493	36.835	116.4881	379	34	68785	1	1381
63574	545711	4076463	36.8348	116.4874	380	36	-3	0	1381

Grid cell identifier	Slope (degrees inclination from horizontal)	Aspect (degrees from northing)	Soil type identifier	Depth class identifier	Modeled soil depth (m)	Rock type identifier	Topographic position	Blocking ridge angle 1	Blocking ridge angle 2
59985	9	197	5	1	0.48	17	4	2	1
60288	9	199	5	1	0.48	17	4	2	1
60879	8	201	5	1	0.46	17	5	2	1
61172	10	109	5	1	0.5	17	4	2	1
61179	8	196	5	1	0.46	17	5	2	1
61794	20	259	5	1	0.33	18	4	3	5
61795	10	108	5	1	0.5	17	4	2	1
62076	10	108	5	1	0.5	17	4	2	1
62077	9	193	5	1	0.48	17	4	2	1
62706	19	259	5	1	0.35	18	4	5	9
62707	19	263	5	1	0.35	18	4	6	7
62708	10	108	5	1	0.5	17	4	2	1
62711	12	197	5	1	0.47	17	4	2	1
63010	18	258	5	1	0.36	18	4	5	6
63011	10	112	5	1	0.5	17	5	2	1
63573	18	248	5	1	0.36	18	4	5	6
63574	9	125	5	1	0.48	17	5	2	1

Table IV-3. Lookup table in INFIL V2.0 providing properties for each grid block, consisting of rock-type identifier, source, geologic description (formation and lithology), corresponding lithostratigraphic unit and hydrogeologic identifier, and estimated fracture density and bulk bedrock saturated hydraulic conductivity based on filled 250-um fractures.[F/m, fractures per meter; mm/d, millimeters per day.] (DTN: GS000308311221.004)

Geologic Identifier	Source	Geologic descriptions from sources		Corres-ponding lithostratigraphic unit	Corres-ponding hydrogeologic unit	Estimated Fracture density (F/m)	Bulk Bedrock Saturated Hydraulic Conductivity w/filled 250-um fractures (mm/d)
		Formation	Lithology				
2	Scott and Bonk (1984)	Rhyolite of Pinnacles Ridge	Lava flows	Tptrv1	TC	25.0	0.41
3	Scott and Bonk (1984)	Rhyolite of Pinnacles Ridge	Pyroclastic rocks	Tpbt2	BT3	0.5	46.66
4	Scott and Bonk (1984)	Rhyolite of Comb Peak	Lava flows	Tpcpll	CW	7.0	0.09
5	Scott and Bonk (1984)	Rhyolite of Comb Peak	Pyroclastic rocks	Tpbt3	BT3	0.5	46.66
6	Scott and Bonk (1984)	Rhyolite of Vent Pass	Lava flows	Tptrv1	TC	25.0	0.41
7	Scott and Bonk (1984)	Rhyolite of Vent Pass	Pyroclastic rocks	Tpbt3	BT3	0.5	46.66
8	Scott and Bonk (1984)	Rhyolite of Black Glass Canyon	Lava flows	Tpcpll	CW	7.0	0.09
9	Scott and Bonk (1984)	Rhyolite of Black Glass Canyon	Pyroclastic rocks	Tpbt3	BT3	0.5	46.66
10	Scott and Bonk (1984)	Basalt Dikes of Yucca Mountain	Welded	Tpcplnc	CW	7.0	0.09
11	Scott and Bonk (1984)	Timber Mountain Tuff-Rainier Mesa	Welded ash-flow tuff	Tptpmn	TMN	5.0	0.06
12	Scott and Bonk (1984)	Timber Mountain Tuff-Rainier Mesa	Nonwelded ash-flow tuff	Tpcpv1	CNW	6.0	2.74
13	Scott and Bonk (1984)	Bedded Tuff	Bedded Tuff	Tpbt4	BT4	0.5	13.83
14	Scott and Bonk (1984)	Rhyolite of Windy Wash	Lava flows	Tpcpll	CW	7.0	0.09
15	Scott and Bonk (1984)	Rhyolite of Windy Wash	Pyroclastic rocks	Tpbt3	BT3	0.5	46.66
16	Scott and Bonk (1984)	Tiva Canyon Tuff	Undifferentiated	Tpcpll	CW	7.0	0.09
17	Scott and Bonk (1984)	Tiva Canyon Tuff	Caprock	Tpcrv	TC	20.0	0.35
18	Scott and Bonk (1984)	Tiva Canyon Tuff	Upper cliff	Tpcrn	CUC	5.0	3.34
19	Scott and Bonk (1984)	Tiva Canyon Tuff	Upper lithophysal	Tpcpul	CUL	5.0	1.13
20	Scott and Bonk (1984)	Tiva Canyon Tuff	Clinkstone	Tpcpmn	CW	5.0	0.06
21	Scott and Bonk (1984)	Tiva Canyon Tuff	Lower cliff	Tpcpmn	CW	5.0	0.06
22	Scott and Bonk (1984)	Tiva Canyon Tuff	Clinkstone	Tpcpmn	CW	5.0	0.06
23	Scott and Bonk (1984)	Tiva Canyon Tuff	Clinkstone	Tpcpmn	CW	5.0	0.06
24	Scott and Bonk (1984)	Tiva Canyon Tuff	Clinkstone	Tpcpmn	CW	5.0	0.06
25	Scott and Bonk (1984)	Tiva Canyon Tuff	Middle lithophysal	Tpcpmn	CW	5.0	0.06
26	Scott and Bonk (1984)	Tiva Canyon Tuff	Clinkstone	Tpcpmn	CW	5.0	0.06
27	Scott and Bonk (1984)	Tiva Canyon Tuff	Rounded step	Tpcpmn	CW	5.0	0.06
28	Scott and Bonk (1984)	Tiva Canyon Tuff	Lower Lithophysal	Tpcpll	CW	5.0	0.06

Geologic Identifier	Source	Geologic descriptions from sources		Corres-ponding lithostratigraphic unit	Corres-ponding hydrogeologic unit	Estimated Fracture density (F/m)	Bulk Bedrock Saturated Hydraulic Conductivity w/filled 250-um fractures (mm/d)
		Formation	Lithology				
29	Scott and Bonk (1984)	Tiva Canyon Tuff	Hackly zone	Tpcplnh	CW	5.0	0.06
30	Scott and Bonk (1984)	Tiva Canyon Tuff	Hackly zone	Tpcplnh	CW	5.0	0.06
31	Scott and Bonk (1984)	Tiva Canyon Tuff	Columnar	Tpcplnc	CW	5.0	0.06
32	Scott and Bonk (1984)	Tiva Canyon Tuff	Bedded Tuff	Tpbt4	BT4	0.5	13.83
33	Scott and Bonk (1984)	Yucca Mountain Tuff	Undifferentiated	Tpbt4	BT4	0.5	13.83
34	Scott and Bonk (1984)	Yucca Mountain Tuff	Upper	Tpbt4	BT4	0.5	13.83
35	Scott and Bonk (1984)	Yucca Mountain Tuff	Middle	Tpy	CW	5.0	0.06
36	Scott and Bonk (1984)	Yucca Mountain Tuff	Lower	Tpy	BT3	0.5	46.66
37	Scott and Bonk (1984)	Yucca Mountain Tuff	Rhyolite Flows	Tpcpll	CW	7.0	0.09
38	Scott and Bonk (1984)	Yucca Mountain Tuff	Bedded Tuff	Tpbt3	BT3	0.5	46.66
39	Scott and Bonk (1984)	Pah Canyon Tuff	Undifferentiated	Tpp	TPP	1.0	75.62
40	Scott and Bonk (1984)	Pah Canyon Tuff	Upper	Tpp	TPP	1.0	75.62
41	Scott and Bonk (1984)	Pah Canyon Tuff	Middle	Tpp	CW	5.0	0.06
42	Scott and Bonk (1984)	Pah Canyon Tuff	Lower	Tpbt2	BT2	0.5	276.49
43	Scott and Bonk (1984)	Pah Canyon Tuff	Bedded Tuff	Tpbt2	BT2	0.5	276.49
44	Scott and Bonk (1984)	Topopah Spring Tuff	Undifferentiated	Tptpll	CW	7.0	0.09
45	Scott and Bonk (1984)	Topopah Spring Tuff	Caprock	Tptrv1	TC	25.0	0.41
99	Scott and Bonk (1984)	Topopah Spring Tuff	Caprock/rounded	Tptrn	TC	10.0	0.25
46	Scott and Bonk (1984)	Topopah Spring Tuff	Rounded	Tptrn	TR	5.0	0.20
47	Scott and Bonk (1984)	Topopah Spring Tuff	Thin lithophysal	Tptpul	TUL	3.0	0.05
48	Scott and Bonk (1984)	Topopah Spring Tuff	Red lithophysal	Tptpul	TUL	3.0	0.05
49	Scott and Bonk (1984)	Topopah Spring Tuff	Upper lithophysal	Tptpul	TUL	3.0	0.05
50	Scott and Bonk (1984)	Topopah Spring Tuff	Lower lithophysal	Tptpul	TUL	3.0	0.05
51	Scott and Bonk (1984)	Topopah Spring Tuff	Lithophysal	Tptpul	TUL	3.0	0.05
52	Scott and Bonk (1984)	Topopah Spring Tuff	Nonlithophysal	Tptpmn	TMN	7.0	0.09
53	Scott and Bonk (1984)	Topopah Spring Tuff	Gray nonlithophysal	Tptpmn	TMN	7.0	0.09
54	Scott and Bonk (1984)	Topopah Spring Tuff	Nonlithophysal	Tptpmn	TMN	7.0	0.09
55	Scott and Bonk (1984)	Topopah Spring Tuff	Brick	Tptpmn	TMN	7.0	0.09

Geologic Identifier	Source	Geologic descriptions from sources		Corres-ponding lithostratigraphic unit	Corres-ponding hydrogeologic unit	Estimated Fracture density (F/m)	Bulk Bedrock Saturated Hydraulic Conductivity w/filled 250-um fractures (mm/d)
		Formation	Lithology				
56	Scott and Bonk (1984)	Topopah Spring Tuff	Middle nonlithophysal	Tptpmn	TMN	7.0	0.09
57	Scott and Bonk (1984)	Topopah Spring Tuff	Orange brick lithophysal	Tptpmn	TMN	7.0	0.09
58	Scott and Bonk (1984)	Topopah Spring Tuff	Orange brick	Tptpmn	TMN	7.0	0.09
59	Scott and Bonk (1984)	Topopah Spring Tuff		Tptpmn	TMN	7.0	0.09
60	Scott and Bonk (1984)	Topopah Spring Tuff		Tptpmn	TMN	7.0	0.09
61	Scott and Bonk (1984)	Topopah Spring Tuff		Tptpmn	TMN	7.0	0.09
62	Scott and Bonk (1984)	Topopah Spring Tuff	Mottled lithophysal	Tptpll	TLL	5.0	0.07
63	Scott and Bonk (1984)	Topopah Spring Tuff	Lower Lithophysal	Tptpll	TLL	5.0	0.07
64	Scott and Bonk (1984)	Topopah Spring Tuff	Lower Lithophysal	Tptpll	TLL	5.0	0.07
65	Scott and Bonk (1984)	Topopah Spring Tuff	Lower Lithophysal	Tptpll	TLL	5.0	0.07
66	Scott and Bonk (1984)	Topopah Spring Tuff	Mottled	Tptpln	TM1	12.0	0.14
67	Scott and Bonk (1984)	Topopah Spring Tuff	Vitrophyre	Tptpv3	PV3	15.0	0.17
68	Scott and Bonk (1984)	Topopah Spring Tuff	Partially welded	Tptpv2,1	PV2	0.5	0.07
69	Scott and Bonk (1984)	Calico Hills Formation	Pyroclastic rocks	Tac	CHZ	0.5	0.02
70	Scott and Bonk (1984)	Calico Hills Formation	Lava flows	Tptpln	TM1	12.0	0.14
71	Scott and Bonk (1984)	Calico Hills Formation	Autobrecciated lavas	Tac	CHZ	0.5	0.01
72	Scott and Bonk (1984)	Prow Pass Tuff	Partially welded	Tcp, unit3	PP3	1.0	1.65
73	Scott and Bonk (1984)	Prow Pass Tuff	Moderately welded	Tcp, unit2	PP2	2.0	0.05
74	Scott and Bonk (1984)	Prow Pass Tuff	Undifferentiated	Tcp, unit2	PP2	2.0	0.05
75	Scott and Bonk (1984)	Prow Pass Tuff	Bedded Tuffs	Tcp, unit1	PP1	1.0	0.02
76	Scott and Bonk (1984)	Bullfrog Tuff	Ash-flow tuff	Tcb, unit3	BF3	1.0	0.09
77	Scott and Bonk (1984)		Disturbed ground				0.25
201	Sawyer et al. (1995)	Tiva Canyon Tuff	Undifferentiated	Tpcpll	CW	1.0	0.09
202	Sawyer et al. (1995)	Timber Mountain Tuff-Rainier Mesa	Welded ash-flow tuff	Tptpmn	TMN	5.0	0.06
203	Sawyer et al. (1995)	Rhyolite of Windy Wash	Lava flows	Tpcpll	CW	1.0	0.09
204	Sawyer et al. (1995)		Alluvium				500.00
205	Sawyer et al. (1995)	Rhyolite of Vent Pass	Lava flows	Tptrv1	TC	25.0	0.41

Geologic Identifier	Source	Geologic descriptions from sources		Corres-ponding lithostratigraphic unit	Corres-ponding hydrogeologic unit	Estimated Fracture density (F/m)	Bulk Bedrock Saturated Hydraulic Conductivity w/filled 250-um fractures (mm/d)
		Formation	Lithology				
206	Sawyer et al. (1995)	Rhyolite of Pinnacles Ridge	Lava flows	Tptrv1	TC	25.0	0.41
207	Sawyer et al. (1995)	Rhyolite of Pinnacles Ridge	Pyroclastic rocks	Tpbt2	BT3	0.5	46.66
208	Sawyer et al. (1995)	Calico Hills Formation	Lava flows	Tptpln	TM1	12.0	0.14
209	Sawyer et al. (1995)	Yucca Mountain Tuff	Middle	Tpy	CW	5.0	0.06
210	Sawyer et al. (1995)	Rhyolite of Comb Peak	Lava flows	Tpcpll	CW	1.0	0.09
211	Sawyer et al. (1995)	Bullfrog Tuff	Ash-flow tuff	Tcb, unit3	BF3	1.0	0.09
212	Sawyer et al. (1995)	Bullfrog Tuff	Ash-flow tuff	Tcb, unit3	BF3	1.0	0.09
213	Sawyer et al. (1995)	Topopah Spring Tuff	Nonlithophysal	Tptpmn	TMN	1.0	0.09
214	Sawyer et al. (1995)	Prow Pass Tuff	Moderately welded	Tcp, unit2	PP2	2.0	0.05
301	Day et al. (1998)	Alluvial & Colluvial deposits	Alluvial & Colluvial deposits	QTac	QTac		500.00
302	Day et al. (1998)	Colluvial deposits	Colluvial deposits	Qtc	QTac		500.00
303	Day et al. (1998)	Miocene Intrusives	basalt dike	Td	CW	5.0	0.06
304	Day et al. (1998)	Timber Mountain Group	Rainier Mesa Tuff, welded	Tmrw	TMN	1.0	0.09
305	Day et al. (1998)	Timber Mountain Group	Rainier Mesa Tuff, nonwelded	Tmr	CNW	6.0	2.74
306	Day et al. (1998)	Rhyolite of Comb Peak	Rhyolite lava flow	Tpkl	BT3	0.5	46.66
307	Day et al. (1998)	Rhyolite of Comb Peak	Ash-flow tuff	Tpkt	BT3	0.5	46.66
308	Day et al. (1998)	Rhyolite of Comb Peak	bedded tuff	Tbt5	BT3	0.5	46.66
309	Day et al. (1998)	Rhyolite of Comb Peak	undivided	Tpu	CW	5.0	0.06
310	Day et al. (1998)	Tiva Canyon Tuff	undivided	Tcu	CW	5.0	0.06
311	Day et al. (1998)	Tiva Canyon Tuff	crystal rich vitric zone	Tcrv	TC	20.0	0.35
312	Day et al. (1998)	Tiva Canyon Tuff	subvitric transition zone	Tcrn4	TC	20.0	0.35
313	Day et al. (1998)	Tiva Canyon Tuff	pumice-poor zone	Tcrn3	CUC	5.0	3.34
314	Day et al. (1998)	Tiva Canyon Tuff	mixed-pumice zone	Tcr2	CUC	5.0	3.34
315	Day et al. (1998)	Tiva Canyon Tuff	crystal transition zone	Tcr1	CW	5.0	0.06
316	Day et al. (1998)	Tiva Canyon Tuff	upper lithophysal	Tcpul	CUL	5.0	1.13
317	Day et al. (1998)	Tiva Canyon Tuff	upper nonlithophysal	Tcpun	CW	5.0	0.06
318	Day et al. (1998)	Tiva Canyon Tuff	middle nonlithophysal	Tcpmn	CW	5.0	0.06

Geologic Identifier	Source	Geologic descriptions from sources		Corres-ponding lithostratigraphic unit	Corres-ponding hydrogeologic unit	Estimated Fracture density (F/m)	Bulk Bedrock Saturated Hydraulic Conductivity w/filled 250-um fractures (mm/d)
		Formation	Lithology				
319	Day et al. (1998)	Tiva Canyon Tuff	upper & middle nonlith, undivided	Tcpum	CW	5.0	0.06
320	Day et al. (1998)	Tiva Canyon Tuff	lower lith	Tcpll	CW	5.0	0.06
321	Day et al. (1998)	Tiva Canyon Tuff	lower nonlith	Tcpln	CW	5.0	0.06
322	Day et al. (1998)	Tiva Canyon Tuff	columnar subzone	Tcplnc	CW	5.0	0.06
323	Day et al. (1998)	Tiva Canyon Tuff	crystal poor vitric	Tcplncv	CNW	6.0	2.74
324	Day et al. (1998)	Yucca Mt. Tuff	Yucca Mt. Tuff	Tpy	BT4	0.5	13.83
325	Day et al. (1998)	Pah Canyon Tuff	Pah Canyon Tuff, nonwelded	Tpp	TPP	1.0	75.62
326	Day et al. (1998)	Pah Canyon Tuff	Pah Canyon Tuff, welded	Tppw	CW	5.0	0.06
327	Day et al. (1998)	pre-Pah Canyon Tuff	pre-Pah Canyon Tuff	Tpbt2	BT2	0.5	276.49
328	Day et al. (1998)	Topopah Spring Tuff	undifferentiated	Tptu	TR	5.0	0.20
329	Day et al. (1998)	crystal rich member	crystal rich vitric, undivided	Tptrv	TC	20.0	0.35
330	Day et al. (1998)	crystal rich member	densely welded zone	Tptrn3	TC	20.0	0.35
331	Day et al. (1998)	crystal rich member	pumice-rich zone	Tptrn2	TR	5.0	0.20
332	Day et al. (1998)	crystal rich member	crystal transition zone	Tptr1	TUL	3.0	0.05
333	Day et al. (1998)	crystal poor member	upper lith	Tptpul	TUL	3.0	0.05
334	Day et al. (1998)	crystal poor member	middle nonlith	Tptpmn	TMN	7.0	0.09
335	Day et al. (1998)	crystal poor member	lithophysal bearing subzone	Tptmnl	TMN	7.0	0.09
336	Day et al. (1998)	crystal poor member	lower lith	Tptpll	TLL	7.0	0.09
345	Day et al. (1998)	Topopah Spring Tuff	undivided	Tptrn	TR	10.0	0.24

Table IV-4. Summary of soil properties used as input for INFIL V2.0.
[m/s, meters per second; Pa, pascals; %, percent; g/cm^3, grams per cubic centimeter; ——, not applicable] (DTN: GS000308311221.004)

Soil unit	Saturated hydraulic conductivity (simulated, m/s)	alpha (1/Pa)	n	Porosity (%)	Rock fragments(%)	Bulk Density (g/cm^3)	Water content at -0.1 bar water potential (%)	Water content at -60 bars water potential (%)
1	$5.6x10^{-6}$	0.00052	1.24	36.6	10.5	1.60	24.2	5.4
2	$1.2x10^{-5}$	0.00062	1.31	31.5	11.6	1.73	17.3	2.3
3	$1.3x10^{-5}$	0.00066	1.36	32.5	18.7	1.70	16.3	1.7
4	$3.8x10^{-5}$	0.00087	1.62	28.1	21.9	1.81	7.3	0.2
5	$6.7x10^{-6}$	0.00056	1.28	33.0	15.2	1.69	20.0	3.5
6	$2.7x10^{-5}$	0.00074	1.40	33.9	11.7	1.66	15.0	1.1
7	$5.6x10^{-6}$	0.00055	1.26	37.0	17.1	1.58	23.4	4.6
9	$5.7x10^{-6}$	0.00055	1.30	32.2	19.1	1.72	18.9	2.8

ATTACHMENT V

DEVELOPMENT OF DAILY CLIMATE INPUT USING DAILY09 V1.0

TOTAL PAGES: 30

Development of Daily Climate Input using DAILY09 V1.0

1. Name of routine/macro with version/OS/hardware environment and user information:

Name of software routine: DAILY09 V1.0
OS and hardware environment: Windows NT 4.0, Pentium Pro PC
Computer Identification: SM321276 with a USGS specific host-name P720dcasr
Software Users: Joseph Hevesi (916-278-3274), Alan Flint (916-278-3221)
User Location: U.S. Geological Survey, Room 5000E, Placer Hall, 6000 J Street, Sacramento, CA 95819-6129

2. Name of commercial software with version/OS/hardware used to develop routine/macro:

The source code for DAILY09 V1.0 was developed using the standard FORTRAN77 programming language. The source code was written, debugged, and compiled (for PC platforms using INTEL processors) using DIGITAL Visual Fortran with Microsoft Developer Studio, v. 5.0.

3. General Description of routine/macro:

DAILY09 V1.0 is a FORTRAN77 routine developed in accordance with AP-SI.1Q, specifically for the analysis/model activity documented in this AMR. The routine source code (DAILY09.FOR), compiled executable file (DAILY09.EXE), routine control file (DAILY09.CTL), input and output files used for routine validation, supplemental files created as part of validation testing, and a copy of this attachment, are located under the directory DAILY09 on a CD-ROM labeled DAYINPUT-1. The routine source code, control file, and the input and output files are ASCII text files that can be read using any standard ASCII text editor and can be imported into standard word processing applications such as Microsoft Word. The executable file can be used to run DAILY09 V1.0 on any PC with an INTEL processor (with adequate RAM).

4. Test plan for the software routine DAILY09 V1.0:

- **Explain whether this is a routine or macro and describe what it does:**

DAILY09 V1.0 is a routine that creates a daily climate input file for INFIL. It reformats EARTHINFO precipitation and air temperature files into a format that can be used as input to INFIL V2.0. Daily climate records from the analog precipitation sites were exported from the EARTHINFO database (using the NCDC format option), and the exported files (Nogales.dat and Hobbs.dat) were provided as input to the program DAILY09, which reformats the NCDC format into the xyz column format required by INFIL V2.0. In addition to reformatting, DAILY09 also identifies gaps in the precipitation and the maximum and minimum air temperature records. Minor gaps (10 days or less for precipitation and 20 days or less for air temperature) are filled using an estimate of zero for precipitation and linear interpolation (arithmetic mean) between the days having records on either side of the gap for

air temperature. Years having major gaps in the record are identified and omitted from the reformatted output. Average daily air temperature is estimated as the mean of the recorded maximum and minimum daily air temperatures. Output from DAILY09, which includes the average daily air temperature estimate, is provided directly as input to INFIL V2.0.

- **Listing of FORTRAN77 Source code:**

A listing of the FORTRAN77 source code for the routine DAILY09 V1.0 along with examples of the input and output files used in the test plan are included at the end of this attachment.

- **Description of test(s) to be performed:**

To evaluate the accuracy of the functions performed by the routine, the test plan utilizes the auxiliary output files created by DAILY09 so that the individual functions can be tested separately. The primary function performed by the routine is the re-formatting of the EARTHINFO export file (exported using the NCDC export format option) consisting of the daily climate record for a selected monitoring site. The EARTHINFO exported file consists of measured daily precipitation (in hundredths of inches), daily maximum air temperature (in degrees Fahrenheit), daily minimum air temperature (in degrees Fahrenheit), and daily snowfall depth (in tenths of inches). It is an ASCII file with the data organized in a pseudo-matrix format.

There are 4 test cases used to evaluate the accuracy of DAILY09 in performing its expected calculations and formatting: (1) A visual inspection to ascertain that the reformatting of the data from the pseudo-matrix (EARTHINFO) into the column format required for input into INFIL doesn't change the values, (2) a visual inspection of the identification of gaps that eliminate years with gaps in precipitation > 10 days and air temperature > 20 days, (3) an arithmetic check to ensure that the mean of the maximum and minimum air temperature is correctly calculated for the day, and (4) a visual inspection of gaps in the record that identify gaps in precipitation < 10 days and insert zeros, and a visual and arithmetic check to ensure that gaps in air temperature < 20 days calculate a linear interpolation between the number preceding the gap and the number at the end of the gap.

- **Specify the range of input values to be used and why the range is valid:**

An example input is used for each test case that represents a random selection of values from the EARTHINFO output file that is transformed into the INFIL daily precipitation input file. A matching output file is used to determine if the transformation is accurate.

5. Test Results.

- **Output from test (explain difference between input range used and possible input):**

The output must provide, for each of the 4 test cases: (1) an accurate representation of the values reformatted, (2) the omission of years with gaps that exceed those number of days

specified, (3) the correct averaging of minimum and maximum air temperatures for a given day to no greater accuracy than zero decimal places, and (4) the insertion of zeros into precipitation records that have gaps for < 10 days and the correct interpolation of air temperatures for gaps < 20 days, to no greater accuracy than zero decimal places.

- **Description of how the testing shows that the results are correct for the specified input:**

If the testing results in output that conforms to the above criteria then the results are correct for the specified input.

- **List limitations or assumptions to this test case and code in general:**

Limitations to the developed test case consist of the selection only of a small number of values that are assumed to be representative of the entire file.

- **Electronic files identified by name and location:**

The following electronic files including DAILY09 V1.0 and selected analog input and output files are provided:

DAILY09.CTL:	input file consisting of the input and output file names for BLOCKR7, along with parameters needed to perform the 36 blocking ridge angle calculations.
DAILY09.FOR:	FORTRAN source code listing for the routine BLOCKR7. A printout of the source code is included as part of this attachment.
DAILY09.EXE:	Executable file for the routine BLOCKR7, compiled for INTEL processors.
ROSALIA.DAT:	ASCII text file exported from the EARTHINFO NOAA daily climate records WEST2 database. This file is the input file to DAILY09 V1.0.
ROSALIA.DAY:	Auxiliary output file created by DAILY09 V1.0. The file contains all daily climate data provided by ROSALIA.DAT and is used to test for the proper re-formatting. The calculated average daily air temperature is included. This file is used only as part of the validation test for DAILY09.
ROSALIA.INP:	Primary output file created by DAILY09 V1.0. This file is used directly as input to INFIL V2.0 for defining the daily climate input parameters needed for simulating net infiltration.

6. **Supporting Information. (Include background information, such as revision to a previous routine or macro, or explanation of the steps performed to run the software. Include listings of all electronic files and codes used).**

- **Procedure for running routine:**

To run the routine DAILY09, an executable version of the code and all input files must be placed in the same directory. The routine is executed by typing DAILY09 in a DOS window or by double clicking on the file DAILY09.EXE in Windows NT. The input and output file names and the parameters used for the blocking ridge calculations must be in the correct sequential order as specified in the routine control file DAILY09.CTL (see example listing in this section)

- **Example listing of ROSALIA.DAT.** This ASCII file is exported from EARTHINFO using the NCDC export format option. The data shown in this subset is for maximum daily air temperature (TMAX), followed by precipitation (PRCP), with the record starting in May (5) of 1948, continuing through November (11) of 1948. On the first 2 monthly records it is noted just above the top line how to read the file. Month 5 has no data (-99999) for temperature, month 6 has data in degrees Fahrenheit.

```
            Tmax   1948  5 (May)      1 (Day)         2 (Day)         3 (Day)
DLY45718002TMAX F19480599990310198-99999M10298-99999M10398-99999M10498-99999M10598-
99999M10698-99999M10798-99999M10898-99999M10998-99999M11098-99999M11198-99999M11298-
99999M11398-99999M11498-99999M11598-99999M11698-99999M11798-99999M11898-99999M11998-
99999M12098-99999M12198-99999M12298-99999M12398-99999M12498-99999M12598-99999M12698-
99999M12798-99999M12898-99999M12998-99999M13098-99999M13198-99999M1

            Tmax   1948  6 (June)     1        77 (F) 2        81 (F) 3        67 (F)
DLY45718002TMAX F19480699990310198 00077 10298 00081 10398 00067 10498 00066 10598 00079
10698 00084 10798 00088 10898 00086 10998 00087 11098 00077 11198 00069 11298 00074 11398
00071 11498 00076 11598 00071 11698 00066 11798 00069 11898 00073 11998 00077 12098 00065
12198 00061 12298 00069 12398 00075 12498 00069 12598 00077 12698 00077 12798 00081 12898
00086 12998 00091 13098 00083 13198-99999M1

DLY45718002PRCPHI19480599990310198-99999M10298-99999M10398-99999M10498-99999M10598-
99999M10698-99999M10798-99999M10898-99999M10998-99999M11098-99999M11198-99999M11298-
99999M11398-99999M11498-99999M11598-99999M11698-99999M11798-99999M11898-99999M11998-
99999M12098-99999M12198-99999M12298-99999M12398-99999M12498-99999M12598-99999M12698-
99999M12798-99999M12898-99999M12998-99999M13098-99999M13198-99999M1

DLY45718002PRCPHI19480699990310198 00000 10298 00000 10398 00000 10498 00017 10598 00001
10698 00000 10798 00000 10898 00000 10998 00000 11098 00040 11198 00000 11298 00057 11398
00005 11498 00002 11598 00000 11698 00046 11798 00012 11898 00000 11998 00000 12098 00000
12198 00034 12298 00005 12398 00004 12498 00000 12598 00005 12698 00005 12798 00000 12898
00000 12998 00000 13098 00002 13198-99999M1
```

- **Example listing of ROSALIA.DAY.** DAILY09 uses the EARTHINO data to reformat into *.DAY format prior to identification of gaps, conversions and averaging. When compared to the above EARTHINFO file it indicates that the reformatting done in DAILY09 is correct. This file also includes the conversion of air temperature from Fahrenheit to Celsius. June 1, 1948 in the EARTHINFO file above is 77 (F), June 2 is 81 (F). In file below the conversion results in June 1 = 25(C) and June 2 = 27.2(C), calculated as degrees C = (degrees F – 32) * (5/9).

```
Output file generated using program DAILY09.FOR
Output file = Rosalia.day
```

Daily climate record for Rosalia, Washington
GU1 Upper bound glacial transition climate analog (4/12/1999)

Station ID = 457180

Dy = day
Mo = month
Yr = year
Max = maximum
Min = minimum
Precip = total daily precipitation
Temp = daily air temperature
mm = millimeters
deg C = degrees Celsius

Data Flags:

-999.9 = missing data value
M = missing data flag
A = accumulated measurement (multiple days)
T = trace amount (less than measurement resolution)

Record Day Number	Year	Mo	Dy of Mo	Dy of Yr	Precip mm	Max Temp deg C	Min Temp deg C	Snow Fall mm
54177	1948	5	1	122	-999.9 M	-999.9 M	-999.9 M	-999.9 M
54178	1948	5	2	123	-999.9 M	-999.9 M	-999.9 M	-999.9 M
54179	1948	5	3	124	-999.9 M	-999.9 M	-999.9 M	-999.9 M
54180	1948	5	4	125	-999.9 M	-999.9 M	-999.9 M	-999.9 M
54181	1948	5	5	126	-999.9 M	-999.9 M	-999.9 M	-999.9 M
54182	1948	5	6	127	-999.9 M	-999.9 M	-999.9 M	-999.9 M
54183	1948	5	7	128	-999.9 M	-999.9 M	-999.9 M	-999.9 M
54184	1948	5	8	129	-999.9 M	-999.9 M	-999.9 M	-999.9 M
54185	1948	5	9	130	-999.9 M	-999.9 M	-999.9 M	-999.9 M
54186	1948	5	10	131	-999.9 M	-999.9 M	-999.9 M	-999.9 M
54187	1948	5	11	132	-999.9 M	-999.9 M	-999.9 M	-999.9 M
54188	1948	5	12	133	-999.9 M	-999.9 M	-999.9 M	-999.9 M
54189	1948	5	13	134	-999.9 M	-999.9 M	-999.9 M	-999.9 M
54190	1948	5	14	135	-999.9 M	-999.9 M	-999.9 M	-999.9 M
54191	1948	5	15	136	-999.9 M	-999.9 M	-999.9 M	-999.9 M
54192	1948	5	16	137	-999.9 M	-999.9 M	-999.9 M	-999.9 M
54193	1948	5	17	138	-999.9 M	-999.9 M	-999.9 M	-999.9 M
54194	1948	5	18	139	-999.9 M	-999.9 M	-999.9 M	-999.9 M
54195	1948	5	19	140	-999.9 M	-999.9 M	-999.9 M	-999.9 M
54196	1948	5	20	141	-999.9 M	-999.9 M	-999.9 M	-999.9 M
54197	1948	5	21	142	-999.9 M	-999.9 M	-999.9 M	-999.9 M
54198	1948	5	22	143	-999.9 M	-999.9 M	-999.9 M	-999.9 M
54199	1948	5	23	144	-999.9 M	-999.9 M	-999.9 M	-999.9 M
54200	1948	5	24	145	-999.9 M	-999.9 M	-999.9 M	-999.9 M
54201	1948	5	25	146	-999.9 M	-999.9 M	-999.9 M	-999.9 M
54202	1948	5	26	147	-999.9 M	-999.9 M	-999.9 M	-999.9 M
54203	1948	5	27	148	-999.9 M	-999.9 M	-999.9 M	-999.9 M
54204	1948	5	28	149	-999.9 M	-999.9 M	-999.9 M	-999.9 M
54205	1948	5	29	150	-999.9 M	-999.9 M	-999.9 M	-999.9 M

Record Number	Year	Mo	Dy of Mo	Dy of Yr	Precip mm	Max Temp deg C	Min Temp deg C	Snow Fall mm
54206	1948	5	30	151	-999.9 M	-999.9 M	-999.9 M	-999.9 M
54207	1948	5	31	152	-999.9 M	-999.9 M	-999.9 M	-999.9 M
54208	1948	6	1	153	0.0	25.0	7.8	0.0
54209	1948	6	2	154	0.0	27.2	7.2	0.0
54210	1948	6	3	155	0.0	19.4	10.0	0.0
54211	1948	6	4	156	4.3	18.9	8.9	0.0
54212	1948	6	5	157	0.3	26.1	7.2	0.0
54213	1948	6	6	158	0.0	28.9	8.9	0.0
54214	1948	6	7	159	0.0	31.1	8.9	0.0
54215	1948	6	8	160	0.0	30.0	10.6	0.0
54216	1948	6	9	161	0.0	30.6	15.0	0.0
54217	1948	6	10	162	10.2	25.0	9.4	0.0
54218	1948	6	11	163	0.0	20.6	10.6	0.0
54219	1948	6	12	164	14.5	23.3	7.2	0.0
54220	1948	6	13	165	1.3	21.7	11.7	0.0
54221	1948	6	14	166	0.5	24.4	7.2	0.0
54222	1948	6	15	167	0.0	21.7	10.6	0.0
54223	1948	6	16	168	11.7	18.9	10.0	0.0
54224	1948	6	17	169	3.0	20.6	7.2	0.0
54225	1948	6	18	170	0.0	22.8	6.7	0.0
54226	1948	6	19	171	0.0	25.0	7.2	0.0
54227	1948	6	20	172	0.0	18.3	8.3	0.0
54228	1948	6	21	173	8.6	16.1	8.3	0.0
54229	1948	6	22	174	1.3	20.6	6.7	0.0
54230	1948	6	23	175	1.0	23.9	7.2	0.0
54231	1948	6	24	176	0.0	20.6	7.8	0.0
54232	1948	6	25	177	1.3	25.0	5.6	0.0
54233	1948	6	26	178	1.3	25.0	6.7	0.0
54234	1948	6	27	179	0.0	27.2	6.7	0.0
54235	1948	6	28	180	0.0	30.0	8.9	0.0
54236	1948	6	29	181	0.0	32.8	9.4	0.0
54237	1948	6	30	182	0.5	28.3	14.4	0.0

- **Example listing of ROSALIA.DAY. DAILY09** uses the EARTHINO data to reformat into *.DAY format prior to identification of gaps and averaging, but following conversion from Fahrenheit to Celsius. The file below is precipitation for 1971 (Dec), 1972 (all) and 1973 (Jan and Feb only), following the reformatting and conversion to Celsius. The year 1972 has large gaps and when compared to the final input file will be omitted.

```
Output file generated using program DAILY09.FOR
Output file = Rosalia.day
Daily climate record for Rosalia, Washington
GU1 Upper bound glacial transition climate analog (4/12/1999)

Station ID = 457180

Dy          = day
Mo          = month
Yr          = year
Max         = maximum
Min         = minimum
Precip      = total daily precipitation
Temp        = daily air temperature
mm          = millimeters
deg C       = degrees Celsius

Data Flags:

-999.9  =  missing data value
M       =  missing data flag
A       =  accumulated measurement (multiple days)
T       =  trace amount (less than measurement resolution)
```

Record Day Number	Year	Mo	Dy of Mo	Dy of Yr	Precip mm		Max Temp deg C	Min Temp deg C	Snow Fall mm	
62791	1971	12	1	335	0.0		1.1	-3.9	0.0	
62792	1971	12	2	336	0.0		3.9	-2.8	0.0	
62793	1971	12	3	337	0.0	T	2.8	-4.4	0.0	T
62794	1971	12	4	338	0.0		1.7	-6.1	0.0	
62795	1971	12	5	339	5.1		2.2	-1.7	63.5	
62796	1971	12	6	340	0.0		2.8	-5.0	0.0	
62797	1971	12	7	341	0.0		-2.8	-16.1	0.0	
62798	1971	12	8	342	0.0		-6.7	-15.6	0.0	
62799	1971	12	9	343	0.0		2.8	-7.8	0.0	
62800	1971	12	10	344	0.0		2.2	-2.2	0.0	
62801	1971	12	11	345	7.6		0.0	-8.9	50.8	
62802	1971	12	12	346	2.0		1.1	-8.9	25.4	
62803	1971	12	13	347	0.0		0.0	-9.4	0.0	
62804	1971	12	14	348	0.0		0.6	-7.8	0.0	
62805	1971	12	15	349	0.0		1.1	-7.2	0.0	
62806	1971	12	16	350	3.6		-1.7	-13.3	76.2	
62807	1971	12	17	351	0.0		4.4	-1.7	0.0	
62808	1971	12	18	352	0.3		5.0	0.6	0.0	
62809	1971	12	19	353	0.0		3.3	-3.3	0.0	
62810	1971	12	20	354	0.0		0.6	-1.1	0.0	
62811	1971	12	21	355	3.0		2.2	-0.6	12.7	
62812	1971	12	22	356	2.0		3.9	0.0	0.0	
62813	1971	12	23	357	0.3		5.6	-1.7	0.0	
62814	1971	12	24	358	0.3		3.9	0.0	0.0	
62815	1971	12	25	359	0.0		6.1	-0.6	0.0	
62816	1971	12	26	360	0.0		3.3	-4.4	0.0	
62817	1971	12	27	361	0.0		-3.3	-10.0	0.0	
62818	1971	12	28	362	0.0		-1.7	-10.6	0.0	
62819	1971	12	29	363	3.0		-4.4	-8.9	25.4	
62820	1971	12	30	364	0.0		-5.0	-16.1	0.0	
62821	1971	12	31	365	0.8		0.6	-9.4	25.4	
62822	1972	1	1	1	0.0		0.6	-5.0	0.0	
62823	1972	1	2	2	0.0		2.8	-2.8	0.0	
62824	1972	1	3	3	0.0		-1.1	-12.8	0.0	
62825	1972	1	4	4	0.0		-3.9	-12.2	0.0	
62826	1972	1	5	5	1.3		-1.1	-6.7	2.5	
62827	1972	1	6	6	0.0		2.2	-1.7	0.0	
62828	1972	1	7	7	0.0		3.3	0.6	0.0	
62829	1972	1	8	8	0.5		3.9	-3.3	12.7	
62830	1972	1	9	9	0.0		2.8	-2.8	0.0	
62831	1972	1	10	10	0.0		2.2	-5.0	0.0	
62832	1972	1	11	11	1.8		1.7	-3.9	12.7	
62833	1972	1	12	12	0.0		4.4	-3.9	0.0	
62834	1972	1	13	13	0.0		-1.7	-11.7	0.0	
62835	1972	1	14	14	0.0		-5.0	-12.2	0.0	
62836	1972	1	15	15	0.0		-0.6	-6.7	0.0	
62837	1972	1	16	16	0.0		2.8	-1.7	0.0	
62838	1972	1	17	17	0.0		5.0	0.6	0.0	
62839	1972	1	18	18	1.3		4.4	-2.8	12.7	
62840	1972	1	19	19	7.6		3.9	-2.8	12.7	
62841	1972	1	20	20	14.7		6.7	2.8	0.0	
62842	1972	1	21	21	9.9		8.3	2.2	0.0	
62843	1972	1	22	22	0.0		7.2	1.1	0.0	
62844	1972	1	23	23	1.5		5.0	0.0	2.5	
62845	1972	1	24	24	0.0		1.7	-4.4	0.0	
62846	1972	1	25	25	8.9		-0.6	-7.2	101.6	
62847	1972	1	26	26	5.6		-6.1	-16.7	76.2	
62848	1972	1	27	27	0.0		-13.9	-18.9	0.0	
62849	1972	1	28	28	0.0		-12.2	-18.9	0.0	
62850	1972	1	29	29	2.0		-10.0	-18.3	12.7	
62851	1972	1	30	30	0.0		-6.7	-18.9	0.0	
62852	1972	1	31	31	0.0		-5.6	-16.1	0.0	
62853	1972	2	1	32	2.3		-8.9	-20.6	38.1	
62854	1972	2	2	33	0.0		-8.9	-23.3	0.0	
62855	1972	2	3	34	0.0		-6.7	-23.9	0.0	
62856	1972	2	4	35	0.0		-3.9	-21.1	0.0	

Record Day Number	Year	Mo	Dy of Mo	Dy of Yr	Precip mm	Max Temp deg C	Min Temp deg C	Snow Fall mm	
62857	1972	2	5	36	3.8	-3.3	-16.1	50.8	
62858	1972	2	6	37	5.3	0.6	-7.8	76.2	
62859	1972	2	7	38	0.0	1.7	-2.8	0.0	
62860	1972	2	8	39	0.0	3.3	-2.8	0.0	
62861	1972	2	9	40	0.0	2.8	-3.9	0.0	
62862	1972	2	10	41	0.0	1.1	-6.7	0.0	
62863	1972	2	11	42	0.0	1.7	-6.1	0.0	
62864	1972	2	12	43	0.0	3.9	0.0	0.0	
62865	1972	2	13	44	3.6	6.7	0.0	0.0	
62866	1972	2	14	45	0.0	3.3	-1.7	0.0	
62867	1972	2	15	46	5.1	2.2	-1.7	0.0	T
62868	1972	2	16	47	0.0	8.3	1.7	0.0	
62869	1972	2	17	48	0.0	9.4	-2.2	0.0	
62870	1972	2	18	49	4.1	2.8	-1.7	0.0	
62871	1972	2	19	50	0.0	12.8	2.2	0.0	
62872	1972	2	20	51	4.1	13.3	1.1	0.0	
62873	1972	2	21	52	0.0	6.7	-1.1	0.0	
62874	1972	2	22	53	1.8	8.3	0.0	0.0	
62875	1972	2	23	54	0.0	6.1	-1.7	0.0	
62876	1972	2	24	55	6.6	5.0	-1.1	50.8	
62877	1972	2	25	56	0.0	6.1	-2.2	0.0	
62878	1972	2	26	57	0.0	3.9	-2.8	0.0	
62879	1972	2	27	58	7.6	11.1	0.6	0.0	
62880	1972	2	28	59	0.0	12.8	7.2	0.0	
62881	1972	2	29	60	0.0	13.9	0.0	0.0	
62882	1972	3	1	61	0.0	5.0	-3.3	0.0	
62883	1972	3	2	62	4.1	1.7	-2.2	25.4	
62884	1972	3	3	63	0.0	5.0	-2.8	0.0	
62885	1972	3	4	64	0.0	4.4	-2.8	0.0	
62886	1972	3	5	65	2.0	9.4	-2.2	0.0	
62887	1972	3	6	66	0.0	12.2	1.1	0.0	
62888	1972	3	7	67	0.0	4.4	-3.9	0.0	
62889	1972	3	8	68	0.0	4.4	-3.3	0.0	
62890	1972	3	9	69	0.0	12.2	0.6	0.0	
62891	1972	3	10	70	0.3	18.9	2.2	0.0	
62892	1972	3	11	71	4.6	13.9	5.6	0.0	
62893	1972	3	12	72	5.6	12.8	3.9	0.0	
62894	1972	3	13	73	7.9	10.0	6.7	0.0	
62895	1972	3	14	74	0.0	12.8	1.7	0.0	
62896	1972	3	15	75	0.0	10.6	2.2	0.0	
62897	1972	3	16	76	0.0	14.4	4.4	0.0	
62898	1972	3	17	77	0.0	18.3	5.6	0.0	
62899	1972	3	18	78	0.0	20.6	6.7	0.0	
62900	1972	3	19	79	0.8	11.7	2.8	0.0	
62901	1972	3	20	80	0.0	10.0	2.2	0.0	
62902	1972	3	21	81	0.0	12.8	1.7	0.0	
62903	1972	3	22	82	0.0	15.6	4.4	0.0	
62904	1972	3	23	83	0.0	14.4	0.0	0.0	
62905	1972	3	24	84	0.0	7.2	-0.6	0.0	
62906	1972	3	25	85	2.3	8.9	-3.9	0.0	
62907	1972	3	26	86	0.0	5.6	-3.9	0.0	
62908	1972	3	27	87	0.0	5.0	-1.7	0.0	
62909	1972	3	28	88	1.5	6.1	-1.1	25.4	
62910	1972	3	29	89	0.0	7.2	-2.8	0.0	
62911	1972	3	30	90	0.0	11.7	0.0	0.0	
62912	1972	3	31	91	0.0	13.3	0.6	0.0	
62913	1972	4	1	92	3.3	16.1	5.6	0.0	
62914	1972	4	2	93	0.0	14.4	-3.9	0.0	
62915	1972	4	3	94	0.0	10.0	-3.3	0.0	
62916	1972	4	4	95	0.0	12.2	0.6	0.0	
62917	1972	4	5	96	0.5	12.8	5.6	0.0	
62918	1972	4	6	97	2.3	13.9	3.9	0.0	
62919	1972	4	7	98	1.5	11.7	0.0	0.0	
62920	1972	4	8	99	0.0	8.3	-0.6	0.0	
62921	1972	4	9	100	1.5	8.9	-1.7	0.0	
62922	1972	4	10	101	0.0	8.3	-3.3	0.0	

Record Day Number	Year	Mo	Dy of Mo	Dy of Yr	Precip mm	Max Temp deg C	Min Temp deg C	Snow Fall mm
62923	1972	4	11	102	1.3	10.0	1.7	0.0
62924	1972	4	12	103	3.3	6.7	1.7	0.0
62925	1972	4	13	104	1.3	5.6	-2.2	0.0
62926	1972	4	14	105	0.0	8.3	-2.2	0.0
62927	1972	4	15	106	0.0	12.2	2.2	0.0
62928	1972	4	16	107	0.0	11.7	0.6	0.0
62929	1972	4	17	108	0.0	7.8	-2.8	0.0
62930	1972	4	18	109	0.0	5.6	-5.0	0.0
62931	1972	4	19	110	0.0	8.9	-3.9	0.0
62932	1972	4	20	111	0.0	12.8	0.0	0.0
62933	1972	4	21	112	0.0	12.8	3.3	0.0
62934	1972	4	22	113	0.0	9.4	-5.0	0.0
62935	1972	4	23	114	0.0	8.9	-1.1	0.0
62936	1972	4	24	115	0.0	21.1	7.2	0.0
62937	1972	4	25	116	0.0	13.3	0.6	0.0
62938	1972	4	26	117	0.0	11.7	-1.7	0.0
62939	1972	4	27	118	0.0	15.0	0.6	0.0
62940	1972	4	28	119	0.0	23.3	5.6	0.0
62941	1972	4	29	120	0.0	8.3	-3.3	0.0
62942	1972	4	30	121	0.0	10.6	-3.9	0.0
62943	1972	5	1	122	0.0	11.7	-3.3	0.0
62944	1972	5	2	123	0.0	16.7	0.6	0.0
62945	1972	5	3	124	0.0	20.6	2.8	0.0
62946	1972	5	4	125	0.0	22.2	4.4	0.0
62947	1972	5	5	126	0.0	23.3	4.4	0.0
62948	1972	5	6	127	0.0	22.2	8.3	0.0
62949	1972	5	7	128	0.0	18.9	5.6	0.0
62950	1972	5	8	129	16.8	15.6	4.4	0.0
62951	1972	5	9	130	24.4	6.7	2.8	0.0
62952	1972	5	10	131	1.8	8.9	4.4	0.0
62953	1972	5	11	132	0.0	15.6	5.6	0.0
62954	1972	5	12	133	0.0	17.8	6.7	0.0
62955	1972	5	13	134	0.0	21.7	8.3	0.0
62956	1972	5	14	135	0.0	25.0	7.2	0.0
62957	1972	5	15	136	0.0	23.9	10.0	0.0
62958	1972	5	16	137	0.0	21.1	8.3	0.0
62959	1972	5	17	138	0.0	22.2	9.4	0.0
62960	1972	5	18	139	2.3	15.0	2.2	0.0
62961	1972	5	19	140	0.0	14.4	3.9	0.0
62962	1972	5	20	141	0.0	25.0	8.9	0.0
62963	1972	5	21	142	0.0	22.2	8.3	0.0
62964	1972	5	22	143	5.6	9.4	6.1	0.0
62965	1972	5	23	144	0.0	15.6	3.3	0.0
62966	1972	5	24	145	0.0	14.4	3.3	0.0
62967	1972	5	25	146	0.0	13.9	0.6	0.0
62968	1972	5	26	147	0.0	18.3	3.9	0.0
62969	1972	5	27	148	0.0	22.8	8.3	0.0
62970	1972	5	28	149	0.0	27.2	12.2	0.0
62971	1972	5	29	150	0.0	28.3	12.2	0.0
62972	1972	5	30	151	0.0	31.1	13.3	0.0
62973	1972	5	31	152	0.0	29.4	13.9	0.0
62974	1972	6	1	153	-999.9 M	-999.9 M	-999.9 M	-999.9 M
62975	1972	6	2	154	-999.9 M	-999.9 M	-999.9 M	-999.9 M
62976	1972	6	3	155	-999.9 M	-999.9 M	-999.9 M	-999.9 M
62977	1972	6	4	156	-999.9 M	-999.9 M	-999.9 M	-999.9 M
62978	1972	6	5	157	-999.9 M	-999.9 M	-999.9 M	-999.9 M
62979	1972	6	6	158	-999.9 M	-999.9 M	-999.9 M	-999.9 M
62980	1972	6	7	159	-999.9 M	-999.9 M	-999.9 M	-999.9 M
62981	1972	6	8	160	-999.9 M	-999.9 M	-999.9 M	-999.9 M
62982	1972	6	9	161	-999.9 M	-999.9 M	-999.9 M	-999.9 M
62983	1972	6	10	162	-999.9 M	-999.9 M	-999.9 M	-999.9 M
62984	1972	6	11	163	-999.9 M	-999.9 M	-999.9 M	-999.9 M
62985	1972	6	12	164	-999.9 M	-999.9 M	-999.9 M	-999.9 M
62986	1972	6	13	165	-999.9 M	-999.9 M	-999.9 M	-999.9 M
62987	1972	6	14	166	-999.9 M	-999.9 M	-999.9 M	-999.9 M
62988	1972	6	15	167	-999.9 M	-999.9 M	-999.9 M	-999.9 M

Record Day Number	Year	Mo	Dy of Mo	Dy of Yr	Precip mm	Max Temp deg C	Min Temp deg C	Snow Fall mm
62989	1972	6	16	168	-999.9 M	-999.9 M	-999.9 M	-999.9 M
62990	1972	6	17	169	-999.9 M	-999.9 M	-999.9 M	-999.9 M
62991	1972	6	18	170	-999.9 M	-999.9 M	-999.9 M	-999.9 M
62992	1972	6	19	171	-999.9 M	-999.9 M	-999.9 M	-999.9 M
62993	1972	6	20	172	-999.9 M	-999.9 M	-999.9 M	-999.9 M
62994	1972	6	21	173	-999.9 M	-999.9 M	-999.9 M	-999.9 M
62995	1972	6	22	174	-999.9 M	-999.9 M	-999.9 M	-999.9 M
62996	1972	6	23	175	-999.9 M	-999.9 M	-999.9 M	-999.9 M
62997	1972	6	24	176	-999.9 M	-999.9 M	-999.9 M	-999.9 M
62998	1972	6	25	177	-999.9 M	-999.9 M	-999.9 M	-999.9 M
62999	1972	6	26	178	-999.9 M	-999.9 M	-999.9 M	-999.9 M
63000	1972	6	27	179	-999.9 M	-999.9 M	-999.9 M	-999.9 M
63001	1972	6	28	180	-999.9 M	-999.9 M	-999.9 M	-999.9 M
63002	1972	6	29	181	-999.9 M	-999.9 M	-999.9 M	-999.9 M
63003	1972	6	30	182	-999.9 M	-999.9 M	-999.9 M	-999.9 M
63004	1972	7	1	183	0.0	27.8	6.1	0.0
63005	1972	7	2	184	0.0	23.3	7.8	0.0
63006	1972	7	3	185	0.0	23.9	8.3	0.0
63007	1972	7	4	186	0.0	26.7	7.8	0.0
63008	1972	7	5	187	0.0	31.1	6.7	0.0
63009	1972	7	6	188	0.0	32.2	16.1	0.0
63010	1972	7	7	189	5.8	33.3	10.6	0.0
63011	1972	7	8	190	0.0	27.8	11.1	0.0
63012	1972	7	9	191	1.5	25.6	8.9	0.0
63013	1972	7	10	192	0.0	20.0	3.3	0.0
63014	1972	7	11	193	3.0	21.1	9.4	0.0
63015	1972	7	12	194	0.0	20.0	10.6	0.0
63016	1972	7	13	195	0.0	29.4	15.6	0.0
63017	1972	7	14	196	0.0	26.7	8.3	0.0
63018	1972	7	15	197	0.0	27.2	6.1	0.0
63019	1972	7	16	198	0.0	27.8	7.2	0.0
63020	1972	7	17	199	0.0	29.4	10.6	0.0
63021	1972	7	18	200	0.0	28.3	10.0	0.0
63022	1972	7	19	201	0.0	26.7	9.4	0.0
63023	1972	7	20	202	0.0	20.6	10.6	0.0
63024	1972	7	21	203	5.6	21.7	8.9	0.0
63025	1972	7	22	204	0.5	18.3	8.9	0.0
63026	1972	7	23	205	0.0	27.2	10.6	0.0
63027	1972	7	24	206	0.0	28.9	9.4	0.0
63028	1972	7	25	207	0.0	24.4	10.0	0.0
63029	1972	7	26	208	0.0	28.9	7.2	0.0
63030	1972	7	27	209	0.0	30.6	8.3	0.0
63031	1972	7	28	210	0.0	29.4	8.9	0.0
63032	1972	7	29	211	0.0	33.9	10.0	0.0
63033	1972	7	30	212	0.0	35.0	12.8	0.0
63034	1972	7	31	213	0.0	33.9	11.1	0.0
63035	1972	8	1	214	0.0	33.3	11.7	0.0
63036	1972	8	2	215	0.0	30.0	7.8	0.0
63037	1972	8	3	216	0.0	28.3	8.9	0.0
63038	1972	8	4	217	0.0	30.6	7.8	0.0
63039	1972	8	5	218	0.0	32.8	8.9	0.0
63040	1972	8	6	219	0.0	35.0	10.0	0.0
63041	1972	8	7	220	0.0	37.2	10.6	0.0
63042	1972	8	8	221	0.0	38.3	14.4	0.0
63043	1972	8	9	222	0.0	39.4	18.3	0.0
63044	1972	8	10	223	0.0	35.0	12.8	0.0
63045	1972	8	11	224	0.0	32.8	11.7	0.0
63046	1972	8	12	225	0.0	29.4	12.2	0.0
63047	1972	8	13	226	0.0	27.2	11.7	0.0
63048	1972	8	14	227	0.0	26.7	7.8	0.0
63049	1972	8	15	228	0.0	32.2	13.3	0.0
63050	1972	8	16	229	21.6 A	23.3	7.8	0.0
63051	1972	8	17	230	0.5	23.9	10.0	0.0
63052	1972	8	18	231	0.0	20.0	5.0	0.0
63053	1972	8	19	232	0.0	26.7	6.7	0.0
63054	1972	8	20	233	0.0	25.6	10.0	0.0

Record Day Number	Year	Mo	Dy of Mo	Dy of Yr	Precip mm	Max Temp deg C	Min Temp deg C	Snow Fall mm
63055	1972	8	21	234	0.0	31.7	12.2	0.0
63056	1972	8	22	235	0.8	29.4	9.4	0.0
63057	1972	8	23	236	2.3	23.3	4.4	0.0
63058	1972	8	24	237	0.0	23.9	7.2	0.0
63059	1972	8	25	238	0.0	26.1	8.9	0.0
63060	1972	8	26	239	0.0	31.1	11.7	0.0
63061	1972	8	27	240	0.0	32.8	11.7	0.0
63062	1972	8	28	241	0.0	35.0	13.3	0.0
63063	1972	8	29	242	0.0	36.7	11.7	0.0
63064	1972	8	30	243	0.0	33.3	10.0	0.0
63065	1972	8	31	244	0.0	25.6	2.2	0.0
63066	1972	9	1	245	0.0	26.1	4.4	0.0
63067	1972	9	2	246	0.0	26.7	2.8	0.0
63068	1972	9	3	247	0.0	29.4	5.6	0.0
63069	1972	9	4	248	0.0	30.0	5.0	0.0
63070	1972	9	5	249	0.0	31.1	9.4	0.0
63071	1972	9	6	250	0.0	22.2	5.6	0.0
63072	1972	9	7	251	0.0	19.4	3.3	0.0
63073	1972	9	8	252	0.0	22.2	7.2	0.0
63074	1972	9	9	253	0.5	23.9	5.6	0.0
63075	1972	9	10	254	0.0	18.3	0.6	0.0
63076	1972	9	11	255	0.0	20.6	1.1	0.0
63077	1972	9	12	256	6.6	21.1	6.7	0.0
63078	1972	9	13	257	0.3	13.3	1.7	0.0
63079	1972	9	14	258	0.0	22.2	3.3	0.0
63080	1972	9	15	259	0.0	25.0	4.4	0.0
63081	1972	9	16	260	0.0	25.6	6.7	0.0
63082	1972	9	17	261	0.0	25.0	10.6	0.0
63083	1972	9	18	262	0.0	20.6	2.2	0.0
63084	1972	9	19	263	0.0	22.2	6.7	0.0
63085	1972	9	20	264	0.3	14.4	3.9	0.0
63086	1972	9	21	265	0.0	15.0	3.3	0.0
63087	1972	9	22	266	7.6	19.4	1.1	0.0
63088	1972	9	23	267	5.1	14.4	2.2	0.0
63089	1972	9	24	268	3.0	12.8	0.6	0.0
63090	1972	9	25	269	0.0	10.6	-2.2	0.0
63091	1972	9	26	270	0.0	12.2	-0.6	0.0
63092	1972	9	27	271	0.0	13.9	-3.3	0.0
63093	1972	9	28	272	0.0	11.7	-1.7	0.0
63094	1972	9	29	273	0.0	14.4	-0.6	0.0
63095	1972	9	30	274	0.0	18.3	0.0	0.0
63096	1972	10	1	275	0.0	23.3	1.1	0.0
63097	1972	10	2	276	0.0	22.8	4.4	0.0
63098	1972	10	3	277	0.0	23.9	2.8	0.0
63099	1972	10	4	278	0.0	23.3	3.3	0.0
63100	1972	10	5	279	0.0	19.4	2.8	0.0
63101	1972	10	6	280	0.0	20.0	-3.9	0.0
63102	1972	10	7	281	0.0	20.0	-2.8	0.0
63103	1972	10	8	282	0.0	21.7	-1.7	0.0
63104	1972	10	9	283	0.0	23.9	3.9	0.0
63105	1972	10	10	284	0.0	18.3	5.6	0.0
63106	1972	10	11	285	4.8	14.4	3.9	0.0
63107	1972	10	12	286	0.0	15.0	1.7	0.0
63108	1972	10	13	287	0.0	18.3	1.7	0.0
63109	1972	10	14	288	0.0	11.1	3.9	0.0
63110	1972	10	15	289	0.0	18.3	-1.7	0.0
63111	1972	10	16	290	0.0	16.7	-1.1	0.0
63112	1972	10	17	291	0.0	17.8	0.0	0.0
63113	1972	10	18	292	0.0	17.2	-1.7	0.0
63114	1972	10	19	293	0.0	18.3	-2.8	0.0
63115	1972	10	20	294	0.0	17.2	-3.3	0.0
63116	1972	10	21	295	0.0	17.2	-1.1	0.0
63117	1972	10	22	296	0.0	17.8	1.1	0.0
63118	1972	10	23	297	0.0	18.9	2.8	0.0
63119	1972	10	24	298	0.0	13.9	-4.4	0.0
63120	1972	10	25	299	0.0	12.8	-2.2	0.0

Record Day Number	Year	Mo	Dy of Mo	Dy of Yr	Precip mm		Max Temp deg C	Min Temp deg C	Snow Fall mm	
63121	1972	10	26	300	0.5		17.2	-0.6	0.0	
63122	1972	10	27	301	0.3		9.4	-3.3	0.0	
63123	1972	10	28	302	0.0	T	7.2	-3.9	0.0	T
63124	1972	10	29	303	8.6		3.9	-3.9	0.0	
63125	1972	10	30	304	0.0		3.3	-5.0	0.0	
63126	1972	10	31	305	0.0		2.2	-3.3	0.0	
63127	1972	11	1	306	0.0		4.4	-1.1	0.0	
63128	1972	11	2	307	3.8		5.0	1.1	0.0	
63129	1972	11	3	308	0.0		11.1	3.9	0.0	
63130	1972	11	4	309	6.4		11.1	4.4	0.0	
63131	1972	11	5	310	2.3		12.2	2.8	0.0	
63132	1972	11	6	311	0.0		9.4	0.0	0.0	
63133	1972	11	7	312	0.0		10.0	2.8	0.0	
63134	1972	11	8	313	0.0		11.7	3.3	0.0	
63135	1972	11	9	314	0.0		4.4	0.6	0.0	
63136	1972	11	10	315	0.0		10.0	1.7	0.0	
63137	1972	11	11	316	0.0		11.7	1.1	0.0	
63138	1972	11	12	317	0.0		11.1	2.8	0.0	
63139	1972	11	13	318	0.0		5.6	-1.1	0.0	
63140	1972	11	14	319	0.0		11.1	0.0	0.0	
63141	1972	11	15	320	0.5		10.6	0.6	0.0	
63142	1972	11	16	321	0.0		10.0	0.6	0.0	
63143	1972	11	17	322	0.0		13.3	1.1	0.0	
63144	1972	11	18	323	0.0		6.1	2.2	0.0	
63145	1972	11	19	324	1.5		7.8	1.1	0.0	
63146	1972	11	20	325	0.0		7.2	-1.1	0.0	
63147	1972	11	21	326	0.0		4.4	-2.8	0.0	
63148	1972	11	22	327	0.0		6.1	-3.3	0.0	
63149	1972	11	23	328	0.0		6.1	-2.8	0.0	
63150	1972	11	24	329	0.0		2.8	-1.7	0.0	
63151	1972	11	25	330	0.0		3.9	-1.7	0.0	
63152	1972	11	26	331	5.8		3.9	-1.7	0.0	
63153	1972	11	27	332	0.0		5.6	-5.6	0.0	
63154	1972	11	28	333	0.0		3.9	-5.0	0.0	
63155	1972	11	29	334	0.0		3.3	-5.0	0.0	
63156	1972	11	30	335	0.0		2.8	-0.6	0.0	
63157	1972	12	1	336	0.0		4.4	1.1	0.0	
63158	1972	12	2	337	1.8		8.9	-0.6	0.0	
63159	1972	12	3	338	0.0		5.0	-8.9	0.0	
63160	1972	12	4	339	0.0		-5.6	-15.0	0.0	
63161	1972	12	5	340	0.0		-7.8	-16.7	0.0	
63162	1972	12	6	341	0.0		-7.8	-14.4	0.0	
63163	1972	12	7	342	0.0		-10.6	-15.6	0.0	
63164	1972	12	8	343	0.0		-11.1	-21.7	0.0	
63165	1972	12	9	344	0.0		-12.2	-23.3	0.0	
63166	1972	12	10	345	0.0		-10.0	-23.9	0.0	
63167	1972	12	11	346	0.0		-11.1	-17.8	0.0	
63168	1972	12	12	347	2.5		-7.2	-12.2	50.8	
63169	1972	12	13	348	1.8		-6.1	-21.1	63.5	
63170	1972	12	14	349	0.0		-8.3	-19.4	0.0	
63171	1972	12	15	350	0.0		-2.8	-12.2	0.0	
63172	1972	12	16	351	0.0		0.6	-8.9	0.0	
63173	1972	12	17	352	6.6		3.3	0.0	0.0	
63174	1972	12	18	353	6.6		4.4	1.1	0.0	
63175	1972	12	19	354	3.8		7.2	1.7	0.0	
63176	1972	12	20	355	0.0		7.8	3.3	0.0	
63177	1972	12	21	356	6.9		9.4	3.3	0.0	
63178	1972	12	22	357	13.0		10.6	3.3	0.0	
63179	1972	12	23	358	0.0		7.2	2.8	0.0	
63180	1972	12	24	359	13.2		6.1	1.1	0.0	
63181	1972	12	25	360	0.0		5.0	0.6	0.0	
63182	1972	12	26	361	0.0		9.4	2.2	0.0	
63183	1972	12	27	362	1.3		8.3	3.3	0.0	
63184	1972	12	28	363	1.8		8.9	-0.6	0.0	
63185	1972	12	29	364	0.0		3.9	-4.4	0.0	
63186	1972	12	30	365	0.0		1.7	-4.4	0.0	

Record Day Number	Year	Mo	Dy of Mo	Dy of Yr	Precip mm	Max Temp deg C	Min Temp deg C	Snow Fall mm	
63187	1972	12	31	366	0.0	0.6	-4.4	0.0	
63188	1973	1	1	1	0.0	1.1	-3.9	0.0	
63189	1973	1	2	2	0.0	3.9	-5.0	0.0	
63190	1973	1	3	3	0.0	2.2	-8.9	0.0	
63191	1973	1	4	4	0.0	-1.7	-13.9	0.0	
63192	1973	1	5	5	0.0	-5.6	-12.8	0.0	
63193	1973	1	6	6	0.0	-7.8	-16.7	0.0	
63194	1973	1	7	7	0.0	-6.7	-17.2	0.0	
63195	1973	1	8	8	0.0	-9.4	-16.1	0.0	
63196	1973	1	9	9	0.0	-7.8	-15.6	0.0	
63197	1973	1	10	10	0.0	-5.0	-16.1	0.0	
63198	1973	1	11	11	5.6	-2.8	-15.6	25.4	
63199	1973	1	12	12	8.4	2.8	-6.7	0.0	T
63200	1973	1	13	13	13.5	6.1	-3.9	0.0	
63201	1973	1	14	14	1.3	8.9	4.4	0.0	
63202	1973	1	15	15	0.0	11.1	4.4	0.0	
63203	1973	1	16	16	5.6	10.6	3.9	0.0	
63204	1973	1	17	17	4.3	7.2	0.6	0.0	
63205	1973	1	18	18	0.0	7.2	0.0	0.0	
63206	1973	1	19	19	0.0	5.0	-1.7	0.0	
63207	1973	1	20	20	0.0	1.7	-2.8	0.0	
63208	1973	1	21	21	2.5	0.6	-4.4	12.7	
63209	1973	1	22	22	0.0	2.8	-5.0	0.0	
63210	1973	1	23	23	0.0	1.7	-5.6	0.0	
63211	1973	1	24	24	0.0	5.6	-1.1	0.0	
63212	1973	1	25	25	0.0	4.4	0.0	0.0	
63213	1973	1	26	26	0.0	4.4	-6.1	0.0	
63214	1973	1	27	27	0.0	2.8	-6.7	0.0	
63215	1973	1	28	28	0.0	3.9	-6.1	0.0	
63216	1973	1	29	29	0.0	6.1	-3.3	0.0	
63217	1973	1	30	30	3.0	2.8	-3.3	12.7	
63218	1973	1	31	31	4.1	4.4	-1.7	25.4	
63219	1973	2	1	32	0.0	2.2	-3.9	0.0	
63220	1973	2	2	33	0.0	5.0	-3.9	0.0	
63221	1973	2	3	34	0.0	6.1	0.6	0.0	
63222	1973	2	4	35	0.0	5.6	-1.7	0.0	
63223	1973	2	5	36	0.0	3.9	-3.9	0.0	
63224	1973	2	6	37	0.0	2.8	-5.6	0.0	
63225	1973	2	7	38	0.0	0.0	-6.7	0.0	
63226	1973	2	8	39	0.0	3.9	-8.9	0.0	
63227	1973	2	9	40	0.0	4.4	-8.9	0.0	
63228	1973	2	10	41	0.0	2.2	-5.0	0.0	

- **Example listing of ROSALIA.INP.** This is the main output file from DAILY09 V1.0, generated using the exported EARTHINFO record for Rosalia, WA. The file is used directly as input to INFIL V2.0. The file includes 1971 and 1973. As the data from the entire month of June in 1972 was missing in the above file, it is omitted from the final file indicated below. This verifies the omission of years when the gap identified is large (> 10 days for precipitation and > 20 for air temperature). In addition, the following file illustrates the additional column of mean air temperature calculated as (TMAX+TMIN)/2.

```
Output file generated using program DAILY09.FOR
Output file = Rosalia.inp
Daily climate record for Rosalia, Washington
GU1 Upper bound glacial transition climate analog (4/12/1999)

Station ID = 457180

Dy          = day
Mo          = month
Yr          = year
Max         = maximum
```

```
Min       = minimum
Precip    = total daily precipitation
Temp      = daily air temperature
mm        = millimeters
deg C     = degrees Celsius

Data Flags:

-999.9  =  missing data
M       =  missing data flag
A       =  accumulated measurement (multiple days)
T       =  trace amount (less than measurement resolution)
C1      =  calculated value (type 1 calculation)
E1      =  estimated value (type 1 estimation)
E2      =  estimated value (type 2 estimation)
E3      =  estimated value (type 3 estimation)
```

Record Day Number	Year	Mo	Dy of Mo	Dy of Yr	Precip mm	Max Temp deg C	Min Temp deg C	Mean Temp deg C	Snow Fall mm
62791	1971	12	1	335	0.0	1.1	-3.9	-1.4 C1	0.0
62792	1971	12	2	336	0.0	3.9	-2.8	0.6 C1	0.0
62793	1971	12	3	337	0.0 T	2.8	-4.4	-0.8 C1	0.0 T
62794	1971	12	4	338	0.0	1.7	-6.1	-2.2 C1	0.0
62795	1971	12	5	339	5.1	2.2	-1.7	0.3 C1	63.5
62796	1971	12	6	340	0.0	2.8	-5.0	-1.1 C1	0.0
62797	1971	12	7	341	0.0	-2.8	-16.1	-9.4 C1	0.0
62798	1971	12	8	342	0.0	-6.7	-15.6	-11.1 C1	0.0
62799	1971	12	9	343	0.0	2.8	-7.8	-2.5 C1	0.0
62800	1971	12	10	344	0.0	2.2	-2.2	0.0 C1	0.0
62801	1971	12	11	345	7.6	0.0	-8.9	-4.4 C1	50.8
62802	1971	12	12	346	2.0	1.1	-8.9	-3.9 C1	25.4
62803	1971	12	13	347	0.0	0.0	-9.4	-4.7 C1	0.0
62804	1971	12	14	348	0.0	0.6	-7.8	-3.6 C1	0.0

Record Day Number	Year	Mo	Dy of Mo	Dy of Yr	Precip mm	Max Temp deg C	Min Temp deg C	Mean Temp deg C		Snow Fall mm	
62805	1971	12	15	349	0.0	1.1	-7.2	-3.1	C1	0.0	
62806	1971	12	16	350	3.6	-1.7	-13.3	-7.5	C1	76.2	
62807	1971	12	17	351	0.0	4.4	-1.7	1.4	C1	0.0	
62808	1971	12	18	352	0.3	5.0	0.6	2.8	C1	0.0	
62809	1971	12	19	353	0.0	3.3	-3.3	0.0	C1	0.0	
62810	1971	12	20	354	0.0	0.6	-1.1	-0.3	C1	0.0	
62811	1971	12	21	355	3.0	2.2	-0.6	0.8	C1	12.7	
62812	1971	12	22	356	2.0	3.9	0.0	1.9	C1	0.0	
62813	1971	12	23	357	0.3	5.6	-1.7	1.9	C1	0.0	
62814	1971	12	24	358	0.3	3.9	0.0	1.9	C1	0.0	
62815	1971	12	25	359	0.0	6.1	-0.6	2.8	C1	0.0	
62816	1971	12	26	360	0.0	3.3	-4.4	-0.6	C1	0.0	
62817	1971	12	27	361	0.0	-3.3	-10.0	-6.7	C1	0.0	
62818	1971	12	28	362	0.0	-1.7	-10.6	-6.1	C1	0.0	
62819	1971	12	29	363	3.0	-4.4	-8.9	-6.7	C1	25.4	
62820	1971	12	30	364	0.0	-5.0	-16.1	-10.6	C1	0.0	
62821	1971	12	31	365	0.8	0.6	-9.4	-4.4	C1	25.4	
63188	1973	1	1	1	0.0	1.1	-3.9	-1.4	C1	0.0	
63189	1973	1	2	2	0.0	3.9	-5.0	-0.6	C1	0.0	
63190	1973	1	3	3	0.0	2.2	-8.9	-3.3	C1	0.0	
63191	1973	1	4	4	0.0	-1.7	-13.9	-7.8	C1	0.0	
63192	1973	1	5	5	0.0	-5.6	-12.8	-9.2	C1	0.0	
63193	1973	1	6	6	0.0	-7.8	-16.7	-12.2	C1	0.0	
63194	1973	1	7	7	0.0	-6.7	-17.2	-11.9	C1	0.0	
63195	1973	1	8	8	0.0	-9.4	-16.1	-12.8	C1	0.0	
63196	1973	1	9	9	0.0	-7.8	-15.6	-11.7	C1	0.0	
63197	1973	1	10	10	0.0	-5.0	-16.1	-10.6	C1	0.0	
63198	1973	1	11	11	5.6	-2.8	-15.6	-9.2	C1	25.4	
63199	1973	1	12	12	8.4	2.8	-6.7	-1.9	C1	0.0	T
63200	1973	1	13	13	13.5	6.1	-3.9	1.1	C1	0.0	
63201	1973	1	14	14	1.3	8.9	4.4	6.7	C1	0.0	
63202	1973	1	15	15	0.0	11.1	4.4	7.8	C1	0.0	
63203	1973	1	16	16	5.6	10.6	3.9	7.2	C1	0.0	
63204	1973	1	17	17	4.3	7.2	0.6	3.9	C1	0.0	
63205	1973	1	18	18	0.0	7.2	0.0	3.6	C1	0.0	
63206	1973	1	19	19	0.0	5.0	-1.7	1.7	C1	0.0	
63207	1973	1	20	20	0.0	1.7	-2.8	-0.6	C1	0.0	
63208	1973	1	21	21	2.5	0.6	-4.4	-1.9	C1	12.7	
63209	1973	1	22	22	0.0	2.8	-5.0	-1.1	C1	0.0	
63210	1973	1	23	23	0.0	1.7	-5.6	-1.9	C1	0.0	
63211	1973	1	24	24	0.0	5.6	-1.1	2.2	C1	0.0	
63212	1973	1	25	25	0.0	4.4	0.0	2.2	C1	0.0	
63213	1973	1	26	26	0.0	4.4	-6.1	-0.8	C1	0.0	
63214	1973	1	27	27	0.0	2.8	-6.7	-1.9	C1	0.0	
63215	1973	1	28	28	0.0	3.9	-6.1	-1.1	C1	0.0	
63216	1973	1	29	29	0.0	6.1	-3.3	1.4	C1	0.0	
63217	1973	1	30	30	3.0	2.8	-3.3	-0.3	C1	12.7	
63218	1973	1	31	31	4.1	4.4	-1.7	1.4	C1	25.4	
63219	1973	2	1	32	0.0	2.2	-3.9	-0.8	C1	0.0	
63220	1973	2	2	33	0.0	5.0	-3.9	0.6	C1	0.0	
63221	1973	2	3	34	0.0	6.1	0.6	3.3	C1	0.0	
63222	1973	2	4	35	0.0	5.6	-1.7	1.9	C1	0.0	
63223	1973	2	5	36	0.0	3.9	-3.9	0.0	C1	0.0	
63224	1973	2	6	37	0.0	2.8	-5.6	-1.4	C1	0.0	
63225	1973	2	7	38	0.0	0.0	-6.7	-3.3	C1	0.0	
63226	1973	2	8	39	0.0	3.9	-8.9	-2.5	C1	0.0	
63227	1973	2	9	40	0.0	4.4	-8.9	-2.2	C1	0.0	
63228	1973	2	10	41	0.0	2.2	-5.0	-1.4	C1	0.0	

- **Example listing of ROSALIA.DAY indicating small gaps in precipitation and air temperature data.**

```
Output file generated using program DAILY09.FOR
Output file = Rosalia.day
Daily climate record for Rosalia, Washington
GU1 Upper bound glacial transition climate analog (4/12/1999)

Station ID = 457180

Dy          = day
Mo          = month
Yr          = year
Max         = maximum
Min         = minimum
Precip      = total daily precipitation
Temp        = daily air temperature
mm          = millimeters
deg C       = degrees Celsius

Data Flags:

-999.9  =  missing data value
M       =  missing data flag
A       =  accumulated measurement (multiple days)
T       =  trace amount (less than measurement resolution)
```

Record Number	Year	Mo	Dy of Mo	Dy of Yr	Precip mm	Max Temp deg C	Min Temp deg C	Snow Fall mm
71263	1995	2	10	41	0.0	8.3	-1.7	0.0
71264	1995	2	11	42	0.0	6.1	-2.8	0.0
71265	1995	2	12	43	0.0	1.1	-8.9	0.0
71266	1995	2	13	44	-999.9 M	-6.7	-12.2	-999.9 M
71267	1995	2	14	45	0.8	-7.2	-12.2	12.7
71268	1995	2	15	46	0.0	-6.7	-11.7	0.0
71269	1995	2	16	47	3.8	2.2	-999.9 M	50.8
71270	1995	2	17	48	13.7	4.4	0.0	0.0
71271	1995	2	18	49	0.0	7.8	1.1	0.0
71272	1995	2	19	50	8.9	11.1	2.8	0.0
71273	1995	2	20	51	5.8	13.3	8.3	0.0

- **Example listing of ROSALIA.INP illustrating that the gap in precipitation is replaced by a zero, and the gap in air temperature is replaced with a linear interpolation between the numbers on either side of the gap.**

```
Output file generated using program DAILY09.FOR
Output file = Rosalia.inp
Daily climate record for Rosalia, Washington
GU1 Upper bound glacial transition climate analog (4/12/1999)

Station ID = 457180

Dy          = day
Mo          = month
Yr          = year
Max         = maximum
Min         = minimum
Precip      = total daily precipitation
Temp        = daily air temperature
mm          = millimeters
deg C       = degrees Celsius
```

Data Flags:

-999.9 = missing data
M = missing data flag
A = accumulated measurement (multiple days)
T = trace amount (less than measurement resolution)
C1 = calculated value (type 1 calculation)
E1 = estimated value (type 1 estimation)
E2 = estimated value (type 2 estimation)
E3 = estimated value (type 3 estimation)

Record Day Number	Year	Mo	Dy of Mo	Dy of Yr	Precip mm		Max Temp deg C		Min Temp deg C		Mean Temp deg C		Snow Fall mm	
71263	1995	2	10	41	0.0		8.3		-1.7		3.3	C1	0.0	
71264	1995	2	11	42	0.0		6.1		-2.8		1.7	C1	0.0	
71265	1995	2	12	43	0.0		1.1		-8.9		-3.9	C1	0.0	
71266	1995	2	13	44	0.0	E1	-6.7		-12.2		-9.4	C1	-999.9	M
71267	1995	2	14	45	0.8		-7.2		-12.2		-9.7	C1	12.7	
71268	1995	2	15	46	0.0		-6.7		-11.7		-9.2	C1	0.0	
71269	1995	2	16	47	3.8		2.2		-5.8	E2	-1.8	C1	50.8	
71270	1995	2	17	48	13.7		4.4		0.0		2.2	C1	0.0	
71271	1995	2	18	49	0.0		7.8		1.1		4.4	C1	0.0	
71272	1995	2	19	50	8.9		11.1		2.8		6.9	C1	0.0	
71273	1995	2	20	51	5.8		13.3		8.3		10.8	C1	0.0	

- **Listing of source code for routine DAILY09 V1.0:**

```
      program daily09
c     version 1.0
c
c
c---- This routine is used to compile and re-format
c     EarthInfo NCDC (cr/lf) format export files
c     (daily NOAA climate data) into a single
c     ASCII (column format) daily climate input file used as
c     input to INFIL version 2.0.
c
c     The routine also estimates data values in cases of missing data,
c     or skips years if record is too incomplete. Criteria for
c     skipping years due to excessive data gaps is currently
c     hard-wired into the code:
c
c     current settings allow for daily precip gaps of 10 days or less
c     and daily air temperature gaps of 20 days or less.
c     If gaps are exceeded the entire year is excluded from
c     the developed daily climate file. Gaps in the snowfall
c     record are allowed because this parameter is
c     not used directly as input by INFIL version 2.0.
c
c     program written by Joe Hevesi, U.S. Geological Survey, WRD
c
c
c---- NCDC export format input variables (NCDCfile)
      character*20 NCDCfile
      character*3 dly
      character*6 statid,station
      character*2 code1
      character*4  dtype
      character*2  dunit
      integer*4 dyear
      integer*2 dmonth
      character*6 df1
      character*1 df2(31)
      integer dday(31)
      integer df3(31)
      real ddat(31)
      character*1 dflag(31)
c
c---- calendar variables (good for dates 01/01/1800 - 12/31/2000)
      integer yr(100000),mo(100000),dy(100000)
      integer lpyr(1800:2000)
      integer ndmon(12)
      integer ndmonth(1800:2000,12)
      integer modays
      integer iday(1800:2000,12,31)
      integer nday,iprcp,itmax,itmin,isnow
      integer nend,nbeg,n10,n20,n30,n40
c
c---- precip data variables
      real ppt(100000)
      character*2 pflg(100000)
      real moppt,yrppt,aappt
      integer ndmoppt,n1
      integer imisppt(1800:2000)
c
c---- max air temp data variables
      real tmax(100000)
      character*2 tmaxflg(100000)
      real motmax,yrtmax,tmax0,tmax1,tmax2,aatmax
      integer ndmotmax,nmistmax,n2
      integer imistmax(1800:2000)
c
c---- min air temp data variables
      real tmin(100000)
      character*2 tminflg(100000)
```

```
      real motmin,yrtmin,tmin0,tmin1,tmin2,aatmin
      integer ndmotmin,nmistmin,n3
      integer imistmin(1800:2000)
c
c---- average air temp data variables
      real tavg(100000)
      character*2 tavgflg(100000)
      real yrtavg,aatavg
c
c---- snow fall data variables
      real snow(100000)
      character*2 snowflg(100000)
      real mosnow,yrsnow
      integer ndmosnow,n4
c
c---- output variables
      character*20 outfile,outfil2,monthfil,yearfile
      character*120 header,headout1,headout2
      integer iout(100000)
      real maxppt
c
c
c---- start program
c
1     format(a)
11    format('Output file generated using program DAILY09.FOR')
21    format('Output file = ',a20)
      open(unit=7,file='daily09.ctl')
      read(7,1) header
      read(7,1) headout1
      read(7,1) headout2
      read(7,1) NCDCfile
      read(7,1) outfile
      read(7,1) outfil2
      read(7,1) monthfil
      read(7,1) yearfile
c
c
c==== Import EARTH-INFO NCDC export files
c     ---------------------------------
c---- open EARTH-INFO NCDC export files
      open(unit=8,file=NCDCfile)
c
c---- open output files
c     outfile (unit 18) = compiled NCDC data output
c     outfil2 (unit 19) = daily climate input file for infil model
c     monthfil (unit 20) = monthly summary file
c     yearfile (unit 21) = yearly summary file
      open(unit=18,file=outfile)
      open(unit=19,file=outfil2)
      open(unit=20,file=monthfil)
      open(unit=21,file=yearfile)
c
      write(18,11)
      write(18,21) outfile
      write(18,1) headout1
      write(18,1) headout2
      write(19,11)
      write(19,21) outfil2
      write(19,1) headout1
      write(19,1) headout2
      write(20,11)
      write(20,21) monthfil
      write(20,1) headout1
      write(20,1) headout2
      write(21,11)
      write(21,21) yearfile
      write(21,1) headout1
      write(21,1) headout2
c
C---- Set up months and leap years for up to 200 years starting at 1800
```

```
c     initialize flags for identifying incomplete years
      do i2 = 1800,2000
            lpyr(i2) = 0
            imisppt(i2) = 0
            imistmax(i2) = 0
            imistmin(i2) = 0
      enddo
      do i2 = 1800,2000,4
            lpyr(i2) = 1
      enddo
      lpyr(1800) = 0
      lpyr(1900) = 0
c
      ndmon(1) = 31
      ndmon(2) = 28
      ndmon(3) = 31
      ndmon(4) = 30
      ndmon(5) = 31
      ndmon(6) = 30
      ndmon(7) = 31
      ndmon(8) = 31
      ndmon(9) = 30
      ndmon(10) = 31
      ndmon(11) = 30
      ndmon(12) = 31
c
c
c---- set up calendar counters for checking NCDC input
c     and initialize record input arrays
c     date 01/01/1800 = day 1 for input record array
c     this algorithm works only for dates 01/01/1800 through 12/31/2000
c
      nday = 0
      do 50 i = 1800,2000
            do 50 j = 1,12
                  ndmon2 = ndmon(j)
                  if((j.eq.2).and.(lpyr(i).eq.1)) ndmon2 = 29
                  ndmonth(i,j) = ndmon2
                  do 50 k = 1,ndmon2
                        nday = nday + 1
                        iday(i,j,k) = nday
                        ppt(nday) = -999.9
                        tmax(nday) = -999.9
                        tmin(nday) = -999.9
                        snow(nday) = -999.0
c
                        pflg(nday) = 'M'
                        tmaxflg(nday) = 'M'
                        tminflg(nday) = 'M'
                        snowflg(nday) = 'M'
50    continue
      nbeg = iday(2000,12,31)
      nend = 1
c
c     initialize array counters
      iprcp = 0
      itmax = 0
      itmin = 0
      isnow = 0
c
c     initialize monthly statistics
      moppt = 0.
      maxppt = -999.
      maxflg = '-9'
      nmpflg = 0
      napflg = 0
      ntpflg = 0

      nmtmxflg = 0
      natmxflg = 0
      nttmxflg = 0
```

```
      nmtmnflg = 0
      natmnflg = 0
      nttmnflg = 0

      nmsnoflg = 0
      nasnoflg = 0
      ntsnoflg = 0

      ndaymo = 0

      n1 = 0
      n2 = 0
      n3 = 0
      n4 = 0
c
c---- Read in NCDC format daily data by month (each line = 31 days)
c
      ndat = 1
200   read(8,101,end=900) dly,statid,code1,dtype,dunit,
      1             dyear,dmonth,df1,
      2             (df2(i),dday(i),df3(i),ddat(i),dflag(i),i=1,31)
c
101         format(a3,a6,a2,a4,a2,
     1                    i4,i2,a6,
     2                    31(a1,i2,i2,f6.0,a1))
c
c------- check station id
            if(ndat.eq.1) then
                  station = statid
                  ndat = 0
            else
                  if(statid.ne.station) stop
            endif
c
c-------     import daily precip data
            if(dtype.eq.'PRCP') then
            if(iprcp.eq.0) then
                  n10 = iday(dyear,dmonth,dday(1))
                  n1 = n10 - 1
                  iprcp = 1
                  if(n10.lt.nbeg) nbeg = n10
            endif
            moppt = 0.
            motmax = 0.
            motmin = 0.
            mosnow = 0.
c
c           read-in daily precip data for each month
            do 300 j = 1,ndmonth(dyear,dmonth)
                  n1 = n1 + 1
                  ndaymo = ndaymo + 1
                  yr(n1) = dyear
                  mo(n1) = dmonth
                  dy(n1) = dday(j)
c
c                 get precip data (convert HIN to mm)
                  if(ddat(j).ne.-99999.) then
                        ppt(n1) = 0.254*ddat(j)
                        moppt = moppt + ppt(n1)
                        if(ppt(n1).gt.maxppt) maxppt = ppt(n1)
                  else
                        ppt(n1) = -999.9
                  endif
                  pflg(n1) = dflag(j)
                  if(pflg(n1).eq.'M') nmpflg = nmpflg + 1
                  if(pflg(n1).eq.'A') napflg = napflg + 1
                  if(pflg(n1).eq.'T') ntpflg = ntpflg + 1
c
300         continue
c
```

```
c
c-------    import maximum daily air temp data
            else if(dtype.eq.'TMAX') then
            if(itmax.eq.0) then
                    n20 = iday(dyear,dmonth,dday(1))
                    n2 = n20 - 1
                    itmax= 1
                    if(n20.lt.nbeg) nbeg = n20
            endif
            motmax = 0.
c
c           read-in maximum daily air temp data for each month
            do 310 j = 1,ndmonth(dyear,dmonth)
                    n2 = n2 + 1
                    ndaymo = ndaymo + 1
c
c                   get air temp data (convert deg F to deg C)
                    if(ddat(j).ne.-99999.) then
                            tmax(n2) = (ddat(j)-32.)*5/9
                            motmax = motmax + tmax(n2)
                            if(tmax(n2).gt.maxtmax) maxtmax = tmax(n2)
                    else
                            tmax(n2) = -999.9
                    endif
                    tmaxflg(n2) = dflag(j)
                    if(tmaxflg(n2).eq.'M') nmtmxflg = nmtmxflg + 1
                    if(tmaxflg(n2).eq.'A') natmxflg = natmxflg + 1
                    if(tmaxflg(n2).eq.'T') nttmxflg = nttmxflg + 1
c
c
310         continue
c
c-------    import minimum daily air temp data
            else if(dtype.eq.'TMIN') then
            if(itmin.eq.0) then
                    n30 = iday(dyear,dmonth,dday(1))
                    n3  = n30 - 1
                    itmin = 1
                    if(n30.lt.nbeg) nbeg = n30
            endif
            motmin = 0.
c
c           read-in minimum daily air temp data for each month
            do 320 j = 1,ndmonth(dyear,dmonth)
                    n3 = n3 + 1
                    ndaymo = ndaymo + 1
c
c                   get air temp data (convert deg F to deg C)
                    if(ddat(j).ne.-99999.) then
                            tmin(n3) = (ddat(j)-32.)*5/9
                            motmin = motmin + tmin(n3)
                            if(tmin(n3).gt.maxtmin) maxtmin = tmin(n3)
                    else
                            tmin(n3) = -999.9
                    endif
                    tminflg(n3) = dflag(j)
                    if(tminflg(n3).eq.'M') nmtmnflg = nmtmnflg + 1
                    if(tminflg(n3).eq.'A') natmnflg = natmnflg + 1
                    if(tminflg(n3).eq.'T') nttmnflg = nttmnflg + 1
c
c
320         continue
c
c-------    import daily snow fall data
            else if(dtype.eq.'SNOW') then
            if(isnow.eq.0) then
                    n40 = iday(dyear,dmonth,dday(1))
                    n4 = n40 - 1
                    isnow = 1
                    if(n40.lt.nbeg) nbeg = n40
            endif
```

```
      mosnow = 0.
c
c     read-in daily snow fall data for each month
      do 330 j = 1,ndmonth(dyear,dmonth)
            n4 = n4 + 1
            ndaymo = ndaymo + 1
c
c           get snow fall data (convert deg F to deg C)
            if(ddat(j).ne.-99999.) then
                  snow(n4) = 2.54*ddat(j)
                  mosnow = mosnow + snow(n4)
                  if(snow(n4).gt.maxsnow) maxsnow = snow(n4)
            else
                  snow(n4) = -999.9
            endif
            snowflg(n4) = dflag(j)
            if(snowflg(n4).eq.'M') nmsnoflg = nmsnoflg + 1
            if(snowflg(n4).eq.'A') nasnoflg = nasnoflg + 1
            if(snowflg(n4).eq.'T') ntsnoflg = ntsnoflg + 1
c
c
330   continue
c
      endif
      goto 200
c
c
900   continue
c
c     find ending array indices

      if(n1.gt.nend) nend = n1
      if(n2.gt.nend) nend = n2
      if(n3.gt.nend) nend = n3
      if(n4.gt.nend) nend = n4
c
c==== Process Results
c     ---------------
c---- output to 1st output file (data file)
c     write header info 1st
c     unit 18 = data output file
c
      write(18,8111) station
8111  format(/,'Station ID = 'a6)
      write(18,8001)
8001  format(/,'Dy          = day',
     1             /,'Mo          = month',
     2             /,'Yr          = year',
     3             /,'Max         = maximum',
     4             /,'Min         = minimum',
     5             /,'Precip      = total daily precipitation',
     6             /,'Temp        = daily air temperature',
     7             /,'mm          = millimeters',
     8             /,'deg C       = degrees Celsius',
     9            //,'Data Flags:',
     1            //,'-999.9  =  missing data value',
     1             /,'M       =  missing data flag',
     2             /,'A       =  accumulated measurement (multiple days)',
     3             /,'T       =  trace amount ',
     4                    '(less than measurement resolution)')
c
      write(18,8011)
8011  format(   /'  Record',1x,'    ',1x,'  ',1x,'Dy',1x,' Dy',
     1            2x,'      ',3x,'    Max',3x,'    Min',3x,'   Snow',
     2              /'     Day',1x,'    ',1x,'  ',1x,'of',1x,' of',
     3            2x,'Precip',3x,'   Temp',3x,'   Temp',3x,'   Fall',
     4              /'  Number',1x,'Year',1x,'Mo',1x,'Mo',1x,' Yr',
     5            2x,'    mm',3x,'  deg C',3x,'  deg C',3x,'     mm',
     6              /'--------',1x,'----',1x,'--',1x,'--',1x,'---',
     7            2x,'------',3x,'-------',3x,'-------',3x,'-------',/)
c
```

```
c
c---- write header info to monthly summary file
c
      write(20,8801) station
8801  format(/,'Station ID = 'a6)
      write(20,8901)
8901  format('Monthly summary of input record',
     1                    /'no data flag = -999.9',/)
      write(20,8921)
8921  format( /'        ',1x,'    ',1x,'  ',1x,'  ',1x,'   ',2x,
      1             '   ',1x,'      ',2x,'   ',
      2             1x,'  Mean',2x,'   ',1x,'  Mean',2x,'   ',1x,' Total',
      1               /'        ',1x,'    ',1x,'  ',1x,'Dy',1x,' Dy',2x,
      1             '  #',1x,' Total',2x,'  #',
      2             1x,'   Max',2x,'  #',1x,'   Min',2x,'  #',1x,'  Snow',
      3               /'     Day',1x,'    ',1x,'  ',1x,'of',1x,' of',2x,
      4             ' of',1x,'Precip',2x,' of',
      5             1x,'  Temp',2x,' of',1x,'  Temp',2x,' of',1x,'  Fall',
      6               /'  Number',1x,'Year',1x,'Mo',1x,'Mo',1x,' Yr',2x,
      7             'Rec',1x,'    mm',2x,'Rec',
      8             1x,' deg C',2x,'Rec',1x,' deg C',2x,'Rec',1x,'    mm',
      9               /'--------',1x,'----',1x,'--',1x,'--',1x,'---',2x,
      1             '---',1x,'------',2x,'---',
      2             1x,'------',2x,'---',1x,'------',2x,'---',1x,'------',/)
c
c
c---- initialize monthly stats
      moppt = 0.
      motmax = 0.
      motmin = 0.
      mosnow = 0.
      modays = 0
c
      ndmoppt = 0
      ndmotmax = 0
      ndmotmin = 0
      ndmosnow = 0
c
      istart = 0
      ndyear = 0
      nmisppt = 0
      nmisppt2 = 0
      nmistmax = 0
      nmistmx2 = 0
      nmistmin = 0
      nmistmn2 = 0
c
      do 8000 i = nbeg,nend
c
c           set up annual counters
            ndyear = ndyear + 1
            if(i.gt.1) then
                  if(yr(i).ne.yrold) ndyear = 1
            endif
            if(ndyear.eq.1) then
                  nmisppt2 = 0
                  nmistmx2 = 0
                  nmistmn2 = 0
            endif
            yrold = yr(i)
c
c
c           flag missing data at beginning and of record
            if((ppt(i).eq.-999.9).and.(istart.eq.0)) then
                  iout(i) = 0
            else if((tmax(i).eq.-999.9).and.(istart.eq.0)) then
                  iout(i) = 0
            else if((tmin(i).eq.-999.9).and.(istart.eq.0)) then
                  iout(i) = 0
            else if((snow(i).eq.-999.9).and.(istart.eq.0)) then
                  iout(i) = 0
```

```
      else
             istart = 1
             iout(i) = 1
      endif
c
c
c     write output to intermediate file for checking
      write(18,111) i,yr(i),mo(i),dy(i),ndyear,
     1       ppt(i),pflg(i),
     2       tmax(i),tmaxflg(i),
     3       tmin(i),tminflg(i),
     4       snow(i),snowflg(i)
c
111   format(1x,i7,1x,i4,1x,i2,1x,i2,1x,i3,1x,
     1                    4(1x,f6.1,1x,a2))
c
c     collect monthly statistics prior to filling gaps
      modays = modays + 1
      if(ppt(i).ne.-999.9) then
             ndmoppt = ndmoppt + 1
             moppt = moppt + ppt(i)
      endif
      if(tmax(i).ne.-999.9) then
             ndmotmax = ndmotmax + 1
             motmax = motmax + tmax(i)
      endif
      if(tmin(i).ne.-999.9) then
             ndmotmin = ndmotmin + 1
             motmin = motmin + tmin(i)
      endif
      if(snow(i).ne.-999.9) then
             ndmosnow = ndmosnow + 1
             mosnow = mosnow + snow(i)
      endif
c
c     write output to monthly summary file
      if(dy(i).eq.ndmonth(yr(i),mo(i))) then
             if(ndmoppt.eq.0) moppt = -999.9
             if(ndmosnow.eq.0) mosnow = -999.9
             if(ndmotmax.eq.0) then
                    motmax = -999.9
             else
                    motmax = motmax/ndmotmax
             endif
             if(ndmotmin.eq.0) then
                    motmin = -999.9
             else
                    motmin = motmin/ndmotmin
             endif
             write(20,8911) i,yr(i),mo(i),dy(i),ndyear,
     1                      ndmoppt,moppt,ndmotmax,motmax,
     2                      ndmotmin,motmin,ndmosnow,mosnow
8911         format(1x,i7,1x,i4,1x,i2,1x,i2,1x,i3,
     1                                   4(3x,i2,1x,f6.1))
             moppt = 0.
             motmax = 0.
             motmin = 0.
             mosnow = 0.
             ndmoppt = 0
             ndmotmax = 0
             ndmotmin = 0
             ndmosnow = 0
      endif
c
c
c======== Create developed data file
c      (fill in minor gaps, flag years with large gaps)
c
c-------- estimate precip for gaps of 10 days or less
c      E1 = type 1 estimation (assume no precip)
c      E3 - type 3 estimation (assume snow fall density = 0.1)
```

```
      nmisppt = 0
      if(ppt(i).eq.-999.9) then
            if(snow(i).le.0.) then
                  ppt(i) = 0.
                  pflg(i) = 'E1'
            else
                  ppt(i) = snow(i)/10
                  pflg(i) = 'E3'
            endif
            nmisppt = 1
            nmisppt2 = nmisppt2 + 1
8540        if(((i+nmisppt).le.n1).or.(nmisppt.le.10)) then
                  if(ppt(i+nmisppt).eq.-999.9) then
                        nmisppt = nmisppt + 1
                        goto 8540
                  endif
            endif
            if(nmisppt.gt.10)      imisppt(yr(i)) = 1
            if(nmisppt2.gt.20) imisppt(yr(i)) = 1
      endif
c
c
c-------- estimate max air temp for gaps less than 20 days
c     (type 2 estimation)
      nmistmax = 0
      if((tmax(i).eq.-999.9).and.(tmaxflg(i-1).ne.'E2')) then
            nmistmax = 1
            tmax0 = tmax(i-1)
            nmistmx2 = nmistmx2 + 1
8550        if(i+nmistmax.gt.n1) then
                  tmax2 = tmax0
            else if((tmax(i+nmistmax).eq.-999.9).and.
     1      (i+nmistmax.lt.n1)) then
                  nmistmax = nmistmax + 1
                  goto 8550
            endif
            tmax2 = tmax(i+nmistmax)
            tmax(i) = (tmax0 + tmax2)/2.
            tmaxflg(i) = 'E2'
            tmax1 = tmax(i)
      else if((tmax(i).eq.-999.9).and.(tmaxflg(i-1).eq.'E2')) then
            tmax(i) = tmax1
            tmaxflg(i) = 'E2'
            nmistmx2 = nmistmx2 + 1
      endif
      if(nmistmax.gt.20) imistmax(yr(i)) = 1
      if(nmistmx2.gt.40) imistmax(yr(i)) = 1
c
c
c-------- estimate min air temp for gaps less than 20 days
c     (type 2 estimation)
      nmistmin = 0
      if((tmin(i).eq.-999.9).and.(tminflg(i-1).ne.'E2')) then
            nmistmin = 1
            tmin0 = tmin(i-1)
            nmistmn2 = nmistmn2 + 1
8560        if(i+nmistmin.gt.n1) then
                  tmin2 = tmin0
            else if((tmin(i+nmistmin).eq.-999.9).and.
     1      (i+nmistmin.lt.n1)) then
                  nmistmin = nmistmin + 1
                  goto 8560
            endif
            tmin2 = tmin(i+nmistmin)
            tmin(i) = (tmin0 + tmin2)/2.
            tminflg(i) = 'E2'
            tmin1 = tmin(i)
      else if((tmin(i).eq.-999.9).and.(tminflg(i-1).eq.'E2')) then
            tmin(i) = tmin1
            tminflg(i) = 'E2'
            nmistmn2 = nmistmn2 + 1
```

```
            endif
            if(nmistmin.gt.20) imistmin(yr(i)) = 1
            if(nmistmn2.gt.40) imistmin(yr(i)) = 1
c
c
8000  continue
c
c
c---- output to 2nd output file (infil model input file)
c     write header info 1st
c     unit 19 = model input file
c
      write(19,9111) station
9111  format(/,'Station ID = 'a6)
      write(19,9001)
9001  format(/,'Dy          = day',
     1              /,'Mo          = month',
     2              /,'Yr          = year',
     3              /,'Max         = maximum',
     4              /,'Min         = minimum',
     5              /,'Precip      = total daily precipitation',
     6              /,'Temp        = daily air temperature',
     7              /,'mm          = millimeters',
     8              /,'deg C       = degrees Celsius',
     9             //,'Data Flags:',
c    1             //,'r       =  measured (recorded) data',
     1             //,'-999.9  =  missing data',
     1              /,'M       =  missing data flag',
     2              /,'A       =  accumulated measurement (multiple days)',
     3              /,'T       =  trace amount ',
     4                    '(less than measurement resolution)',
     5              /,'C1      =  calculated value (type 1 calculation)',
     6              /,'E1      =  estimated value (type 1 estimation)',
     7              /,'E2      =  estimated value (type 2 estimation)',
     8              /,'E3      =  estimated value (type 3 estimation)')
c
c
      write(19,9011)
9011  format(   /'  Record',1x,'    ',1x,'  ',1x,'Dy',1x,' Dy',
     1            2x,'      ',3x,'    Max',3x,'    Min',3x,'   Mean',
     2            3x,'   Snow',
     2              /'     Day',1x,'    ',1x,'  ',1x,'of',1x,' of',
     3            2x,'Precip',3x,'   Temp',3x,'   Temp',3x,'   Temp',
     3            3x,'   Fall',
     4              /'  Number',1x,'Year',1x,'Mo',1x,'Mo',1x,' Yr',
     5            2x,'    mm',3x,'  deg C',3x,'  deg C',3x,'  deg C',
     5            3x,'     mm',
     6              /'--------',1x,'----',1x,'--',1x,'--',1x,'---',
     7            2x,'------',3x,'-------',3x,'-------',3x,'-------',
     7            3x,'-------',/)
c
c
c---- output to yearly summary file (unit 21)
c     write header info 1st
c
      write(21,9501) station
9501  format(/,'Station ID = 'a6)
      write(21,9511)
9511  format('Annual summary of input record',/)
c
      write(21,9521)
9521  format('      ',3x,'    ',2x,'    ',3x,'  Total',3x,'   Mean',
     1            3x,'   Mean',3x,'   Mean',
     2            /'Number',3x,'    ',2x,'Days',3x,' Annual',3x,' Annual',
     2            3x,' Annual',3x,' Annual',
     3            /'    of',3x,'    ',2x,'  in',3x,' Precip',3x,'   Tmax',
     3            3x,'   Tmin',3x,'   Tavg',
     4            /' Years',3x,'Year',2x,'Year',3x,'   (mm)',3x,'(deg C)',
     4            3x,'(deg C)',3x,'(deg C)',
     5            /'------',3x,'----',2x,'----',3x,'-------',3x,'-------',
     5            3x,'-------',3x,'-------')
```

```
c
c
      yrppt = 0.
      yrtmax = 0.
      yrtmin = 0.
      yrtavg = 0.
      yrsnow = 0.
c
      aappt = 0.
      aatmax = 0.
      aatmin = 0.
      aatavg = 0.
c
      istart = 0
      ndyear = 0
      do 9000 i = nbeg,nend
            ndyear = ndyear + 1
            if(i.gt.1) then
                  if(yr(i).ne.yrold) ndyear = 1
            endif
            yrold = yr(i)
c
c           calculate mean daily air temperature
            tavg(i) = (tmax(i) + tmin(i))/2.
            tavgflg(i) = 'C1'
c
c
c           bypass gaps in record
            if(iout(i).eq.0) goto 9000
            if(imisppt(yr(i)).eq.1) goto 9000
            if(imistmax(yr(i)).eq.1) goto 9000
            if(imistmin(yr(i)).eq.1) goto 9000
c
            yrppt = yrppt + ppt(i)
            yrtmax = yrtmax + tmax(i)
            yrtmin = yrtmin + tmin(i)
            yrtavg = yrtavg + tavg(i)
            if((i.gt.1).and.(yr(i+1).ne.yrold)) then
                  nyr = nyr + 1
                  yrtmax = yrtmax/ndyear
                  yrtmin = yrtmin/ndyear
                  yrtavg = yrtavg/ndyear
                  write(*,9301) nyr,yr(i),ndyear,yrppt,yrtmax,
     1                                          yrtmin,yrtavg
                  write(21,9301) nyr,yr(i),ndyear,yrppt,yrtmax,
     1                                          yrtmin,yrtavg
9301              format(i6,3x,i4,3x,i3,4(3x,f7.1))
                  aappt = aappt + yrppt
                  aatmax = aatmax + yrtmax
                  aatmin = aatmin + yrtmin
                  aatavg = aatavg + yrtavg
                  yrppt = 0.
                  yrtmax = 0.
                  yrtmin = 0.
                  yrtavg = 0.
            endif
c
c
            write(19,1111) i,yr(i),mo(i),dy(i),ndyear,
     1                     ppt(i),pflg(i),
     2                     tmax(i),tmaxflg(i),
     3                     tmin(i),tminflg(i),
     4                     tavg(i),tavgflg(i),
     5                     snow(i),snowflg(i)
c
1111              format(1x,i7,1x,i4,1x,i2,1x,i2,1x,i3,1x,
     1                           5(1x,f6.1,1x,a2))
c
c
9000  continue
c
```

```
c       calculate and print annual averages
                aappt = aappt/nyr
                aatmax = aatmax/nyr
                aatmin = aatmin/nyr
                aatavg = aatavg/nyr
                write(*,9311) aappt,aatmax,aatmin,aatavg
                write(21,9311) aappt,aatmax,aatmin,aatavg
9311            format(/,4x,'Averages:',6x,4(3x,f7.1))
c
c
      close(18)
      close(19)
      close(20)
      close(21)
      stop
      end
```

ATTACHMENT VI

CALCULATION OF BLOCKING RIDGES USING BLOCKR7 V1.0

TOTAL PAGES: 40

Calculation of Blocking Ridges using BLOCKR7 V1.0

1. Name of routine/macro with version/OS/hardware environment and user information:

Name of software routine: BLOCKR7 V1.0,
OS and hardware environment: Windows NT 4.0, Pentium Pro PC
Computer Identification: SM321276 with a USGS specific host-name P720dcasr
Software Users: Joseph Hevesi (916-278-3274), Alan Flint (916-278-3221)
User Location: U.S. Geological Survey, Room 5000E, Placer Hall, 6000 J Street, Sacramento, CA 95819-6129

2. Name of commercial software with version/OS/hardware used to develop routine/macro:

The source code for BLOCKR7 V1.0 was developed using the standard FORTRAN77 programming language. The source code was written, debugged, and compiled (for PC platforms using INTEL processors) using DIGITAL Visual FORTRAN with Microsoft Developer Studio, V. 5.0.

3. General Description of routine/macro:

BLOCKR7 V1.0 is a FORTRAN77 routine developed in accordance with AP-SI.1Q, specifically for the analysis/model activity documented in this AMR. The routine source code (BLOCKR7.FOR), compiled executable file (BLOCKR7.EXE), routine control file (BLOCKR7.CTL), input and output files, validation test files, and a copy of this attachment, are located under the directory BLOCKR7 on a CD-ROM labeled GEOINPUT-1. The routine source code, control file, and the input and output files are ASCII text files that can be read using any standard ASCII text editor and can be imported into standard word processing applications such as Microsoft Word. The executable file can be used to run BLOCKR7 V1.0 on any PC with an INTEL processor (with adequate RAM).

All parameters included in the output file developed by BLOCKR7 V1.0 are used for the development of the geospatial parameter input file for INFIL V2.0. The parameters used and developed by BLOCKR7 V1.0 are equivalent to the parameters used in the input file for INFIL V1.0 (Flint and others, 1996).

4. Test plan for the software routine BLOCKR7 V1.0:

- **Explain whether this is a routine or macro and describe what it does:**

BLOCKR7 V1.0 is the first routine in a sequence of developed FORTRAN77 routines that are used in the development of the geospatial parameter input files for INFIL V2.0. The routine performs two functions required as part of the development of the geospatial parameter input files for INFIL V2.0. The first function consists of assembling nine individual ASCII matrix grid files developed in ARCINFO (corresponding to 9 separate input parameters) into a single column formatted ASCII output file. The second function consists of the calculation of 36 blocking ridge angles for each grid location defined by the

ASCII matrix grids. The blocking ridge angles are defined by the angle of inclination above the horizontal plane that the surrounding topography obstructs a location's "view" of the sky and potential direct beam solar radiation. The 36 blocking ridge angles are calculated at each 10-degree horizontal arc (with the azimuth aligned in the UTM northing direction) for each grid cell.

The input and output files used by the routine are defined in the routine control file BLOCKR7.CTL that is itself an input file for the routine. The input files defined in BLOCKR7.CTL consist of the 9 ASCII matrix grid files (one file for each parameter defined above). The output files defined in BLOCKR7.CTL consist of 30MSITE.INP which is the main output file (this file is used as input by GEOMAP7 V1.0) and two auxiliary output files, 30MSITE.SKY and SKYVIEW.ASC, consisting of the calculated sky-view factor for each grid location. Also included in BLOCKR7.CTL are parameters used as input for the calculation of the 36 approximate 10-degree azimuth angles based on the input grid geometry.

The calculated sky-view factor that included as output in the two auxiliary output files is the percentage of sky viewed from the ground surface, relative to the sky-view for an infinite horizontal plane, and is calculated for each grid cell location using the 36 blocking ridge angles generated by BLOCKR7. The two auxiliary output files provide the sky-view factor in two different output formats (ASCII column and ASCII matrix) and are used as a part of the test plan for BLOCKR7.

- **Listing of FORTRAN77 Source code:**

A listing of the FORTRAN77 source code for the routine BLOCKR7 V1.0 along with examples of the input and output files used in the test plan are included at the end of this attachment.

- **Description of test(s) to be performed:**

To determine that the two functions performed by the routine are operating correctly, two separate test plans are applied. The first test case involves a visual inspection of the column-formatted ASCII output file 30MSITE.INP to confirm that the file format is correct and that there are a total of 253,597 rows and 48 columns. The testing procedure consists of a direct comparison of parameter values in the input files to the ordering and values of parameters in the corresponding line of the output file. This provides a validation check of the first function performed by BLOCKR7 V1.0, which is the assembling of individual ASCII matrix grids for each of the input parameters into a single column formatted ASCII output file. For example, the parameter value of the first column of the first line of the input matrix for the first input parameter (latitude) must correspond to the parameter value located in the third column of the first line of the output file. The parameter value of the first column of the first line of the input matrix for the second input parameter (longitude) must correspond to the parameter value located in the fourth column of the first line of the output file, and so-on for all parameters assembled into the output file.

The second test consists of a visual evaluation of the second function performed by BLOCKR7 that consists of the calculation of the 36 blocking ridge angles and the output of these values as 36 separate columns that are included in the output file. To test this function, a visual test is conducted in ARCVIEW by a comparison of the map image obtained using the input elevation grid with the map image obtained using the sky-view values that are included in the auxiliary output file created by BLOCKR7. The sky-view values are calculated using the same 36 blocking ridge values that are included in the main output file. The testing criteria used in this test are based on the following known conditions: 1. Grid locations that are not surrounded by ridges blocking incoming solar radiation will result in a calculation of approximately 100 percent of the sky viewed (the sky-view value is the percentage of the sky viewed). 2. Grid locations in deep valleys and washes where there is blockage of solar radiation by ridges will result in the maximum reduction in sky-view within the model domain of approximately 25 to 30 percent. For the hypothetical upper bound case of an infinite horizontal plane, the calculated sky-view factor is 100 percent (no reduction in the percentage of sky viewed). In the case of mountainous terrain such as the Yucca Mountain site and the area of the net infiltration model, the occurrence of rugged topography including steep ridges with significant relief of 100 meters and greater should result in an appropriate reduction of the percent of sky viewed.

The testing is performed in ARCVIEW by a visual comparison of both a shaded-relief and a contoured representation of the DEM to map images generated using the sky-view factor obtained from the auxiliary output file SKYVIEW.ASC. The test criteria are subjectively based on the determination that the sky-view factor provides a reasonable representation of the percentage of sky viewed relative to expected reductions in sky view based on the known topography surrounding a given grid cell.

For ridge-top locations and flat or gently sloping terrain where there are no ridges blocking sky-view, expected reductions in sky-view should be minimal (from 90 to 100 percent sky-view). In comparison, for steep side-slopes and deep washes or valleys characterized by more rugged terrain, larger reductions in sky-view are expected (less than 80 percent sky-view).

The subjective acceptance criteria used in the test plan for the calculation of blocking ridges are based on the sensitivity of estimated net infiltration to the inclusion of blocking ridges in the calculation of available energy to drive potential evapotranspiration. The inclusion of the reduction in sky-view for locations with surrounding ridges provides a slight increase in the accuracy of estimated net infiltration. For example, the impact of excluding the reduction in sky-view from the estimation of net infiltration is a maximum reduction in net infiltration estimates of approximately two to three percent as compared to estimates obtained if the reduction in sky-view is included.

- **Specify the range of input values to be used and why the range is valid:**

All 9 ASCII matrix grid files used as input by BLOCKR7 V1.0 consist of six standard ARCINFO and ARCVIEW header lines specifying the dimensions of the input grid (copies of the first nine lines of these input files are included at the end of this attachment). The header lines are followed by a matrix of 691 rows by 367 columns for a total of 253,597 input values for each input file. The matrix consists of the parameter values for a specific parameter (one file per parameter) and is the standard raster-data format that can be exported or imported by ARCINFO or ARCVIEW. The nine ASCII matrix grid files listed below consist of one file for each input parameter and must be listed in the same order in the routine control file BLOCKR7.CTL. The range of input values specified in the listing below is valid because these values were obtained from ARCINFO using the source data as input.

1. **30MLAT.ASC:** Latitude coordinate input file (in decimal degrees from 36.7501 to 36.9373) for each grid location.

2. **30MLONG.ASC:** Absolute-value longitude coordinate input file (in decimal degrees from 116.3752 to 116.4997) for each grid cell location.

3. **30MSLOPE.ASC:** Ground surface slope input file (in degrees from 0 to 47).

4. **30MASPCT.ASC:** Ground surface aspect input file (in degrees from –1 to 358).

5. **30MELEV.ASC:** Ground surface elevation (in meters from 918 to 1969)

6. **30MSOIL.ASC:** Soil type identification number (an integer value from 1 to 10)

7. **30MDEPTH.ASC:** Soil depth class number (an integer value from 1 to 4)

8. **30MROCK.ASC:** Rock type identification number (an integer value from 1 to 214)

9. **30MTOPO.ASC:** Topographic location number (an integer value from 1 to 6)

5. Test Results.

- **Output from test (explain difference between input range used and possible input):**

The output for the first part of the test (input parameters from ARCINFO are properly combined into a single column formatted ASCII text file) is the main output file 30MSITE.INP generated by BLOCKR7 V1.0 and the nine ASCII matrix input files (see listing of files below). The output for the second part of the test (qualitative evaluation of blocking ridge angles using sky-view) is the value of calculated percent sky-view for every grid cell and is included in the two auxiliary output files created by BLOCKR7 (30MSITE.SKY and SKYVIEW.ASC).

- **Description of how the testing shows that the results are correct for the specified input:**

A visual inspection of the input and output files indicates that the test criteria for the first part of the test plan is satisfied. Comparison of input and output parameter values shows that all input parameters have been assembled into the correct order and line of the output file, and thus the first function of the routine is being correctly executed. The test results are reproduced in this attachment by including a partial print-out of the input and output files. Inspection of the file copies indicates that the parameter value in the first grid cell position of each matrix (hi-lighted in red) is in the correct column position of the corresponding grid cell location of the output file (first line of the output file, hi-lighted in red), the parameter value in the second grid cell position of the of each matrix (hi-lighted in blue) is in the correct column position of the corresponding grid cell location of the output file (second line of file, hi-lighted in blue), and so on. Inspection of the complete output file indicates 253,597 rows and 48 columns, with the columns ordered according to the following sequence:

Column number	Parameter description
1	Grid cell location number
2	UTM easting coordinate , in meters
3	UTM northing coordinate, in meters
4	Latitude coordinate, in decimal degrees
5	Longitude coordinate, in decimal degrees
6	Ground surface slope, in degrees
7	Ground surface aspect, in degrees
8	Ground surface elevation, in meters
9	Soil type identification number, integer value
10	Soil depth class number, integer value
11	Rock type Identification number, integer value
12	Topographic identification number, integer value
13	First of 36 blocking ridge angles, in degrees
14	Second of 36 blocking ridge angles, in degrees
15	Third of 36 blocking ridge angles, in degrees
16-47	blocking ridge angles 4 through 35
48	Last blocking ridge angle, in degrees.

The second part of the test consists of a visual evaluation of the sky-view factor calculated using the blocking ridge angles generated by BLOCKR7. Comparison of Figures VI-1 through VI-3 indicates that the test criteria for the second part of the test are satisfied. The elevation values in the main output file are used in ARCVIEW to develop Figure VI-1, which is a shaded relief map of the Yucca Mountain site. Both the elevation values in the main output file and the sky-view values provided in the auxiliary output file 30MSITE.SKY are used in ARCVIEW to develop Figures VI-2 and VI-3. Overlaying the sky view factor and topography into a combined map image allows for a visual evaluation that the test criteria are satisfied. Visual inspection of Figures VI-2 and VI-3 indicates a high percentage of sky-view (90 percent and higher) for ridge-top and flat, open area locations, and a low percentage of

sky-view (80 percent and lower) for steep side-slope locations and for deep, narrow washes. These test results indicate that the routine is functioning properly for the intended use.

- **List limitations or assumptions to this test case and code in general:**

Limitations are only those inherent in the DEM, and in the ability of the reviewer to discern topography from the shaded relief representation of the DEM. To provide an enhanced test result, the visual test is performed in ARCVIEW, allowing for the map of calculated sky-view to be draped over the shaded relief map and overlain with elevation contours generated from the DEM.

- **Electronic files identified by name and location:**

Electronic files are located on CD-ROM labeled GEOINPUT-1, under the directory BLOCKR7, included as an attachment to the AMR. The following electronic files are provided:

BLOCKR7.CTL: input file consisting of the input and output file names for BLOCKR7, along with parameters needed to perform the 36 blocking ridge angle calculations.

BLOCKR7.FOR: FORTRAN source code listing for the routine BLOCKR7. A printout of the source code is included as part of this attachment.

BLOCKR7.EXE: Executable file for the routine BLOCKR7, compiled for INTEL processors.

30MLAT.ASC: input file consisting of the grid cell latitude coordinates (in decimal degrees) for all 253,597 grid cell locations of the base grid, developed using ARCINFO and exported as a standard ARCINFO format ASCII matrix grid file. A partial printout of the first part of this file is included as part of this attachment.

30MLONG.ASC: input file consisting of the grid cell longitude coordinates (in decimal degrees) for all 253,597 grid cell locations of the base grid, developed using ARCINFO and exported as a standard ARCINFO format ASCII matrix grid file. A partial printout of the first part of this file is included as part of this attachment.

30MSLOPE.ASC: input file consisting of ground surface slope (in degrees) for all 253,597 grid cell locations of the base grid, calculated from the DEM using ARCINFO and exported as a standard ARCINFO format ASCII matrix grid file. A partial printout of the first part of this file is included as part of this attachment.

30MASPCT.ASC: input file consisting of ground surface aspect (in degrees) for all 253,597 grid cell locations of the base grid, calculated from the DEM using ARCINFO and exported as a standard ARCINFO format ASCII matrix grid file. A partial printout of the first part of this file is included as part of this attachment.

30MELEV.ASC: input file consisting of ground surface elevation (in meters) for all 253,597 grid cell locations of the base grid. The source data consists of two standard 7.5 minute USGS 30-meter digital elevation models (DEMs), which are merged into a single composite DEM using ARCINFO, and exported as a standard ARCINFO format ASCII matrix grid file. A partial printout of the first part of this file is included as part of this attachment.

30MSOIL.ASC: input file consisting of the soil type identification number (an integer value from 1 to 10) for all 253,597 grid cell locations of the base grid. The source data consists of a standard ARCINFO vector coverage that is rasterized onto the cell locations of the base grid using ARCINFO and exported as a standard ARCINFO format ASCII matrix grid file. A partial printout of the first part of this file is included as part of this attachment.

30MDEPTH.ASC: input file consisting of the soil depth class identification number (an integer value from 1 to 4) for all 253,597 grid cell locations of the base grid. The source data consists of a standard ARCINFO vector coverage that is rasterized onto the cell locations of the base grid using ARCINFO and exported as a standard ARCINFO format ASCII matrix grid file. A partial printout of the first part of this file is included as part of this attachment.

30MROCK.ASC: input file consisting of the rock type identification number (an integer value from 1 to 214) for all 253,597 grid cell locations of the base grid. The source data consists of a standard ARCINFO vector coverage that is rasterized onto the cell locations of the base grid using ARCINFO and exported as a standard ARCINFO format ASCII matrix grid file. A partial printout of the first part of this file is included as part of this attachment.

30MTOPO.ASC: input file consisting of the topographic position identification number (an integer value from 1 to 6) for all 253,597 grid cell locations of the base grid. The parameter is generated in ARCINFO using the source DEM as input, rasterized onto the cell locations of the base grid and exported as a standard ARCINFO format ASCII matrix grid file. A partial printout of the first part of this file is included as part of this attachment.

30MSITE.INP: main output file consisting of 253,597 rows and 48 columns (see section 5 above for column ordering and descriptions. This file includes 36 columns that are the 36 blocking ridge angles calculated by BLOCKR7 for each grid location. A partial printout of the first part of this file is included as part of this attachment.

30MSITE.SKY: auxiliary output file consisting of 253,597 rows and 3 columns. The first two columns are the UTM coordinates and the third column is the calculated sky-view factor (in percent). This file is used only as part of the test plan. It is not required for the intended application of the routine.

SKYVIEW.ASC: auxiliary output file consisting of the 253,597 sky-view values in the ASCII grid matrix format that is imported directly into ARCVIEW. This file is used only as part of the test plan. It is not required for the intended application of the routine.

6. Supporting Information. (Include background information, such as revision to a previous routine or macro, or explanation of the steps performed to run the software. Include listings of all electronic files and codes used).

- **Procedure for running routine:**

To run the routine BLOCKR7, an executable version of the code and all input files must be placed in the same directory. The routine is executed by typing BLOCKR7 in a DOS window, by double clicking on the file BLOCKR7.EXE in the Microsoft Windows OS, or by typing in the path and filename in the RUN window of the Windows NT or Windows 98 start menu. The input and output file names and the parameters used for the blocking ridge calculations must be in the correct sequential order as specified in the routine control file BLOCKR7.CTL (see example printouts provided below).

- **Example printout of routine control file BLOCKR7.CTL**

```
blockr7.ctl INFIL v2.0 geospatial parameter pre-processing, step 1, routine BLOCKR7
v1.0
30mlat.asc
30mlong.asc
30mslope.asc
30maspct.asc
30melev.asc
30msoil.asc
30mdepth.asc
30mrock.asc
30mtopo.asc
30msite.xyz
30msite.sky
skyview.asc
blockr7.sum
32
1    1      3
2    1      2
```

```
3    2    3
4    1    1
5    3    2
6    2    1
7    3    1
8    1    0
9    3    -1
10   2    -1
11   3    -2
12   1    -1
13   2    -3
14   1    -2
15   1    -3
16   0    -1
17   -1   -3
18   -1   -2
19   -2   -3
20   -1   -1
21   -3   -2
22   -2   -1
23   -3   -1
24   -1   0
25   -3   1
26   -2   1
27   -3   2
28   -1   1
29   -2   3
30   -1   2
31   -1   3
32   0    1
```

- **Example printout of 30MLAT.ASC: ARCINFO ASCII grid format input file for latitude, in decimal degrees (only the 6 header lines and the first 3 lines of the input matrix are listed).**

```
ncols                 367
nrows                 691
xllcorner         544661.000000
yllcorner        4067133.000000
cellsize              30.000000
NODATA_value       -9999.000000
  36.9373  36.9373  36.9373  36.9373  36.9373  36.9373  36.9373  36.9373  36.9373
36.9373  36.9373  36.9373  36.9373  36.9373  36.9373  36.9373  36.9373  36.9373
36.9373  36.9373  36.9373  36.9373  36.9373  36.9373  36.9373  36.9373  36.9373
36.9373  36.9373  36.9373  36.9373  36.9373  36.9373  36.9373  36.9373  36.9373
36.9373  36.9373  36.9373  36.9373  36.9373  36.9373  36.9372  36.9372  36.9372
36.9372  36.9372  36.9372  36.9372  36.9372  36.9372  36.9372  36.9372  36.9372
36.9372  36.9372  36.9372  36.9372  36.9372  36.9372  36.9372  36.9372  36.9372
36.9372  36.9372  36.9372  36.9372  36.9372  36.9372  36.9372  36.9372  36.9372
36.9372  36.9372  36.9372  36.9372  36.9372  36.9372  36.9372  36.9372  36.9372
36.9372  36.9372  36.9372  36.9372  36.9372  36.9372  36.9372  36.9372  36.9372
36.9372  36.9372  36.9372  36.9372  36.9372  36.9372  36.9372  36.9372  36.9372
36.9372  36.9372  36.9372  36.9372  36.9372  36.9372  36.9372  36.9372  36.9372
36.9372  36.9372  36.9372  36.9372  36.9372  36.9372  36.9372  36.9372  36.9371
36.9371  36.9371  36.9371  36.9371  36.9371  36.9371  36.9371  36.9371  36.9371
36.9371  36.9371  36.9371  36.9371  36.9371  36.9371  36.9371  36.9371  36.9371
36.9371  36.9371  36.9371  36.9371  36.9371  36.9371  36.9371  36.9371  36.9371
36.9371  36.9371  36.9371  36.9371  36.9371  36.9371  36.9371  36.9371  36.9371
36.9371  36.9371  36.9371  36.9371  36.9371  36.9371  36.9371  36.9371  36.9371
36.9371  36.9371  36.9371  36.9371  36.9371  36.9371  36.9371  36.9371  36.9371
```

36.9371	36.9371	36.9370	36.9370	36.9370	36.9370	36.9370	36.9370	36.9370
36.9370	36.9370	36.9370	36.9370	36.9370	36.9370	36.9370	36.9370	36.9370
36.9370	36.9370	36.9370	36.9370	36.9370	36.9370	36.9370	36.9370	36.9370
36.9370	36.9370	36.9370	36.9370	36.9370	36.9370	36.9370	36.9370	36.9370
36.9370	36.9370	36.9370	36.9370	36.9370	36.9370	36.9370	36.9370	36.9370
36.9370	36.9370	36.9370	36.9370	36.9370	36.9370	36.9370	36.9370	36.9370
36.9370	36.9370	36.9370	36.9370	36.9370	36.9370	36.9370	36.9370	36.9370
36.9370	36.9370	36.9370	36.9370	36.9370	36.9370	36.9370	36.9369	36.9369
36.9369	36.9369	36.9369	36.9369	36.9369	36.9369	36.9369	36.9369	36.9369
36.9369	36.9369	36.9369	36.9369	36.9369	36.9369	36.9369	36.9369	36.9369
36.9369	36.9369	36.9369	36.9369	36.9369	36.9369	36.9369	36.9369	36.9369
36.9369	36.9369	36.9369	36.9369	36.9369	36.9369	36.9369	36.9369	36.9369
36.9369	36.9369	36.9369	36.9369	36.9369	36.9369	36.9369	36.9369	36.9369
36.9369	36.9369	36.9369	36.9369	36.9369	36.9369	36.9369	36.9369	36.9369
36.9369	36.9369	36.9369	36.9369	36.9368	36.9368	36.9368	36.9368	36.9368
36.9368	36.9368	36.9368	36.9368	36.9368	36.9368	36.9368	36.9368	36.9368
36.9368	36.9368	36.9368	36.9368	36.9368	36.9368	36.9368	36.9368	36.9368
36.9368	36.9368	36.9368	36.9368	36.9368	36.9368	36.9368	36.9368	36.9368
36.9368	36.9368	36.9368	36.9368	36.9368	36.9368	36.9368	36.9368	36.9368
36.9368	36.9368	36.9368	36.9368	36.9368	36.9368	36.9368	36.9368	36.9368
36.9368	36.9368	36.9368	36.9368	36.9368	36.9368	36.9368	36.9367	36.9367
36.9367	36.9367	36.9367	36.9367	36.9367	36.9367	36.9367		
36.9370	36.9370	36.9370	36.9370	36.9370	36.9370	36.9370	36.9370	36.9370
36.9370	36.9370	36.9370	36.9370	36.9370	36.9370	36.9370	36.9370	36.9370
36.9370	36.9370	36.9370	36.9370	36.9370	36.9370	36.9370	36.9370	36.9370
36.9370	36.9370	36.9370	36.9370	36.9370	36.9370	36.9370	36.9370	36.9370
36.9370	36.9370	36.9370	36.9370	36.9370	36.9370	36.9370	36.9370	36.9370
36.9370	36.9370	36.9370	36.9370	36.9370	36.9370	36.9370	36.9370	36.9370
36.9370	36.9370	36.9370	36.9370	36.9370	36.9370	36.9370	36.9370	36.9370
36.9370	36.9370	36.9370	36.9370	36.9370	36.9370	36.9369	36.9369	36.9369
36.9369	36.9369	36.9369	36.9369	36.9369	36.9369	36.9369	36.9369	36.9369
36.9369	36.9369	36.9369	36.9369	36.9369	36.9369	36.9369	36.9369	36.9369
36.9369	36.9369	36.9369	36.9369	36.9369	36.9369	36.9369	36.9369	36.9369
36.9369	36.9369	36.9369	36.9369	36.9369	36.9369	36.9369	36.9369	36.9369
36.9369	36.9369	36.9369	36.9369	36.9369	36.9369	36.9369	36.9369	36.9369
36.9369	36.9369	36.9369	36.9369	36.9369	36.9369	36.9369	36.9369	36.9369
36.9369	36.9369	36.9369	36.9369	36.9369	36.9369	36.9369	36.9369	36.9369
36.9368	36.9368	36.9368	36.9368	36.9368	36.9368	36.9368	36.9368	36.9368
36.9368	36.9368	36.9368	36.9368	36.9368	36.9368	36.9368	36.9368	36.9368
36.9368	36.9368	36.9368	36.9368	36.9368	36.9368	36.9368	36.9368	36.9368
36.9368	36.9368	36.9368	36.9368	36.9368	36.9368	36.9368	36.9368	36.9368
36.9368	36.9368	36.9368	36.9368	36.9368	36.9368	36.9368	36.9368	36.9368
36.9368	36.9368	36.9368	36.9368	36.9368	36.9368	36.9368	36.9368	36.9368
36.9368	36.9368	36.9368	36.9368	36.9368	36.9368	36.9368	36.9368	36.9368
36.9367	36.9367	36.9367	36.9367	36.9367	36.9367	36.9367	36.9367	36.9367
36.9367	36.9367	36.9367	36.9367	36.9367	36.9367	36.9367	36.9367	36.9367
36.9367	36.9367	36.9367	36.9367	36.9367	36.9367	36.9367	36.9367	36.9367
36.9367	36.9367	36.9367	36.9367	36.9367	36.9367	36.9367	36.9367	36.9367
36.9367	36.9367	36.9367	36.9367	36.9367	36.9367	36.9367	36.9367	36.9367
36.9367	36.9367	36.9367	36.9367	36.9367	36.9367	36.9367	36.9367	36.9367
36.9367	36.9367	36.9367	36.9367	36.9367	36.9367	36.9367	36.9366	36.9366
36.9366	36.9366	36.9366	36.9366	36.9366	36.9366	36.9366	36.9366	36.9366
36.9366	36.9366	36.9366	36.9366	36.9366	36.9366	36.9366	36.9366	36.9366
36.9366	36.9366	36.9366	36.9366	36.9366	36.9366	36.9366	36.9366	36.9366
36.9366	36.9366	36.9366	36.9366	36.9366	36.9366	36.9366	36.9366	36.9366
36.9366	36.9366	36.9366	36.9366	36.9366	36.9366	36.9366	36.9366	36.9366
36.9366	36.9366	36.9366	36.9366	36.9366	36.9366	36.9365	36.9365	36.9365
36.9365	36.9365	36.9365	36.9365	36.9365	36.9365	36.9365	36.9365	36.9365
36.9365	36.9365	36.9365	36.9365	36.9365	36.9365	36.9365	36.9365	36.9365
36.9365	36.9365	36.9365	36.9365	36.9365	36.9365	36.9365	36.9365	36.9365
36.9365	36.9365	36.9365	36.9365	36.9365	36.9365	36.9365	36.9365	36.9365
36.9365	36.9365	36.9365	36.9365	36.9365	36.9365	36.9365	36.9365	36.9365
36.9365	36.9365	36.9365	36.9365	36.9365	36.9365	36.9365		

```
  36.9368  36.9368  36.9368  36.9368  36.9368  36.9368  36.9368  36.9368  36.9368
36.9368  36.9368  36.9368  36.9368  36.9368  36.9368  36.9368  36.9368  36.9368
36.9368  36.9368  36.9368  36.9367  36.9367  36.9367  36.9367  36.9367  36.9367
36.9367  36.9367  36.9367  36.9367  36.9367  36.9367  36.9367  36.9367  36.9367
36.9367  36.9367  36.9367  36.9367  36.9367  36.9367  36.9367  36.9367  36.9367
36.9367  36.9367  36.9367  36.9367  36.9367  36.9367  36.9367  36.9367  36.9367
36.9367  36.9367  36.9367  36.9367  36.9367  36.9367  36.9367  36.9367  36.9367
36.9367  36.9367  36.9367  36.9367  36.9367  36.9367  36.9367  36.9367  36.9367
36.9367  36.9367  36.9367  36.9367  36.9367  36.9367  36.9367  36.9367  36.9366
36.9366  36.9366  36.9366  36.9366  36.9366  36.9366  36.9366  36.9366  36.9366
36.9366  36.9366  36.9366  36.9366  36.9366  36.9366  36.9366  36.9366  36.9366
36.9366  36.9366  36.9366  36.9366  36.9366  36.9366  36.9366  36.9366  36.9366
36.9366  36.9366  36.9366  36.9366  36.9366  36.9366  36.9366  36.9366  36.9366
36.9366  36.9366  36.9366  36.9366  36.9366  36.9366  36.9366  36.9366  36.9366
36.9366  36.9366  36.9366  36.9365  36.9365  36.9365  36.9365  36.9365  36.9365
36.9365  36.9365  36.9365  36.9365  36.9365  36.9365  36.9365  36.9365  36.9365
36.9365  36.9365  36.9365  36.9365  36.9365  36.9365  36.9365  36.9365  36.9365
36.9365  36.9365  36.9365  36.9365  36.9365  36.9365  36.9365  36.9365  36.9365
36.9365  36.9365  36.9365  36.9365  36.9365  36.9365  36.9365  36.9365  36.9365
36.9365  36.9365  36.9365  36.9365  36.9365  36.9365  36.9365  36.9365  36.9365
36.9365  36.9365  36.9365  36.9365  36.9365  36.9365  36.9365  36.9365  36.9365
36.9364  36.9364  36.9364  36.9364  36.9364  36.9364  36.9364  36.9364  36.9364
36.9364  36.9364  36.9364  36.9364  36.9364  36.9364  36.9364  36.9364  36.9364
36.9364  36.9364  36.9364  36.9364  36.9364  36.9364  36.9364  36.9364  36.9364
36.9364  36.9364  36.9364  36.9364  36.9364  36.9364  36.9364  36.9364  36.9364
36.9364  36.9364  36.9364  36.9364  36.9364  36.9364  36.9364  36.9364  36.9364
36.9364  36.9364  36.9364  36.9364  36.9364  36.9364  36.9364  36.9364  36.9364
36.9364  36.9363  36.9363  36.9363  36.9363  36.9363  36.9363  36.9363  36.9363
36.9363  36.9363  36.9363  36.9363  36.9363  36.9363  36.9363  36.9363  36.9363
36.9363  36.9363  36.9363  36.9363  36.9363  36.9363  36.9363  36.9363  36.9363
36.9363  36.9363  36.9363  36.9363  36.9363  36.9363  36.9363  36.9363  36.9363
36.9363  36.9363  36.9363  36.9363  36.9363  36.9363  36.9363  36.9363  36.9363
36.9363  36.9363  36.9363  36.9363  36.9363  36.9363  36.9363  36.9363  36.9363
36.9363  36.9363  36.9362  36.9362  36.9362  36.9362  36.9362  36.9362  36.9362
36.9362  36.9362  36.9362  36.9362  36.9362  36.9362  36.9362  36.9362  36.9362
36.9362  36.9362  36.9362  36.9362  36.9362  36.9362  36.9362  36.9362  36.9362
36.9362  36.9362  36.9362  36.9362  36.9362  36.9362  36.9362
```

- **Example listing of 30MLONG.ASC: ARCINFO ASCII grid format input file for longitude, in decimal degrees (only the 6 header lines and the first 3 lines of the input matrix are listed).**

```
ncols                   367
nrows                   691
xllcorner        544661.000000
yllcorner       4067133.000000
cellsize             30.000000
NODATA_value       -9999.000000
 116.4985 116.4981 116.4978 116.4975 116.4971 116.4968 116.4965 116.4961
116.4958 116.4955 116.4951 116.4948 116.4944 116.4941 116.4938 116.4934
116.4931 116.4928 116.4924 116.4921 116.4917 116.4914 116.4911 116.4907
116.4904 116.4901 116.4897 116.4894 116.4891 116.4887 116.4884 116.4880
116.4877 116.4874 116.4870 116.4867 116.4864 116.4860 116.4857 116.4853
116.4850 116.4847 116.4843 116.4840 116.4837 116.4833 116.4830 116.4827
116.4823 116.4820 116.4816 116.4813 116.4810 116.4806 116.4803 116.4800
116.4796 116.4793 116.4789 116.4786 116.4783 116.4779 116.4776 116.4773
116.4769 116.4766 116.4762 116.4759 116.4756 116.4752 116.4749 116.4746
```

116.4742 116.4739 116.4736 116.4732 116.4729 116.4725 116.4722 116.4719
116.4715 116.4712 116.4709 116.4705 116.4702 116.4698 116.4695 116.4692
116.4688 116.4685 116.4682 116.4678 116.4675 116.4672 116.4668 116.4665
116.4661 116.4658 116.4655 116.4651 116.4648 116.4645 116.4641 116.4638
116.4634 116.4631 116.4628 116.4624 116.4621 116.4618 116.4614 116.4611
116.4608 116.4604 116.4601 116.4597 116.4594 116.4591 116.4587 116.4584
116.4581 116.4577 116.4574 116.4571 116.4567 116.4564 116.4560 116.4557
116.4554 116.4550 116.4547 116.4544 116.4540 116.4537 116.4533 116.4530
116.4527 116.4523 116.4520 116.4517 116.4513 116.4510 116.4507 116.4503
116.4500 116.4496 116.4493 116.4490 116.4486 116.4483 116.4480 116.4476
116.4473 116.4469 116.4466 116.4463 116.4459 116.4456 116.4453 116.4449
116.4446 116.4443 116.4439 116.4436 116.4432 116.4429 116.4426 116.4422
116.4419 116.4416 116.4412 116.4409 116.4405 116.4402 116.4399 116.4395
116.4392 116.4389 116.4385 116.4382 116.4378 116.4375 116.4372 116.4368
116.4365 116.4362 116.4358 116.4355 116.4351 116.4348 116.4345 116.4341
116.4338 116.4335 116.4331 116.4328 116.4325 116.4321 116.4318 116.4314
116.4311 116.4308 116.4304 116.4301 116.4298 116.4294 116.4291 116.4287
116.4284 116.4281 116.4277 116.4274 116.4271 116.4267 116.4264 116.4261
116.4257 116.4254 116.4250 116.4247 116.4244 116.4240 116.4237 116.4234
116.4230 116.4227 116.4223 116.4220 116.4217 116.4213 116.4210 116.4207
116.4203 116.4200 116.4197 116.4193 116.4190 116.4186 116.4183 116.4180
116.4176 116.4173 116.4170 116.4166 116.4163 116.4160 116.4156 116.4153
116.4149 116.4146 116.4143 116.4139 116.4136 116.4133 116.4129 116.4126
116.4122 116.4119 116.4116 116.4112 116.4109 116.4106 116.4102 116.4099
116.4096 116.4092 116.4089 116.4085 116.4082 116.4079 116.4075 116.4072
116.4069 116.4065 116.4062 116.4058 116.4055 116.4052 116.4048 116.4045
116.4042 116.4038 116.4035 116.4032 116.4028 116.4025 116.4021 116.4018
116.4015 116.4011 116.4008 116.4005 116.4001 116.3998 116.3994 116.3991
116.3988 116.3984 116.3981 116.3978 116.3974 116.3971 116.3968 116.3964
116.3961 116.3957 116.3954 116.3951 116.3947 116.3944 116.3940 116.3937
116.3934 116.3930 116.3927 116.3924 116.3920 116.3917 116.3914 116.3910
116.3907 116.3904 116.3900 116.3897 116.3893 116.3890 116.3887 116.3883
116.3880 116.3876 116.3873 116.3870 116.3866 116.3863 116.3860 116.3856
116.3853 116.3850 116.3846 116.3843 116.3840 116.3836 116.3833 116.3829
116.3826 116.3823 116.3819 116.3816 116.3812 116.3809 116.3806 116.3802
116.3799 116.3796 116.3792 116.3789 116.3786 116.3782 116.3779 116.3776
116.3772 116.3769 116.3765 116.3762 116.3759 116.3755 116.3752

116.4985 116.4982 116.4978 116.4975 116.4971 116.4968 116.4965 116.4961
116.4958 116.4955 116.4951 116.4948 116.4944 116.4941 116.4938 116.4934
116.4931 116.4928 116.4924 116.4921 116.4918 116.4914 116.4911 116.4907
116.4904 116.4901 116.4897 116.4894 116.4891 116.4887 116.4884 116.4880
116.4877 116.4874 116.4870 116.4867 116.4864 116.4860 116.4857 116.4854
116.4850 116.4847 116.4843 116.4840 116.4837 116.4833 116.4830 116.4827
116.4823 116.4820 116.4816 116.4813 116.4810 116.4806 116.4803 116.4800
116.4796 116.4793 116.4789 116.4786 116.4783 116.4779 116.4776 116.4773
116.4769 116.4766 116.4762 116.4759 116.4756 116.4752 116.4749 116.4746
116.4742 116.4739 116.4736 116.4732 116.4729 116.4725 116.4722 116.4719
116.4715 116.4712 116.4709 116.4705 116.4702 116.4698 116.4695 116.4692
116.4688 116.4685 116.4682 116.4678 116.4675 116.4672 116.4668 116.4665
116.4661 116.4658 116.4655 116.4651 116.4648 116.4645 116.4641 116.4638
116.4634 116.4631 116.4628 116.4624 116.4621 116.4618 116.4614 116.4611
116.4608 116.4604 116.4601 116.4597 116.4594 116.4591 116.4587 116.4584
116.4581 116.4577 116.4574 116.4571 116.4567 116.4564 116.4560 116.4557
116.4554 116.4550 116.4547 116.4544 116.4540 116.4537 116.4533 116.4530
116.4527 116.4523 116.4520 116.4517 116.4513 116.4510 116.4507 116.4503
116.4500 116.4496 116.4493 116.4490 116.4486 116.4483 116.4480 116.4476
116.4473 116.4469 116.4466 116.4463 116.4459 116.4456 116.4453 116.4449
116.4446 116.4443 116.4439 116.4436 116.4432 116.4429 116.4426 116.4422
116.4419 116.4416 116.4412 116.4409 116.4405 116.4402 116.4399 116.4395
116.4392 116.4389 116.4385 116.4382 116.4379 116.4375 116.4372 116.4368
116.4365 116.4362 116.4358 116.4355 116.4351 116.4348 116.4345 116.4341
116.4338 116.4335 116.4331 116.4328 116.4325 116.4321 116.4318 116.4315
116.4311 116.4308 116.4304 116.4301 116.4298 116.4294 116.4291 116.4287

116.4284 116.4281 116.4277 116.4274 116.4271 116.4267 116.4264 116.4261
116.4257 116.4254 116.4251 116.4247 116.4244 116.4240 116.4237 116.4234
116.4230 116.4227 116.4223 116.4220 116.4217 116.4213 116.4210 116.4207
116.4203 116.4200 116.4197 116.4193 116.4190 116.4187 116.4183 116.4180
116.4176 116.4173 116.4170 116.4166 116.4163 116.4160 116.4156 116.4153
116.4149 116.4146 116.4143 116.4139 116.4136 116.4133 116.4129 116.4126
116.4123 116.4119 116.4116 116.4112 116.4109 116.4106 116.4102 116.4099
116.4096 116.4092 116.4089 116.4085 116.4082 116.4079 116.4075 116.4072
116.4069 116.4065 116.4062 116.4058 116.4055 116.4052 116.4048 116.4045
116.4042 116.4038 116.4035 116.4032 116.4028 116.4025 116.4021 116.4018
116.4015 116.4011 116.4008 116.4005 116.4001 116.3998 116.3994 116.3991
116.3988 116.3984 116.3981 116.3978 116.3974 116.3971 116.3968 116.3964
116.3961 116.3957 116.3954 116.3951 116.3947 116.3944 116.3940 116.3937
116.3934 116.3930 116.3927 116.3924 116.3920 116.3917 116.3914 116.3910
116.3907 116.3904 116.3900 116.3897 116.3893 116.3890 116.3887 116.3883
116.3880 116.3876 116.3873 116.3870 116.3866 116.3863 116.3860 116.3856
116.3853 116.3850 116.3846 116.3843 116.3840 116.3836 116.3833 116.3829
116.3826 116.3823 116.3819 116.3816 116.3812 116.3809 116.3806 116.3802
116.3799 116.3796 116.3792 116.3789 116.3786 116.3782 116.3779 116.3776
116.3772 116.3769 116.3765 116.3762 116.3759 116.3755 116.3752
116.4985 116.4982 116.4978 116.4975 116.4971 116.4968 116.4965 116.4961
116.4958 116.4955 116.4951 116.4948 116.4944 116.4941 116.4938 116.4934
116.4931 116.4928 116.4924 116.4921 116.4918 116.4914 116.4911 116.4907
116.4904 116.4901 116.4897 116.4894 116.4891 116.4887 116.4884 116.4880
116.4877 116.4874 116.4870 116.4867 116.4864 116.4860 116.4857 116.4854
116.4850 116.4847 116.4843 116.4840 116.4837 116.4833 116.4830 116.4827
116.4823 116.4820 116.4816 116.4813 116.4810 116.4806 116.4803 116.4800
116.4796 116.4793 116.4790 116.4786 116.4783 116.4779 116.4776 116.4773
116.4769 116.4766 116.4762 116.4759 116.4756 116.4752 116.4749 116.4746
116.4742 116.4739 116.4736 116.4732 116.4729 116.4726 116.4722 116.4719
116.4715 116.4712 116.4709 116.4705 116.4702 116.4698 116.4695 116.4692
116.4688 116.4685 116.4682 116.4678 116.4675 116.4672 116.4668 116.4665
116.4662 116.4658 116.4655 116.4651 116.4648 116.4645 116.4641 116.4638
116.4634 116.4631 116.4628 116.4624 116.4621 116.4618 116.4614 116.4611
116.4608 116.4604 116.4601 116.4598 116.4594 116.4591 116.4587 116.4584
116.4581 116.4577 116.4574 116.4571 116.4567 116.4564 116.4560 116.4557
116.4554 116.4550 116.4547 116.4544 116.4540 116.4537 116.4533 116.4530
116.4527 116.4523 116.4520 116.4517 116.4513 116.4510 116.4507 116.4503
116.4500 116.4496 116.4493 116.4490 116.4486 116.4483 116.4480 116.4476
116.4473 116.4469 116.4466 116.4463 116.4459 116.4456 116.4453 116.4449
116.4446 116.4443 116.4439 116.4436 116.4432 116.4429 116.4426 116.4422
116.4419 116.4416 116.4412 116.4409 116.4405 116.4402 116.4399 116.4395
116.4392 116.4389 116.4385 116.4382 116.4379 116.4375 116.4372 116.4368
116.4365 116.4362 116.4358 116.4355 116.4351 116.4348 116.4345 116.4341
116.4338 116.4335 116.4331 116.4328 116.4325 116.4321 116.4318 116.4315
116.4311 116.4308 116.4304 116.4301 116.4298 116.4294 116.4291 116.4287
116.4284 116.4281 116.4277 116.4274 116.4271 116.4267 116.4264 116.4261
116.4257 116.4254 116.4251 116.4247 116.4244 116.4240 116.4237 116.4234
116.4230 116.4227 116.4223 116.4220 116.4217 116.4213 116.4210 116.4207
116.4203 116.4200 116.4197 116.4193 116.4190 116.4187 116.4183 116.4180
116.4176 116.4173 116.4170 116.4166 116.4163 116.4160 116.4156 116.4153
116.4149 116.4146 116.4143 116.4139 116.4136 116.4133 116.4129 116.4126
116.4123 116.4119 116.4116 116.4112 116.4109 116.4106 116.4102 116.4099
116.4096 116.4092 116.4089 116.4085 116.4082 116.4079 116.4075 116.4072
116.4069 116.4065 116.4062 116.4059 116.4055 116.4052 116.4048 116.4045
116.4042 116.4038 116.4035 116.4032 116.4028 116.4025 116.4021 116.4018
116.4015 116.4011 116.4008 116.4005 116.4001 116.3998 116.3995 116.3991
116.3988 116.3984 116.3981 116.3978 116.3974 116.3971 116.3968 116.3964
116.3961 116.3957 116.3954 116.3951 116.3947 116.3944 116.3941 116.3937
116.3934 116.3931 116.3927 116.3924 116.3920 116.3917 116.3914 116.3910
116.3907 116.3904 116.3900 116.3897 116.3893 116.3890 116.3887 116.3883
116.3880 116.3877 116.3873 116.3870 116.3867 116.3863 116.3860 116.3856
116.3853 116.3850 116.3846 116.3843 116.3840 116.3836 116.3833 116.3829

```
116.3826 116.3823 116.3819 116.3816 116.3813 116.3809 116.3806 116.3803
116.3799 116.3796 116.3792 116.3789 116.3786 116.3782 116.3779 116.3776
116.3772 116.3769 116.3765 116.3762 116.3759 116.3755 116.3752
```

- **Example listing of 30MSLOPE.ASC: ARCINFO ASCII grid format input file for ground surface slope, in degrees (only the 6 header lines and the first 3 lines of the input matrix are listed).**

```
ncols                 367
nrows                 691
xllcorner        544661.000000
yllcorner       4067133.000000
cellsize             30.000000
NODATA_value         -9999
    21    25    26    24    25    28    28    24    16    13    21    20
16    19    22    20    20    21    23    23    22    16    10    18    27
27    25    23    15     9    14    19    21    23    24    23    23    24
26    27    23    19    21    24    25    26    30    36    37    33    30
25    28    36    34    32    31    29    24    20    21    28    34    35
33    32    30    27    25    23    22    20    17    15    15    16    14
13    13    11    14    17    16    11    13    20    22    22    19    16
15    16    18    20    18    16    17    19    21    22    20    19    20
22    21    18    16    18    22    26    30    29    28    30    29    21
19    23    24    24    23    23    26    26    26    28    30    28    26
25    26    26    27    30    33    32    32    30    30    34    37    35
33    32    32    32    32    32    33    35    38    38    36    32    26
23    26    27    25    24    28    33    33    29    25    23    20    17
15    16    17    17    18    18    16    11    12    19    18    16    16
19    22    20    11     8    18    27    32    36    39    40    41    40
32    17    14    24    28    28    32    37    33    19    18    26    26
25    27    30    26    18    19    24    22    18    22    26    28    29
31    31    31    32    29    24    21    22    25    29    32    37    38
34    31    31    31    32    30    26    19    18    29    35    35    31
28    30    33    35    36    32    19    11    18    22    23    21    17
18    20    18    14    15    19    25    27    26    26    25    17    13
21    28    30    35    43    46    42    39    35    25    14    12    12
12    12    13    12    11    10    11    12    13    14    16    13    10
12    15    16    14    13    15    17    17    15    14    14    15    16
16    15    13    11    10    11    15    17    19    18    18    19    20
19    16    15    14    15    16    16    17    21    23    22    19    16
13    14    16    17    18    21    19    15    12     9     8     7    11
15    15    16    16    17    16    16    14    12    13    18    18     7
1     1     2     2
    24    28    28    26    27    28    26    19    11    14    20    18
15    17    22    20    21    22    23    24    21    13     8    15    27
28    27    25    18    10    12    17    20    22    24    21    20    24
26    25    19    17    23    25    25    26    30    35    37    33    27
23    28    35    35    33    30    28    24    16    12    19    32    36
35    33    31    28    25    25    25    22    17    14    15    17    15
12    12    12    14    18    15    11    14    20    21    21    18    16
15    16    17    17    14    15    17    18    22    23    20    17    17
17    17    15    15    19    21    25    30    30    27    27    28    24
23    24    23    21    21    21    24    25    28    30    31    28    24
23    25    22    21    26    27    28    28    27    26    29    33    32
31    30    30    30    30    31    32    34    38    39    35    29    24
26    31    31    30    28    26    28    30    28    25    23    20    15
12    14    18    22    25    26    28    28    23    17    14    15    17
18    14    12    17    22    18    15    27    35    40    42    43    44
41    32    19    13    20    25    28    35    38    31    18    13    19
23    28    31    29    24    21    23    23    21    21    25    26    29
31    31    32    32    29    23    20    22    29    34    38    40    38
33    32    32    32    32    30    28    22    18    28    33    33    30
```

```
28    29    33    36    40    38    28    17    13    21    26    22    15
15    21    24    26    29    31    32    34    32    27    23    24    28
27    26    28    34    44    46    41    39    36    25    14    14    12
11    11    11    11     9     9    10    13    13    12    13    12     9
10    14    16    15    15    16    17    16    15    14    15    14    14
14    14    12     9     9    12    15    14    14    14    15    16    17
17    16    16    15    14    15    15    16    18    18    18    17    15
13    13    16    16    18    22    22    17    11     8     7     7     7
11    12    12    12    12    12    11     9     5     9    20    21     9
1     1     1     1
    26    28    27    26    28    28    24    14     8    17    20    17
13    14    20    20    21    21    22    21    16    12    12    15    27
28    27    26    21    13    10    15    17    19    20    19    21    26
25    21    19    22    25    24    23    26    31    35    37    33    24
20    28    34    35    33    30    30    29    25    18    16    27    36
37    35    32    28    25    26    26    23    19    15    14    15    13
11    12    13    14    18    14    10    15    19    19    20    18    15
14    15    16    16    14    15    17    19    23    25    23    18    16
15    14    15    18    20    20    22    26    28    27    25    24    22
21    23    22    21    21    19    22    24    26    28    28    26    22
21    26    25    23    25    25    25    25    25    23    23    28    27
26    26    27    29    30    31    33    35    39    40    35    27    25
32    34    33    31    29    27    25    26    26    26    26    24    20
15     9     7    16    25    29    30    33    33    31    29    28    29
27    24    27    29    30    29    22    20    32    40    41    41    43
42    39    33    20    12    20    26    30    35    37    33    25    15
12    24    31    30    27    24    24    26    23    19    22    24    27
30    31    32    32    29    22    21    27    34    38    39    38    34
31    30    30    31    31    32    31    24    21    29    32    33    31
28    29    32    36    40    41    35    24    14    17    25    22    13
9    13    18    25    31    35    36    36    38    36    30    25    30
38    41    40    36    40    44    40    38    34    23    19    19    17
14     9     8     8     8     9    11    14    14    13    12    12     9
7    11    16    16    16    14    12    12    13    16    16    14    11
11    11    12    10     9    12    13    12    12    13    13    13    14
16    16    16    15    14    14    14    15    15    14    14    16    17
15    13    14    15    17    24    24    18    12     8     7     7     8
8    10     9     9     8     8     9     9     8    10    18    23    11
2     1     2     2
```

- **Example listing of 30MASPCT.ASC: ARCINFO ASCII grid format input file for ground surface aspect, in degrees (only the 6 header lines and the first 3 lines of the input matrix are listed).**

```
ncols                   367
nrows                   691
xllcorner        544661.000000
yllcorner       4067133.000000
cellsize             30.000000
NODATA_value         -9999
   238   259   269   277   284   286   284   277   241   169   127   128
166   220   232   224   204   188   178   162   141   136   122    88    85
86    88    93   117   174   218   225   225   224   218   202   204   226
246   253   244   220   193   180   187   208   229   242   247   247   241
206   147   125   130   143   149   139   118    92    66    57    62    70
76    80    82    84    84    87    98   113   128   137   128   116   129
177   206   166   120   120   120   167   251   262   263   259   249   229
203   179   161   152   170   205   229   228   223   220   209   192   189
192   184   180   206   244   255   257   258   257   255   251   243   205
153   148   166   185   179   160   159   169   158   132   122   136   160
188   208   203   181   159   146   141   141   149   176   204   207   196
186   191   201   206   211   223   232   238   245   251   253   246   221
```

180 155 153 155 144 117 101 96 94 92 87 78 66
60 63 65 64 63 59 59 99 162 164 153 148 148
142 124 103 100 133 183 202 212 218 224 222 214 210
203 158 82 48 46 47 53 60 68 114 181 186 179
193 221 233 225 188 132 113 120 158 200 212 212 215
220 221 224 225 216 199 175 154 145 145 139 129 129
133 132 126 118 110 106 111 140 202 244 248 248 243
236 232 231 233 239 240 210 134 81 81 96 109 108
91 80 77 83 98 107 108 113 128 146 156 145 93
45 41 51 65 78 85 85 82 82 88 100 118 136
151 158 156 151 154 150 149 167 168 140 114 130 169
192 217 224 206 189 185 187 188 180 165 159 167 180
189 188 185 191 183 158 153 164 172 179 181 182 196
198 180 167 162 145 132 136 152 156 147 135 132 131
118 99 92 91 91 94 100 106 107 102 110 151 200
206 193 176 163 157 157 147 118 73 43 60 77 126
184 184 238 245
274 281 283 285 288 290 289 284 228 137 125 128
160 219 231 212 192 182 177 168 159 181 167 74 80
80 81 84 94 142 206 221 220 218 214 209 227 255
264 261 238 199 177 176 193 219 240 249 252 252 241
199 140 124 125 135 149 153 150 145 115 74 72 75
78 81 83 83 82 83 87 94 107 127 136 130 130
168 219 181 117 115 126 177 250 259 257 250 236 215
192 175 160 149 174 218 224 214 215 219 210 190 186
195 191 200 235 255 257 256 255 253 250 245 233 198
155 144 160 186 186 158 147 161 166 148 130 130 151
189 215 204 171 151 142 135 133 139 165 201 209 197
190 196 205 212 222 234 242 248 254 257 256 243 210
170 157 158 164 164 140 109 91 82 78 79 81 82
75 58 42 35 35 30 27 35 44 42 36 40 69
102 113 72 20 34 77 145 205 213 219 211 205 213
216 205 182 125 61 58 62 63 60 61 87 137 173
197 221 227 221 195 150 120 116 142 190 211 210 215
220 221 223 224 222 205 178 155 140 143 145 139 134
137 139 134 130 125 118 118 145 208 251 255 250 240
228 224 226 229 233 231 217 182 123 78 75 72 61
50 49 37 28 34 42 48 54 63 87 129 169 170
157 137 115 104 95 92 90 91 93 88 77 76 92
119 144 152 154 158 151 140 150 169 157 117 110 140
184 217 220 200 183 179 184 195 186 167 160 163 178
192 196 201 203 181 150 142 152 167 178 178 180 200
203 182 171 169 154 134 127 132 139 142 134 129 137
142 126 105 97 92 93 102 115 125 117 95 105 157
201 194 173 158 150 148 146 150 218 223 67 78 81
104 174 239 240
287 283 280 279 280 282 283 275 210 119 121 129
163 220 224 200 187 181 175 171 189 242 195 61 79
79 79 78 81 110 176 219 219 219 224 239 261 271
267 248 210 176 169 180 207 235 250 256 257 254 237
188 134 123 122 128 141 154 166 179 178 137 88 80
79 79 80 80 80 83 85 87 90 100 113 121 127
161 212 189 125 107 121 183 256 259 251 239 226 210
187 172 160 154 179 214 211 201 208 217 211 193 189
197 204 235 269 280 279 273 262 253 247 240 227 196
158 142 155 185 192 162 135 143 159 153 137 128 140
180 215 202 167 148 144 134 127 129 153 197 213 200
194 202 211 222 234 242 247 252 257 257 251 231 190
160 159 161 167 173 162 136 112 100 100 105 113 126
139 138 85 18 23 20 19 27 28 20 12 20 46
52 147 323 205 29 59 97 160 203 211 206 208 220
219 212 211 194 133 71 66 63 57 50 48 56 86
156 219 225 217 199 168 138 126 140 182 210 209 215

```
220   223   225   231   232   208   173   155   140   138   143   144   139
135   136   134   130   129   128   128   157   219   247   245   238   229
221   220   223   225   228   225   220   220   172    85    80    79    78
73    54    24    10    22    34    41    48    58    68    85   122   161
171   166   155   138   110    95    92    90    81    60    47    59    69
81    97   116   135   152   153   138   135   160   176   147   116   119
161   210   212   193   181   182   196   204   183   167   163   168   183
196   204   216   209   171   141   135   142   160   174   174   180   203
203   180   173   175   165   143   125   118   120   126   126   122   130
152   150   117   101    96    93    99   113   135   152   134   103   122
176   197   174   153   142   134   131   159   223   191    81    81    78
97   169   234   246
```

- **Example listing of 30MELEV.ASC: ARCINFO ASCII grid format input file for ground surface elevation, in meters (only the 6 header lines and the first 3 lines of the input matrix are listed).**

```
ncols                   367
nrows                   691
xllcorner        544661.000000
yllcorner       4067133.000000
cellsize             30.000000
NODATA_value         -9999
  1739  1750  1767  1781  1794  1807  1824  1838  1851  1854  1846  1836
1829  1833  1843  1852  1858  1861  1862  1861  1854  1846  1841  1836  1821
1805  1791  1777  1765  1763  1766  1772  1781  1789  1799  1805  1807  1814
1825  1840  1854  1863  1868  1868  1867  1871  1881  1898  1920  1939  1955
1969  1969  1950  1932  1919  1910  1900  1889  1878  1869  1857  1841  1821
1803  1784  1766  1750  1734  1722  1708  1697  1689  1684  1680  1673  1664
1659  1663  1666  1660  1653  1646  1638  1641  1652  1663  1676  1688  1696
1700  1701  1699  1693  1689  1690  1696  1704  1711  1719  1727  1730  1730
1733  1735  1735  1735  1742  1753  1766  1783  1800  1815  1831  1848  1861
1858  1850  1844  1843  1845  1843  1836  1833  1832  1825  1809  1793  1786
1785  1790  1797  1799  1796  1787  1776  1764  1752  1744  1750  1763  1772
1774  1776  1782  1790  1797  1807  1822  1838  1859  1881  1904  1924  1939
1944  1939  1932  1926  1922  1911  1892  1871  1852  1838  1824  1812  1803
1796  1788  1778  1770  1762  1754  1745  1739  1738  1737  1734  1729  1725
1722  1716  1704  1692  1688  1688  1694  1704  1714  1731  1751  1766  1778
1792  1802  1797  1788  1775  1764  1752  1733  1710  1695  1695  1699  1700
1699  1705  1719  1732  1740  1736  1724  1710  1702  1705  1711  1720  1728
1740  1752  1763  1777  1791  1798  1799  1796  1789  1780  1771  1756  1735
1719  1707  1693  1678  1661  1642  1626  1614  1611  1623  1641  1662  1681
1695  1708  1722  1738  1756  1776  1791  1793  1781  1770  1755  1741  1733
1725  1714  1704  1696  1689  1681  1670  1655  1643  1637  1635  1635  1631
1623  1611  1600  1585  1563  1529  1499  1475  1454  1434  1423  1416  1412
1409  1407  1405  1401  1398  1396  1392  1390  1390  1388  1380  1372  1370
1370  1373  1380  1385  1387  1388  1389  1390  1391  1390  1387  1384  1383
1384  1386  1386  1387  1388  1388  1384  1380  1378  1377  1378  1378  1379
1384  1386  1384  1383  1379  1373  1366  1361  1358  1353  1344  1335  1329
1323  1316  1309  1299  1290  1279  1268  1259  1252  1246  1241  1238  1240
1243  1246  1247  1245  1241  1237  1234  1229  1223  1218  1214  1201  1194
1195  1194  1195  1196
  1738  1754  1770  1785  1800  1815  1830  1843  1850  1848  1839  1830
1823  1824  1836  1845  1848  1848  1848  1847  1843  1838  1839  1839  1824
1808  1793  1778  1764  1759  1760  1765  1771  1779  1787  1793  1796  1807
1823  1838  1851  1856  1856  1855  1854  1859  1871  1889  1911  1933  1949
1959  1955  1938  1921  1905  1893  1888  1881  1876  1873  1866  1852  1829
1807  1786  1768  1751  1736  1723  1709  1695  1684  1677  1673  1667  1660
1654  1657  1663  1658  1648  1640  1635  1639  1649  1661  1672  1682  1689
1692  1692  1690  1685  1680  1683  1691  1696  1702  1710  1718  1721  1721
1723  1726  1726  1730  1740  1750  1762  1778  1796  1811  1825  1839  1850
1848  1839  1831  1830  1834  1833  1825  1819  1817  1812  1799  1783  1772
```

1770 1777 1787 1788 1782 1774 1763 1750 1739 1732 1733 1743 1751
1755 1758 1764 1772 1783 1797 1813 1829 1850 1876 1899 1917 1929
1931 1924 1916 1910 1907 1902 1889 1871 1853 1839 1827 1816 1808
1801 1794 1787 1780 1771 1763 1757 1749 1738 1733 1730 1728 1724
1715 1706 1701 1697 1696 1688 1682 1690 1700 1714 1732 1741 1755
1773 1785 1794 1793 1784 1773 1761 1744 1723 1701 1686 1684 1683
1685 1694 1708 1721 1731 1730 1719 1707 1696 1692 1699 1707 1714
1726 1737 1750 1763 1775 1785 1787 1785 1777 1765 1754 1739 1719
1703 1692 1680 1665 1652 1637 1622 1608 1605 1617 1635 1655 1672
1685 1696 1708 1723 1744 1765 1779 1784 1783 1773 1759 1745 1736
1733 1726 1714 1707 1700 1690 1678 1664 1647 1631 1617 1617 1622
1624 1621 1608 1588 1563 1526 1500 1476 1452 1431 1422 1416 1409
1403 1400 1397 1395 1393 1392 1389 1385 1382 1382 1378 1369 1365
1364 1367 1374 1379 1379 1379 1378 1379 1383 1382 1380 1377 1375
1376 1378 1380 1382 1384 1383 1377 1372 1370 1369 1370 1369 1370
1375 1378 1376 1375 1374 1369 1361 1355 1347 1341 1336 1329 1323
1319 1316 1307 1298 1289 1277 1264 1255 1249 1246 1242 1237 1234
1236 1239 1239 1237 1234 1231 1228 1225 1224 1224 1218 1203 1194
1194 1194 1194 1195

1742 1758 1774 1788 1803 1820 1834 1845 1849 1843 1832 1824
1818 1819 1828 1834 1836 1836 1836 1834 1831 1833 1841 1840 1827
1811 1795 1780 1766 1757 1753 1759 1764 1770 1776 1783 1793 1808
1823 1837 1846 1846 1842 1838 1840 1850 1865 1884 1905 1927 1943
1951 1944 1928 1910 1891 1879 1870 1865 1864 1866 1865 1854 1834
1811 1789 1770 1753 1739 1726 1710 1696 1684 1675 1668 1660 1655
1651 1652 1658 1655 1645 1635 1631 1637 1648 1658 1669 1677 1682
1684 1683 1682 1678 1675 1679 1684 1688 1691 1699 1708 1712 1712
1714 1717 1719 1728 1737 1748 1760 1774 1790 1806 1819 1830 1837
1836 1828 1821 1819 1823 1823 1816 1805 1800 1796 1787 1775 1764
1760 1767 1777 1778 1770 1763 1754 1742 1730 1720 1718 1729 1736
1739 1743 1750 1760 1771 1786 1804 1824 1845 1870 1894 1911 1918
1913 1904 1898 1892 1889 1889 1883 1872 1858 1844 1829 1815 1804
1798 1795 1794 1791 1786 1779 1775 1768 1758 1748 1743 1742 1734
1716 1705 1706 1713 1712 1699 1681 1674 1679 1692 1705 1713 1728
1751 1766 1778 1788 1789 1779 1766 1752 1736 1718 1701 1686 1677
1675 1681 1694 1707 1716 1719 1712 1701 1687 1681 1689 1694 1702
1712 1723 1736 1749 1765 1777 1778 1775 1765 1747 1730 1716 1704
1691 1678 1667 1653 1639 1626 1612 1598 1598 1614 1631 1649 1663
1674 1683 1695 1709 1725 1746 1764 1774 1780 1776 1763 1749 1739
1734 1729 1724 1724 1719 1708 1695 1681 1664 1642 1620 1605 1598
1596 1593 1587 1576 1560 1527 1500 1475 1450 1432 1429 1421 1412
1403 1397 1394 1391 1389 1388 1385 1379 1374 1376 1376 1370 1363
1359 1361 1367 1370 1370 1370 1370 1373 1376 1375 1372 1369 1369
1369 1371 1375 1379 1380 1377 1372 1367 1364 1363 1362 1361 1362
1367 1369 1367 1367 1365 1363 1357 1350 1343 1337 1331 1325 1316
1311 1310 1304 1297 1290 1279 1263 1251 1244 1242 1241 1238 1234
1231 1233 1234 1232 1230 1227 1224 1220 1222 1228 1222 1206 1196
1194 1194 1194 1195

- Example listing of 30MSOIL.ASC: ARCINFO ASCII grid format input file for soil type identification (only the 6 header lines and the first 3 lines of the input matrix are listed).

```
ncols                   367
nrows                   691
xllcorner          544661.000000
yllcorner         4067133.000000
cellsize             30.000000
NODATA_value         -9999
    5    5    5    5    5    5    5    5    5    5    5    5
5   5    5    5    5    5    5    5    5    5    5    5    5
5   5    5    5    3    5    5    5    5    5    5    5    5
5   5    5    5    5    5    5    5    5    5    5    5    5
5   5    5    5    5    5    5    5    5    5    5    5    5
5   5    5    5    5    5    5    5    5    5    5    5    5
5   5    5    5    5    5    5    5    5    5    5    5    5
5   5    5    5    5    5    5    5    5    5    5    5    5
5   5    5    5    5    5    5    5    5    5    5    5    5
5   5    5    5    5    5    5    5    5    5    5    5    5
5   5    5    5    5    5    5    5    5    5    5    5    5
5   5    5    5    5    5    5    5    5    5    5    5    5
5   5    5    4    4    9    9    9    5    5    5    5    5
5   5    5    5    5    5    5    5    5    5    5    5    5
5   5    5    5    5    5    5    5    9    9    9    9    9
9   5    5    5    5    5    5    5    5    5    5    5    5
5   5    5    5    5    5    5    5    5    5    5    5    5
5   5    5    5    5    5    5    5    5    5    5    5    5
5   5    5    5    5    5    5    5    5    5    5    5    5
5   5    5    5    5    5    5    5    5    5    3    3    3
3   2    2    2    2    2    2    5    5    5    5    5    5
5   5    5    5    5    5    5    5    5    2    5    9    9
9   9    9    9    5    5    5    5    5    5    9    9    5
5   5    5    5    5    5    5    5    5    5    5    5    5
5   5    5    5    5    5    5    1    1    1    2    5    1
1   1    1    1    1    1    5    5    5    5    5    3    3
4   4    3    3
    5    5    5    5    5    5    5    5    5    5    5    5
5   5    5    5    5    5    5    5    5    5    5    5    5
5   5    5    5    3    5    5    5    5    5    5    5    5
5   5    5    5    5    5    5    5    5    5    5    5    5
5   5    5    5    5    5    5    5    5    5    5    5    5
5   5    5    5    5    5    5    5    5    5    5    5    5
5   5    5    5    5    5    5    5    5    5    5    5    5
5   5    5    5    5    5    5    5    5    5    5    5    5
5   5    5    5    5    5    5    5    5    5    5    5    5
5   5    5    5    5    5    5    5    5    5    5    5    5
5   5    5    5    5    5    5    5    5    5    5    5    5
5   5    5    5    5    5    5    5    5    5    5    5    5
5   5    4    5    5    5    9    9    9    5    5    5    5
5   5    5    5    5    5    5    5    5    5    5    5    5
5   5    5    5    5    5    5    5    9    9    9    9    9
9   9    9    5    5    5    5    5    5    5    5    5    5
9   5    5    5    5    5    5    5    5    5    5    5    5
5   5    5    5    5    5    5    5    5    5    5    5    5
5   5    5    5    5    5    5    5    5    5    5    5    5
5   5    5    5    5    5    5    5    5    5    3    3    3
3   3    2    2    2    2    2    5    5    5    5    5    5
5   5    5    5    5    5    5    5    5    2    5    9    9
```

```
9    9    9    9    5    5    5    5    9    9    9    9    9
5    5    5    5    5    5    5    5    5    5    5    5    5
5    5    5    5    5    5    5    9    1    1    1    2    3
1    1    1    1    1    1    1    5    5    5    5    5    3
4    3    3    3
     5    5    5    5    5    5    5    5    5    5    5    5
5    5    5    5    5    5    5    5    5    5    5    5    5
5    5    5    5    5    5    5    5    5    5    5    5    5
5    5    5    5    5    5    5    5    5    5    5    5    5
5    5    5    5    5    5    5    5    5    5    5    5    5
5    5    5    5    5    5    5    5    5    5    5    5    5
5    5    5    5    5    5    5    5    5    5    5    5    5
5    5    5    5    5    5    5    5    5    5    5    5    5
5    5    5    5    5    5    5    5    5    5    5    5    5
5    5    5    5    5    5    5    5    5    5    5    5    5
5    5    5    5    5    5    5    5    5    5    5    5    5
5    5    5    5    5    5    5    5    5    5    5    5    5
5    5    5    5    5    5    5    5    5    5    5    5    5
5    5    5    5    5    5    5    9    9    9    5    5    5
5    5    5    5    5    5    5    5    5    5    5    5    5
5    5    5    5    5    5    5    9    9    9    9    9    9
9    9    9    5    5    5    5    5    5    5    5    9    9
9    9    9    5    5    9    9    5    5    5    5    5    5
5    5    5    5    5    5    5    5    5    5    5    5    5
5    5    5    5    5    5    5    5    5    5    5    5    5
5    5    5    5    5    5    5    5    5    5    5    5    5
3    3    3    3    2    2    2    2    5    5    5    5    5
5    5    5    5    5    5    5    5    5    2    5    3    9
9    9    9    5    5    5    5    5    9    9    9    9    9
5    5    5    5    5    5    5    5    5    5    5    5    5
5    5    5    5    5    5    9    9    9    1    1    1    2
1    1    1    1    1    1    1    1    5    5    5    5    4
4    3    3    3
```

- **Example listing of 30MSOIL.ASC: ARCINFO ASCII grid format input file for soil type identification (only the 6 header lines and the first 3 lines of the input matrix are listed).**

```
ncols                  367
nrows                  691
xllcorner        544661.000000
yllcorner       4067133.000000
cellsize          30.000000
NODATA_value        -9999
     1    1    1    1    1    1    1    1    1    1    1    1
1    1    1    1    1    1    1    1    1    1    1    1    1
1    1    1    1    3    1    1    1    1    1    1    1    1
1    1    1    1    1    1    1    1    1    1    1    1    1
1    1    1    1    1    1    1    1    1    1    1    1    1
1    1    1    1    1    1    1    1    1    1    1    1    1
1    1    1    1    1    1    1    1    1    1    1    1    1
1    1    1    1    1    1    1    1    1    1    1    1    1
1    1    1    1    1    1    1    1    1    1    1    1    1
1    1    1    1    1    1    1    1    1    1    1    1    1
1    1    1    1    1    1    1    1    1    1    1    1    1
1    1    1    1    1    1    1    1    1    1    1    1    1
1    1    1    1    1    1    1    1    1    1    1    1    1
1    1    1    3    3    2    2    2    1    1    1    1    1
1    1    1    1    1    1    1    1    1    1    1    1    1
1    1    1    1    1    1    1    1    2    2    2    2    2
```

2	1	1	1	1	1	1	1	1	1	1	1	1
1	1	1	1	1	1	1	1	1	1	1	1	1
1	1	1	1	1	1	1	1	1	1	1	1	1
1	1	1	1	1	1	1	1	1	1	1	1	1
1	1	1	1	1	1	1	1	1	1	3	4	4
4	4	4	4	4	3	3	1	1	1	1	1	1
1	1	1	1	1	1	1	1	1	3	1	2	2
2	2	2	2	1	1	1	1	1	1	2	2	1
1	1	1	1	1	1	1	1	1	1	1	1	1
1	1	1	1	1	1	1	3	4	4	3	1	1
3	3	3	3	3	3	1	1	1	1	1	3	3
4	4	4	4									
1	1	1	1	1	1	1	1	1	1	1	1	
1	1	1	1	1	1	1	1	1	1	1	1	1
1	1	1	1	3	1	1	1	1	1	1	1	1
1	1	1	1	1	1	1	1	1	1	1	1	1
1	1	1	1	1	1	1	1	1	1	1	1	1
1	1	1	1	1	1	1	1	1	1	1	1	1
1	1	1	1	1	1	1	1	1	1	1	1	1
1	1	1	1	1	1	1	1	1	1	1	1	1
1	1	1	1	1	1	1	1	1	1	1	1	1
1	1	1	1	1	1	1	1	1	1	1	1	1
1	1	1	1	1	1	1	1	1	1	1	1	1
1	1	1	1	1	1	1	1	1	1	1	1	1
1	1	1	1	1	1	1	1	1	1	1	1	1
1	1	1	1	1	1	1	1	1	1	1	1	1
1	1	3	1	1	1	2	2	2	1	1	1	1
1	1	1	1	1	1	1	1	1	1	1	1	1
1	1	1	1	1	1	1	1	2	2	2	2	2
2	2	2	1	1	1	1	1	1	1	1	1	1
2	1	1	1	1	1	1	1	1	1	1	1	1
1	1	1	1	1	1	1	1	1	1	1	1	1
1	1	1	1	1	1	1	1	1	1	1	1	1
1	1	1	1	1	1	1	1	1	1	3	3	3
4	4	4	4	4	4	3	1	1	1	1	1	1
1	1	1	1	1	1	1	1	1	3	1	2	2
2	2	2	2	1	1	1	1	2	2	2	2	2
1	1	1	1	1	1	1	1	1	1	1	1	1
1	1	1	1	1	1	1	2	3	4	4	3	3
4	4	4	4	4	4	3	1	1	1	1	1	3
4	4	4	4									
1	1	1	1	1	1	1	1	1	1	1	1	
1	1	1	1	1	1	1	1	1	1	1	1	1
1	1	1	1	1	1	1	1	1	1	1	1	1
1	1	1	1	1	1	1	1	1	1	1	1	1
1	1	1	1	1	1	1	1	1	1	1	1	1
1	1	1	1	1	1	1	1	1	1	1	1	1
1	1	1	1	1	1	1	1	1	1	1	1	1
1	1	1	1	1	1	1	1	1	1	1	1	1
1	1	1	1	1	1	1	1	1	1	1	1	1
1	1	1	1	1	1	1	1	1	1	1	1	1
1	1	1	1	1	1	1	1	1	1	1	1	1
1	1	1	1	1	1	1	1	1	1	1	1	1
1	1	1	1	1	1	1	1	1	1	1	1	1
1	1	1	1	1	1	1	1	1	1	1	1	1
1	1	1	1	1	1	1	2	2	2	1	1	1
1	1	1	1	1	1	1	1	1	1	1	1	1
1	1	1	1	1	1	1	2	2	2	2	2	2
2	2	2	1	1	1	1	1	1	1	1	2	2
2	2	2	1	1	2	2	1	1	1	1	1	1
1	1	1	1	1	1	1	1	1	1	1	1	1
1	1	1	1	1	1	1	1	1	1	1	1	1
1	1	1	1	1	1	1	1	1	1	1	1	1

```
3     3     4     4     4     4     4     3     1     1     1     1     1
1     1     1     1     1     1     1     1     1     3     1     3     2
2     2     2     1     1     1     1     1     2     2     2     2     2
1     1     1     1     1     1     1     1     1     1     1     1     1
1     1     1     1     1     1     2     2     2     3     4     4     4
4     4     4     4     4     4     4     3     1     1     1     1     3
4     4     4     4
```

- **Example listing of 30MDEPTH.ASC: ARCINFO ASCII grid format input file for soil depth class identification (only the 6 header lines and the first 3 lines of the input matrix are listed).**

```
ncols                   367
nrows                   691
xllcorner        544661.000000
yllcorner       4067133.000000
cellsize             30.000000
NODATA_value           -9999
     1     1     1     1     1     1     1     1     1     1     1     1
1    1     1     1     1     1     1     1     1     1     1     1     1
1    1     1     1     3     1     1     1     1     1     1     1     1
1    1     1     1     1     1     1     1     1     1     1     1     1
1    1     1     1     1     1     1     1     1     1     1     1     1
1    1     1     1     1     1     1     1     1     1     1     1     1
1    1     1     1     1     1     1     1     1     1     1     1     1
1    1     1     1     1     1     1     1     1     1     1     1     1
1    1     1     1     1     1     1     1     1     1     1     1     1
1    1     1     1     1     1     1     1     1     1     1     1     1
1    1     1     1     1     1     1     1     1     1     1     1     1
1    1     1     1     1     1     1     1     1     1     1     1     1
1    1     1     1     1     1     1     1     1     1     1     1     1
1    1     1     1     1     1     1     1     1     1     1     1     1
1    1     1     3     3     2     2     2     1     1     1     1     1
1    1     1     1     1     1     1     1     1     1     1     1     1
1    1     1     1     1     1     1     1     2     2     2     2     2
2    1     1     1     1     1     1     1     1     1     1     1     1
1    1     1     1     1     1     1     1     1     1     1     1     1
1    1     1     1     1     1     1     1     1     1     1     1     1
1    1     1     1     1     1     1     1     1     1     1     1     1
1    1     1     1     1     1     1     1     1     1     3     4     4
4    4     4     4     4     3     3     1     1     1     1     1     1
1    1     1     1     1     1     1     1     1     3     1     2     2
2    2     2     2     1     1     1     1     1     1     2     2     1
1    1     1     1     1     1     1     1     1     1     1     1     1
1    1     1     1     1     1     1     3     4     4     3     1     1
3    3     3     3     3     3     1     1     1     1     1     3     3
4    4     4     4
     1     1     1     1     1     1     1     1     1     1     1     1
1    1     1     1     1     1     1     1     1     1     1     1     1
1    1     1     1     3     1     1     1     1     1     1     1     1
1    1     1     1     1     1     1     1     1     1     1     1     1
1    1     1     1     1     1     1     1     1     1     1     1     1
1    1     1     1     1     1     1     1     1     1     1     1     1
1    1     1     1     1     1     1     1     1     1     1     1     1
1    1     1     1     1     1     1     1     1     1     1     1     1
1    1     1     1     1     1     1     1     1     1     1     1     1
1    1     1     1     1     1     1     1     1     1     1     1     1
1    1     1     1     1     1     1     1     1     1     1     1     1
1    1     1     1     1     1     1     1     1     1     1     1     1
1    1     1     1     1     1     1     1     1     1     1     1     1
1    1     3     1     1     1     2     2     2     1     1     1     1
```

```
1    1    1    1    1    1    1    1    1    1    1    1    1
1    1    1    1    1    1    1    1    2    2    2    2    2
2    2    2    1    1    1    1    1    1    1    1    1    1
2    1    1    1    1    1    1    1    1    1    1    1    1
1    1    1    1    1    1    1    1    1    1    1    1    1
1    1    1    1    1    1    1    1    1    1    1    1    1
1    1    1    1    1    1    1    1    1    1    3    3    3
4    4    4    4    4    4    3    1    1    1    1    1    1
1    1    1    1    1    1    1    1    1    3    1    2    2
2    2    2    2    1    1    1    1    2    2    2    2    2
1    1    1    1    1    1    1    1    1    1    1    1    1
1    1    1    1    1    1    1    2    3    4    4    3    3
4    4    4    4    4    4    3    1    1    1    1    1    3
4    4    4    4
     1    1    1    1    1    1    1    1    1    1    1    1
1    1    1    1    1    1    1    1    1    1    1    1    1
1    1    1    1    1    1    1    1    1    1    1    1    1
1    1    1    1    1    1    1    1    1    1    1    1    1
1    1    1    1    1    1    1    1    1    1    1    1    1
1    1    1    1    1    1    1    1    1    1    1    1    1
1    1    1    1    1    1    1    1    1    1    1    1    1
1    1    1    1    1    1    1    1    1    1    1    1    1
1    1    1    1    1    1    1    1    1    1    1    1    1
1    1    1    1    1    1    1    1    1    1    1    1    1
1    1    1    1    1    1    1    1    1    1    1    1    1
1    1    1    1    1    1    1    1    1    1    1    1    1
1    1    1    1    1    1    1    1    1    1    1    1    1
1    1    1    1    1    1    1    1    1    1    1    1    1
1    1    1    1    1    1    1    2    2    2    1    1    1
1    1    1    1    1    1    1    1    1    1    1    1    1
1    1    1    1    1    1    1    2    2    2    2    2    2
2    2    2    1    1    1    1    1    1    1    1    2    2
2    2    2    1    1    2    2    1    1    1    1    1    1
1    1    1    1    1    1    1    1    1    1    1    1    1
1    1    1    1    1    1    1    1    1    1    1    1    1
1    1    1    1    1    1    1    1    1    1    1    1    1
3    3    4    4    4    4    4    3    1    1    1    1    1
1    1    1    1    1    1    1    1    1    3    1    3    2
2    2    2    1    1    1    1    1    2    2    2    2    2
1    1    1    1    1    1    1    1    1    1    1    1    1
1    1    1    1    1    1    2    2    2    3    4    4    4
4    4    4    4    4    4    4    3    1    1    1    1    3
4    4    4    4
```

- **Example listing of 30MROCK.ASC: ARCINFO ASCII grid format input file for rock type identification number (only the 6 header lines and the first 3 lines of the input matrix are listed).**

```
ncols                   367
nrows                   691
xllcorner        544661.000000
yllcorner       4067133.000000
cellsize             30.000000
NODATA_value         -9999
   201   201   201   201   201   201   201   201   201   202   202   202
202   202   201   201   201   201   201   201   201   201   201   201   201
201   203   203   203   203   203   201   201   201   201   201   201   201
201   201   201   201   201   201   201   201   201   201   201   201   201
201   201   201   201   201   201   201   201   201   201   201   201   201
201   201   201   201   201   201   201   201   201   201   201   201   201
201   201   201   201   201   201   201   204   204   201   201   201   201
```

```
201  201  201  201  201  201  201  201  201  201  201  201  203
203  201  201  201  201  201  201  201  201  201  201  201  201
201  201  201  201  201  201  201  201  201  201  201  201  201
201  201  201  205  205  205  205  205  205  205  205  205  205
205  205  206  206  206  206  206  206  206  206  206  206  206
206  206  206  206  206  206  206  206  206  206  206  206  206
206  206  206  206  206  206  206  206  206  206  206  206  206
206  206  206  206  206  204  204  204  206  206  206  206  206
206  206  206  206  206  206  206  206  206  206  206  206  206
206  206  207  207  207  207  207  206  206  206  206  206  206
206  206  206  206  206  206  206  206  206  206  206  206  206
206  206  206  206  206  206  206  208  208  208  205  205  205
205  205  205  202  202  202  202  202  202  202  202  202  202
202  202  202  202  202  202  202  202  202  202  202  202  202
202  202  202  202  202  202  202  202  202  202  202  202  204
204  204  204  204  204  204  204  202  202  202  202  204  204
204  202  202  202  202  202  202  202  202  202  202  202  204
204  204  202  202  202  202  202  202  202  202  202  202  202
205  205  205  205  205  205  205  205  205  205  205  205  205
205  205  205  205  205  205  204  204  204  204  204  204  204
204  205  205  205  205  205  205  205  205  205  209  209  204
204  204  204  204
   201  201  201  201  201  201  201  201  201  201  201  202  202
202  202  201  201  201  201  201  201  201  201  201  201  201
201  203  203  203  203  203  203  201  201  201  201  201  201
201  201  201  201  201  201  201  201  201  201  201  201  201
201  201  201  201  201  201  201  201  201  201  201  201  201
201  201  201  201  201  201  201  201  201  201  201  201  201
201  201  201  201  201  201  201  204  204  201  201  201  201
201  201  201  201  201  201  201  201  201  201  201  201  203
203  201  201  201  201  201  201  201  201  201  201  201  201
201  201  201  201  201  201  201  201  201  201  201  201  201
201  201  201  201  205  205  205  205  205  205  205  205  205
205  205  206  206  206  206  206  206  206  206  206  206  206
206  206  206  206  206  206  206  206  206  206  206  206  206
206  206  206  206  206  206  206  206  206  206  206  206  206
206  206  206  206  206  206  204  204  204  204  206  206  206
206  206  206  206  206  206  206  206  206  206  206  206  206
206  206  207  207  207  207  207  206  206  206  206  206  206
206  206  206  206  206  206  206  206  206  206  206  206  206
206  206  206  202  202  202  202  208  208  208  205  205  205
205  205  205  202  202  202  202  202  202  202  202  202  202
202  202  202  202  202  202  202  202  202  202  202  202  202
202  202  202  202  202  202  202  202  202  202  202  202  204
204  204  204  204  204  204  204  204  202  202  202  202  204
204  204  202  202  202  202  202  202  202  202  202  204  204
204  204  202  202  202  202  202  202  202  202  202  202  202
202  205  205  205  205  205  205  205  205  205  205  205  205
205  205  205  205  205  205  204  204  204  204  204  204  204
204  204  205  205  205  205  205  205  205  209  209  209  204
204  204  204  204
   201  201  201  201  201  201  201  201  201  201  201  202  202
201  201  201  201  201  201  201  201  201  201  201  201  201
201  203  203  203  203  203  203  201  201  201  201  201  201
201  201  201  201  201  201  201  201  201  201  201  201  201
201  201  201  201  201  201  201  201  201  201  201  201  201
201  201  201  201  201  201  201  201  201  201  201  201  201
201  201  201  201  201  201  201  204  204  201  201  201  201
201  201  201  201  201  201  201  201  201  201  201  201  203
203  201  201  201  201  201  201  201  201  201  201  201  201
201  201  201  201  201  201  201  201  201  201  201  201  201
201  201  201  201  205  205  205  205  205  205  205  205  205
205  205  206  206  206  206  206  206  206  206  206  206  206
```

```
206   206   206   206   206   206   206   206   206   206   206   206   206
206   206   206   206   206   206   206   206   206   206   206   206   206
206   206   206   206   206   206   206   204   204   204   206   206   206
206   206   206   206   206   206   206   206   206   206   206   206   206
206   206   206   207   207   207   207   206   206   206   206   206   206
206   206   206   206   206   206   206   206   206   206   206   206   202
202   202   202   202   202   202   202   208   208   208   205   205   205
205   205   205   205   202   202   202   202   202   202   202   202   202
202   202   202   202   202   202   202   202   202   202   202   202   202
202   202   202   202   202   202   202   202   202   202   202   202   202
204   204   204   204   204   204   204   204   204   204   204   204   204
204   204   202   202   202   202   202   202   202   202   202   204   204
204   202   202   202   202   202   202   202   202   202   202   202   202
202   205   205   205   205   205   205   205   205   205   205   205   205
205   205   205   205   205   205   204   204   204   204   204   204   204
204   204   204   204   205   205   205   205   205   209   209   209   204
204   204   204   204
```

- **Example listing of 30MTOPO.ASC: ARCINFO ASCII grid format input file for topographic location number (only the 6 header lines and the first 3 lines of the input matrix are listed).**

```
ncols                  367
nrows                  691
xllcorner        544661.000000
yllcorner       4067133.000000
cellsize          30.000000
NODATA_value          -9999
      4     4     4     4     4     4     4     4     4     4     4     4
4     4     4     4     4     4     4     4     4     4     4     4     4
4     4     4     4     2     4     4     4     4     4     4     4     4
4     4     4     4     4     4     4     4     4     4     4     4     4
4     4     4     4     4     4     4     4     4     4     4     4     4
4     4     4     4     4     4     4     4     4     4     4     4     4
4     4     4     4     4     4     4     4     4     4     4     4     4
4     4     4     4     4     4     4     4     4     4     4     4     4
4     4     4     4     4     4     4     4     4     4     4     4     4
4     4     4     4     4     4     4     4     4     4     4     4     4
4     4     4     4     4     4     4     4     4     4     4     4     4
4     4     4     4     4     4     4     4     4     4     4     4     4
4     4     4     4     4     4     4     4     5     4     4     4     4
4     4     4     1     1     3     3     3     4     4     4     4     4
4     4     5     4     4     4     4     4     4     4     4     4     4
4     4     4     4     4     4     4     4     3     3     3     3     3
3     4     4     4     4     4     4     4     4     4     4     4     4
4     4     4     4     4     4     4     4     4     4     4     4     4
4     4     4     4     4     4     4     5     4     4     4     4     4
4     4     4     4     4     4     4     4     4     4     4     4     4
4     4     4     4     4     4     4     4     4     4     2     1     2
2     2     2     2     2     2     2     4     4     4     4     4     4
4     4     4     4     4     4     4     4     4     2     4     3     3
3     3     3     3     2     2     2     2     2     2     3     3     2
2     2     2     2     2     2     2     2     2     2     2     2     2
2     2     2     2     2     2     2     2     2     2     2     5     4
2     2     2     2     2     2     4     4     4     4     4     2     2
1     1     2     2
      4     4     4     4     4     4     4     4     4     4     4     4
4     4     4     4     4     4     4     4     4     4     5     5     4
4     4     4     4     2     4     4     4     4     4     4     4     4
4     4     4     4     4     4     4     4     4     4     4     4     4
4     4     4     4     4     4     4     4     4     4     4     4     4
```

```
 4  4  4  4  4  4  4  4  4  4  4  4  4
 4  4  4  4  4  4  4  4  4  4  4  4  4
 4  4  4  4  4  4  4  4  4  4  4  4  4
 4  4  1  4  4  4  4  4  4  4  4  4  4
 4  4  4  4  4  4  4  4  4  4  4  4  4
 4  4  4  4  4  4  4  4  4  4  4  4  4
 4  4  4  4  4  4  4  4  4  4  4  4  4
 4  4  4  4  4  4  4  4  4  4  4  4  4
 4  4  4  4  4  4  4  4  4  4  4  4  4
 4  4  1  4  4  4  3  3  3  4  4  4  4
 4  4  4  4  4  4  4  4  4  4  4  4  4
 4  4  4  4  4  4  4  4  3  3  3  3  3
 3  3  3  4  4  4  4  4  4  4  4  4  4
 3  4  4  4  4  4  4  4  4  4  4  4  4
 4  4  4  4  4  4  4  4  4  4  4  4  4
 4  4  4  4  4  4  4  4  4  4  4  4  4
 4  4  4  4  4  4  4  4  4  4  2  2  2
 2  2  2  2  2  2  2  4  4  4  4  4  4
 4  4  4  4  4  4  4  4  4  2  4  3  3
 3  3  3  3  5  2  2  2  3  3  3  3  3
 2  2  2  2  2  2  2  2  2  2  2  2  2
 2  2  2  2  2  2  2  3  2  2  2  2  2
 2  2  2  2  2  2  2  4  5  5  4  4  2
 1  2  2  2
    4  4  4  4  4  4  4  4  5  4  4  4
 4  4  4  4  4  4  4  4  4  4  4  4  4
 4  4  4  4  4  5  4  4  4  4  4  4  4
 4  4  4  4  4  4  4  4  4  4  4  4  4
 4  4  4  4  4  4  4  4  4  4  4  4  4
 4  4  4  4  4  4  4  4  4  4  4  4  4
 4  4  4  4  4  4  5  4  4  4  4  4  4
 4  4  4  4  4  4  4  4  4  4  4  4  4
 4  4  4  4  4  4  4  4  4  4  4  4  4
 4  4  4  4  4  4  4  4  4  4  4  4  4
 4  4  4  4  4  4  4  4  4  4  4  4  4
 4  4  4  4  4  4  4  4  4  4  4  4  4
 4  4  4  4  4  4  4  4  4  4  4  4  4
 4  4  6  4  4  4  4  4  4  4  4  4  4
 4  4  4  4  4  4  4  3  3  3  4  4  4
 4  4  4  4  5  4  4  4  4  4  4  4  4
 5  4  4  4  4  4  4  3  3  3  3  3  3
 3  3  3  4  4  4  4  4  4  4  4  3  3
 3  3  3  4  4  3  3  4  4  4  4  4  4
 4  4  4  4  4  4  4  4  4  4  4  4  4
 4  4  4  4  4  4  4  4  4  4  4  4  4
 4  4  4  4  4  4  4  4  4  4  4  4  4
 2  2  2  2  2  2  2  2  4  4  4  4  4
 5  5  4  4  4  4  4  4  4  2  4  2  3
 3  3  3  2  5  2  2  2  3  3  3  3  3
 2  2  2  2  2  2  2  2  2  2  2  2  2
 2  2  2  2  2  2  3  3  3  2  2  2  2
 2  2  2  2  2  2  2  2  5  4  4  4  1
 1  2  2  2
```

- **Example listing of 30MSITE.INP: main output file generated by BLOCKR7 V1.0 and supplied as input to GEOMAP7 (only the 6 header lines and the first 3 lines of the input matrix are listed).**

```
     1  544661.  4087833. 36.9373 116.4985  21 238  1739  5  1 201  4  0  0
0  0  0  0  0  2 25 25 25 24 23 21 19 16 11 11  1  0  0  0  0  0  0  0  0  0
0  0  0  0  0  0  0  0 .
```

```
      2  544691.  4087833. 36.9373 116.4981  25 259  1750  5  1 201  4  0  0
0  0  0  0  0  3 29 28 27 26 25 22 19 17 11 11  1  0  0  0  0  0  0  0  0  0
0  0  0  0  0  0  0  0
      3  544721.  4087833. 36.9373 116.4978  26 269  1767  5  1 201  4  0  0
0  0  0  0  0  2 25 25 26 26 24 20 18 17 10 10  1  0  0  0  0  0  0  0  0  0
0  0  0  0  0  0  0  0
      4  544751.  4087833. 36.9373 116.4975  24 277  1781  5  1 201  4  0  0
0  0  0  0  0  2 25 25 26 26 25 22 18 16  9  9  2  0  0  0  0  0  0  0  0  0
0  0  0  0  0  0  0  0
      5  544781.  4087833. 36.9373 116.4971  25 284  1794  5  1 201  4  0  0
0  0  0  0  0  2 26 26 27 26 25 23 21 17 11 11  2  0  0  0  0  0  0  0  0  0
0  0  0  0  0  0  0  0
      6  544811.  4087833. 36.9373 116.4968  28 286  1807  5  1 201  4  0  0
0  0  0  0  0  3 29 28 24 25 24 23 20 17 14 14  2  0  0  0  0  0  0  0  0  0
0  0  0  0  0  0  0  0
      7  544841.  4087833. 36.9373 116.4965  28 284  1824  5  1 201  4  0  0
0  0  0  0  0  2 25 23 15 16 15 17 15 13 11 11  1  0  0  0  0  0  0  0  0  0
0  0  0  0  0  0  0  0
      8  544871.  4087833. 36.9373 116.4961  24 277  1838  5  1 201  4  0  0
0  0  0  0  0  2 23 20  2  5  6  6  6  5  8  9  0  0  0  0  0  0  0  0  0  0
0  0  0  0  0  0  0  0
      9  544901.  4087833. 36.9373 116.4958  16 241  1851  5  1 201  4  0  0
0  0  0  0  0  0  5  4  0  0  0  0  0  0  1  2  0  0  0  0  0  0  0  0  0  0
0  0  0  0  0  0  0  0
     10  544931.  4087833. 36.9373 116.4955  13 169  1854  5  1 202  4  0  0
0  0  0  0  0  0  5  4  0  0  0  0  0  0  0  0  1  0  0  0  0  0  0  0  0  0
0  0  0  0  0  0  0  0
     11  544961.  4087833. 36.9373 116.4951  21 127  1846  5  1 202  4  0  0
0  0  0  0  0  0  5  4  0  0  0  0  0  0  0  0  2  1  0  1  1  1  2  1 14 12
0  0  0  0  0  0  0  0
     12  544991.  4087833. 36.9373 116.4948  20 128  1836  5  1 202  4  0  0
0  0  0  0  0  0  8  7  1  1  0  0  0  0  0  0  2  4  4  4  4  7  9  9 18 15
0  0  0  0  0  0  0  0
     13  545021.  4087833. 36.9373 116.4944  16 166  1829  5  1 202  4  0  0
0  0  0  0  0  1 14 13  8  3  1  0  0  0  0  0  2  5  6  6  6  7  8 11 15 13
0  0  0  0  0  0  0  0
     14  545051.  4087833. 36.9373 116.4941  19 220  1833  5  1 202  4  0  0
0  0  0  0  0  2 18 16  8  6  2  1  0  0  0  0  0  3  4  4  3  3  3  3  9  7
0  0  0  0  0  0  0  0
     15  545081.  4087833. 36.9373 116.4938  22 232  1843  5  1 201  4  0  0
0  0  0  0  0  1 16 14  3  2  0  0  0  0  0  0  0  0  1  2  1  1  1  1  4  3
0  0  0  0  0  0  0  0
     16  545111.  4087833. 36.9373 116.4934  20 224  1852  5  1 201  4  0  0
0  0  0  0  0  1 11  9  0  0  0  0  0  0  0  0  0  0  0  0  0  0  0  0  0  0
0  0  0  0  0  0  0  0
     17  545141.  4087833. 36.9373 116.4931  20 204  1858  5  1 201  4  0  0
0  0  0  0  0  0  6  5  0  0  0  0  0  0  0  0  0  0  0  0  0  0  0  0  0  0
0  0  0  0  0  0  0  0
     18  545171.  4087833. 36.9373 116.4928  21 188  1861  5  1 201  4  0  0
0  0  0  0  0  0  6  5  0  0  0  0  0  0  0  0  0  0  0  0  0  0  0  0  0  0
0  0  0  0  0  0  0  0
     19  545201.  4087833. 36.9373 116.4924  23 178  1862  5  1 201  4  0  0
0  0  0  0  0  0  6  5  0  0  0  0  0  0  0  0  0  0  0  0  0  0  0  0  0  0
0  0  0  0  0  0  0  0
     20  545231.  4087833. 36.9373 116.4921  23 162  1861  5  1 201  4  0  0
0  0  0  0  0  0  6  5  0  0  0  0  0  0  0  0  0  0  0  0  0  0  0  1  0  0
0  0  0  0  0  0  0  0
```

- **Figures used as part of the routine test plan:**

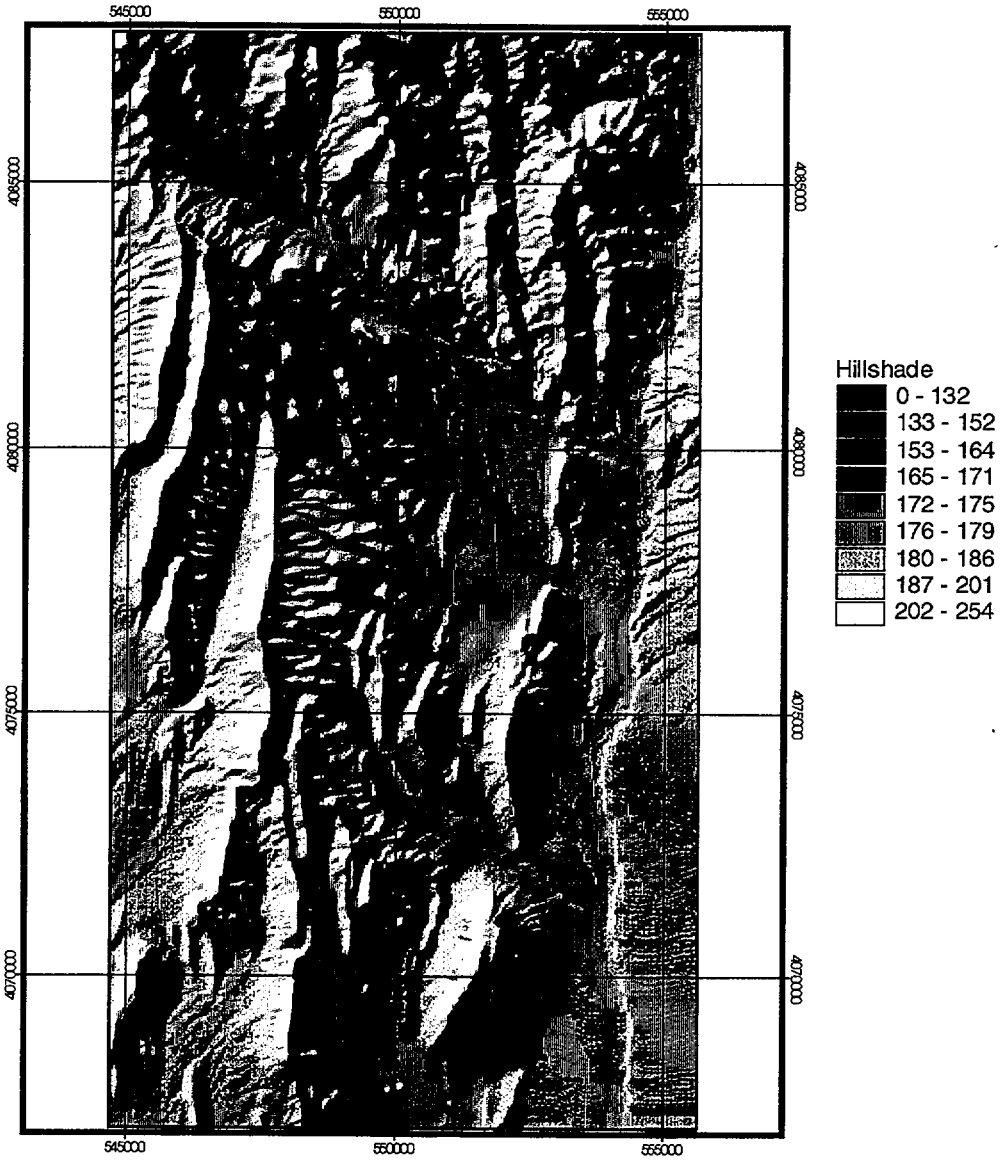

Figure VI-1. Shaded relief representation of the digital elevation model (DEM) used as input to BLOCKR7 V1.0 for calculating the blocking ridge angles required as input to INFIL V2.0 for the Yucca Mountain model domain.

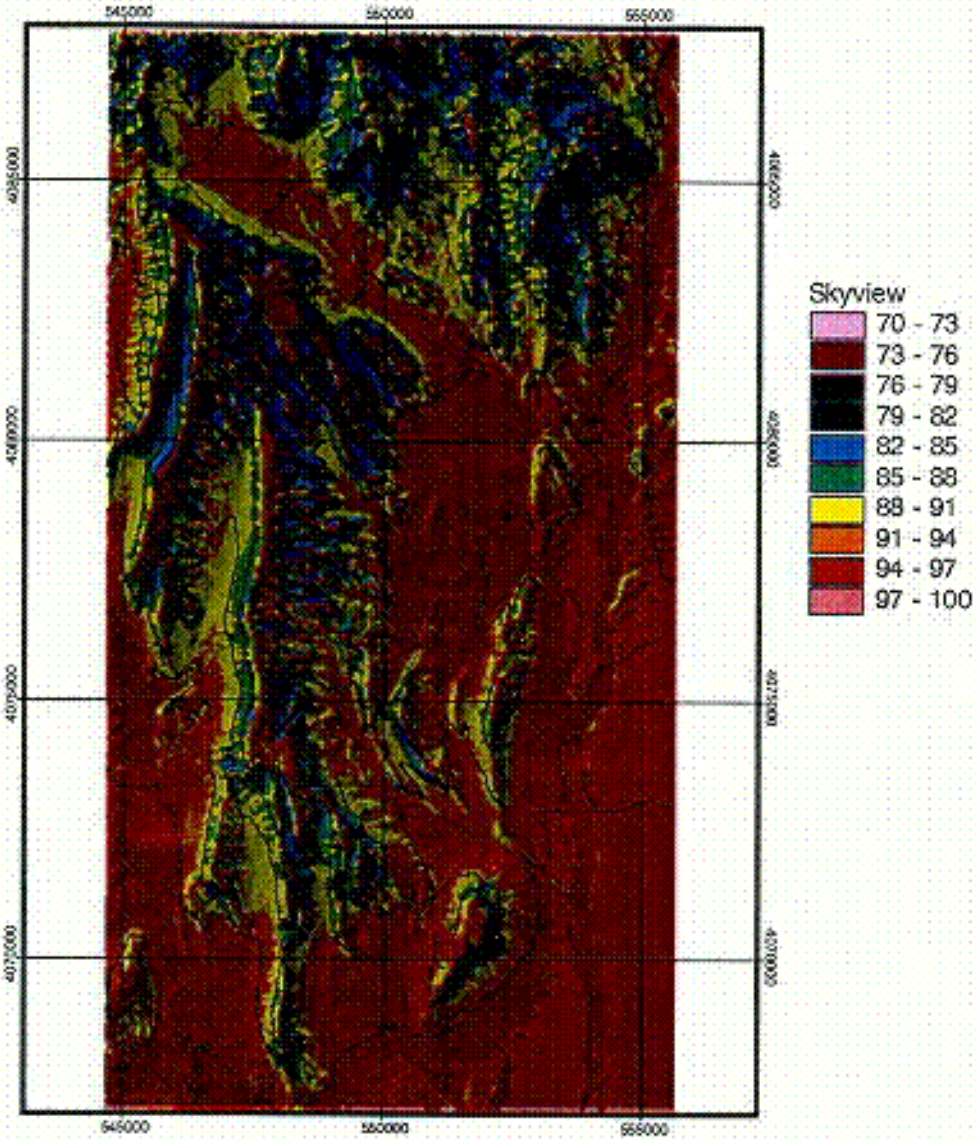

Figure VI-2. Sky-view factor for Yucca Mountain model domain, indicating the percentage of sky viewed from the ground surface relative to the view from an infinite horizontal plane, generated for each model grid cell location using the 36 blocking ridge angles calculated in BLOCKR7 V1.0.

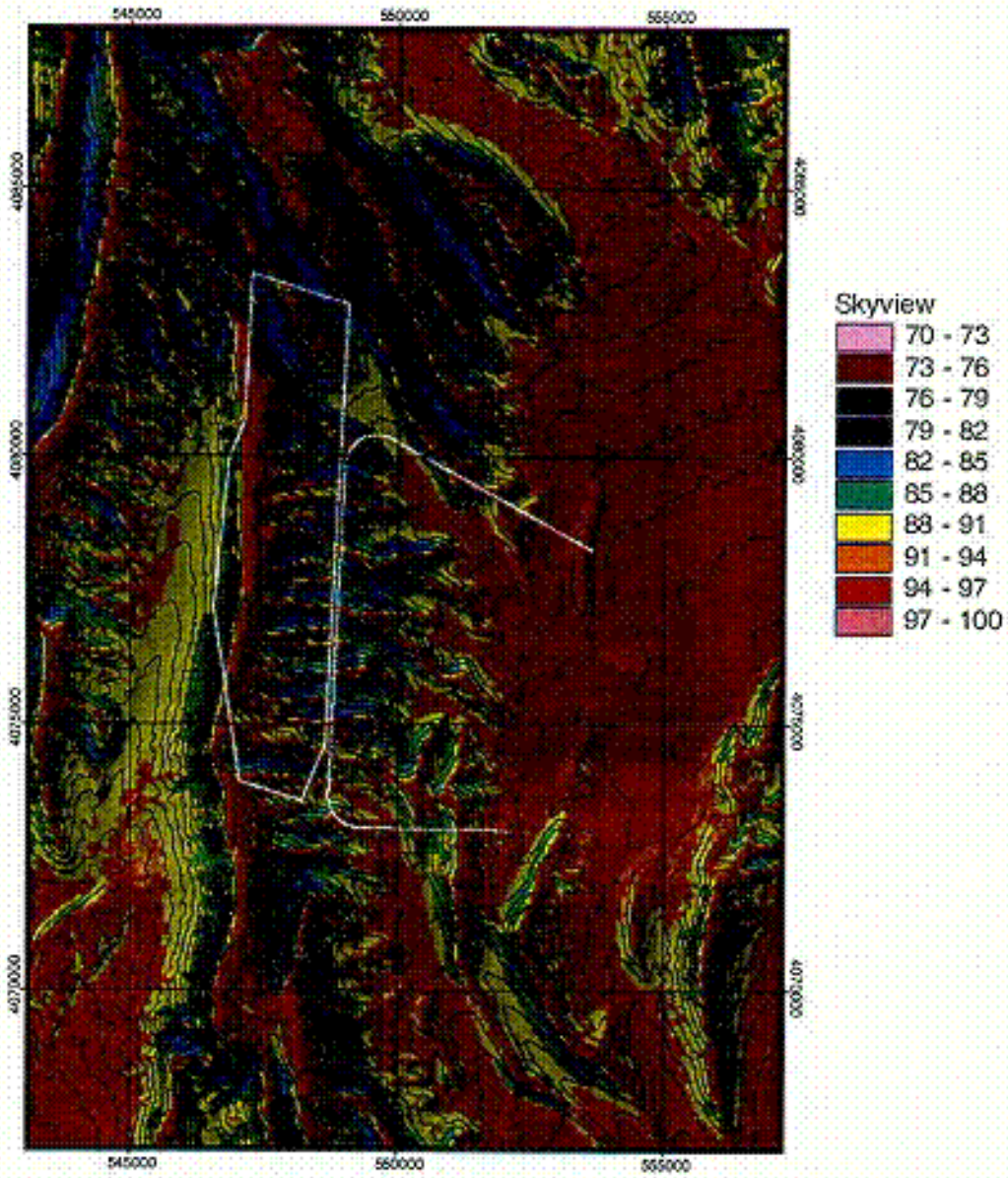

Figure VI-3. Sky-view factor for the area of the potential repository, indicating the expected high (> 90%) sky-view percentages for ridge-tops and alluvial fans, and the expected low (<80%) sky-view percentages on steep side-slopes and narrow washes.

C33

- **Listing of source code for routine BLOCKR7 V1.0:**

```
program blockr7
c     version 1.0
c
c     This routine is the first in a sequence of pre-processing
c     routines used to develop the geospatial input files used
c     for the net infiltration modleing program, INFIL version 2.0.
c
c     BLOCKR7 performs two functions: The first function is to
c     assemble the ASCII grid matrices that are exported from
c     ARCINFO and ARCVIEW using the standard ASCII raster grid
c     export format. A total of 9 ASCII grid matrices (one file
c     per parameter) are input to BLOCKR7. The routine combines
c     the separate parameters into a single xyz column formatted
c     ASCII output file.
c
c     The second function performed by this routine is a calculation
c     of 36 blocking ridge angles (one angle for each 10 degree azimuth
c     direction, starting with 0 degrees for the positive Y direction).
c     The blocking ridge angles are used as input by INFIL version 2.0
c     for the calculation of the reduction in skyview. The skyview factor
c     is calculated (using the blocking ridge angles) and output to
c     to 2 files (a column formatted ASCII text file and an ARCINFO
c     ASCII grid file) that are used to validate the blocking ridge
c     angles.
c
c     The 9 input parameters, 2 UTM coordinates (easting and northing),
c     a row counter used as a grid cell identifier, and the 36
c     blocking ridge angles are assembled into a single column
c     formatted ASCII text file with each row corresponding
c     to a grid cell location and each column corresponding to a
c     grid cell parameter according to the following column order:
c
c     column 1:     LOCID (grid location number)
c     column 2:     X (UTM easting coordinate, in meters)
c     column 3:     Y (UTM northing coordinate, in meters)
c     column 4:     LAT (latitude for X coordinate, in decimal degrees)
c     column 5:     LONG (longitude for Y coordinate, in decimal degress)
c     column 6:     SLOPE (ground surface slope, in degress)
c     column 7:     ASPECT (ground surface aspect, in degrees)
c     column 8:     ELEV (ground surface elevation, in meters)
c     column 9:     SOIL (soil type identification number)
c     column 10:    DEPTH (soil depth class identification number)
c     column 11:    ROCK (rock type identification number)
c     column 12:    TOPOID (topographic position identification number)
c     column 13:    RIDGE(1) (1st blocking ridge angle)
c     "             "
c     "             "
c     column 48     RIDGE(36) (last blocking risge angle)
c
c
c     This routine is a modification of the prototype routine
c     REGRIDGE, version 1.0 (3/24/98),
c     developed by Alan Flint, U.S. Geological Survey.
c     This routine was developed by
c     Joe Hevesi, U.S. Geological Survey, WRD
c     Placer Hall, 6000 J Street
c     Sacramento, CA,
c
c
      double precision east(1000,1000),north(1000,1000)
      double precision xll,yll,cellsize
      double precision easting,northing
      double precision dist,agl,dr,rd
c
      real lat(1000,1000),long(1000,1000)
      real nodata2,x,y
      real angle(36),ang(36)
      real EL,EST,NTH,maxelev,initelev,perdone
```

```
      real sl2,aspect,viewf,costheta,theta
      real ridge2(36)
      real viewfactor(1000)
c
      integer locid(1000,1000),slope(1000,1000),aspct(1000,1000),
      1 elev(1000,1000),soil(1000,1000),dpth(1000,1000),
      2 rock(1000,1000),topo(1000,1000)
c
      integer iang
      integer xang(36),yang(36),ang2(36),anp(36)
      integer rows,cols,nodata1
      integer xx,yy,k,cnt,lp,counter,totcell
c
      character*20 locgrd,latgrd,longgrd,slopgrd,aspgrd,elevgrd,
      1 soilgrd,dpthgrd,rockgrd,topogrd,outfile,skyfil1,skyfil2,
     2  sumfile
      character*120 header
      character*14 ascgrid1,ascgrid2,ascgrid3,ascgrid4,
      1 ascgrid5,ascgrid6
c
c
c---- parameters
c     ----------
      dr    = 0.0174533
      rd    = 57.29579
c
c-------------------------------------------------------------------------72
c---- start routine
c-------------------------------------------------------------------------
c
5     format(A)
      open(unit=7,file='blockr7.ctl')
      read(7,5) header
      read(7,5) latgrd
      read(7,5) longgrd
      read(7,5) slopgrd
      read(7,5) aspgrd
      read(7,5) elevgrd
      read(7,5) soilgrd
      read(7,5) dpthgrd
      read(7,5) rockgrd
      read(7,5) topogrd
      read(7,5) outfile
      read(7,5) skyfil1
      read(7,5) skyfil2
      read(7,5) sumfile
c
c---- read in parameters used for blocking ridge angles
      read(7,*) nang
      do i = 1,nang
        read(7,*) iang,xang(iang),yang(iang)
      enddo
c
c---- open all files
c     -------------------------
      open(unit=9,file=latgrd)
      open(unit=10,file=longgrd)
      open(unit=11,file=slopgrd)
      open(unit=12,file=aspgrd)
      open(unit=13,file=elevgrd)
      open(unit=14,file=soilgrd)
      open(unit=15,file=dpthgrd)
      open(unit=16,file=rockgrd)
      open(unit=17,file=topogrd)
      open(unit=18,file=outfile)
      open(unit=19,file=skyfil1)
      open(unit=20,file=sumfile)
      open(unit=21,file=skyfil2)
c
      write(20,5) header
c
```

```
c---- Begin input of standard ARCINFO ASCII matrix grid files
c     -------------------------------------------------------
77    format(a14,i12)
66    format(a14,f14.4)
c
c---- read-in latitude input grid file
c     and set up header info for skyview ASCII grid matrix
c     -------------------------------------------------------
      read(9,*) ascgrid1,cols
      read(9,*) ascgrid2,rows
      read(9,*) ascgrid3,xll
      read(9,*) ascgrid4,yll
      read(9,*) ascgrid5,cellsize
      read(9,*) ascgrid6,nodata2
c
      write(*,25)
      write(20,25)
25    format(//,'LAT ASCII matrix grid file.....',/)
      write(*,77) ascgrid1,cols
      write(20,77) ascgrid1,cols
      write(21,77) ascgrid1,cols
      write(*,77) ascgrid2,rows
      write(20,77) ascgrid2,rows
      write(21,77) ascgrid2,rows
      write(*,66) ascgrid3,xll
      write(20,66) ascgrid3,xll
      write(21,66) ascgrid3,xll
      write(*,66) ascgrid4,yll
      write(20,66) ascgrid4,yll
      write(21,66) ascgrid4,yll
      write(*,66) ascgrid5,cellsize
      write(20,66) ascgrid5,cellsize
      write(21,66) ascgrid5, cellsize
      write(*,66) ascgrid6,nodata2
      write(20,66) ascgrid6,nodata2
      write(21,66) ascgrid6,nodata2
c
      do i = 1,rows
        read(9,*) (lat(i,j), j=1,cols)
      enddo
c
c
c---- read-in longitude input grid file
c     ---------------------------------
      read(10,*) ascgrid1,cols
      read(10,*) ascgrid2,rows
      read(10,*) ascgrid3,xll
      read(10,*) ascgrid4,yll
      read(10,*) ascgrid5,cellsize
      read(10,*) ascgrid6,nodata2
c
      write(*,35)
      write(20,35)
35    format(//,'LONG ASCII matrix grid file.....',/)
      write(*,77) ascgrid1,cols
      write(20,77) ascgrid1,cols
      write(*,77) ascgrid2,rows
      write(20,77) ascgrid2,rows
      write(*,66) ascgrid3,xll
      write(20,66) ascgrid3,xll
      write(*,66) ascgrid4,yll
      write(20,66) ascgrid4,yll
      write(*,66) ascgrid5,cellsize
      write(20,66) ascgrid5,cellsize
      write(*,66) ascgrid6,nodata2
      write(20,66) ascgrid6,nodata2
c
      do i = 1,rows
        read(10,*) (long(i,j), j=1,cols)
      enddo
c
```

```
c
c---- read-in slope input grid file
c     ------------------------------
      read(11,*) ascgrid1,cols
      read(11,*) ascgrid2,rows
      read(11,*) ascgrid3,xll
      read(11,*) ascgrid4,yll
      read(11,*) ascgrid5,cellsize
      read(11,*) ascgrid6,nodata1
c
      write(*,45)
      write(20,45)
45    format(//,'SLOPE ASCII matrix grid file..........',/)
      write(*,77) ascgrid1,cols
      write(20,77) ascgrid1,cols
      write(*,77) ascgrid2,rows
      write(20,77) ascgrid2,rows
      write(*,66) ascgrid3,xll
      write(20,66) ascgrid3,xll
      write(*,66) ascgrid4,yll
      write(20,66) ascgrid4,yll
      write(*,66) ascgrid5,cellsize
      write(20,66) ascgrid5,cellsize
      write(*,77) ascgrid6,nodata1
      write(20,77) ascgrid6,nodata1
c
      do i = 1,rows
        read(11,*) (slope(i,j), j=1,cols)
      enddo
c
c
c---- read-in aspect input grid file
c     -------------------------------
      read(12,*) ascgrid1,cols
      read(12,*) ascgrid2,rows
      read(12,*) ascgrid3,xll
      read(12,*) ascgrid4,yll
      read(12,*) ascgrid5,cellsize
      read(12,*) ascgrid6,nodata1
c
      write(*,55)
      write(20,55)
55    format(//,'ASPCT ASCII matrix grid file..........',/)
      write(*,77) ascgrid1,cols
      write(20,77) ascgrid1,cols
      write(*,77) ascgrid2,rows
      write(20,77) ascgrid2,rows
      write(*,66) ascgrid3,xll
      write(20,66) ascgrid3,xll
      write(*,66) ascgrid4,yll
      write(20,66) ascgrid4,yll
      write(*,66) ascgrid5,cellsize
      write(20,66) ascgrid5,cellsize
      write(*,77) ascgrid6,nodata1
      write(20,77) ascgrid6,nodata1
c
      do i = 1,rows
        read(12,*) (aspct(i,j), j=1,cols)
      enddo
c
c
c---- read-in elevation input grid file
c     ---------------------------------
      read(13,*) ascgrid1,cols
      read(13,*) ascgrid2,rows
      read(13,*) ascgrid3,xll
      read(13,*) ascgrid4,yll
      read(13,*) ascgrid5,cellsize
      read(13,*) ascgrid6,nodata1
c
      write(*,65)
```

```
      write(20,65)
65    format(//,'ELEV ASCII matrix grid file.....',/)
      write(*,77) ascgrid1,cols
      write(20,77) ascgrid1,cols
      write(*,77) ascgrid2,rows
      write(20,77) ascgrid2,rows
      write(*,66) ascgrid3,xll
      write(20,66) ascgrid3,xll
      write(*,66) ascgrid4,yll
      write(20,66) ascgrid4,yll
      write(*,66) ascgrid5,cellsize
      write(20,66) ascgrid5,cellsize
      write(*,77) ascgrid6,nodata1
      write(20,77) ascgrid6,nodata1
c
      do i =1,rows
        read(13,*) (elev(i,j), j=1,cols)
      enddo
c
c
c---- read-in soil type input grid file
c     --------------------------------
      read(14,*) ascgrid1,cols
      read(14,*) ascgrid2,rows
      read(14,*) ascgrid3,xll
      read(14,*) ascgrid4,yll
      read(14,*) ascgrid5,cellsize
      read(14,*) ascgrid6,nodata2
c
      write(*,75)
      write(20,75)
75    format(//,'SOIL ASCII matrix grid file.....',/)
      write(*,77) ascgrid1,cols
      write(20,77) ascgrid1,cols
      write(*,77) ascgrid2,rows
      write(20,77) ascgrid2,rows
      write(*,66) ascgrid3,xll
      write(20,66) ascgrid3,xll
      write(*,66) ascgrid4,yll
      write(20,66) ascgrid4,yll
      write(*,66) ascgrid5,cellsize
      write(20,66) ascgrid5,cellsize
      write(*,77) ascgrid6,nodata1
      write(20,77) ascgrid6,nodata1
c
      do i = 1,rows
        read(14,*) (soil(i,j), j=1,cols)
      enddo
c
c
c---- read-in soil depth class input grid file
c     ---------------------------------------
      read(15,*) ascgrid1,cols
      read(15,*) ascgrid2,rows
      read(15,*) ascgrid3,xll
      read(15,*) ascgrid4,yll
      read(15,*) ascgrid5,cellsize
      read(15,*) ascgrid6,nodata1
c
      write(*,85)
      write(20,85)
85    format(//,'DPTH ASCII matrix grid file.....',/)
      write(*,77) ascgrid1,cols
      write(20,77) ascgrid1,cols
      write(*,77) ascgrid2,rows
      write(20,77) ascgrid2,rows
      write(*,66) ascgrid3,xll
      write(20,66) ascgrid3,xll
      write(*,66) ascgrid4,yll
      write(20,66) ascgrid4,yll
      write(*,66) ascgrid5,cellsize
```

```
      write(20,66) ascgrid5,cellsize
      write(*,77) ascgrid6,nodata1
      write(20,77) ascgrid6,nodata1
c
      do i = 1,rows
        read(15,*) (dpth(i,j), j=1,cols)
      enddo
c
c
c---- read-in rock type input grid file
c     ---------------------------------
      read(16,*) ascgrid1,cols
      read(16,*) ascgrid2,rows
      read(16,*) ascgrid3,xll
      read(16,*) ascgrid4,yll
      read(16,*) ascgrid5,cellsize
      read(16,*) ascgrid6,nodata1
c
      write(*,95)
      write(20,95)
95    format(//,'ROCK ASCII matrix grid file.....',/)
      write(*,77) ascgrid1,cols
      write(20,77) ascgrid1,cols
      write(*,77) ascgrid2,rows
      write(20,77) ascgrid2,rows
      write(*,66) ascgrid3,xll
      write(20,66) ascgrid3,xll
      write(*,66) ascgrid4,yll
      write(20,66) ascgrid4,yll
      write(*,66) ascgrid5,cellsize
      write(20,66) ascgrid5,cellsize
      write(*,77) ascgrid6,nodata1
      write(20,77) ascgrid6,nodata1
c
      do i = 1,rows
        read(16,*) (rock(i,j), j=1,cols)
      enddo
c
c
c---- read-in topographic ID input grid file
c     --------------------------------------
      read(17,*) ascgrid1,cols
      read(17,*) ascgrid2,rows
      read(17,*) ascgrid3,xll
      read(17,*) ascgrid4,yll
      read(17,*) ascgrid5,cellsize
      read(17,*) ascgrid6,nodata1
c
      write(*,105)
      write(20,105)
105   format(//,'TOPOID ASCII matrix grid file.....',/)
      write(*,77) ascgrid1,cols
      write(20,77) ascgrid1,cols
      write(*,77) ascgrid2,rows
      write(20,77) ascgrid2,rows
      write(*,66) ascgrid3,xll
      write(20,66) ascgrid3,xll
      write(*,66) ascgrid4,yll
      write(20,66) ascgrid4,yll
      write(*,66) ascgrid5,cellsize
      write(20,66) ascgrid5,cellsize
      write(*,77) ascgrid6,nodata1
      write(20,77) ascgrid6,nodata1
c
      do i = 1,rows
        read(17,*) (topo(i,j), j=1,cols)
      enddo
c
c
      totcell = rows * cols
      write(*,115)
```

```
115   format(///)
c
c-------------------------------------------------------------------------72
C     SET UP THE INITIAL BLOCKING RIDGES AS ZERO'S
C     START THE LOOP SEARCHING FOR THE BLOCKING ANGLES FOR EACH LOCATION
c-------------------------------------------------------------------------
c
      cnt=0
      DO 1000 ir = 1,rows
        DO 1300 ic = 1,cols
c
            east(ir,ic) = xll + ((ic-1)*cellsize)
            north(ir,ic) = yll + ((rows-ir)*cellsize)
            sl2 = float(slope(ir,ic))
            aspect = float(aspct(ir,ic))
c
            counter = counter + 1
            perdone = float(counter)/float(totcell)*100.
            if (ic.eq.cols) write (*,1005) counter,ir,perdone
1005        format(i8,i8,f12.1)
c
            do 1500 k = 1,36
                  angle(k)=0.
1500        continue
            initelev = elev(ir,ic)
            maxelev = elev(ir,ic)
c
c------------       search elevation input grid for highest point
c           for each 10 degree angle
            do 2000 k = 1,nang
c                 k = ia
                  x = ic
                  y = ir
                  maxelev = elev(ir,ic)
                  do 3000 lp = 1,1000
                        x = x + xang(k)
                        if((x .gt.cols).or.
     1                        (x.lt.1)) goto 2000
                        y = y + yang(k)
                        if((y.gt.rows).or.
     1                        (y.lt.1)) goto 2000
                        if(maxelev.lt.elev(y,x)) then
                              maxelev = elev(y,x)
                              dist = sqrt((ic-x)**2+(ir-y)**2)*cellsize
                        endif
                        if(dist.eq.0) dist = 1
                        agl = atand((maxelev - initelev)/dist)
                        if(agl.gt.angle(k)) angle(k) = agl
c
3000              continue
2000        continue
c
c
c------------       calculate the 36 blocking ridge angles for each grid cell
c           ---------------------------------------------------------
c------------       1st quadrant
            ANG(1)=(10)/(11.25-0)
     1              *(ANGLE(1)-ANGLE(32))+ANGLE(32)
            ANG(2)=(20-11.25)/(22.5-11.25)
     1              *(ANGLE(2)-ANGLE(1))+ANGLE(1)
            ANG(3)=(30-22.5)/(33.75-22.5)
     1              *(ANGLE(3)-ANGLE(2))+ANGLE(2)
            ANG(4)=(40-33.75)/(45-33.75)
     1              *(ANGLE(4)-ANGLE(3))+ANGLE(3)
            ANG(5)=(50-45)/(56.25-45)
     1              *(ANGLE(5)-ANGLE(4))+ANGLE(4)
            ANG(6)=(60-56.25)/(67.5-56.25)
     1              *(ANGLE(6)-ANGLE(5))+ANGLE(5)
            ANG(7)=(70-67.6)/(78.75-67.5)
     1              *(ANGLE(7)-ANGLE(6))+ANGLE(6)
            ANG(8)=(80-78.75)/(78.75-67.5)
```

```
     1            *(ANGLE(8)-ANGLE(7))+ANGLE(7)
          ANG(9)=ANGLE(8)
c
c------------      2nd quadrant
          ANG(10)=(80-78.75)/(78.75-67.5)
     1            *(ANGLE(9)-ANGLE(8))+ANGLE(8)
          ANG(11)=(70-67.6)/(78.75-67.5)
     1            *(ANGLE(10)-ANGLE(9))+ANGLE(9)
          ANG(12)=(60-56.25)/(67.5-56.25)
     1            *(ANGLE(11)-ANGLE(10))+ANGLE(10)
          ANG(13)=(50-45)/(56.25-45)
     1            *(ANGLE(12)-ANGLE(11))+ANGLE(11)
          ANG(14)=(40-33.75)/(45-33.75)
     1            *(ANGLE(13)-ANGLE(12))+ANGLE(12)
          ANG(15)=(30-22.5)/(33.75-22.5)
     1            *(ANGLE(14)-ANGLE(13))+ANGLE(13)
          ANG(16)=(20-11.25)/(22.5-11.25)
     1            *(ANGLE(15)-ANGLE(14))+ANGLE(14)
          ANG(17)=(10)/(11.25-0)
     1            *(ANGLE(16)-ANGLE(15))+ANGLE(15)
          ANG(18)=ANGLE(16)
c
c------------      3rd quadrant
          ANG(19)=(10)/(11.25-0)
     1            *(ANGLE(17)-ANGLE(16))+ANGLE(16)
          ANG(20)=(20-11.25)/(22.5-11.25)
     1            *(ANGLE(18)-ANGLE(17))+ANGLE(17)
          ANG(21)=(30-22.5)/(33.75-22.5)
     1            *(ANGLE(19)-ANGLE(18))+ANGLE(18)
          ANG(22)=(40-33.75)/(45-33.75)
     1            *(ANGLE(20)-ANGLE(19))+ANGLE(19)
          ANG(23)=(50-45)/(56.25-45)
     1            *(ANGLE(21)-ANGLE(20))+ANGLE(20)
          ANG(24)=(60-56.25)/(67.5-56.25)
     1            *(ANGLE(22)-ANGLE(21))+ANGLE(21)
          ANG(25)=(70-67.6)/(78.75-67.5)
     1            *(ANGLE(23)-ANGLE(22))+ANGLE(22)
          ANG(26)=(80-78.75)/(78.75-67.5)
     1            *(ANGLE(24)-ANGLE(23))+ANGLE(23)
          ANG(27)=ANGLE(24)
c
c------------ 4rth quadrant
          ANG(28)=(80-78.75)/(78.75-67.5)
     1            *(ANGLE(25)-ANGLE(24))+ANGLE(24)
          ANG(29)=(70-67.6)/(78.75-67.5)
     1            *(ANGLE(26)-ANGLE(25))+ANGLE(25)
          ANG(30)=(60-56.25)/(67.5-56.25)
     1            *(ANGLE(27)-ANGLE(26))+ANGLE(26)
          ANG(31)=(50-45)/(56.25-45)
     1            *(ANGLE(28)-ANGLE(27))+ANGLE(27)
          ANG(32)=(40-33.75)/(45-33.75)
     1            *(ANGLE(29)-ANGLE(28))+ANGLE(28)
          ANG(33)=(30-22.5)/(33.75-22.5)
     1            *(ANGLE(30)-ANGLE(29))+ANGLE(29)
          ANG(34)=(20-11.25)/(22.5-11.25)
     1            *(ANGLE(31)-ANGLE(30))+ANGLE(30)
          ANG(35)=(10)/(11.25-0)
     1            *(ANGLE(32)-ANGLE(31))+ANGLE(31)
          ANG(36)=ANGLE(32)
c
c
c------------ calculate viewfactor for validation
c         ----------------------------------
          viewfactor(ic) = 0.
          do 4000 ii = 1,36
                 ridge2(ii) = 90.-ang(ii)
                 costheta = cos(sl2*dr)*cos(ridge2(ii)*dr)
     1                  +sin(sl2*dr)*sin(ridge2(ii)*dr)
     2                  *cos((ii*10.-aspect)*dr)
c
                 theta = -atan(costheta / sqrt(-costheta ** 2. + 1.))
```

```
     1                    + 90. * dr
                  theta = 90. - theta * rd
                  viewf = 90. - theta
                  if(viewf.ge.90.) viewf = 90.
                  viewfactor(ic) = viewfactor(ic) + viewf
4000        continue
            viewfactor(ic) = (viewfactor(ic)/(36.*90.))*100.
            ii = 0.
c
c
c------------       set calculated angles to integer values
c           ------------------------------------
            do 5000 cnt = 1,36
                  ang2(cnt) = INT(ang(cnt))
5000        continue
c
c
c------------       assemble all parameters and write to output file,
c           one line at a time
c           ------------------------------------------------
            topo2 = 1
            write(18,5005) counter,east(ir,ic),north(ir,ic),
     1      lat(ir,ic),long(ir,ic),slope(ir,ic),aspct(ir,ic),
     2      elev(ir,ic),soil(ir,ic),dpth(ir,ic),rock(ir,ic),
     3      topo(ir,ic),(ang2(cnt),cnt=1,36)
c
5005        format(i7,f10.1,f11.1,2f9.4,2i5,i6,i3,i3,i4,i3,36i3)
c
c
            write(19,5105) east(ir,ic),north(ir,ic),viewfactor(ic)
5105        format(f10.1,f11.1,f12.6)
c
1300    continue
c
c-------- write skyview results to ARCINFO ASCII grid file
        write(21,2305) (viewfactor(ic), ic=1,cols)
2305    format(30000f9.2)
c
1000  continue
c
      close(18)
      close(19)
      close(20)
      close(21)
      stop
      END
```